Heterogeneity in the Neural Mechanisms of Adversity: Implications for Developmental Risk and Resilience

by

Felicia A. Hardi

A dissertation submitted in partial fulfillment
of the requirements for the degree of
Doctor of Philosophy
(Psychology)
in the University of Michigan
2024

Doctoral Committee:

Professor Christopher S. Monk, Chair
Associate Professor Adriene Beltz
Professor Luke W. Hyde
Professor Vonnie McLoyd
Research Associate Professor Colter Mitchell
Professor Stephan Taylor

Felicia A. Hardi

felhardi@umich.edu

ORCID iD: 0000-0002-3975-9159

Dedication

In loving memory of my father,

who inspires me to pursue big dreams.

Acknowledgements

This dissertation would not have been possible without the support of many. First and foremost, to my graduate advisor, Dr. Christopher Monk, thank you for all the opportunities you have provided; for encouraging my numerous research ideas and enthusiasm for learning new methodologies; for celebrating my successes and guiding me through each challenge; and for not only providing support in small ways, but also in the most tangible ways. I would also like to express my gratitude to the rest of my committee. To Dr. Luke Hyde, thank you for your continued generosity in welcoming me into your lab community. Your mentorship has challenged me to think deeply about my work and pushed the boundaries of what I thought I could achieve during my training. Thank you to Dr. Colter Mitchell, for guiding me in working with the Future Families and Child Wellbeing Study; Dr. Adriene Beltz, for instilling the importance of statistical rigor and for the opportunity to apply GIMME in my research; Dr. Vonnie McLoyd, for your thought-provoking questions that have made a significant impact on the way I think about the contexts in which children develop; Dr. Stephan Taylor, for your time and for sharing your expertise in psychiatry and neuroscience. Each of you played a pivotal role in my academic journey, and I am immensely grateful for your time, support, and guidance.

I would also like to thank my brilliant colleagues who supported me throughout all stages of my graduate training. Current and past members across TaD and MiND labs, and members of the developmental training grant and area: Sunghyun Hong, Linda Zhang, Dr. Leigh Goetschius, Cleanthis Michael, Gabby Suarez, Deaweh Benson, Heidi Westerman, Jessica Bezek, Joe

Guzman, Ryan Tung, Dr. Scott Tillem, Dr. Melissa Peckins, Montana Boone, Dr. Michael Demidenko, Dr. Ka Ip, Hannah Becker, Chi-Lin Yu, Ella Simmons, Joonyoung Park – thank you for lending me your listening ears during the toughest moments and for the exciting collaborations over the years. I would also like to extend gratitude to other mentors: Dr. Nestor Lopez-Duran, Dr. Jeanne Brooks-Gunn, Dr. Katie Maguire-Jack, as well as to the numerous staff and research assistants who were involved in the SAND project over the years.

The time I spent working on this dissertation and my graduate training was the most exhilarating, both on a professional and personal level. Of course, this would not have been possible without the unwavering support of my partner, Jonathan. Thank you for always indulging my wild ideas and for your steadfast dedication to our family. I would also not be here without my children, Andrea and Sean, who inspire me every day to wrestle with the hard questions. Additionally, I would like to thank my mother and in-laws for their support when we needed it most, as well as to my social circle outside of academia, both in Michigan and the New York area, for keeping me grounded.

I would also like to acknowledge the funding I received from the NIH/NICHD T32 developmental training grant and the Psychology Department at the University of Michigan, which provided the resources necessary to conduct this work. Last but not least, thank you to the individuals and families whose participation made this work possible. Their invaluable contribution to scientific research has not only enriched this work but also stands to advance our understanding of developmental processes that can inform effective policies and interventions.

Table of Contents

List of Tables

List of Figures

Abstract

The wide heterogeneity in adverse outcomes of stressful experiences unexplained in existing literature suggests that more research is needed to understand the developmental risk and resilience to adversity. Specifically, why and how do certain experiences lead to mental health problems for some but not others? What neural mechanisms could account for the long-term effects of adverse experiences on mental health? This dissertation addressed these questions using prospective longitudinal data from a population-based birth cohort sample. The findings demonstrate that the developmental impact of adversity is specific to the types of experiences and neural features, thus requiring approaches that can capture the complexities of both the environment and the brain. Study one examined the differential neural mechanisms implicated in the long-term neural and behavioral consequences of childhood adversity across 21 years. Results show that household instability during childhood was associated with structural brain network organization in adolescence, even after accounting for other types of adversities. Moreover, structural network organization indirectly explained the association between childhood instability and depressive symptoms in young adulthood, demonstrating the prolonged influence of the early environment on mental health through experience-specific neural correlates. In study two, data-driven person-specific functional connectivity subgroups in adolescence were identified to predict mental health outcomes and stress susceptibility six years later, during the highly stressful period of the global pandemic. Findings revealed that individuals with greater functional connectivity involving specific emotion-related key regions (amygdala, subgenual cingulate cortex, ventral striatum) showed an increased trajectory of

anxiety symptoms and were more susceptible to future stress, relative to those with connectivity involving other brain regions (dorsal anterior cingulate cortex, insula). These findings suggest that the associations between adverse experiences and mental health differ based on specific emotion-linked neural regions. Finally, study three built upon the previous studies by addressing heterogeneity in childhood adversity as well as adolescent brain networks using person-oriented approaches. First, data-driven latent profiles were identified using adverse experiences across multiple contexts during the first nine years of life. These profiles were then used to estimate differences in prospective youth mental health outcomes and person-specific functional brain networks. Findings demonstrate that youth with a profile indicated by high exposure to multi-domain adversity, as well as those with an adversity profile characterized by exposure to high maternal depression, exhibited the highest levels of internalizing and externalizing symptoms in adolescence. These patterns were also reflected in the brain function of these youth during emotion processing; specifically, youth with the high-adversity and maternal depression profiles showed the highest density within the default mode network. Additionally, those with the high childhood adversity profile showed attenuated salience network density and greater frontoparietal network density, suggesting aberrant network communication in key emotion regulatory regions. Collectively, this dissertation provides empirical evidence that the neural mechanisms of adversity are specific to the types of experiences, the brain regions involved, and their contextual interactions, which underscore the importance of considering development as an individualized process to parse heterogeneity in the influence of adversity. This work informs future studies by integrating broader environmental measures in characterizing adversity and adopting novel approaches in modeling brain development across multiple levels of analysis.

Chapter 1
Introduction

Childhood adversity is a major risk factor for psychological well-being and is a pervasive problem in the US. Close to 30% of global psychiatric problems were attributed to childhood adversity (Kessler et al., 2010), with approximately two-thirds of US adults surveyed between 2011 and 2020 reporting at least one adverse childhood experience, and one in six indicating exposure to four or more adversities (Swedo, 2023). Childhood adversity also contributes to the vast health inequality within the US, as it is disproportionately experienced by individuals with marginalized identities and those with fewer economic resources (Giano et al., 2020).

Landmark cross-species studies have compellingly shown that adverse experiences can have long-term implications for socioemotional health. For instance, experimental research in rodents and non-human primates has found that stressful conditions, such as disruptions in the early mother-infant relationship, variations in the licking and grooming practices of dams, or limited bedding and nesting, can lead to long-term behavioral disturbances in infants (Champagne et al., 2003; Levine, 2005; Meaney, 2001; Walker et al., 2017a). In nonhuman primates, unpredictable foraging conditions can produce behavioral problems (Rosenblum & Paully, 1984) and cause sustained elevation in the excretion of stress hormones in their infants (Coplan et al., 1996, 2001).

The harmful consequences of early adversity for emotional health are also well-established in humans. Evidence from classical studies examining the influence of maternal separation on orphanage children has shown how severe social deprivation in early childhood

can lead to poor long-term mental health outcomes (Goldfarb, 1945; Gunnar et al., 2007; Rutter, 1998). More contemporary developmental psychology and epidemiological studies have also consistently linked adversity across multiple contexts with a wide range of psychiatric disorders later in life (Chapman et al., 2004; Cicchetti & Lynch, 1993; Finkelhor, 1995; Kessler et al., 1997; Sameroff et al., 1987). These studies collectively demonstrate the long reach of childhood adversity in shaping socioemotional development.

1.1 The Neural Embedding of Adversity

Adverse experiences during the formative period of childhood are particularly influential, as early life experiences can become biologically embedded, shaping the entire life course of development (Berens et al., 2017). Exposure to stress can alter the body's stress regulatory system, responsible for maintaining homeostasis, thus increasing allostatic load—the "wear and tear" on the body—that can have profound health implications (McEwen, 1998). The brain is central to this process, playing a pivotal role in initiating stress regulatory responses (McEwen, 1998). Repeated stress can heighten the activation and release of neurotransmitters, such as glucocorticoids, leading to eventual dysregulation of the hypothalamic-pituitary-adrenocortical (HPA) axis (Loman & Gunnar, 2010), which, in turn, can alter the course of neural development (Berens et al., 2017; Sapolsky, 1992).

Subcortical structures, such as the amygdala and other limbic structures, were found to be important regions because they contain a high density of glucocorticoids receptors (Tottenham & Sheridan, 2010). As a result, they are proposed to be highly susceptible to stressful experiences (see reviews: Hein & Monk, 2017; Tottenham & Sheridan, 2010). In addition to their functional and structural properties, the connections between these structures and regions in the prefrontal

cortex, which are involved in higher-order cognitive processes, have important implications for emotion regulation (Gee et al., 2013; Hanson et al., 2015; Hardi et al., 2022). Other studies have also begun to examine the neural connections between these structures and other regions of the brain in relation to adverse experiences (Goetschius, Hein, McLanahan, et al., 2020; Goetschius, Hein, Mitchell, et al., 2020; McLaughlin et al., 2019) to demonstrate the widespread influence of adversity on the brain.

In humans, the long-term effects of adversity on brain development have been most compellingly demonstrated through longitudinal studies. For instance, the seminal randomized controlled trial of institutionalized children, the Bucharest Early Intervention Project (Zeanah et al., 2003), revealed marked differences in critical neural structures between severely neglected Romanian children and those who were never institutionalized (Sheridan et al., 2012). Similar findings have been observed in other samples of adopted children in the U.S. (Tottenham et al., 2010), as well as in other cases of abuse and neglect in relation to brain function and structure (McLaughlin et al., 2019; Teicher et al., 2016). Collectively, these studies inform how adversity can "get under the skin" to influence health and behaviors across the lifespan (Hertzman, 2012).

1.2 Current Challenges

Despite extensive research on the neural embedding of adversity in relation to mental health outcomes, there remains an urgent need for further studies on this topic. In particular, although childhood adversities are pervasive across multiple contexts (e.g., caregiving, neighborhood, society) and are well-established risk factor for mental health, inconsistencies in the literature suggest that current findings have not adequately captured the broad heterogeneity of environmental influences on neural development (Cohodes et al., 2021). These inconsistencies

encompass the types of adverse experiences, the brain regions linked to these experiences, the direction of effects (i.e., increased or decreased activity in key regions), as well as variations in the developmental timing of experience that relate to neural differences (e.g., early childhood vs. later in development) (Holz et al., 2023; Hosseini-Kamkar et al., 2023; Vannucci et al., 2023). These findings underscore the need for more research to clarify the individual differences in the developmental outcomes of adverse experiences.

1.3 Theoretical Frameworks

1.3.1 Equifinality and multifinality

Conceptual frameworks based on longstanding developmental theories can provide insights into these broad heterogeneous outcomes of adversity. For instance, principles of developmental psychopathology such as the *Equifinality* and *Multifinality* (Cicchetti & Rogosch, 1996) describe the diversity of developmental pathways and outcomes observed in individuals who experience similar or dissimilar risk factors. These principles emphasize the importance of considering individual differences when understanding an individual's onset and course of psychopathology. *Equifinality* refers to the process through which different experiences or processes can lead to the same eventual end state. For instance, two individuals growing up in seemingly contrasting environments can develop similar manifestations of psychopathology through many different circumstances, indicating that multiple pathways can lead to a similar outcome. Conversely, *Multifinality* posits that a single event can lead to vastly different outcomes, resulting in a wide variety of potential consequences. For example, the same adverse event may result in maladaptive behavior in one individual but not in another, suggesting that each mental disorder can have unique causal pathways.

1.3.2 Conceptual models of human development

Both equifinality and multifinality underscore the variability in individuals' responses to risk factors and stressors. These conceptual models are well aligned with the principles of human development described by Bronfenbrenner's *Bioecological Model* (Bronfenbrenner & Morris, 2007). This theoretical model provides a framework for understanding human development within the context of various ecological systems. It emphasizes the bidirectional interplay between individuals and their environment, acknowledging that development is influenced by multiple layers of interacting systems. Individual characteristics, including biology, are nested within multiple contexts—such as family, school, neighborhood, society—and development is shaped by the dynamic interactions of these factors across time.

This complex interplay between nature (i.e., person) and nurture (i.e., environment) is also captured by other person-environment interaction models that address how and why individual differences in developmental outcomes arise. For example, Sameroff's *Transactional Model* (Sameroff, 1975) and subsequently, his *Unified Theory of Development*, focuses on transactional processes across multiple levels of analysis (Sameroff, 2010). These models depict children as active agents who create a continuous feedback loop between individual and various contexts (home, school, community), where they learn, play, and socialize (Bronfenbrenner & Ceci, 1995; Sameroff, 2010). The *Holistic-Interactionistic perspective* and *Dynamic Systems Theory* both outlined how variations in development can emerge from the interactions of multiple factors within the individual (Magnusson, 2001; Molenaar, 2015; Thelen & Smith, 1994). These conceptual models explain how individuals could arrive in similar or differential outcomes through individual factors that are context-dependent, non-linear, and transactional. The interplay between individuals and their environment is also illustrated by the *Gene-*

Environment Interaction models, which posit how shared genetic and environmental variations interact to shape development (Manuck & McCaffery, 2014; Rutter & Silberg, 2002). Other models, such as the *Diathesis-Stress Model* and the *Differential Susceptibility to Stress* model (Belsky et al., 2007; Belsky & Pluess, 2009; Boyce & Ellis, 2005; Rudolph et al., 2016), describe how varying sensitivities to context across individuals can explain the equifinality and multifinality of adverse experiences. Whereas the diathesis-stress model suggests that certain individuals are predisposed to stress (increasing their risk for negative outcomes), the differential susceptibility model extends this principle by positing that highly susceptible individuals may be more sensitive not only to adverse but also to supportive environments. Together, these theoretical frameworks underscore the importance of bidirectional interactions between individual characteristics and environmental contexts as foundational to children's development.

1.3.3 Conceptual models of adversity

While theoretical models of human development explain *how* and *why* individual variations arise, conceptual models of adversity provide contextual understanding of how this could apply to children exposed to adversity. The prevailing approach in understanding how adversity can lead to developmental risks is explained by the *cumulative model*. Rutter and colleagues initiated this model in the Isle of Wight study, where they created a 'Family Adversity Index' to represent the accumulating risk of multiple forms of adversity (Rutter et al., 1979). Similarly, in the Rochester Longitudinal Study, Sameroff and colleagues combined scores from multiple family environment factors to establish cumulative effects on children's cognitive and socioemotional functioning (Sameroff et al., 1987). This model was formalized in the seminal epidemiological studies on Adverse Childhood Experiences (ACEs) (Felitti et al., 1998), which

found that exposure to more than four ACEs led to increased health risks. The cumulative approach has since been widely adopted in research across diverse experiences, such as maltreatment, family violence, maternal stress, parental psychopathology, and financial hardship, with these findings replicated in numerous subsequent studies (see review: Evans et al., 2013).

While the prevailing cumulative risk model has well established that the risk for mental health problems increases with greater exposure to adverse experiences, addressing multiple risks simultaneously through intervention and prevention efforts is extremely difficult. Thus, there has been considerable interest in identifying specific mechanisms that can inform more targeted strategies, potentially enhancing the feasibility of interventions. Pollak and colleagues (2000), for instance, examined potential differences in emotion recognition among children who were physically abused compared to those who were neglected. They found that neglected children had difficulty distinguishing between different emotions, while those who were physically abused were particularly attuned to angry facial expressions (Pollak et al., 2000). These disparate patterns of emotion processing have motivated research to further explore whether differential mechanisms underlie abuse and neglect. Identifying such mechanisms could increase the specificity of neural targets for interventions and improve our understanding of the vast individual differences in childhood maltreatment outcomes.

Thus, new conceptual models of adversity were proposed. The *Dimensional Model of Adversity and Psychopathology* (Sheridan & McLaughlin, 2014) posits that discrete neural mechanisms are associated with different dimensions of adversity (threat vs. deprivation), which can lead to either emotion-linked or cognitive-linked difficulties. Belsky and colleagues differentiate the mechanistic processes underlying unpredictability from those associated with environmental harshness (e.g., poverty) (Belsky et al., 2011). More recently, efforts were made

to integrate unpredictability into the dimensional model of adversity (Ellis et al., 2022; McLaughlin et al., 2021), though more research is needed to establish their differential mechanistic processes. All these theoretical models collectively aim to increase the specificity of identified neural mechanisms underlying adverse experiences.

Evidence on differential neural correlates along the dimensions of threat and deprivation underscores that different adverse experiences can influence brain development through distinct underlying mechanisms (McLaughlin et al., 2021). For instance, studies have found that exposure to violence, but not deprivation, was related to functional connectivity or activity in the amygdala (Goetschius, Hein, McLanahan, et al., 2020; Hein et al., 2020), while others found that deprivation was more strongly linked to deficits in cognitive abilities (Machlin et al., 2019; Miller et al., n.d., 2018). Davis and colleagues (2017) found that unpredictable maternal signals were associated with poor cognitive function in both rats and human samples, and that these fragmented signals were associated with greater density in the white matter tract uncinate fasciculus (Glynn & Baram, 2019). These studies demonstrate how the downstream effects of adversity can influence health through distinct neurodevelopmental pathways.

1.3.4 Heterogeneity problem

Other potential reasons for inconsistencies in current literature is the challenge of translating animal models, which informed the early work on the neural embedding of adversity, to human research. Unlike humans, the sources of stress for rodents are fairly homogeneous and are strictly controlled within an experimental paradigm. Conversely, adverse experiences in humans are incredibly heterogeneous, even within the same type of experience. Abuse, for instance, can be accompanied by physical or emotional violence, occur intermittently or

constantly, be perpetrated by single or multiple parties, and last for short or long periods (Warmingham et al., 2019). Moreover, humans undergo an incredibly protracted ontogenetic process compared to other species, offering an extended opportunity for environmental imprinting (Tottenham, 2020), resulting in greater individual differences over the course of development. This protracted development also provides a prolonged period for exploration in human children, arguably allowing the young developing brain to play a much larger role in driving environmental input, which contributes to greater variations in phenotypic expressions.

This is compounded by recent evidence that convincingly demonstrates how highly idiosyncratic the human brain is, underscoring the need to examine individual differences in brain development (Foulkes & Blakemore, 2018). This observation is evident given that human development is a non-ergodic process (Molenaar, 2004), which attributes to the uniqueness of the developmental process to an individual across time. This implies that inferences that are drawn from intra-individual analyses (comparison among individuals) may not generalize to inter-individual variations (changes occurring within an individual) (Cattell, 1952; Molenaar, 2004; Sterba & Bauer, 2010). Thus, to adeptly examine individual differences, neural models of human development require approaches that can accommodate individual trajectories, factor models, and variances. However, early research on adversity and the brain largely employed common approaches that rely on averages across individuals, precluding granularity in parsing heterogeneity. This is particularly predominant for models examining neural function that conventionally utilize univariate contrast methods (i.e., differences in neural activity in a particular brain region between task conditions). These approaches not only exhibit poor test-retest reliability (Elliott et al., 2020) but are also suboptimal in capturing the vast heterogeneity in brain function across individuals (Finn et al., 2015; Gordon et al., 2017). Thus, there is a

pressing need for further research that adopts new approaches to examining individual differences in the neural embedding of adversity that underlie mental health risks.

1.3.5 Network neuroscience

To address this heterogeneity problem, increased specificity and precision in identified neural correlates of adversity are needed. Just as the individual is an organism of many intersecting processes, the brain is best characterized as a complex system with numerous individual components working in tandem. Multivariate network modeling in neuroscience can provide more holistic models of the brain, and increase reliability in clinical prediction (Spisak et al., 2023). Studies examining individual brain patterns using resting-state functional neuroimaging data, for instance, have found that brain function is highly individualized and that the locations of brain regions differ among individuals (Gordon et al., 2017). This implies that the localized function of one particular region may vary from individual to individual, suggesting that methods focusing on only one specific region may not adequately capture the brain's complexity. Furthermore, network approaches circumvent the need for an overreliance on singular seed-to-target connectivity, which has been shown to be less reliable (Noble et al., 2019), and provide greater statistical power by summarizing more information across the connectome (Kragel et al., 2021; Taxali et al., 2021). Thus, beyond the activation of specific structures and their correspondence with other brain regions, further consideration is needed to understand how stressful experiences relate to brain networks (Menon, 2011; Pessoa, 2017).

Beyond connectivity, the topological organization of these connections can also provide important insights into the development of neural systems. Network organization can be quantified by applying graph analytical methods to reveal the structural organization of neural

connections (E. T. Bullmore & Sporns, 2009). These metrics have been shown to be important for providing new insights into brain development. For instance, studies have found that network structures become increasingly efficient over time as the brain optimizes to its environment (Hagmann et al., 2010), and that brain organization is sensitive to environmental influences (Astle et al., 2023; Guassi Moreira et al., 2021). These studies establish that employing a network approach to model brain organization can reveal novel insights into individual differences in how adverse experiences modulate the brain and mental health.

1.3.6 Person-oriented approaches

Moreover, studies on the neural mechanisms of adversity predominantly examines questions using variable-centered methods. These methods focus on the characteristics of individual variables, quantifying the role of a particular variable in a study, rather than the characteristics of individuals or groups. When used to examine variations between individuals, variable-centered approaches can obscure important information about individuals and reduce the generalizability of inferences from groups to individuals (Curran & Bauer, 2011; Fisher et al., 2018; Molenaar, 2015). In contrast, person-oriented approaches place emphasis on the individual and are powerful tools for elucidating heterogeneity in ways that variable-centered methods cannot (Bergman & Magnusson, 1997; Cicchetti & Rogosch, 1996). Methods under the umbrella of person-oriented approaches vary from less restrictive variable-oriented methods such as latent growth curve models, to classification methods such as mixture models or cluster analysis and single-subject or person-specific methods (Sterba & Bauer, 2010). Collectively, these approaches consider development as a product of complex interaction of various processes and factors occurring within the individual.

1.3.6.1 Person-centered approach

While variable-centered approaches operate under the assumption that relationships between variables are consistent across the entire sample, person-centered methods assumes that there are multiple subpopulations within the overall population that are qualitatively different from one another (Howard & Hoffman, 2018; Morin et al., 2016). Person-centered approach has been applied in research for decades to try to describe psychological processes within particular individuals (Laursen & Hoff, 2006; Magnusson & Stattin, 2007). These methods utilize individual-specific information to identify groups of individuals who share similar experiences or characteristics in the sample (Lanza & Cooper, 2016; Scotto Rosato & Baer, 2012). Moreover, unlike variable-centered approaches that treat experiences as separate entities, person-centered approaches do not assume equal weight for each variable (Bergman & Magnusson, 1997; Laursen & Hoff, 2006). This is critical given that not all adverse experiences operate similarly across individuals (Briggs et al., 2021; Lacey & Minnis, 2020), nor do we fully understand what constitutes high or low risk for each person (Masten, 2001). To address this, a holistic approach to characterizing the child's environment can be achieved using person-centered methods that can account for the complex interactions among contextual factors that contribute to development (Bergman & Magnusson, 1997).

1.3.6.2 Person-specific approach

Whereas a variable-centered approach relies on *population* averages and person-centered approach summarize patterns across *subpopulations*, the person-specific approach is capable of capturing finer-grained information of *individuals*. Person-specific analyses operate under the assumption that individuals within a population are unique, thus questions that seek to

understand variations among people require individualized models (Howard & Hoffman, 2018; Molenaar, 2004; Molenaar & Campbell, 2009). This is particularly notable for brain function (as captured by functional neuroimaging data) that represents moment-to-moment fluctuations in neural activity that are highly amenable to person-specific features (Finn et al., 2015; Gordon et al., 2017; Gratton et al., 2018). One such person-specific method is the application of Group Iterative Multiple Model Estimation (GIMME) (Gates & Molenaar, 2012) on the time-series of functional neuroimaging data. GIMME produce personalized networks that contain connections that are common across the sample, as well as those that are unique to the individual. Thus, allowing for more granularity in modeling individual brain function while simultaneously preserving information across individuals.

1.4 Specific Aims of the Dissertation

This dissertation focused in addressing three aims: 1) examine variations stemming from types of adversity by establishing differential neural mechanisms underlying the long-term influence of adversity on development; 2) examine variations stemming from brain regions by examining the differential neural patterns associated with prospective stressful experiences and psychopathology; and 3) examine variations across types and neural networks by parsing population heterogeneity in experiences to identify more precise neural models of adversity. In all three studies, I employed a network neuroscience approach in examining differences in neural structures and function implicated in psychopathology using a longitudinal analytic design across multiple developmental stages. In the first study, I examined the differential neural mechanisms associated with various types of adverse experiences using topological measures of structural connectivity. The second and third studies applied a similar network principle, with the addition

of a person-specific estimation method (i.e., GIMME) in modeling functional brain networks to address the highly individualized nature of brain function. The second study established differential mental health outcomes related to economic stress during the COVID-19 pandemic, as predicted by person-specific functional network connectivity. In the third study, person-centered multi-domain adversity profiles were examined in association with functional network connectivity and adolescent mental health.

1.4.1 Sample

All three studies in this dissertation examined data from the Future Families and Child Wellbeing Study (FFCWS; formerly known as the Fragile Families and Child Wellbeing Study) (Reichman et al., 2001) and the Study of Adolescent Neurodevelopment (SAND). The FFCWS is a population-based longitudinal cohort of 4,898 families recruited from large cities (population over 200,000) across the U.S. The study oversampled for children of non-marital births at a ratio of 3:1, and included a large representation of minority and low-income families (49% Black, 25% Hispanic, 18% White, 8% other/multiracial; median household income at child's birth $22,500)—groups who are underrepresented in neuroimaging research (Falk et al., 2013). Data were collected at child's birth and at ages 1, 3, 5, 9, and 15 through a series of home visitations, phone interviews, and survey administrations. At age 15, a subsample of individuals was invited to participate in the SAND study at the University of Michigan, Ann Arbor, where data (both mental health and neuroimaging) were collected from 237 youth and families (76% Black, 13% White, 6% Hispanic, 5% other/multiracial; median household income $36,195). This subsample was continually followed, with non-neuroimaging data collected through phone interviews two years later, and again six years later during the COVID-19 pandemic.

Chapter 2 [1]

Early Childhood Household Instability, Adolescent Structural Neural Network Architecture, and Young Adulthood Depression: A 21-Year Longitudinal Study

2.1 Introduction

Childhood adversity is experienced by 40% of individuals and is linked to close to 30% of mental health disorders (Kessler et al., 2010; McLaughlin et al., 2012). Early adversity can increase susceptibility for psychopathology later in life through modulation of critical neural systems as demonstrated by both animal (Sánchez et al., 2001) and human studies (Gur et al., 2019; McLaughlin et al., 2019; Nelson & Gabard-Durnam, 2020; Tottenham et al., 2010).

Though theoretical and empirical work has linked several types of adversities to specific developmental and neurobehavioral outcomes, little research has examined the links between unstable environments with human brain development despite growing interest in cross-species translation of neural mechanisms associated with unpredictability (Ellis et al., 2022; Gee, 2021; McLaughlin et al., 2021). Highly variable or stressful environments (e.g., limited bedding or nesting, maternal separation or unpredictable rearing) have primarily been linked to synaptic maturation in rodents (Bath et al., 2016; Guadagno et al., 2020; Ono et al., 2008; Strzelewicz et al., 2019; Walker et al., 2017b), and studies focusing on unpredictability and human brain development have only recently emerged (Granger et al., 2021).

[1] Chapter 2 corresponds to Hardi et al., 2023 published in *Developmental Cognitive Neuroscience*

Instability can create unique challenges as environments that are constantly shifting heighten demands for adaptation and increase the production of stress hormones (Coplan et al., 2001; Martf & Armario, 1997; Muir & Pfister, 1986) that play important roles for neural regions implicated in socioemotional development (Dallman et al., 2004; McEwen, 2008). These effects are especially pronounced during early childhood when rapid neural development is occurring, with long-lasting implications through adolescence and young adulthood (Hensch & Bilimoria, 2012; Luby et al., 2020; Pechtel & Pizzagalli, 2011). For example, unstable environments marked by frequent residential moves (Ziol-Guest & McKenna, 2014) and family instability (Fomby & Osborne, 2017; Mitchell et al., 2015) during early childhood were linked to increased child internalizing and externalizing behaviors. Similarly, environmental unpredictability was associated with increased behavioral problems in adolescence (Belsky et al., 2011), specifically when these changes were experienced during early years of childhood (Doom et al., 2016).

These observed differences in both neural development and mental health outcomes could potentially vary as a function of instability that reflects environmental adaptation. Such inference is consistent with the life history strategy theory (Belsky et al., 2011; Promislow & Harvey, 1990), which posits that early experiences shape one's strategy for survival, leading to certain phenotypic traits that increase the organism's chances of survival and reproduction. These patterns were established in animal models such as squirrels (Dantzer et al., 2013), birds (Martin, 1995), nonhuman primates (Pereira & Fairbanks, 2002), and rodents (Careau et al., 2009), whereby variations in the environment are associated with reproductive behaviors and offspring growth. Such increased growth, however, could come with a potential trade-off cost of shorter lifespans. The "weathering hypothesis" for instance, posits that exposures to adversities could increase allostatic load and accelerate aging (Geronimus, 1992; McEwen, 2007),

suggesting that while increased pace of development could be advantageous in the short-term, it could also pose long-term health consequences.

Despite evidence linking unstable early environments, neural development, and mental health, no study to date has examined environmental unpredictability and white matter networks. White matter structures are particularly important markers of neural development as myelination of white matter solidifies neural connections and limits the extent to which the brain remains plastic and sensitive to the environment (Hensch & Bilimoria, 2012). While unpredictable maternal signals have been linked to density of preadolescence white matter corticolimbic structures (Granger et al., 2021), little is known about how unstable environment across early childhood relate to network organization of structural connections. Furthermore, most work examining white matter tractography relating to early adverse experiences and psychopathology have focused on specific major white matter tracts (Granger et al., 2021; Hanson et al., 2013; Hein et al., 2018) or microstructures (Goetschius, Hein, Mitchell, et al., 2020; Hardi et al., 2022), which do not capture the spatial characteristics of structural networks that represent information exchange in the brain (E. T. Bullmore & Sporns, 2009; Menon, 2011; Rubinov & Sporns, 2010). Measures of network organization can be accomplished by applying graph analysis to reconstructed white matter fibers streamlines using diffusion magnetic resonance imaging (dMRI) data (Nucifora et al., 2007). Network integration quantified by global efficiency represents how quickly information can travel across the brain through network connections (E. T. Bullmore & Sporns, 2009). Network organization can also be characterized by the presence of interconnected nodes (i.e., clusters) that quantify network robustness, which signifies the degree to which structural integrity is retained when the network is perturbed (e.g., removal of any individual node) (E. T. Bullmore & Sporns, 2009). Finally, network segregation measured by the

modularity index represents the extent to which a network can be subdivided into separate modules (E. T. Bullmore & Sporns, 2009). These network organization measures leverage the strength of structural connectivity among brain regions to provide valuable insight into how information is transmitted across the brain via white matter structures.

Beyond examining the direct link between unstable early environment and neural mechanisms relating to mental health, more work is needed to establish evidence for neural specificity linked to different types of childhood experiences. Extant research on childhood adversity has largely focused on distinguishing the effects of emotional and cognitive enrichment that parents are able to provide to children (Brooks-Gunn & Duncan, 1997; McLoyd, 1998); parent-child interaction (e.g., harsh or supportive parenting) (Chang et al., 2003; Gard et al., 2017; Wiggins et al., 2015); or differential dimensions of adversity across threat-related or deprivation exposures (Goetschius, Hein, McLanahan, et al., 2020; Goetschius, Hein, Mitchell, et al., 2020; Hein et al., 2020; McLaughlin et al., 2019; Sheridan & McLaughlin, 2014). These efforts have collectively shown that specific types of childhood experiences could have differential impact on children's brain and socioemotional development. In regards to unpredictability, events such as residential moves and caregiver transitions contain elements of stochasticity that may not be present in the experiences of poverty or parental harshness (Belsky et al., 2011; Ellis et al., 2022).

The present investigation sought to examine the neural developmental pathways between unstable environments and white matter structures by testing three aims: (1) examine the association between childhood household instability (i.e., residential moves, household composition, and caregiver transitions during first five years of life) (age 0-5) and adolescent structural network architecture (age 15); (2) determine the specificity in childhood adversity by

examining the associations between household instability and structural networks are distinct from the association of other types of adversity (i.e., harsh parenting, neglect, poverty) and structural organization; and (3) test indirect effects of household instability through structural networks on prospective anxiety and depressive symptoms during young adulthood (age 21). Additionally, to provide specificity, an exploratory aim of the study was to identify specific regions that may be particularly important by examining the association of early instability and structural connectivity strength of network regions (overall, within-region, between-regions). We hypothesized that greater childhood instability would be related to patterns of more developed structural networks that are more integrated (i.e., increased global efficiency), more robust (i.e., increased transitivity), and less segregated (i.e., decreased modularity) (Hagmann et al., 2010), and that these associations would be distinct from associations with other types of adverse experiences. Furthermore, we hypothesized that instability would predict subsequent symptoms of anxiety and depression via individual differences in white matter organization.

2.2 Methods

2.2.1 Samples and procedures

Participants were recruited from Future Families and Child Wellbeing Study (FFCWS), a population-based sample of 4,898 children born in large cities in the United States (population over 200,000) with a 3:1 oversampling for non-marital births (Reichman et al., 2001). Given this sampling strategy (i.e., urban births to unmarried parents), low-income families were disproportionately represented in the FFCWS. These children were followed throughout childhood and when children were 15-17 years old, a cohort of 237 families from midwestern sites (Detroit, MI; Toledo, OH; Chicago, IL) participated in the Study of Adolescent Neural

Development (SAND) (*N*=237; mean age 15.87 years; 52% females, 76% Black, median household income $36,195; descriptive statistics on included sample are in Supplemental Table 2-2). Six years later (coinciding with the pandemic), participants self-reported their anxiety and depressive symptoms through online and phone interviews. All participants provided informed consent or verbal assent as minors with parents' consent at each wave, and study protocols were approved by the University of Michigan ethics committee.

2.2.2 Household instability

The early household instability construct was adapted from prior literature examining environmental unpredictability (Belsky et al., 2011; Doom et al., 2016) and applied to the Future Families and Child Wellbeing Study longitudinal data (Reichman et al., 2001). The construct of early household instability in the present study includes the extent of residential moves (i.e., number of times family moved from one wave to the next), change in household composition (i.e., difference in the number of individuals living within the home between waves), and change in living situation with caregivers (i.e., mother, father, mother's cohabitating partners, and grandparents moved in and out of the home between waves) during the first five years (between ages 0-1, 1-3, 3-5). Scores across each component were then standardized and summed to create an overall household instability score for each individual. More details on this construct are available in the Supplement.

2.2.3 Neuroimaging measures

2.2.3.1 Data acquisition and preprocessing

Magnetic Resonance Imaging (MRI) scans were acquired using 3T GE Discovery MR750 scanner with 8-channel head coil at the University of Michigan Functional MRI laboratory. Head movement was limited through the use of head paddings and detailed instructions provided to participants. T1-weighted gradient echo images were first captured (TR=12ms, TE=5ms, TI=500ms, flip angle=15°, field of view=26cm, slice thickness=1.44mm, 256x192 matrix, 110 slices). Diffusion MRI (dMRI) data were then acquired using spin-echo EPI diffusion sequence using repetition time of 7250ms, minimum echo time, 128x128 acquisition matrix, FOV=22cm, 3mm no-gap thick slices with 40 slices acquired using alternating-increasing order, b-value of 1000s/mm^2, 64 non-linear directions. dMRI images were first inspected visually for quality, and slices with an average intensity < 4 standard deviations or more were marked as outliers and replaced with predicted models (Andersson et al., 2016). Participants were excluded if more than 5% of slides were replaced and images for 10 participants who had most replaced slices were further visually inspected. These data were also utilized in previous publications (Calabrese et al., 2022; Goetschius et al., 2019; Goetschius, Hein, Mitchell, et al., 2020; Hardi et al., 2022; Hein et al., 2018).

In the present investigation, preprocessed dMRI data were then processed using the MRtrix pipeline to estimate structural connectivity (Tournier et al., 2012). MRtrix utilizes a novel tensor-fitting method called the Constrained Spherical Deconvolution (CSD) (Farquharson et al., 2013; Tournier et al., 2004, 2007) that outperforms diffusion tractography imaging (DTI) or other conventional deterministic methods, especially in crossing fibers regions (Tournier et al., 2012). This improved method of tracking white matter fibers is further strengthened by the addition of Anatomical Constrained Tractography algorithm, which takes into account other

biological tissues (e.g., cerebral spinal fluid) during estimation to restrict fiber tracking only to anatomically plausible fibers (Smith et al., 2012). These advancements in methodology improve the ability to estimate white matter fibers more precisely using dMRI data. Ten million streamlines were generated using probabilistic tractography, which were then combined with nodes from the anatomical AAL2 atlas (Rolls et al., 2015) to create a 94x94 individualized connectome matrix representing the number of streamlines or structural connectivity (i.e., edges) between each brain regions (i.e., nodes). Additionally, to examine regional specificity, these nodes were subdivided into 8 brain regions based on AAL2 anatomical parcellation (Rolls et al., 2015): frontal lateral, frontal medial, orbitofrontal, temporal, limbic, subcortical, parietal, and occipital (Figure 2-1). Details on specific nodes and coordinates are in Supplemental Table 2-5 and more specific details on steps of MRtrix pipeline are available in the Supplement.

2.2.3.2 Graph analysis

The resulting white matter connectomes were subsequently processed as weighted, undirected, and unthresholded (Civier et al., 2019) graphs using the Brain Connectivity Toolbox (Rubinov & Sporns, 2010) in MATLAB to generate three weighted global metrics of network architecture: global efficiency (Latora & Marchiori, 2001; Onnela et al., 2005; Y. Wang et al., 2017); transitivity (Opsahl & Panzarasa, 2009); and modularity (Newman, 2006; Reichardt & Bornholdt, 2006). Additionally, a localized metric of nodal strength (i.e., strengths of edge connections attached to individual nodes) (Sporns, 2002) was computed and within-region strength (i.e., strength of connections that are within the same region) and between-region strength (i.e., strength of connections between one region and other regions) using custom codes in R. For a weighted graph, global efficiency is the inverse of path with greatest structural

connectivity within the network. Thus, highly efficient networks typically contain strong network connections that facilitate faster information transfer within the network (E. T. Bullmore & Sporns, 2009). As a measure of network clustering, transitivity was utilized in this study to reduce bias of identifying clusters in a weighted graph (Opsahl & Panzarasa, 2009). Transitivity is a localized measure of efficiency, and captures the presence of triangles in the network. A greater transitivity score indicates a greater number of triangles and often signifies the robustness of information transfer when individual nodes are removed on a local level (E. T. Bullmore & Sporns, 2009). Modularity is a measure of network segregation and quantifies the extent to which the network can be subdivided into separate modules (E. T. Bullmore & Sporns, 2009); greater modularity score indicates a more segregated network. These metrics were computed for each person based on individual structural connectomes and extracted for further analysis. More information on their computation is in the Supplement.

2.2.4 Anxiety and depressive symptoms

Anxiety and depressive symptoms during young adulthood (age 21) were self-reported using the 21-item Beck Anxiety Inventory (BAI) (Beck et al., 1988) and 20-item Beck Depression Inventory (BDI) (Beck et al., 1996). The scales showed good internal reliability (Cronbach's $\alpha = .95$ for BAI; Cronbach's $\alpha = .91$for BDI). These data were collected during the early peak of the COVID-19 pandemic (between April 30th, 2020 and June 26th, 2021).

2.2.5 Covariates

The following covariates were included to adjust for demographical characteristics: gender (male, female); ethnoracial identity (Black, white, Hispanic/LatinX, other), a social construct included to control for differences in exposure to structural racism and other discrimination; birth city (Detroit, Toledo, Chicago, other), to account for any sampling differences by geographical location; pubertal development (parent and self-reported at age 15), to account for neural developmental stemming from puberty; economic hardship (parent-reported at ages 1, 3, 5), to account for differences in socioeconomic circumstances. The following variables were also included to examine the specificity of instability in predicting neurobehavioral outcomes versus other adverse experiences during early childhood: harsh parenting (standardized sum score of parent-reported physical violence and psychological aggression subscales in the Conflict Tactics Scale at ages 3 and 5, and parent-reported spanking at age 1); neglect (sum score of parent-reported neglect in the Conflict Tactics Scale at ages 3, 5); food insecurity (parent-reported at ages 3, 5). In addition, to ensure that anxiety and depressive symptoms during young adulthood were not confounded by earlier levels of symptoms, pre-pandemic levels of symptoms (scores measuring anxiety and depression using self-reported Screen for Anxiety Related Disorders (Birmaher et al., 1997) and Mood and Feelings Questionnaire (Angold et al., 1995) at age 17 (Cronbach's $\alpha = .95$ and Cronbach's $\alpha = .96$ respectively) were also accounted for during sensitivity analyses. More details on these constructs and sensitivity analyses are available in Supplement.

2.2.6 Statistical analyses

All statistical analyses were conducted using R Statistical Software v4.2.1 and MPlus v8 (Muthén & Muthén, 2017). For the first aim, zero-order correlations between early childhood

instability and structural network properties (i.e., global efficiency, transitivity, modularity) were examined. Distribution of each variable was examined, and models were tested without extreme or influential outliers as robustness checks. For the second aim, a path model was tested using MPlus v8 with early instability, other types of early adversity, and demographic covariates (gender, puberty, ethnoracial identity, birth city, economic hardship) predicting structural network metrics (global efficiency, transitivity, modularity). For the third aim, indirect effects models predicting anxiety and depressive symptoms during young adulthood were separately tested in association with instability, other adverse experiences, and demographic covariates. Pre-pandemic symptoms were subsequently also added in the mediation model as sensitivity analyses (see Supplement for additional information on robustness checks and sensitivity analyses). Finally, for the fourth exploratory aim, zero-order correlations were tested between childhood instability and structural connections of each lateral subregion. False Discovery Rate (FDR) (Benjamini & Hochberg, 1995) was applied to correct for multiple comparisons across 8 structural subregions. Path models were assessed using standard fit indices (Hu & Bentler, 1999) and were utilized to account for shared variance across multiple types of adverse experiences while retaining the full number of participants in the sample. Full Information Maximum Likelihood estimation with robust standard errors (MLR) was used to account for missing data and to deviations in normality of variables and residuals for the path models tested using Mplus. For the models examining zero-order correlations between instability and network metrics or subregion-specific structural connections, subjects with missing household instability data were listwise deleted (N=161). There were no demographical differences across the full sample (N=237) and subsample with missing instability data (N=161) (Supplemental Table 2-4), and results do not differ when path models were tested using either sample (see Supplement).

2.3 Results

2.3.1 Early instability was related to greater adolescent structural networks efficiency.

Greater instability during early childhood was related to greater global efficiency in structural networks (b^*=.180, p=.028; Figure 2-1). Instability was not related to clustering or modularity (transitivity: b^*=.143, p=.149; modularity: b^*=-.062, p=.432) (Figure 2-2). The association between instability and global efficiency remained after adjusting for covariates (b^*=.164, p=.042) (see Supplemental Table 2-3 for zero-order correlations of all variables).

2.3.2 Associations between early childhood instability and adolescent structural network efficiency remained after accounting for other types of early adverse experiences.

The association between early instability and global efficiency remained after controlling for harsh parenting, neglect, and food insecurity (b^* [*SE*]=.183 [.077], p=.017) (Figure 2-3). Beyond instability, increased harsh parenting also related to increased transitivity (b^* [*SE*]=.312 [.142], p=.029). Path model showed excellent model fit (CFI=.986, TLI=.968, RMSEA=.036, SRMR=.042) and included controls for all demographics (gender, ethnoracial identity, puberty, birth city, economic hardship; see Supplemental Figure 2-1 for full path model).

2.3.3 Greater structural network efficiency in adolescence related to increased depressive symptoms in young adulthood. Household instability predicted depressive symptoms via network efficiency.

Greater adolescent global efficiency was related to increased depressive symptoms during young adulthood (b^* [*SE*]=.523 [.168], p=.002). Further, instability predicted depressive

symptoms later in adulthood via global efficiency during adolescence (specific indirect effect via global efficiency *b** [*SE*]=.100 [.049], *p*=.042) (Figure 2-4). There were no indirect effects via transitivity (*b** [*SE*]=-.041 [.031], *p*=.190) or modularity (*b** [*SE*]=-.007 [.011], *p*=.510). The model showed excellent fit to the data (CFI=.987, TLI=.957, RMSEA=.035, SRMR=.039; see Supplemental Figure 2-2 for full path model). Additionally, results remained after sensitivity analyses including previous levels of depressive symptoms (instability related to global efficiency *b** [*SE*]=.179 [.077], *p*=.021; efficiency related to depression *b** [*SE*]=.582 [.156], *p*<.001; specific indirect effect via efficiency *b** [*SE*]=.104 [.052], *p*=.043; model fit: CFI=.988, TLI=.947, RMSEA=.035, SRMR=.037). There were no significant direct or indirect effects between instability, structural networks, and anxiety symptoms (model fit: CFI=.986, TLI=.955, RMSEA=.036, SRMR=.040; association between anxiety and global efficiency *b** [*SE*]=.201 [.156], *p*=.196; indirect association through global efficiency *b** [*SE*]=.038 [.032], *p*=.245). Furthermore, beyond instability, harsh parenting was associated with transitivity (*b** [*SE*]=.317 [.142], *p*=.025), but transitivity was not related to symptomatology, nor did transitivity indirectly explain the association between harsh parenting and depression (*b** [*SE*]=-.101 [.067], *p*=.131).

2.3.4 Structural connectivity of the fronto-lateral and temporal regions was associated with early instability.

Exploratory analyses on to identify regional specificity found that early instability was most strongly related to structural connectivity strength of the left frontolateral nodes (*b**=.23, *q*=.029) (Figure 2-5). Furthermore, early instability was related to between-region strength connectivity (i.e., connectivity among left frontolateral nodes and all other regions) (*b**=.22, *q*=.037), as well as between-region connectivity among left temporal nodes and all other regions

(b^*=.20, q=.037) (Figure 2-5). All results from subregional connectivity analyses are available in Supplemental Table 2-6.

2.4 Discussion

Using a longitudinal design across 21 years, childhood household instability during the first five years of childhood was associated with greater structural network efficiency in adolescence, which in turn predicted to greater depressive symptoms in young adulthood. Furthermore, structural network efficiency indirectly explained the association between instability and depression, and these associations remained even after accounting for other types of adversity (i.e., harsh parenting, neglect, food insecurity) and earlier symptoms of depression. Moreover, exploratory findings showed that associations with structural connectivity were strongest within the left frontolateral subregion and between temporal and other subregions were associated with greater instability. These results suggest that instability during early childhood was related to greater structural network efficiency, particularly in regions important for regulation and cognition, and that these associations may have consequences for mental health later in life. These findings demonstrate the potential long-term neurobehavioral consequences of exposure to early instability and highlight a model in which early instability may lead to greater risk for psychopathology via modulation of structural white matter networks.

Increased attention has been placed recently to identify the differential influence of unpredictability and instability for child development (Ellis et al., 2022; Gee, 2021; McLaughlin et al., 2021). Our findings here are one of the first to establish associations between household instability and white matter network organization in relation to mental health. While previous work has focused on unpredictability within the caregiving environment through observations of

mother-child dyads at a more granular timescale (Granger et al., 2021), the present results provide complementary evidence by examining neural mechanisms associated with unstable environment across several years. While parent-child interaction is critical for understanding how caregiving environments impact brain development, a multi-year snapshot of the child's environment could capture the potential accumulation of stress resulting from unstable environment. The interplay between these constructs would be an intriguing avenue for further inquiry as instability at large timescales is likely to be correlated with instability at smaller timescales. For instance, frequent residential moves can lead to an array of experiences such as changes in schools or routines that create instability on a daily basis. Furthermore, instability caused by relocations or fathers moving in and out of the home could also have downstream effects on child development through caregiving practices, given that these events could also function as a potential source of stress for the mothers.

Greater levels of instability during early childhood in the present investigation was associated with network organization that facilitates faster information flow in the brain (i.e., greater global efficiency)—a pattern commonly observed with brain maturation (Chen et al., 2013; Hagmann et al., 2010; Richmond et al., 2016; Vértes & Bullmore, 2015). It is possible that this increased efficiency in structural network reflects an adaptive response to household instability, though with potential long-term implications for mental health. Such inference is consistent with theoretical models such as life history theories (Belsky et al., 2011; Promislow & Harvey, 1990) and the stress acceleration hypothesis (Callaghan & Tottenham, 2016), which posit that less predictable early environments or increased exposure to early life stress accelerates biological maturation to increase organism survival, though potentially at later costs. Relatedly, evidence on the "weathering hypothesis" (Geronimus, 1992; McEwen, 2007) have

also demonstrated how adverse environments are associated with increased allostatic load, more rapid aging, and health inequalities, especially among Black mothers. For humans, the prolonged juvenile period may be developmentally advantageous as it allows for continued sensitivity to the environment. Thus, a reduced window of plasticity due to early maturation of neural structures may limit opportunities for subsequent enrichment, potentially increasing susceptibility to psychopathology. From a network theoretical perspective, increased efficiency relating to greater risk for mental health may reflect a greater topological cost of maintaining a more densely structured networks (E. Bullmore & Sporns, 2012). While greater network density could improve communication efficiency, greater allostatic load and vulnerability to environmental stressors could occur if such increase in wiring cost were attained prematurely and constrain future development and adaption to later contexts.

Despite these inferences, conclusive evidence for accelerated neural development relating to instability requires multiple timepoints of neuroimaging data, which is not possible in present investigation. Even though many studies have found efficiency of structural networks to increase with age (Chen et al., 2013; Hagmann et al., 2010; Richmond et al., 2016; Vértes & Bullmore, 2015), there are evidence to show that global efficiency of streamline-based structural connectivity decreases (Koenis et al., 2015) or stabilizes during adolescence (Koenis et al., 2018). It is important to note however, that current developmental trajectories of structural network organization are predominantly based on samples that are markedly distinct from present investigation. This emphasizes the critical need for developmental trajectories of brain development using more diverse and representative samples (Falk et al., 2013; Garcini et al., 2022; Ricard et al., 2022) to allow for a more definitive understanding of how white matter structures change across time.

The associations between household instability with structural networks was observed after adjusting for other types of early adverse experiences, suggesting that instability could have unique neural correlates for mental health. Additionally, whereas instability had the strongest association with global efficiency, harsh parenting during early childhood was related to greater network clustering. Furthermore, although harsh parenting was related to more clustered networks, transitivity was not related to symptomatology. These results suggest that instability is qualitatively different from exposure to harsh parenting and that different types of early adverse experiences may contribute to the development of different elements of network organization that are potentially implicated in psychopathology. These findings are also in line with the integrated model of childhood adversity (Ellis et al., 2022; McLaughlin et al., 2021) that proposed distinct neural mechanisms through which different types of adverse experiences (i.e., threat, deprivation, unpredictability) could lead to psychopathology. Further research is warranted to identify the common facets between the different types of adversity (e.g., household instability and harsh parenting), and whether the intersections of multiple types of adverse experiences may contribute to more unique neural mechanisms relating to psychopathology or, conversely, whether an environment with differential combinations of adverse experiences can contribute to similarities in neural correlates (i.e., equifinality and multifinality) (Cicchetti & Rogosch, 1996).

While the present study does not examine the directional nature of household changes (e.g., whether the child moved into a better or worse neighborhood; or whether a grandparent's move into the home produced beneficial caregiving support or introduced novel stress for the child), these findings suggest that changes in either direction were linked to the organization of white matter networks. This is consistent with evidence showing that adjustment to both positive

and negative life changes can produce stress with consequences for health (Brown & McGill, 1989). However, future investigations on the destination of residential moves or children's perception of these changes are warranted, in addition to their developmental timing effects. For instance, Moving to Opportunity (Chetty et al., 2016), a randomized control trial in which families were given the opportunity to move to a lower-poverty area or remain in their homes, found that relocating to a more economically affluent neighborhood produced more beneficial developmental outcomes for youth who moved during early, but not later, childhood. These findings suggest that the impact of household instability on development could be age or developmental stage specific.

In the present investigation, we found associations between efficiency with depression during COVID-19, a period marked with heightened stress. The pandemic has presented stressors such as social isolation, financial adversity, and uncertainty that increase risk for anxiety and depression, especially for young adults (Lee et al., 2020). Thus, it is possible that these elevated symptoms of depression indicate a potential susceptibility to stress. There were also no associations observed between network metrics and depression at age 17 (before the pandemic), suggesting that these effects could be unique to the circumstance of heightened stress during COVID, or could indicate that these brain-depression findings only emerge later in development when rates of depression continue to increase. Interestingly, we found no association between network connectivity and anxiety symptoms, echoing the potentially differential neural mechanisms relating to anxiety and depression during this period (Hardi, Goetschius, McLoyd, et al., 2023), thus indicating a future direction to further tease apart the distinct etiology preceding these mental health disorders.

Results on subregional structural connectivity in the current study suggests that early instability was particularly related to structural connectivity of the frontolateral and temporal regions. Specifically, the average strength of edges within the frontolateral regions (i.e., within-region connectivity strength), as well as connectivity between the frontolateral and temporal nodes with other brain regions (i.e., between-region connectivity strength) were related to greater early instability. These regions play an important role in higher-order processing and are sensitive to rearing environment in rodents (Greenough et al., 1973). More work is thus needed to further examine the significance of structural connectivity of these regions in relation to early environment and mental processes implicated in psychopathology.

Though the current study had several strengths including a 21-year longitudinal study with a well sampled and underrepresented sample, the combination of early measures of adversity with cutting-edge metrics of white matter organization, and the ability to control for multiple other types of adversity, there are a few limitations. First, longitudinal data during early childhood were collected in intervals of one to two years and no data were collected at ages 2 and 4, thus, additional changes occurring within the household (specifically, parental transitions) during that period may not be accounted for. Nevertheless, the present study captured changes across four waves within a period of five years for all individuals. Second, no information regarding experience of other types of adverse experiences (i.e., neglect, food insecurity) were collected prior to age 1; however, these experiences are unlikely to vastly differ across time, and the present investigation showed consistent results when accounting for a multitude of factors across multiple timepoints (i.e., ages 3 and 5). Third, while events such as residential moves and caregiver transitions could be unpredictable and have been deemed as such in previous works, we were not able to determine whether these events are truly unpredictable for the child in

present investigation (i.e., regular moves may be interpreted as predicted by a child). Thus, more research is needed to establish whether household changes experienced by the child and family as those measured here are unpredictable. Fourth, the present investigation focused on a narrow age range (ages 0-5) as data were collected at longer and unequal intervals in subsequent waves. This limited our ability to capture developmental timing-specific effects of instability during later childhood or preadolescence; thus, more research is needed to test the developmental timing hypothesis of instability using other longitudinal samples in the future. Lastly, no data on externalizing behaviors were collected at age 21.

2.5 Conclusion

Household instability during childhood is a known risk factor for subsequent mental health problems, but less is known about its neurodevelopmental correlates. Here, using a network analysis approach with diffusion tractography of white matter, we found that early childhood instability related to greater structural network efficiency in adolescence and these network differences were linked to greater depressive symptoms in a lower-income, well-sampled cohort of young adults who are underrepresented in neuroimaging research (Falk et al., 2013). These findings suggest that early childhood household instability was related to greater efficiency in neural networks, which, in turn increased susceptibility for mental health problems in young adulthood. At the same time, these associations may also reflect neural adaptation that is protective against increased instability early in life, thus it is possible that there may be benefits of increased efficiency in structural networks that were not examined in this study. Taken together, these results could inform interventions that promote household stability during early childhood to benefit long-term development of child mental health and well-being.

Figure 2-1 Structural networks subdivided into 8 subregions

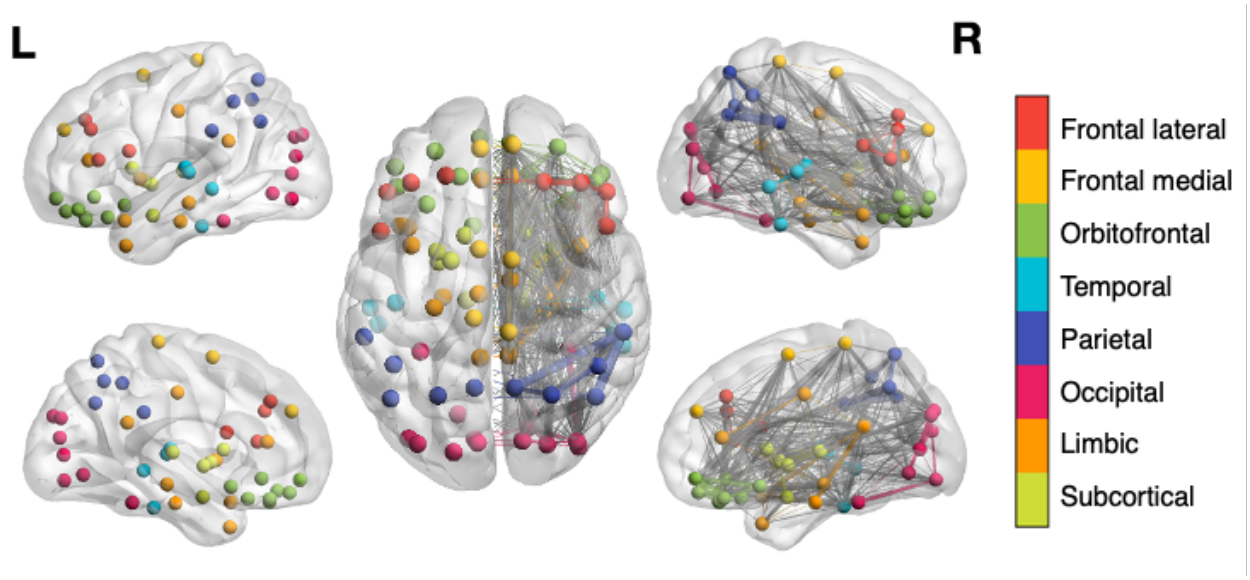

Structural nodes and edges for one subject. Structural networks were subdivided into 8 regions based on the AAL2 anatomical parcellation (Rolls et al., 2015). Details on each node and coordinates are available in Supplemental. Within-region connections are depicted in the same color as the subregion, while between-regions connections are shown in grey. Thickness of edges (i.e., connections) differ based on edge weight (i.e., structural connectivity strength). Edges shown in 25% sparsity for visualization purposes only and figures were created using BrainNet Viewer (Xia et al., 2013).

Figure 2-2 Associations between household instability and white matter structural networks

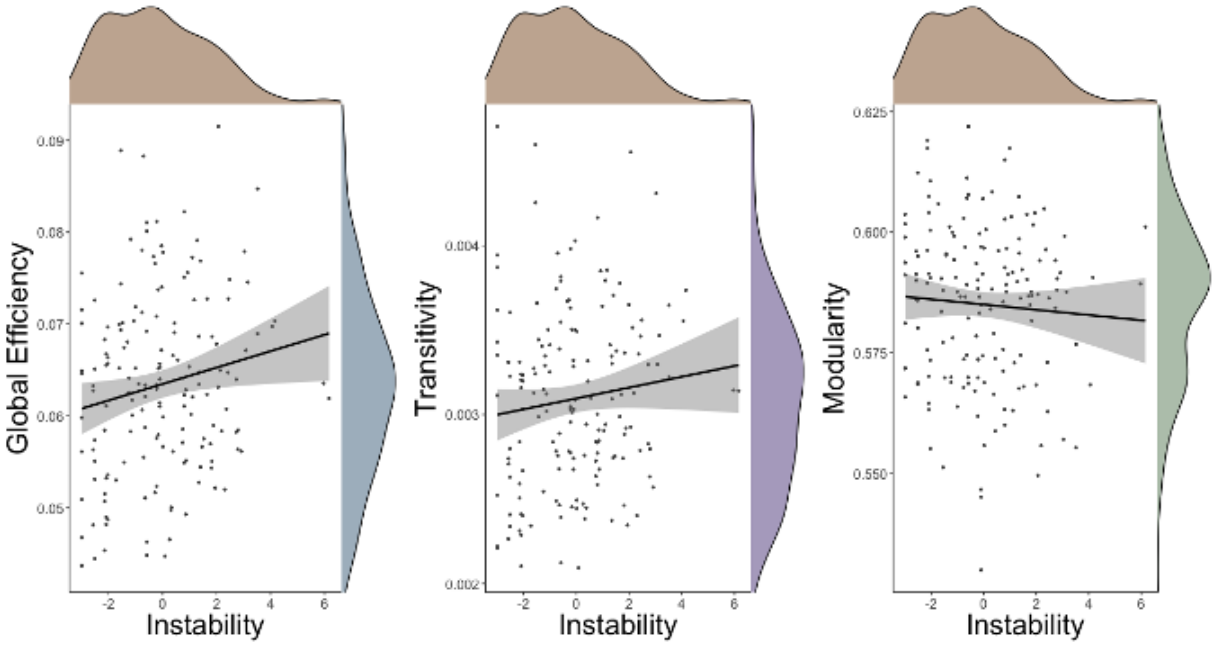

Zero-order correlations between instability and structural network properties. From left to right: greater instability was related to greater structural network efficiency (b*=.173, p=.028), but not transitivity (b*=.143, p=.149) or modularity (b*= -.062, p=.432). Distributions for each variable are shown in brown (instability), blue (global efficiency), purple (clustering), and green (modularity). Outliers (n=2) were omitted for ease of visualization; results were consistent with or without inclusion of outliers. Household instability was represented by standardized scores.

Figure 2-3 Path model testing associations among early instability, other types of childhood adversity, and adolescent structural networks

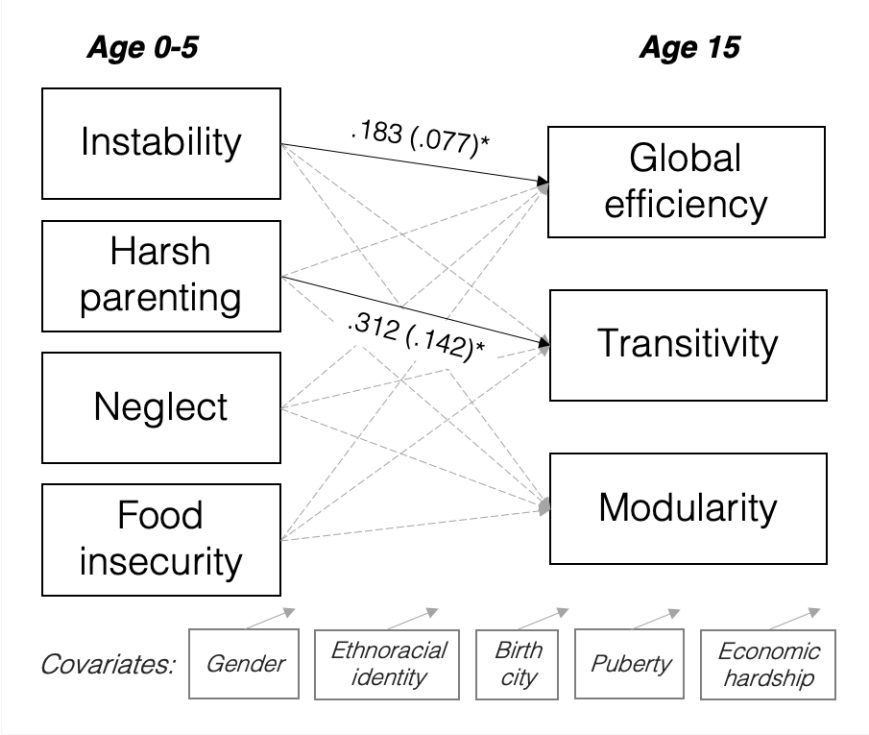

Associations between instability and global efficiency remained (*b** [*SE*] = .183 [.077], *p* = .017) even after adjusting for other types of early adversity (i.e., harsh parenting, neglect, food insecurity). Additionally, harsh parenting was also associated with greater transitivity (*b** [*SE*] = .312 [.142], *p* = .029). Model was adjusted for demographic covariates (gender, ethnoracial identity, birth city, puberty, economic hardship) and had excellent fit (CFI = .986; TLI = .968; RMSEA = .036; SRMR = .042). Standardized coefficients are shown, and dotted path lines indicate non-significant estimated paths.

Figure 2-4 Early household instability indirectly related to depression at young adulthood via adolescent structural network efficiency

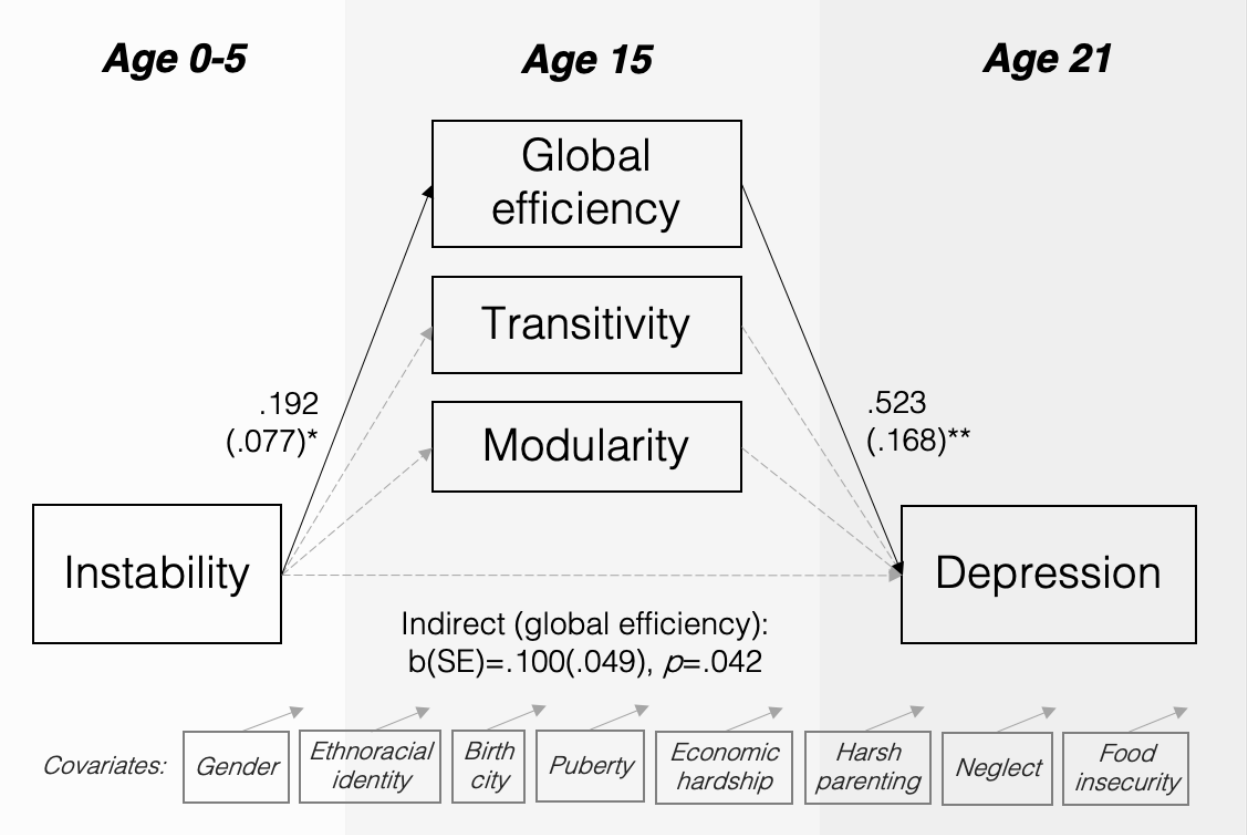

Childhood instability was related to greater structural network efficiency (b*[SE] = .192 [.077], p = .013), which in turn related to greater depressive symptoms at young adulthood (b*[SE] = .523 [.168], p = .002). Global efficiency indirectly explains the association between instability and depression (b*[SE] = .100 [.049], p = .042). Model had excellent fit (CFI = .987; TLI = .957; RMSEA = .035; SRMR = .039) and was adjusted for all covariates (gender, ethnoracial identity, birth city, puberty, economic hardship, harsh parenting, neglect, food insecurity). Standardized coefficients are shown, and dotted path lines indicate non-significant estimated paths.

Figure 2-5 Associations between regional structural connectivity and early instability

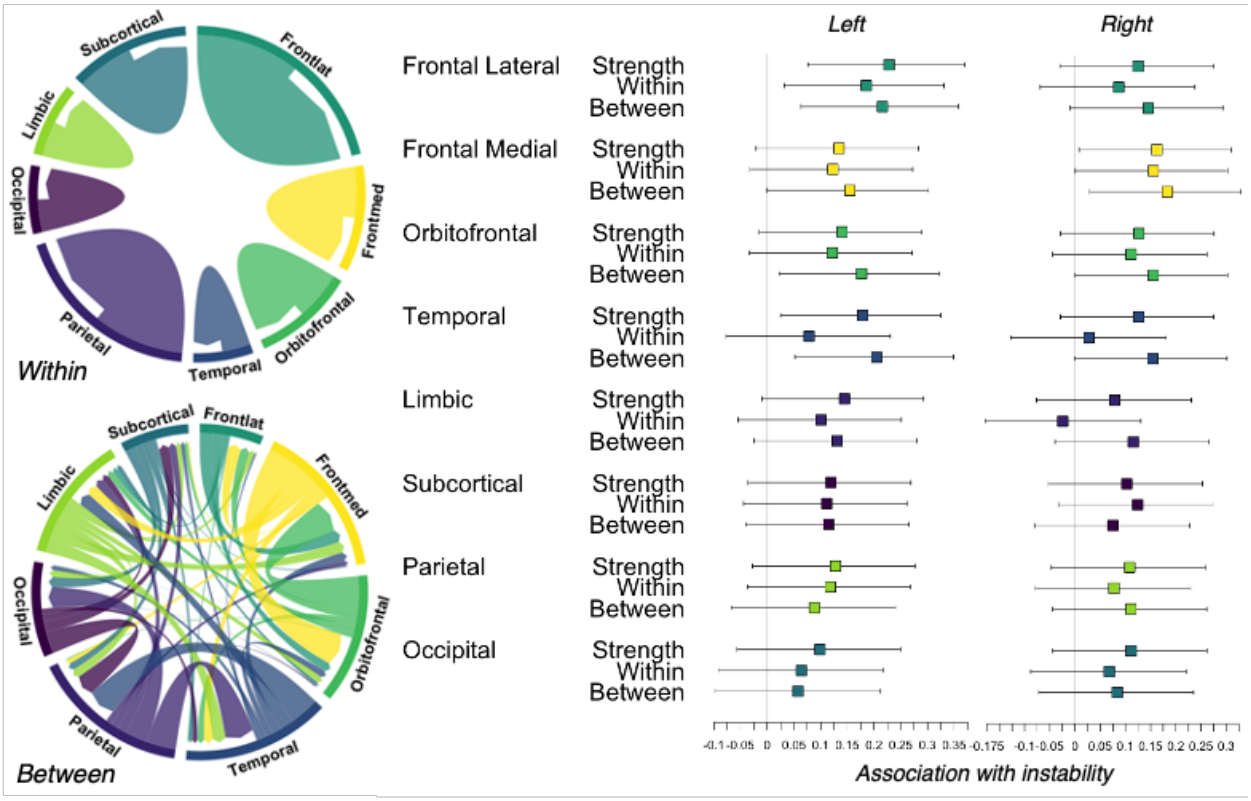

LEFT: Circular plots illustrating within-region (i.e., connections between nodes within each region) and between-regions (i.e., connections between nodes of each region with all other regions) structural connectivity of one individual in the sample.

RIGHT: Instability was particularly associated with the overall strength of structural paths connected to the left frontal lateral nodes ($b^* = .23$, $q = .029$). Additionally, instability was related to connections between left frontal lateral nodes and other regions ($b^* = .19$, $q = .037$), as well as connections between left temporal nodes and other regions ($b^* = .20$, $q = .037$). Each square box denotes standardized estimate of the association between instability and each subregion connectivity metrics, and whiskers indicate confidence intervals.

2.6 Appendix

2.6.1 Exclusionary criteria

Participants were excluded based on whether or not they completed MRI scan (for reasons including refused MRI, exceeded weight limit, medical restrictions, braces or other metal in the body, pregnancy, Autism Spectrum Disorder diagnosis, not completing dMRI scan), and imaging artefact (found in preprocessed structural or tractography during quality control, extreme outliers in network measures) (Supplemental Table 2-1).

2.6.2 Household instability

Household instability construct was adapted from (Belsky et al., 2011) and measured by composite score comprising of residential moves, changes in household composition, and caregiver transition between ages 0 to 5. At each wave (child aged 0, 1, 3, and 5), mother reported on the number of individuals living in the home and who those individuals are. At child ages 1, 3, and 5, mother also reported on the number of times that the family had moved since last wave. Residential moves were computed by adding up the number of moves between ages 0-1, 1-3, and 3-5. Similarly, change in household composition was computed by adding the difference in the number of people who are living in the household between ages 0-1, 1-3, and 3-5. Finally, caregiver transition was computed by adding the number of times that mother, father, mother's cohabitating partners, and either grandparent moved in and out of the home from ages 0-1, 1-3, and 3-5. Scores across each component were then standardized and summed to create an overall household instability score for each individual.

2.6.3 Covariates

The following covariates were included to adjust for demographical characteristics: gender (dummy-coded variable of male, female); ethnoracial identity (dummy-coded variables of Black, white, Hispanic/LatinX, other), a social construct included to control for differences in exposure to structural racism and other discrimination; birth city (parent-reported during child's birth; dummy-coded variables of Detroit, Toledo, Chicago, other); pubertal development (composite score of self-reported and parent-reported responses on the Pubertal Development Scale (Petersen et al., 1988) at age 15 that measured changes in child height, body hair, skin, facial hair and voice (males only), breast development and menarche (females only). Responses on the scale were coded on 4-point scale: 1 = no development to 4 = completed development, and score was a sum of all items endorsed; economic hardship status (parent-reported at ages 1, 3, 5 averaged across time) were based on the sum of 8-items (1 = yes, 0 = no) on whether the family had difficulty paying bills or experienced other financial difficulties and was included as a proximal measure of in-home poverty (Bauman, 1999; Hardi et al., 2022; Mayer & Jencks, 1989). The following variables were included to adjust for other types of adverse experiences during early childhood: harsh parenting, neglect, and food insecurity. Harsh parenting was measured as a standardized sum score of parent-reported 5-items physical violence, 5-items psychological aggression subscales taken from the Conflict Tactics Scale (Straus et al., 1998) across ages 3 and 5 (1 = has happened one or more times, 0 = has never happened), and parent responses to 2 questions at age 1 about spanking (1 = yes, 0 = no). Neglect was a sum of 5-items parent-reported neglect subscale in the Conflict Tactics Scale across ages 3, 5 (1 = has happened one or more times, 0 = has never happened). Food insecurity was measured as a sum score of

parent responses to 16 questions (1 = yes, 0 = no) averaged across ages 3, 5 that captures the extent that the families skipped meals or could not afford more food (Bickel et al., 2000). Additionally, pre-pandemic levels of anxiety and depressive symptoms were included to account for any initial levels of symptoms. Data on anxiety and depression were collected at age 17 using the self-reported 38-items Screen for Anxiety Related Disorders (SCARED) anxiety scale (Birmaher et al., 1997) and the self-reported 30-items Mood and Feelings Questionnaire (MFQ) (Angold et al., 1995) depression scale.

2.6.4 dMRI-based streamline connectome and graph analysis metrics estimation

Preprocessed dMRI data was further processed using MRtrix pipeline for streamline tractography estimation (Tournier et al., 2012) and steps outlined in recommended publications (Tahedl, 2018; Tournier et al., 2012) were followed. Fiber orientation densities (FOD) were estimated using the *dhollander* algorithm and *dwi2fod* command. Resulting diffusion images were visually inspected and normalized for further processing. Next, T1-weighted images were utilized to create a mask for MRtrix's Anatomically Constrained Tractography (ACT) that would restrict streamline estimation to biologically plausible spaces, and then streamlines were estimated using probabilistic tractography using *tckgen* command. Ten (10) million streamlines were estimated based on recommendations of published pipeline (Tahedl, 2018) and resulting streamline maps were again visually inspected then refined using *tcksift*. Individualized structural connectivity connectomes were then created by registering the streamlines to the AAL2 (Rolls et al., 2015) structural atlas and imported into MATLAB for graph analysis using Brain Connectivity Toolbox (Rubinov & Sporns, 2010).

Structural connectivity connectomes were treated as weighted undirected unthresholded graphs (Civier et al., 2019) and three weighted whole-brain metrics (i.e., global efficiency, transitivity, modularity) were estimated using scripts available in the Brain Connectivity Toolbox (Rubinov & Sporns, 2010). Global efficiency was measured by the average of the inverse shortest path length, and represents the efficiency of the network (Latora & Marchiori, 2003; Onnela et al., 2005; Y. Wang et al., 2017). Global efficiency in a weighted network is defined by $E^{\mathrm{w}} = \frac{1}{n}\sum_{i\neq N}\frac{\sum_{j\in N, j\neq i}({d_{ij}}^{w})^{-1}}{n-1}$ where N indicates the set of nodes in a network, n to be the number of nodes, (i,j) is the edge between nodes, and ${d_{ij}}^{w}$ to be the shortest weighted path length between i and j (Latora & Marchiori, 2003; Rubinov & Sporns, 2010). Transitivity is defined as the ratio of triangles to triplets or the presence of triangles in the network and is a classical version of clustering coefficient that is recommended for use in weighted graphs (Onnela et al., 2005; Opsahl & Panzarasa, 2009; Rubinov & Sporns, 2010). Transitivity is measured by computing the average efficiency between nodes in a graph defined by $T^{w} = \frac{\sum_{i\in N} 2t_{i}^{w}}{\sum_{i\in N} k_i(k_i-1)}$ in a weighted graph where k_i refers to the degree (number of edges connected to a node) of a node (Newman, 2003; Rubinov & Sporns, 2010). Lastly, weighted modularity measures the extent to which the network can be subdivided into distinct or non-overlapping groups of nodes (Newman, 2006; Reichardt & Bornholdt, 2006) and was computed by $Q^{w} = \frac{1}{l^{w}}\sum_{i,j\in N}\left[w_{ij} - \frac{k_i^{w}k_j^{w}}{l^{w}}\right]\delta_{m_i,m_j}$ where l^{w} refers to the sum of all network weights, w_{ij} refers to the connection weights between i and j, k_i^{w} and k_j^{w} refer to the weighted degree of i and j respectively, and m_i refers to the module including node i (Newman, 2004; Rubinov & Sporns, 2010). In addition to whole-brain network metrics, connectomes were divided into 8 subregions and strength of connectivity (Sporns, 2002; Sporns et al., 2005) of each subregion, as

well as within-region and between-regions strength were computed. Within-region strength was computed by averaging weighted edges connected to each node of a particular region to nodes of the same region by the number of possible connections within that region (total number of nodes minus one), and then taking the average sum of all within-region nodal strength within that region. Between-region strength was computed by averaging weighted edges connected to each node of a region to nodes of different regions by the number of nodes within the region, and then averaging the sum of all between-region nodal strength with all possible connections.

2.6.5 Robustness checks and sensitivity analyses

Outliers in the zero-order correlation models were examined by examining Cook's D to ensure that results were not driven by statistical outlier. One extreme outlier (*N*=1) in graph analysis metric was identified (transitivity value exceeded upper limit of *Q3+3*IQR*) and subject was excluded from analysis as a result (additional robustness check including this subject did not change results). Additionally, to ensure that there were no differences driven by sample size between full sample used in path model (*N*=237) and subsample in the multiple regression analyses (*N*=161), statistical comparisons were performed on key predictors, outcomes, and demographical covariates. Results show that the two samples do not differ in all measures (Supplemental Table 2-4). Furthermore, path models testing the associations between early instability, other types of early adversity, and demographic covariates (i.e., analysis testing the second aim) and mediation model predicting anxiety and depressive symptoms (i.e., third aim) were checked using the subsample (*N*=161) and results were consistent with results using full sample. Associations between early instability and global efficiency remained after accounting for other types of adversity and covariates (*b** [*SE*]=.168 [.069], *p*=.015; path model fit

CFI=.992, TLI=.981, RMSEA=.031, SRMR=.047). Global efficiency indirectly explains the association between early instability and depression (early instability related to global efficiency *b** [*SE*]=.167 [.069], *p*=.015; global efficiency related to depression *b** [*SE*]=.534 [.174], *p*=.002; indirect effect through global efficiency *b** [*SE*]=.089 [.043], *p*=.040; path model fit CFI=.993, TLI=.977, RMSEA=.029, SRMR=.044).

Supplemental Table 2-1. Neuroimaging data excluded from analyses (*n*=56)

Reason for exclusion	Excluded
Refused MRI	16
Exceeded MRI table weight limit	3
Medical restriction	1
Braces or other metal in body	7
Risk of pregnancy	1
Excluded for Autism Spectrum Disorder diagnosis	2
Did not complete dMRI scan	11
Significant structural artefact[a]	14
Extreme outlier in network measure[b]	1

[a] Significant motion or distortion artefacts as detected during visual inspection or those marked with >5% outlier slices during preprocessing.
[b] Extreme outlier determined by values exceeding upper limit of *Q3+3*IQR*; robustness checks including this subject were subsequently performed

Supplemental Table 2-2. Descriptive sample information (*N*=237)

Measures	Frequency (%)			
Gender	Male = 113 (47.7%) Female = 124 (52.3%)			
Ethnoracial identity	Black = 181 (76.4%) White = 32 (13.5%) Hispanic/LatinX = 13 (5.5%) Other/Multi = 11 (4.6%)			
Birth city	Detroit = 154 (64.98%) Toledo = 43 (18.14%) Chicago = 33 (13.92%) Other = 7 (2.95%)			
	Mean	*SD*	Max	Min
Pubertal development	3.270	0.476	4.000	1.500
Instability (ages 0-5) Residential moves	-0.059 1.867	2.108 2.068	10.014 14.000	-2.991 0.000

Change in household composition	3.646	2.365	14.000	1.000
Caregiver transitions	1.785	1.847	8.000	0.000
Harsh parenting (ages 1,3,5)	2.364	1.164	5.522	0.000
Neglect (ages 3,5)	0.356	0.907	8.000	0.000
Food insecurity (ages 3,5)	1.246	2.412	14.000	0.000
Economic hardship (ages 1,3,5)	1.048	1.065	5.333	0.000
Network properties (age 15)				
Global efficiency	0.063	0.010	0.092	0.044
Transitivity (clustering)	0.003	0.001	0.005	0.002
Modularity	0.585	0.017	0.622	0.530
Anxiety (age 17)	15.930	13.220	61.000	0.000
Depression (age 17)	13.620	13.619	56.000	0.000
Anxiety (age 21)	10.269	11.780	63.000	0.000
Depression (age 21)	11.038	9.082	38.000	0.000

Supplemental Table 2-3. Zero-order correlations among key variables

	Variable	1	2	3	4	5	6	7	8	9	10	11	12	13
1	Gender (Male)													
2	Ethnoracial identity (Black)	-.09												
3	Birth city (Detroit)	.05	.30**											
4	Pubertal development	-.66**	-.04	-.04										
5	Instability	.04	.11	.10	.02									
6	Neglect	-.06	.06	.13	.00	.10								
7	Harsh parenting	.22**	.45**	.39**	-.21*	.15	.24**							
8	Food insecurity	.13	.14*	.03	-.12	.16*	.29**	.18*						
9	Economic hardship	.10	.17*	.06	-.11	.18**	.35**	.38**	.42**					
10	Global efficiency	.02	.20**	-.02	-.13	.17*	.05	.25*	.03	.09				
11	Transitivity	-.05	.15*	-.02	-.06	.11	.06	.26**	.06	.09	.86**			
12	Modularity	.01	-.12	-.05	.02	-.06	-.05	-.07	.01	-.01	-.38**	-.27**		
13	Anxiety	-.15	-.11	-.06	.08	-.05	.01	-.14	.09	-.04	.01	-.04	-.12	
14	Depression	-.10	-.02	-.00	-.01	-.06	-.08	-.10	.02	.01	.16	.04	.04	.69**

Note. * indicates $p < .05$. ** indicates $p < .01$.

Supplemental Table 2-4. Sample comparisons across full sample and subsample

Measures		Full sample (*N*=237)		Subsample (*N*=161)		Statistical comparison	
		N	%	N	%	χ^2	*p*
Gender	Female	124	52.321	89	55.280	.229	.632
	Male	113	47.680	72	44.721		
Ethnoracial identity	Black	181	76.371	122	75.776	.700	.873
	White	32	13.502	20	12.422		
	Hispanic/LatinX	13	5.485	12	7.453		
	Other/Multiracial	11	4.641	7	4.348		
Birth city	Detroit	154	64.980	107	66.460	3.795	.285
	Toledo	43	18.143	22	13.665		
	Chicago	33	13.924	30	18.634		
	Other	7	2.954	2	1.242		
		Mean	***SD***	**Mean**	***SD***	***t***	***p***
Pubertal development		3.270	0.476	3.267	0.582	-.508	.612
Instability		-0.059	2.108	-0.047	1.899	-.061	.951
Harsh parenting		2.364	1.164	2.435	1.186	-.465	.643
Neglect		0.356	0.907	0.410	0.998	-.501	.617
Food insecurity		1.246	2.412	1.328	2.546	-.320	.749
Economic hardship		1.048	1.065	1.085	1.105	-.318	.751
Global efficiency		0.063	0.010	0.063	0.010	-.131	.896
Transitivity		0.003	0.001	0.003	0.001	-.063	.950
Modularity		0.585	0.017	0.585	0.017	.387	.700
Anxiety (age 17)		15.930	13.220	16.530	12.767	-.386	.700
Depression (age 17)		13.620	13.619	13.738	12.898	-.076	.940
Anxiety (age 21)		10.269	11.780	10.342	11.012	-.053	.958
Depression (age 21)		11.038	9.082	11.591	9.273	-.485	.628

Supplemental Table 2-5. Subregional nodes coordinates

* adapted from AAL2 anatomical parcellation (Rolls et al., 2015)

Subregions	AAL2 nodes	Coordinates (x, y, z)
Frontal lateral	Superior frontal gyrus	L: -20.20, 36.00, 35.20 | R: 22.60, 33.20, 37.30
	Middle frontal gyrus	L: -35.50, 32.90, 29.90 | R: 38.80, 32.90, 29.30
	Inferior frontal gyrus, oper.	L: -48.80, 11.50, 17.80 | R: 49.90, 13.70, 20.20
	Inf. frontal gyrus, triangular	L: -45.90, 28.70, 12.60 | R: 50.10, 28.90, 12.80
Frontal medial	Superior frontal gyrus, medial	L: -5.20, 47.90, 29.60 | R: 8.80, 49.50, 28.90
	Supplementary motor area	L: -5.70, 3.60, 60.10 | R: 8.20, -1.10, 60.50
	Paracentral lobule	L: -8.00, -26.70, 68.70 | R: 7.10, -32.90, 66.80
Frontal orbital	Superior frontal gyrus, med orb	L: -5.40, 52.20, -8.90 | R: 7.80, 50.40, -8.50
	Frontal inferior orbital	L: -41.40, 31.10, -8.10| R: 45.80, 33.40, -8.00
	Gyrus rectus	L: -5.40, 35.70, -19.60 | R: 8.00, 34.50, -19.40

	Medial orbital gyrus	L: -14.20, 35.60, -21.10 | R: 16.40, 37.10, -21.30
	Anterior orbital gyrus	L: -25.00, 46.80, -16.10 | R: 28.60, 48.50, -16.20
	Posterior orbital gyrus	L: -28.70, 23.40, -19.50 | R: 33.00, 24.90, -19.40
	Lateral orbital gyrus	L: -42.50, 39.90, -15.10 | R: 47.80, 36.70, -16.20
	Olfactory	L: -8.30, 13.90, -12.70 | R: 10.10, 14.70, -12.60
Temporal	Superior temporal gyrus	L: -53.40, -22.00, 5.80 | R: 57.80, -23.00, 5.40
	Heschl's gyrus	L: -42.30, -20.00, 8.70 | R: 45.90, -18.10, 9.00
	Middle temporal gyrus	L: -55.90, -35.00, -3.60 | R: 57.20, -38.60, -2.80
	Inferior temporal gyrus	L: -50.00, -29.30, -24.50 | R: 53.40, -32.10, -23.70
Limbic	Temporal pole: superior	L: -40.20, 13.90, -21.40 | R: 47.90, 13.50, -18.20
	Temporal pole: middle	L: -36.70, 13.30, -35.40 | R: 44.00, 13.20, -33.50
	Anterior cing. & paracing. gyri	L: -4.40, 34.20, 12.50 | R: 8.10, 35.70, 14.40
	Mid cingulate & paracing. gyri	L: -5.90, -16.10, 40.20 | R: 7.70, -10.20, 38.40
	Posterior cingulate gyrus	L: -5.20, -44.20, 23.30 | R: 7.20, -43.10, 20.50
	Hippocampus	L: -25.30, -22.00, -11.40 | R: 28.90, -21.00, -11.60
	Parahippocampal gyrus	L: -21.50, -17.30, -21.90 | R: 25.10, -16.30, -21.70
	Insula	L: -35.40, 5.40, 2.20 | R: 38.70, 5.00, 0.80
Subcortical	Amygdala	L: -23.50, -1.90, -18.50 | R: 27.10, -0.60, -18.80
	Caudate nucleus	L: -11.80, 9.70, 8.10 | R: 14.50, 10.80, 8.10
	Putamen	L: -24.20, 2.60, 1.10 | R: 27.50, 3.70, 1.20
	Pallidum	L: -18.10, -1.40, -1.00 | R: 20.90, -1.10, -1.10
	Thalamus	L: -11.20, -18.80, 6.60 | R: 12.70, -18.80, 6.70
Parietal	Superior parietal gyrus	L: -23.70, -60.80, 57.70 | R: 25.80, -60.40, 60.70
	Inferior parietal gyrus	L: -43.10, -47.00, 45.40 | R: 46.30, -47.60, 48.20
	Angular	L: -44.40, -62.10, 34.30 | R: 45.20, -61.20, 37.30
	Supramarginal	L: -56.10, -34.90, 29.10 | R: 57.30, -32.80, 33.10
	Precuneus	L: -7.60, -57.30, 46.60 | R: 9.70, -57.30, 42.40
Occipital	Superior occipital gyrus	L: -16.80, -85.60, 26.90 | R: 24.00, -82.20, 29.30
	Middle occipital gyrus	L: -32.60, -82.00, 14.80 | R: 37.10, -81.00, 18.10
	Inferior occipital gyrus	L: -36.50, -79.60, -9.20 | R: 37.90, -83.20, -9.00
	Cuneus	L: -6.30, -81.40, 25.80 | R: 13.20, -80.60, 26.90
	Calcarine fiss. and surrounding	L: -7.50, -79.80, 5.10 | R: 15.70, -74.40, 8.00
	Lingual	L: -14.90, -68.90, -6.00 | R: 16.10, -68.10, -5.20
	Fusiform	L: -31.40, -41.40, -21.60 | R: 33.70, -40.20, -21.50

Supplemental Table 2-6. Subregional connectivity analyses results

Subregions	**Strength**		**Within-region**		**Between-regions**	
	Left	*Right*	*Left*	*Right*	*Left*	*Right*
Frontal lateral	*b*=.228, *p*=.004, p_{FDR}=.029	*b*=.125, *p*=.113, p_{FDR}=.223	*b*=.186, *p*=.018, p_{FDR}=.148	*b*=.087, *p*=.275, p_{FDR}=.523	*b*=.216, *p*=.006, p_{FDR}=.037	*b*=.145, *p*=.066, p_{FDR}=.037
Frontal medial	*b*=.134, *p*=.089, p_{FDR}=.141	*b* =.162, *p*=.040, p_{FDR}=.223	*b*=.123, *p*=.120, p_{FDR}=.257	*b*=.155, *p*=.049, p_{FDR}=.394	*b*=.155, *p*=.050, p_{FDR}=.100	*b*=.183, *p*=.020, p_{FDR}=.100

Frontal orbital	*b*=.140, *p*=.076, p_{FDR}=.141	*b*=.127, *p*=.109, p_{FDR}=.223	*b*=.122, *p*=.123, p_{FDR}=.257	*b*=.111, *p*=.160, p_{FDR}=.427	*b*=.176, *p*=.025, p_{FDR}=.067	*b*=.155, *p*=.049, p_{FDR}=.067
Temporal	*b*=.179, *p*=.023, p_{FDR}=.093	*b*=.126, *p*=.110, p_{FDR}=.223	*b*=.079, *p*=.322, p_{FDR}=.368	*b*=.028, *p*=.729, p_{FDR}=.757	*b*=.205, *p*=.009, p_{FDR}=.037	*b*=.154, *p*=.051, p_{FDR}=.037
Limbic	*b*=.147, *p*=.067, p_{FDR}=.141	*b* =.079, *p*=.319, p_{FDR}=.319	*b*=.101, *p*=.204, p_{FDR}=.273	*b*=-.025, *p*=.757, p_{FDR}=.757	*b*=.131, *p*=.098, p_{FDR}=.157	*b*=.116, *p*=.144, p_{FDR}=.157
Subcortical	*b*=.119, *p*=.132, p_{FDR}=.150	*b*=.103, *p*=.195, p_{FDR}=.223	*b*=.111, *p*=.161, p_{FDR}=.257	*b*=.124, *p*=.117, p_{FDR}=.427	*b*=.115, *p*=.147, p_{FDR}=.196	*b*=.075, *p*=.344, p_{FDR}=.196
Parietal	*b*=.128, *p*=.106, p_{FDR}=.141	*b*=.109, *p*=.171, p_{FDR}=.223	*b*=.118, *p*=.136, p_{FDR}=.257	*b*=.077, *p*=.329, p_{FDR}=.523	*b*=.088, *p*=.264, p_{FDR}=.302	*b*=.111, *p*=.161, p_{FDR}=.302
Occipital	*b*=.099, *p*=.212, p_{FDR}=.212	*b*=.111, *p*=.159, p_{FDR}=.223	*b*=.064, *p*=.420, p_{FDR}=.420	*b*=.068, *p*=.393, p_{FDR}=.523	*b*=.058, *p*=.467, p_{FDR}=.467	*b*=.084, *p*=.292, p_{FDR}=.467

Supplemental Table 2-7. Associations among instability, global efficiency, and depression at age 17

Variable	1	2
1. Instability		
2. Global efficiency	.17*	
3. Depression at age 17	-.05	-.07

Note. * indicates $p < .05$.

Supplemental Table 2-8. Associations among instability at specific timepoints and network metrics

Variable	1	2	3	4	5
1. Instability ages 0-1					
2. Instability ages 1-3	.27**				
3. Instability ages 3-5	.15*	.34**			
4. Global efficiency	.08	.14	.12		
5. Transitivity	.03	.13	.05	.86**	
6. Modularity	-.06	-.06	-.00	-.38**	-.27**

Note. * indicates $p < .05$. ** indicates $p < .01$.

Supplemental Figure 2-1. Full path model of instability predicting structural network metrics adjusting for other types of adversity.

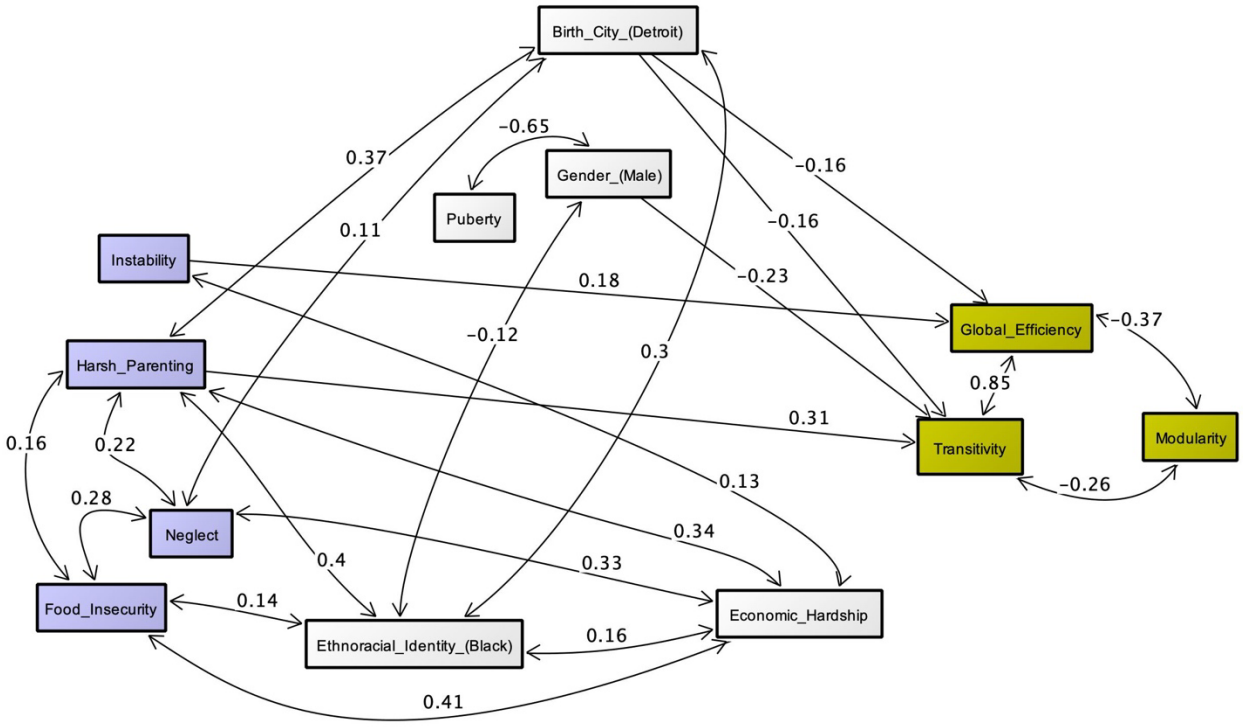

Full path model of instability and other types of adversity (in purple) predicting structural network metrics (in yellow), adjusting for demographical covariates (in grey). Only significant paths are displayed, and estimates shown are standardized coefficients.

Supplemental Figure 2-2. Full path model of main predictors testing indirect effects of instability on young adulthood depression via structural connectivity metrics.

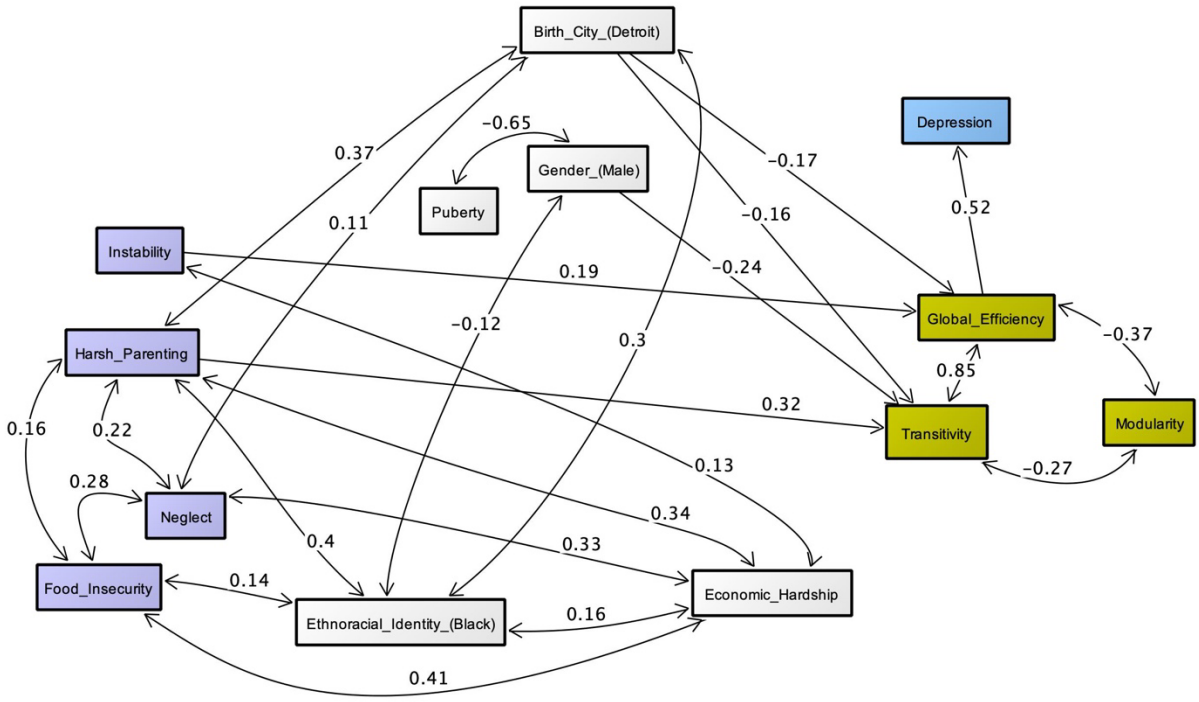

Full path model of instability and other types of adversity (in purple) predicting structural network metrics (in yellow) and depression at young adulthood (in blue), adjusting for demographical covariates (in grey). Only significant paths are displayed, and estimates shown are standardized coefficients.

Chapter 3 [2]

Adolescent Functional Network Connectivity Prospectively Predicts Adult Anxiety Symptoms Related to Perceived COVID-19 Economic Adversity

3.1 Introduction

The COVID-19 pandemic is an unprecedented crisis that has increased the prevalence of mental disorders through profound stressors, including financial hardship, health concerns, and social isolation (Xiong et al., 2020), especially for marginalized and underserved communities that are disproportionately impacted due to systemic inequities (Tai et al., 2021). Although highly stressful experiences often precipitate anxiety and depression (McLaughlin & Nolen-Hoeksema, 2012), only a subset of individuals develop these disorders, potentially due to an increased biological sensitivity to environmental context (Boyce & Ellis, 2005). Young adults may be particularly vulnerable to the stressful impact of the pandemic, given that adolescence and young adulthood are critical developmental stages for neural change as well as shifts in social, occupational, and economic contexts. Further, approximately half of mental health symptoms begin during adolescence and about three quarters manifest before age 24 (Kessler et al., 2005), suggesting that stress susceptibility during these periods may be key in forecasting future anxiety and depression.

Studies have attempted to identify neural signatures from individuals who are more susceptible to stress, finding modest predictive links between brain function during active

[2] Chapter 3 corresponds to Hardi et al., 2023 published in *Journal of Child Psychology and Psychiatry*

emotion processing with later anxiety and depression (Mattson et al., 2016; Swartz et al., 2015). Many studies linking brain function to psychopathology have utilized univariate contrast-based methods that average data across time and individuals (Elliott et al., 2020; Gordon et al., 2017) and recent methodological advances show that multivariate network-based approaches may yield more reliable and predictive estimates of dynamic neural activity (Kragel et al., 2021; Noble et al., 2021; Taxali et al., 2021). Additionally, much of the literature focusing on neural network has utilized neuroimaging data collected at rest; however, without the presence of tasks, resting scans may introduce heterogeneity in cognitive processes that individuals are engaging in during the scan (e.g., one participant may be close to sleep, while another is making lists), leading to greater variance in neural function (Finn, 2021). In contrast, neuroimaging during behavioral tasks may impose boundaries for neural activity that could facilitate better prediction of clinically-relevant traits (Finn et al., 2017; Greene et al., 2018).

In the present investigation, we employed a within-person (in this case, person-specific) approach to map functional connectivity during an emotion task among select neural regions to cluster individuals with similar patterns of connectivity using a data-driven algorithm. This method grouped individuals into subgroups based on similarities and differences in their person-specific networks, thus identifying patterns of heterogeneity (i.e., greater variations in their person-specific connectivity) and homogeneity (i.e., fewer variations in connectivity). Combining hypothesis-driven model-based approaches and data-driven algorithms provides a powerful way to identify patterns of connectivity or clusters of individuals without *a priori* clustering assumptions; this maximizes power by leveraging the within-person nature of functional time series as well as the between-person sample size. We focused on the frontostriatal-limbic circuitry (i.e., amygdala, striatum, insula, cingulate, prefrontal cortex) that is

implicated in anxiety- and depression-like behaviors in both animal models and clinical samples (Etkin & Wager, 2007; Janiri et al., 2020; Price & Drevets, 2010). In addition to clustering individuals based on their functional network, connectivity was characterized in several ways, including network density (i.e., connections within a network) and centrality (i.e., connections involving specific regions of a network) (E. T. Bullmore & Sporns, 2009), revealing both comprehensive brain patterns as well as distinct roles of specific brain regions within networks.

Critically, beyond identifying specific neural patterns that could predict future anxiety and depression, there is a need to examine the psychological impact of stress within groups of individuals who are underrepresented in neuroimaging research and are at increased risk for stress exposure (Falk et al., 2013). The present study examined neural network relating to stress susceptibility in a sample of 174 young adults with a substantial representation of African Americans and low-income families, and tested the following hypotheses: 1) that data-driven neural connectivity network would identify subgroups of adolescents with new onset or worsening symptoms of anxiety and depression six years later during a highly stressful period (COVID-19 pandemic); and 2) these adolescent functional network subgroupings would show differential anxiety and depression susceptibility to COVID-19 adversity. These questions were examined using functional network analyses at a critical time for neural development (age 15) to predict escalation in symptoms over time as well as in response to adversity. Moreover, given the divergent rates of anxiety and depression among men and women (Kessler et al., 1994), we examined sex differences in these associations.

3.2 Methods

3.2.1 Sample and procedures

Participants were recruited from Future Families and Child Wellbeing Study (FFCWS), a population-based sample of 4,898 children born in large US cities (population over 200,000) with an oversampling (3:1) for non-marital births, which resulted in a high representation of low-income families (Reichman et al., 2001). When children were 15-17 years old, a cohort of 237 families from midwestern cities (Detroit, MI; Toledo, OH; Chicago, IL) were invited to participate in the Study of Adolescent Neural Development at the University of Michigan, Ann Arbor, where all neuroimaging data and symptom indicators included in this study were collected. Of these 237 youths who participated in the study, magnetic resonance imaging (MRI) data from 174 youths (mean age 15.9 years) were collected (see Appendix 3.6.1 and Supplemental Figure 3-1 for exclusion criteria). At baseline, the included sample was 54% female, 76% African American, with median household income of $37,000. Two years after their first visit, youth were recontacted, and 128 participants were assessed over the phone. Six years after their first visit (during the pandemic), 119 participants completed online/phone assessments. These data were collected during the peak of the early waves of the pandemic (first participant data was collected on April 30th, 2020; last participant data collected on June 26th, 2021). Participants did not differ in demographic characteristics across each wave or the full sample (Supplemental Table 3-1). Study participants provided informed consent or assent (when minors, with parent consent) at all timepoints. Study protocols were approved by the University of Michigan ethics committee (IRB: HUM00167754; HUM00074392).

3.2.2 Neuroimaging Measures

3.2.2.1 Functional MRI (fMRI) acquisition, task paradigm, and processing

MRIs were acquired using 3T GE Discovery MR750 scanner with 8-channel head coil. Participants completed an emotion faces task in which they identified the gender of the actor (counterbalanced for gender and race). Functional data of each participant across all emotion trials (fear, happy, sad, neutral, angry) during the entire task (including crosshairs presentation) were extracted for subsequent processing (see Supplemental Figure 3-2 for task paradigm). This approach was taken to maximize power and avoid confounds associated with contrast modeling. Standard fMRI preprocessing pipeline were utilized using detailed codes in FSL v6.0 (Beltz et al., 2019) (details on MRI data acquisition, task paradigm, and preprocessing are available in Supplemental Table 3-2 and Supplemental Table 3-3). After preprocessing, time-series functional data were extracted from seven bilateral regions of interest (ROIs): amygdala, dorsal anterior cingulate, dorsomedial prefrontal cortex, insula, orbitofrontal cortex, subgenual anterior cingulate, and ventral striatum. ROIs were 8mm-diameter spheres centered around corresponding Montreal Neurological Institute (MNI) coordinates (Supplemental Table 3-2) extracted from NeuroSynth (Yarkoni et al., 2011), a meta-analytic tool for establishing neural peak activation, and preregistered prior to analyses (see Appendix 3.6.4 for additional information on ROI selection and data extraction). To ensure that results pertained to functional network connectivity of hypothesized ROIs, a sensitivity analysis was completed in which functional connectivity was estimated from other ROIs as a comparison network that was not hypothesized to predict susceptibility to stress (e.g., areas of the brain pertaining to audio, visual, sensorimotor, and language processing), and the resulting subgroup memberships were compared (see Appendix 3.6.5 for details of comparison network, Supplemental Table 3-3 for MNI coordinates of comparison ROIs, and Supplemental Table 3-4 for comparison of resulting subgroups).

3.2.3 Anxiety and depressive symptoms

Symptoms were based on self-reported measures. Anxiety symptoms were measured using Screen for Child Anxiety Related Disorders at wave 1 (baseline) and 2 (pre-COVID), and using the Beck Anxiety Inventory at wave 3 (COVID-19). Depressive symptoms were measured using Mood and Feelings Questionnaire at wave 1 and 2, and using Beck Depression Inventory at wave 3. Scales showed good internal reliability across all waves (see Appendix 3.6.6). Initial (wave 1) anxiety symptoms were related to symptoms at both wave 2 ($r = .58$, $p < .001$) and wave 3 ($r = .31$, $p < .001$); anxiety at waves 2 and 3 were related at $r = .58$, $p < .001$. Initial depression symptoms were related to depression at wave 2 ($r = .39$, $p < .001$) and wave 3 ($r = .38$, $p < .001$), and symptoms at waves 2 and 3 were related at $r = .42$, $p < .001$. Standardized scores were utilized in subsequent analyses.

3.2.4 COVID-19 economic adversity

At wave 3, participants self-reported economic adversity experienced relating to the pandemic ($M = 2.08$, $SD = 1.71$). Participants self-reported yes (1) or no (0) on: employment loss due to the COVID-19 pandemic and income loss due to the COVID-19 pandemic. Participants also reported on the financial state of their household: comfortable (0), enough but not extra (1), have to cut back (2), or cannot make ends meet (3); and any food scarcity experienced by the household: no food insecurity (0), sometimes (1), and often (2). These questions were scaled then summed to compute the economic adversity score (Cronbach's $\alpha = .72$), with higher scores denoting greater pandemic economic adversity. Mean-centered scores were utilized in interaction models to aid interpretation and reduce collinearity (Schumacker et al., 2009).

3.2.5 Covariates

To account for confounding effects, the following covariates were added to statistical models in sensitivity analyses: sex (parent-report: male, female), age during fMRI scan (in years), pubertal development (youth-report), ethnoracial identity (youth-report: Black, white, Hispanic, other/multiracial; a social construct included to account for the impacts of unmeasured structural racism), annual household income at baseline (age 15; parent-report), pandemic duration (number of days since the study commenced, April 20th, 2020; to account for differences in the timing of participation), framewise displacement, early adversity (parent-report: violence exposure; social deprivation (Hein et al., 2020), cognitive ability (reading comprehension; mathematical abilities (Woodcock et al., 2001), cohabitation status (self-report: living with partner or not), parental status (self-report: living with child or not). See Appendix 3.6.7 for details of each covariate.

3.2.6 Statistical Analyses

Data-driven analysis: Subgrouping Group Iterative Multiple Model Estimation (S-GIMME)

Statistical analyses were conducted in R, v4.0.3. S-GIMME (Gates et al., 2017) was applied to extracted functional time-series data. S-GIMME iteratively estimates person-specific unified structural equation models, which contain both positive and negative directed first-order lagged and contemporaneous connections among *a priori* ROIs; those connections can apply to everyone in a sample (reflecting homogeneity), a subset of individuals in a sample (when a subgrouping algorithm is applied through S-GIMME), or just an individual (reflecting heterogeneity). Default GIMME parameters established and supported by largescale simulation studies (Gates et al., 2017; Gates & Molenaar, 2012; Lane et al., 2019) were used in the present

investigation. Beginning with a null model, group-level connections were added for everyone if they significantly improved model fit for at least 75% of the sample as determined by the Lagrange Multiplier tests (Lütkepohl, 2005), then individuals were classified into subgroups using a Walktrap unsupervised community detection algorithm (Gates et al., 2017), which clusters individuals into data-driven subgroups without any *a priori* clustering assumptions and without averaging data across individuals. Finally, subgroup-level connections were added for everyone in a subgroup if they significantly improved model fit for at least 50% of members as determined by Lagrange Multiplier tests. Individual-level connections were estimated for each person (again based on Lagrange Multiplier test) until the networks fit well, and contemporaneous edges were then extracted for subsequent analyses, consistent with previous investigation (e.g., (Goetschius, Hein, McLanahan, et al., 2020)). See Appendix 3.6.8 for more information and Supplemental Figure 3-3 for a visual representation of the S-GIMME process. GIMME and S-GIMME are validated and reliable person-specific functional connectivity analysis approaches that have been used or discussed in over 300 scientific articles (Beltz & Gates, 2017; Gates & Molenaar, 2012). GIMME outperformed 38 commonly-used approaches in modeling functional connectivity (Gates & Molenaar, 2012) and S-GIMME has high precision and recall in estimating connections in largescale simulations of data with similar properties (length and sample size) as this study (Lane et al., 2019). In this study, several robustness checks were performed: psi values were examined to ensure model overfit did not affect inferences; split-half reliability was examined by applying S-GIMME separately to odd versus even volumes of the functional data to ensure data reliability; lastly, S-GIMME was applied to five randomly drawn subsamples, containing 80% of participants (Supplemental Figure 3-4), to ensure stability in subgroup estimation. More details on each procedure are available in Appendix 3.6.9.

3.2.6.1 Subgroup differences analyses

Demographic characteristics in resulting S-GIMME subgroups were first examined using Welsch t-tests to account for heterogeneity of variances between groups. Then, subgroup network characteristics (i.e., density, node centrality) were compared between groups. Density was computed as the number of actual contemporaneous connections divided by the total number of possible connections (Bassett & Bullmore, 2017). Node centrality was computed as a proportion of contemporaneous connections attached to corresponding nodes (i.e., ROIs) from the number of overall contemporaneous connections. Next, two linear multilevel growth curves were estimated separately for anxiety and depression to examine changes in anxiety and depression across three waves. Waves were nested within participants using unstructured error covariance matrices for random intercepts and slopes. Individual intercepts and slopes were then extracted from each model for subsequent analyses. Next, to isolate subgroup differences in symptom change over time, functional network-derived subgroup memberships and intercept (individual symptoms at wave 1; age 15) were used to predict slope (change over waves across ages 15, 17, and 21). As sensitivity analyses, covariates were added in sequential order: main covariates (i.e., age, pubertal development, gender, ethnoracial identity, income, study days), followed by additional sensitivity covariates (i.e., motion, violence exposure, social deprivation, reading comprehension, mathematical abilities, residential status with partner during pandemic, residential status with child during pandemic; see Appendix 3.6.10 for robustness checks). A similar approach was taken to probe ROI specificity by examining the associations between each region node centrality predicting change in anxiety and depressive symptoms over time while adjusting for initial level of symptoms. To account for multiple comparisons, models including node centrality were Bonferroni-corrected (noted by $p_{\text{-adjust}}$). Finally, to probe sex differences,

associations between sex and symptoms were examined at each timepoint, and subgroup-sex interactions were tested to predict symptoms.

3.2.6.2 Subgroup-adversity interaction analyses

Main effects between reported COVID-19 economic adversity with symptoms at wave 3 (during the pandemic) were first tested for anxiety and depression separately. Then, interactions between subgroup-adversity and symptoms (at wave 3; during the pandemic) were tested to examine whether there were subgroup differences in COVID-19 stress susceptibility. In subsequent steps, models were examined with inclusion of initial symptoms (i.e., individual intercepts from growth curves), main covariates, and additional covariates as sensitivity analyses.

3.3 Results

3.3.1 Adolescent data-driven neural network subgroups

S-GIMME derived a two-subgroup model with excellent fit (average model fit indices: root mean square error of approximation = .051, standard root mean residual = .050, non-normed fit index = .924, confirmatory fit index = .952). Subgroup B ($N = 94$) individuals were older and more advanced in pubertal development than Subgroup A ($N = 80$) individuals, but there were no significant differences in other demographic characteristics across the two subgroups (Table 3-1). There were significant subgroup differences in network characteristics. First, Subgroup A network was characterized by greater heterogeneity (i.e., more individual-level connections; $M_A = 17.45$, $SD_A = 4.69$; $M_B = 15$, $SD_B = 3.62$; $t(147.36) = 3.81$, $p < .001$) and relatively greater density compared to subgroup B ($M_A = .36$, $SD_A = .05$; $M_B = .30$, $SD_B = .04$; $t(147.36) = 8.47$, $p <$

.001) (Figure 3-1). Moreover, individuals in subgroup A showed significantly greater centrality in the left amygdala ($t(170.72) = 3.93$, $p_{\text{-adjust}} = .002$), right subgenual anterior cingulate ($t(171.19) = 8.92$, $p_{\text{-adjust}} < .001$), and left ventral striatum ($t(167.23) = 8.17$, $p_{\text{-adjust}} < .001$) (Figure 3-2). In contrast, individuals in subgroup B showed significantly greater centrality in the left dorsal anterior cingulate ($t(171.32) = 4.09$, $p_{\text{-adjust}} < .001$) and bilateral insula (left: $t(171.14) = 3.28$, $p_{\text{-adjust}} = .017$; right: ($t(167.95) = 4.28$, $p_{\text{-adjust}} < .001$) (Figure 3-2) (see Supplemental Table 3-5 for comparison of node centrality across subgroups).

3.3.2 Prospective associations of neural network with symptoms

Accounting for initial symptoms, subgroup A membership predicted greater change in anxiety over time ($\beta = .138$, $p = .042$) relative to subgroup B, and these subgroup differences remained after adjusting for main covariates ($\beta = .194$, $p = .023$) (Table 3-2) and additional covariates ($\beta = .257$, $p = .011$) (Supplemental Table 3-6). Results were specific to anxiety: subgroup membership did not predict change in depression ($\beta = .089$, $p = .243$) (Table 3-2) (Figure 3-3). When examining specific ROIs, individual node centrality did not predict change in anxiety or depression after Bonferroni-correction for multiple comparison (Supplemental Table 3-7). Sex differences in symptoms were most pronounced at age 15 when both anxiety ($\beta = .342$, $p < .001$) and depressive ($\beta = .348$, $p < .001$) symptoms were more prevalent in females than males (Supplemental Figure 3-5), but symptoms did not differ across sex during the pandemic (anxiety: $\beta = .075$, $p = .420$; depression: $\beta = .020$, $p = .829$). Additionally, there were no subgroup-sex interactions predicting anxiety ($\beta = -.0005$, $p = .997$) or depression ($\beta = .070$, $p = .644$) during the pandemic. These results pertained to functional network of hypothesized ROIs;

there were no subgroup differences in symptoms from prediction analyses using comparison network (i.e., non-hypothesized set of ROIs; see Appendix 3.6.5; Supplemental Table 3-4).

3.3.3 Susceptibility to COVID-19 economic adversity

Increased economic adversity during the pandemic was related to greater anxiety symptoms during COVID-19 across all participants ($\beta = .367$, $p < .001$). Moreover, there was a significant adversity-subgroup interaction ($\beta = .307$, $p = .006$), such that participants in the more heterogeneous Subgroup A reported greater anxiety during the pandemic in response to pandemic-related economic adversity relative to subgroup B (Figure 3-4), and this interaction effect remained after adjusting for initial level of anxiety and covariates ($\beta = .237$, $p = .021$) (Table 3-3), and additional covariates ($\beta = .259$, $p = .031$) (Supplemental Table 3-6). There was a similar association in which economic adversity was associated with depression across all participants ($\beta = .356$, $p < .001$), but adversity-subgroup interaction effect was not statistically significant for depression ($\beta = .196$, $p = .088$) (Figure 3-4). Subgroups did not statistically differ in their reports of COVID-19 economic adversity (Table 3-1). Furthermore, subgroup-adversity interaction did not predict symptoms when analyses were done using subgroups that were derived from comparison network (i.e., non-hypothesized set of ROIs; see Appendix 3.6.5; Supplemental Table 3-4).

3.4 Discussion

Using a person-specific functional neural connectivity mapping, data-driven subgroups prospectively predicted increasing anxiety and stress susceptibility during a highly stressful

event. Two subgroups emerged, a more heterogeneous subgroup characterized by relatively greater variation in person-specific networks and greater network density as well as more connections involving the amygdala, subgenual anterior cingulate, and striatum; and a more homogenous subgroup, characterized by lower network density and greater involvement of the insula and dorsal anterior cingulate cortex. Relative to individuals in the more homogenous subgroup, individuals in the more heterogeneous subgroup experienced escalating trajectories of anxiety symptoms from age 15 to 21 (during COVID-19 pandemic) when adjusting for initial symptoms. Moreover, despite exposure to equivalent amounts of economic adversity during the pandemic, the more heterogeneous subgroup experienced greater anxiety as economic adversity increased, and the results remained after controlling for initial levels of anxiety at adolescence and other covariates. These results identify potential neural signatures of susceptibility and resiliency to anxiety-related stress. These conclusions are strengthened by the use of an unsupervised data-driven and personalized approach to network mapping using a six-year longitudinal population-based sample with substantial representation of marginalized participants who are at greater risk for adversity exposure.

The distinction across subgroups in the progression of anxiety symptoms and in relation to adversity demonstrates how network analysis was able to identify individuals whose anxiety symptoms would generally worsen across adolescence and particularly, in response to increased adversity. Notably, reported economic adversity during the pandemic was comparable across the neural subgroups, suggesting that this finding was not driven by disparity in experienced stress, but by individual differences in stress response. Furthermore, though rates of anxiety and depression are often higher in women (Kessler et al., 1994), we found that this sex difference was diminished during the pandemic and there was no evidence that sex interacted with

subgroup membership, nor was a confounder in findings. Thus, these networks appear to be relevant for both men and women. These results are broadly consistent with the biological sensitivity to context model (Boyce & Ellis, 2005), which posits that some individuals are more susceptible to the environment (in this case, economic adversity). However, here we only tested susceptibility related to a negative outcome, leaving open the question of whether these individuals would also achieve more favorable outcomes in a more positive environment.

These results also suggest that more heterogeneous adolescent neural networks, specifically those involving the amygdala, subgenual cingulate, and striatum, may indicate sensitivity to future stress. Individuals with greater heterogeneity in their networks (i.e., more connections that were different from connectivity patterns found in all participants) and greater network density (i.e., more connections among ROIs) showed greater increases in anxiety and susceptibility to stress. These results are consistent with evidence showing that greater reactivity of emotion-related regions predicts risk for psychopathology (Greicius et al., 2007; Schwartz et al., 2003; Stein et al., 2007). Furthermore, greater heterogeneity in the more susceptible group in present investigation suggests that psychopathology may be related to more variations in neural connectivity, consistent with the notion that there may be a greater neural heterogeneity in biological features of psychopathology and fewer variations in neural patterns (i.e., homogeneity) in the general population (Fair et al., 2012; Feczko et al., 2019; Finn et al., 2020). Notably, the detection of neural heterogeneity in the present study was accomplished by clustering individuals using their personalized neural networks, thus demonstrating the strength of person-specific connectivity mapping in teasing apart similarities and differences in neural patterns for prediction of mental health phenotypes. These inferences can be strengthened by future investigations that examine whether such heterogeneity persists with time, or whether

neural function converges to more homogenous patterns of connectivity with improvements in symptomatology. Furthermore, future research can benefit from further testing of whether there are other neural networks implicated in stress susceptibility beyond the brain regions examined in present investigation.

The present results identified distinct responses to stress within an important sample of participants who represent identities and groups that are underrepresented in biomedical research during a historic global event. Though one neural-network based subgroup did appear to be more susceptible to pandemic-related adversity, the other group was relatively resilient, at least on the measures we examined. Evidence of this type of resilience is critical in identifying why and how some individuals thrive despite adversity, particularly for those facing increased stress via marginalization and oppression. Even with compounding economic stress, health-related distress, police brutality, and other forms of social unrest that occurred during the pandemic, individuals with sparser adolescent functional network and more connections involving the insula and dorsal anterior cingulate showed remarkable resilience against accumulating stressors. These findings echo clinical studies showing increased connectivity between the insula and dorsal anterior cingulate in non-anxious individuals (Klumpp et al., 2012), which suggests that adaptive mechanisms involving these regions may be protective against stress. More research is thus needed to identify mechanisms through which resilience can be bolstered for individuals that are facing chronically high stress.

Results showing significant effects for anxiety but not depression are consistent with recent findings on the mental health impact of the COVID-19 pandemic (He et al., 2021; Zeytinoglu et al., 2021). There may be several explanations for these findings. First, the pandemic and economic adversity may have a more immediate effect on anxiety in the short-

term, as compared to depression, which may require a longer time to manifest. Unpredictable external situations such as the pandemic may provoke cognitive states of heightened threat that are more aligned with anxious schemas (Beck & Clark, 1988), and since our measures of symptoms were taken within the first year of the pandemic, we may have captured the rise in anxiety before a later rise in depression (that occurred as the stress became more chronic). Second, our results demonstrate that the group difference in the associations between economic adversity and symptoms was more pronounced for anxiety, suggesting that both groups may be equally more depressed as a function of economic impact of the pandemic. Third, these findings may indicate potential distinct circuitries between anxiety and depression (Z. Wang et al., 2021), but given that our study had only tested for network within selected regions, more research is needed to test the specific processes that are driving these differences.

Though our study is buoyed by several strengths, including prospective longitudinal data of underrepresented individuals and the use of computational methods, there are several limitations. First, COVID-19 adversity was measured at the same time as anxiety and depression; thus, determination of the direction of links between adversity and symptoms is not possible. Nevertheless, the positive associations between adversity and symptoms suggest an increase in psychological distress that was accompanied with increased adversity. Second, we were not able to collect data from all participants from FFCWS that we attempted to recruit, nor did all participants in the neuroimaging study participate at all 3 waves reported on here; however, sampling attrition is expected in longitudinal studies, and included sample did not differ demographically across included waves. Third, anxiety and depression were measured using the same scale at wave 1 and 2, but not wave 3 because the measures were shifted to be more developmentally appropriate, changing from well-validated adolescent to adult measures at age

20 (Y.-P. Wang & Gorenstein, 2013). Nonetheless, correlations between these measures were comparable, suggesting measurement correspondence across waves. Fourth, as with many other neuroimaging studies, the present analyses were conducted with the assumption of functional-structural correspondence across participants. The use of the same location for ROIs across individuals facilitates the estimation of similarities between people and detection of subgroup membership. Finally, we recognize the limitations of our modestly sized sample; however, this study examined within-person symptomatic change that provides critical information about underrepresented individuals during a notable historical period; within-person analyses can boost power and reliability (Curran & Bauer, 2011). Furthermore, the reliability in the data and methods we utilized for subgrouping and functional connectivity estimation was demonstrated by additional checks (i.e., split-half, 80% test), which reflected robustness of model estimation across split-half of the functional data and subsets of the sample (see Appendix 3.6.9).

3.5 Conclusion

In this 6-year prospective study, a data-driven adolescent neural network characterized by relatively more heterogeneity and density involving amygdala, subgenual cingulate, and striatal regions identified a subgroup of individuals with increasing anxiety symptoms that further increased during COVID-19. These findings demonstrate potential neural features indicating susceptibility to future stress, which may confer risk and resilience for mental health in young adults who are making the important transition to adulthood.

Table 3-1 Characteristics of neural-based subgroups

Measure		Subgroup A (*N*=80)		Subgroup B (*N*=94)		Statistical comparison	
		Mean	***SD***	**Mean**	***SD***	***t***	***p***
Age during fMRI scan (years)		15.78	.51	15.94	.53	-2.02	.045
Pubertal development		3.15	.59	3.35	.55	-2.29	.024
Anxiety (wave 1)[1]		17.27	11.33	17.14	11.17	.07	.941
Anxiety (wave 2)[1]		16.51	12.34	14.93	12.22	.72	.475
Anxiety (wave 3; COVID-19)[1]		12.62	13.01	8.67	10.34	1.80	.074
Depression (wave 1)[2]		15.52	10.08	15.43	9.96	.06	.951
Depression (wave 2)[2]		15.37	14.25	12.36	12.44	1.24	.220
Depression (wave 3; COVID-19)[2]		11.91	8.69	10.32	8.53	1.00	.320
COVID-19 economic adversity		2.22	1.67	1.97	1.74	.78	.439
Days since study commenced		168.90	99.10	140.66	84.28	1.75	.083
		N	**%**	**N**	**%**	**χ^2**	***p***
Sex	Female	43	53.75	51	54.26	0	1
	Male	37	46.25	43	45.74		
Ethnoracial identity[3]	Black	63	78.75	70	74.47	0.47	.789
	White	9	11.25	12	12.77		
	Hispanic/LatinX	5	6.25	7	7.45		
	Other/Multiracial	3	3.75	5	5.32		
	<$15,000	24	30	17	18.09	4.86	.182

Annual	$15,000-39,999	18	22.5	31	32.98
household	$40,000-69,999	18	22.5	22	23.40
income	>$70,000	19	23.75	24	25.53
(baseline at	Unknown	1	1.25	0	0
wave 1)[4]					

[1] Wave 1 and 2 anxiety was measured by Screen for Child Anxiety-Related Emotional Disorders. Anxiety during COVID-19 (wave 3) was measured by Beck Anxiety Inventory.

[2] Wave 1 and 2 depression was measured by Mood and Feelings Questionnaire. Depression during COVID-19 (wave 3) was measured using Beck Depression Inventory.

[3] Other/Multiracial group was collapsed with Hispanic/LatinX group for chi-square estimation

[4] Unknown group was collapsed with <$15,000 group for chi-square estimation

Table 3-2 Models with subgroups predicting change in anxiety and depressive symptoms

	Change in anxiety				**Change in depression**			
	Model 1		***Model 2***		***Model 1***		***Model 2***	
	β	***p***	***β***	***p***	***β***	***p***	***β***	***p***
Subgroup (A)	.138	.042	.194	.023	.089	.243	.120	.194
Initial symptoms	-.456	<.001	-.379	<.001	-.100	0.189	.072	.432
Male			.068	.538			.210	.080
Puberty			.008	.937			-.030	.798
Age			.086	.308			.018	.846
White			.160	.078			-.060	.539
Hispanic			-.011	.898			.098	.281
Other			-.118	.155			-.103	.252
Baseline income			.031	.726			.089	.351
Pandemic duration			.022	.795			-.093	.310
	$F(2,170)=24.56$, $p<.001$		$F(10,120)=3.82$, $p<.001$		$F(2,170)=1.46$, $p=.235$		$F(10,120)=1.31$, $p=.233$	

Table 3-3 Models examining subgroup differences in the associations between COVID-19 economic adversity and anxiety/depressive symptoms

	Anxiety during pandemic				**Depression during pandemic**			
	Model 1		***Model 2***		***Model 1***		***Model 2***	
	β	***p***	***β***	***p***	***β***	***p***	***β***	***p***
Subgroup (A)	.136	.106	.181	.024	.069	.428	.048	.473
COVID-19 adversity	.157	.154	.177	.105	.223	.053	.141	.127
Subgroup (A) x adversity	.307	.006	.237	.021	.196	.088	.069	.420
Initial symptoms			.399	<.001			.710	<.001
Gender			.016	.877			.068	.416
Puberty			.055	.574			-.023	.778
Age			.095	.237			.005	.935
White			.207	.015			-.009	.901
Hispanic			.036	.641			.136	.037
Other			-.048	.537			-.001	.989
Baseline income			.067	.435			.056	.434
Pandemic duration			-.008	.924			-.073	.272
	$F(3,114)=10.23$, $p<.001$		$F(12,104)=6.76$, $p<.001$		$F(3,114)=6.97$, $p<.001$		$F(12,104)=13.18$, $p<.001$	

Figure 3-1 Neural networks derived during an emotion processing task

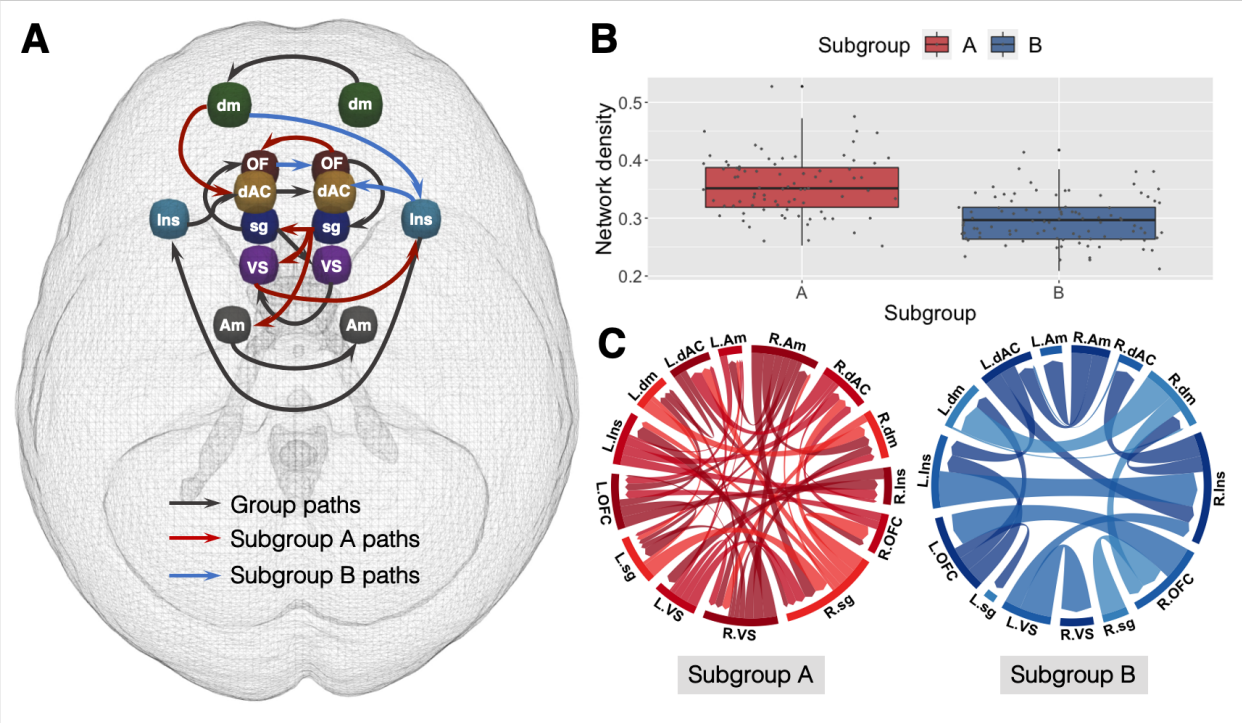

A: S-GIMME derived group-level, subgroup-level, and illustrative individual-level connections. Nodes shown are as follows: amygdala (Am; grey), dorsal anterior cingulate cortex (dAC; yellow), dorsomedial prefrontal cortex (dm; green), insula (Ins; blue), orbitofrontal cortex (OF; dark red), subgenual anterior cingulate cortex (sg; dark blue), and ventral striatum (VS; purple). Eighty (*N*=80) individuals were clustered into Subgroup A while ninety-four (*N*=94) individuals were clustered into Subgroup B. Group-level paths (connections present in at least 75% of the entire sample) are shown in black; subgroup paths (connections present in at least 50% of individuals in each subgroup) are shown in red (Subgroup A) and blue (Subgroup B). Thresholds were default parameters used in connectivity and subgrouping estimation based on large-scale simulations. All connections were positive on average, in exception for left dorsomedial prefrontal cortex (dm) to right insula (Ins) Subgroup B path (all average path estimates reported in Supplemental Table 3-8).

B: Network density (i.e., the proportion of actual contemporaneous connections from the number of possible connections in a network) for each individual in Subgroup A (red) and Subgroup B (blue). Network density was significantly greater in Subgroup A as compared to Subgroup B ($M_A = .36$, $SD_A = .05$; $M_B = .30$, $SD_B = .04$; $t(147.36) = 8.47$, $p < .001$).

C: Person-specific network maps (i.e., individual-level functional connectivity estimated for each individual in the sample) for one individual in Subgroup A (red) and another individual in Subgroup B (blue). L. and R. indicate left/right hemisphere. The Subgroup A individual had a more heterogeneous network, with more connections beyond group- and subgroup-level connections, while Subgroup B individual had a more homogenous network, with fewer connections overall but more similar connections to the group- and subgroup-level patterns. All edges shown were contemporaneous, and figures were created using customized R codes and *circlize* package (Gu et al., 2014).

Figure 3-2 Node centrality across each ROI plotted for each subgroup

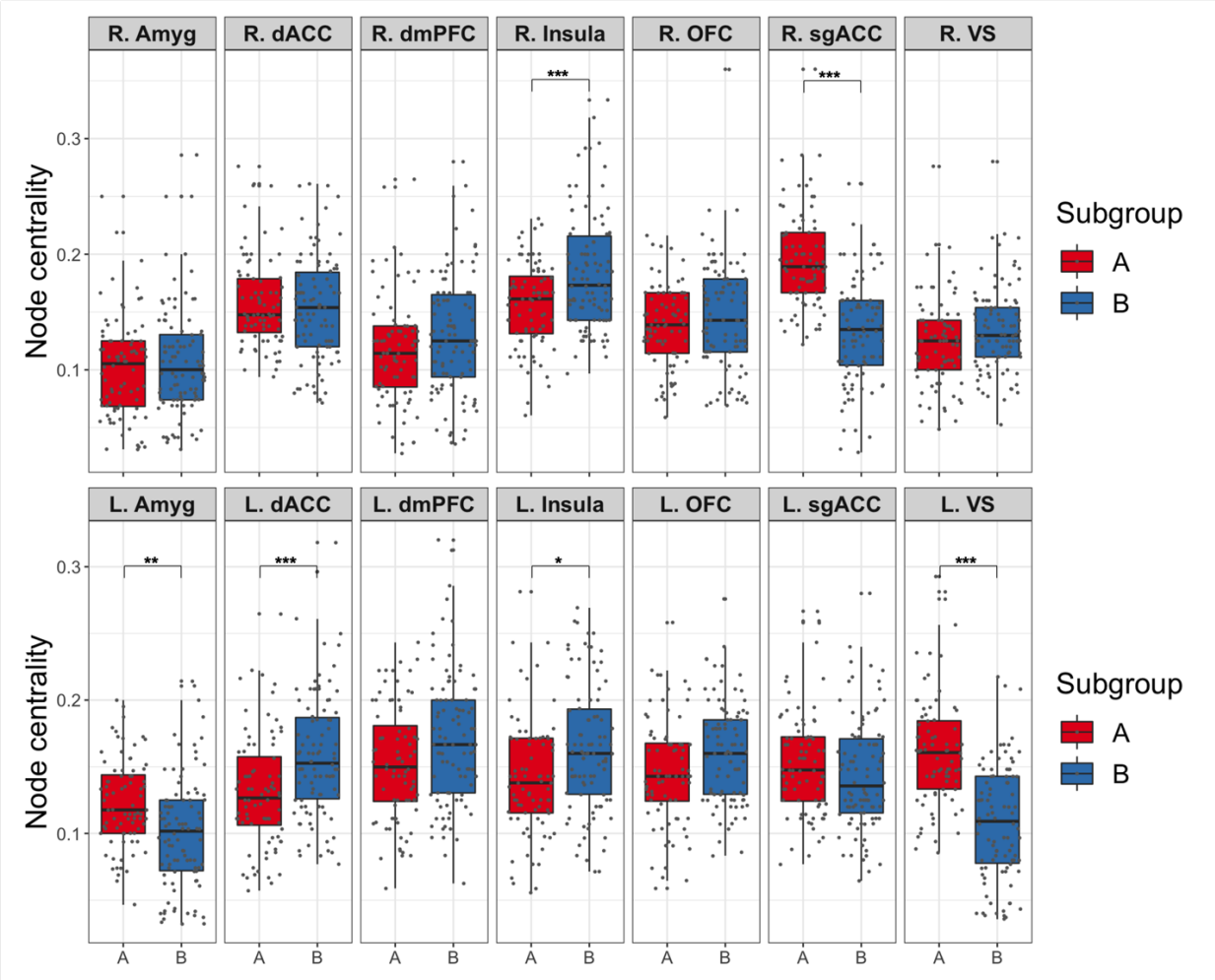

*** *Bonferroni-corrected p*<.001; ** *Bonferroni-corrected p*<.01; * *Bonferroni-corrected p*<.05

Left to right: amygdala (Amyg), dorsal anterior cingulate (dACC), dorsomedial prefrontal cortex (dmPFC), insula, orbitofrontal (OFC), subgenual anterior cingulate (sgACC), ventral striatum (VS). Hemispheres denoted by R. and L. Compared to Subgroup B (blue), Subgroup A (red) showed significantly greater node centrality, specifically in the left amygdala (L.Amyg), left striatum (L.VS), and right subgenual anterior cingulate (R.sgACC). In contrast, Subgroup B showed greater node centrality in the left dorsal anterior cingulate (L.dACC) and bilateral insula (R.Insula, L.Insula). P-values were Bonferroni-corrected for multiple comparisons (Supplemental Table 3-5).

Figure 3-3 Anxiety and depressive symptoms across three waves

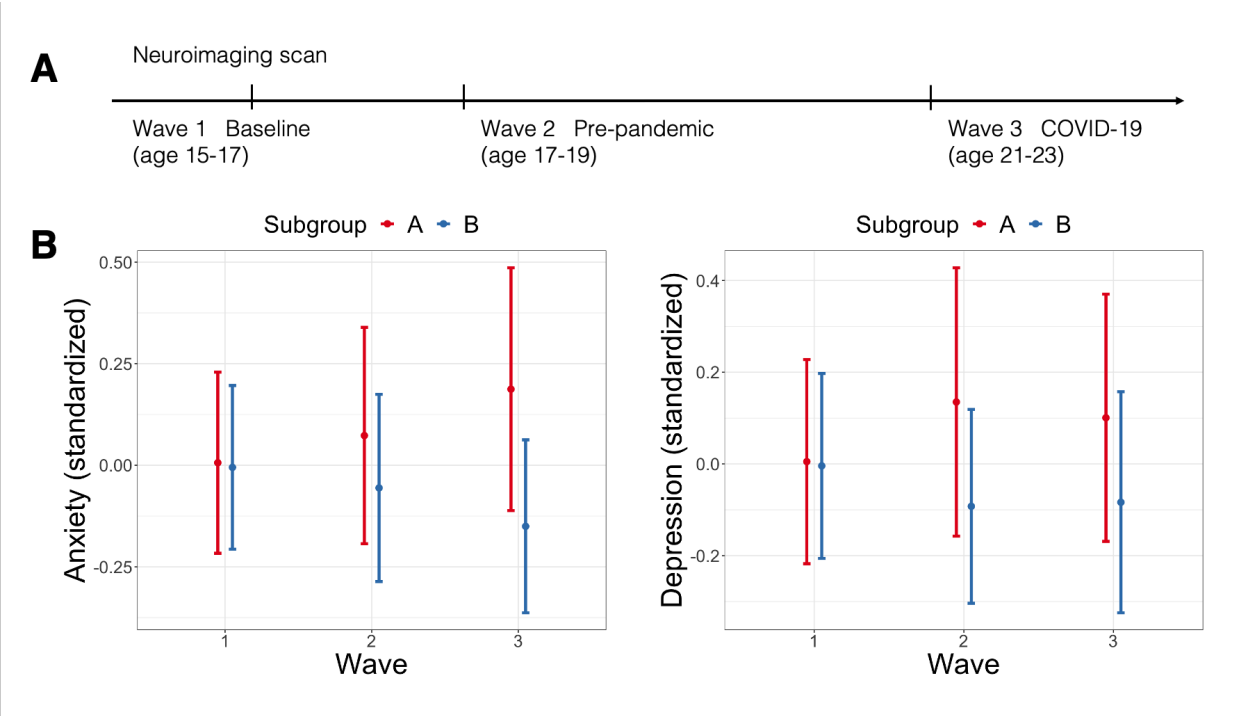

A: Illustration of timepoints and ages at each wave of data collection.

B: Anxiety and depression for each subgroup (A: more heterogeneous network with greater centrality in the amygdala, subgenual, and striatum; B: relatively sparser network with greater centrality in the insula and dorsal anterior cingulate) across each wave. Participants across subgroups did not differ in initial anxiety and depression at wave 1, but symptoms began to diverge at wave 2, which persisted through wave 3. For anxiety, this divergence was exacerbated by COVID-19 at wave 3, whereas subgroup difference for depression during COVID-19 remained similar to pre-pandemic difference. Each point represents mean value, and the bars indicate standard errors.

Figure 3-4 Differential effects of COVID-19 economic adversity on anxiety and depression across neural-based subgroups

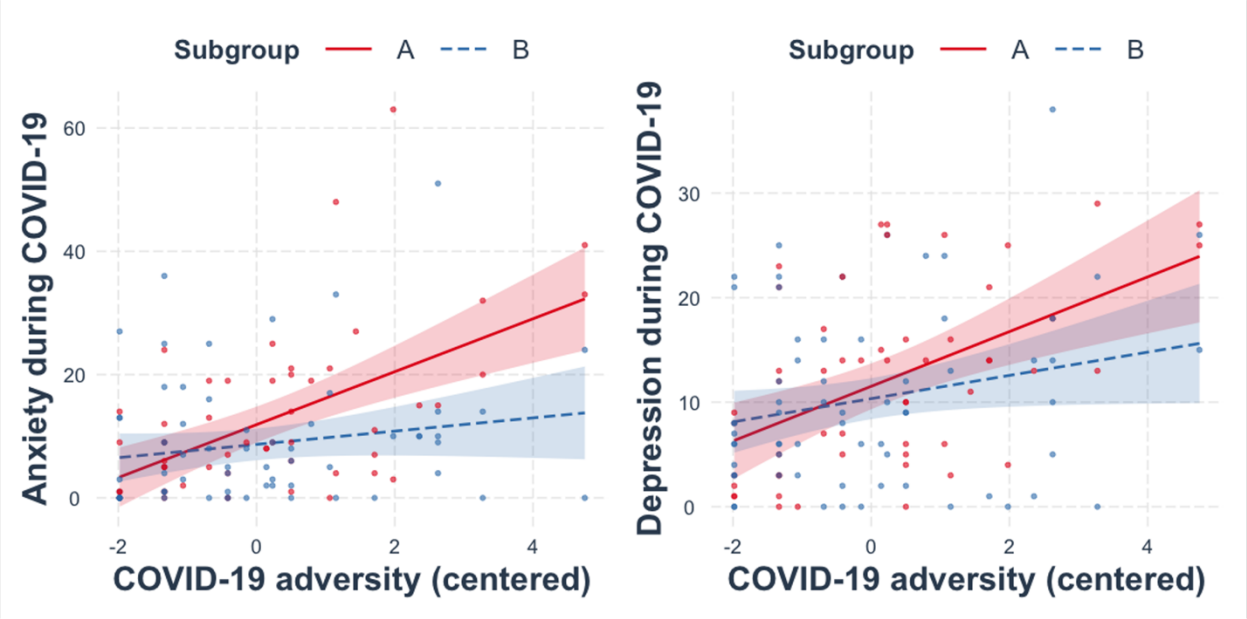

Symptoms during COVID-19 (wave 3) were elevated as a function of COVID-19 economic adversity, especially for subgroup A. Subgroup-adversity interaction was significant for anxiety (*b*=.275, 95% CI=[.470, .080], *p*=.006), but not depression (*b*=.175, 95% CI=[-.026, .376], *p*=.088). Subgroup A slope is depicted in red and Subgroup B slope in blue. COVID-19 adversity scores were mean-centered to aid interpretation.

LEFT: Subgroup-adversity interaction for anxiety symptoms. Subgroup A slope (*b*=.366, 95% CI=[.218, .514], *p*<.001); Subgroup B slope (*b*=.092, 95% CI=[-.035, .219], *p*=.154).

RIGHT: Subgroup-adversity interaction for depressive symptoms. Subgroup A slope (*b*=.304, 95% CI=[.151, .457], *p*<.001); Subgroup B slope (*b*=.129, 95% CI=[-.001, .260], *p*=.053).

3.6 Appendix

3.6.1 Exclusions for neuroimaging scan

Out of 237 youths who participated in the SAND study at baseline, 16 declined to participate in MRI scanning, 3 exceeded MRI table weight limit, 1 reported a medical restriction, 7 had braces or other metal in body, 1 had a risk of pregnancy, and 2 were excluded for diagnosis of Autism Spectrum Disorder. After these exclusions, of 207 youths who participated in MRI scanning, 5 did not finish scan, 6 had significant artifacts in structural anatomical MRI data, 5 was excluded for significant motion artifacts in the functional data, and 17 had accuracy below 70% on fMRI task. The final sample used for time-series extraction and subsequent analyses was 174. See Supplemental Figure 3-1 for illustration.

3.6.2 MRI data acquisition and preprocessing

MRIs were acquired using 3T GEDiscovery MR750 scanner with 8-channel head coil. Head padding and instructions limited movement. T1-weighted gradient echo images were first captured (TR=12ms, TE=5ms, TI=500ms, flip angle=15°, FOV=26cm, slice thickness=1.44mm, 256x192 matrix, 110 slices). fMRI T2*-weighted blood oxygenation level dependent (BOLD) images were then captured using reverse spiral sequence (Glover & Law, 2001) of 40 contiguous axial 3mm slices (TR=2000ms, TE=30ms, flip angle=90°, FOV=22cm, voxel size=3.44x3.44x3mm, ascending acquisition, parallel to AC-PC line). Anatomical images were skull-stripped (f=.25) using Brain Extraction Tool (BET) in FSL version 6.0 (Jenkinson et al., 2012) and segmented into gray matter, white matter, and cerebrospinal fluid using FSL FAST.

After large temporal spikes in the k-space functional data (>2 *SD*) were removed, field maps were corrected, and functional images were reconstructed using MATLAB. Noise from cardiac and respiratory motion were removed using RETROICOR and slice-timing correction using SPM8 (Wellcome Department of Cognitive Neurology, London, UK; http://www.fil.ion.ucl.ac.uk). Moreover, first ten volumes of functional data were removed to ensure the stability of signal intensity. Following these steps, the functional data were further preprocessed using FSL fMRI Expert Analysis Tool (FEAT). Functional images were skull-stripped and spatially smoothed using FSL FMRIB's Automated Segmentation Tool (Woolrich et al., 2001), and registered to subject-specific previously skull-stripped and segmented anatomical images. Motion correction was performed using MCFLIRT and spatial smoothing using a Gaussian kernel of FWHM 6.0mm was applied. Grand-mean intensity of the entire 4D dataset was normalized by a single multiplicative factor and FSL motion outliers were ran to extract framewise displacement motion parameters (Power et al., 2012). ICA-AROMA was used to remove motion-related artifacts in the data, nuisance signal derived from white matter and cerebrospinal fluid were regressed out, and data with signal below 0.01Hz were then high-pass filtered. These preprocessing steps were applied using detailed scripts (Beltz et al., 2019) that were also utilized in previous investigation (Goetschius, Hein, McLanahan, et al., 2020).

3.6.3 fMRI task paradigm

Neuroimaging data was collected using event-related emotion (faces) task (see Supplemental Figure 3-2 for visual representation of task paradigm design). Participants were shown a series of emotional faces (Tottenham et al., 2009) and indicated if they were viewing a female or male face. Gender (female, male), race (European American, African American), and emotion

(fearful, happy, sad, neutral, angry) of the actor were counterbalanced and randomly presented across 100 trials. Each trial consisted of a fixation cross (500ms) followed by 250ms of an emotion stimulus, then 1500ms of blank screen during which participants are expected to respond using button press. Functional data from each participant across all trials of emotion task (without any contrasting) were extracted for subsequent processing.

3.6.4 ROI selection and data extraction

The present investigation focused on seven bilateral regions that have been shown to be implicated in processes related to anxiety and depression: amygdala, anterior cingulate cortex, dorsomedial prefrontal, insula, orbitofrontal, subgenual cingulate, and ventral striatum. The amygdala has most commonly been linked to salience and fear processing (M. Davis, 1992; Janak & Tye, 2015), and amygdala function has been widely found to be implicated in anxiety and depression (Davidson, 2002; Rauch et al., 2003; Thomas et al., 2001; Whalen et al., 2002). Similarly, the anterior cingulate cortex has been found to be substantially involved in processes relating to affective and mood disorders (Drevets et al., 2008; Greicius et al., 2007; Margulies et al., 2007; Stevens et al., 2011). Most prominently, evidence from clinical trials demonstrates that deep brain stimulation of the subgenual cingulate can reduce depressive symptoms (Mayberg et al., 2005), suggesting the importance of this region in mood disorders. Both the dorsomedial and orbitofrontal cortex are believed to be implicated in emotion regulation and higher-order processing. Evidence has shown that disruption in brain function within these regions is important in affective disorders (Drevets, 2007; Eickhoff et al., 2016; Moses-Kolko et al., 2010). The insula is another important region for salience processing (Menon & Uddin, 2010; Uddin, 2015) and the bidirectional communication between insula and dorsal anterior cingulate cortex

has been linked to anxiety disorders in both clinical and non-clinical populations (Klumpp et al., 2012, 2013). Finally, the ventral striatum is central to reward processing and reward-based learning (Pagnoni et al., 2002; Schultz et al., 1992), which are important features of depressive and affective disorders (Robinson et al., 2012).

Consistent with our previous investigation (Goetschius, Hein, McLanahan, et al., 2020), ROI coordinates were extracted from NeuroSynth (Yarkoni et al., 2011) (https://neurosynth.org/analyses/) and preregistered (https://osf.io/tgj3s/). NeuroSynth is a meta-analytic tool that combines results from published neuroimaging articles using an automated parser. Findings from published articles are tagged with a specific term to produce a statistical inference map for activation maps associated with tagged keywords. Specific ROI names (i.e., "amygdala", "anterior cingulate", "dorsomedial", "insula", "orbitofrontal", "subgenual", "ventral striatum") were used as keywords to search for peak activity on the NeuroSynth website and corresponding association maps were then downloaded. Voxel coordinates from downloaded images were subsequently extracted using FSL and then utilized to create an ROI 8mm-diameter sphere using fslmaths. To ensure that there were no significant differences in functional data driven by sphere size, functional data were extracted from one ROI (i.e., left and right amygdala) using 6.5mm-radii sphere that were previously used in prior investigation (Goetschius, Hein, McLanahan, et al., 2020), and extracted data were compared with data extracted using 8mm-diameter sphere used in present investigation. There were no significant differences between the two, and results can be found in Supplemental Table 3-9.

3.6.5 Comparison network

To ensure that the results pertained to hypothesized ROIs we selected based on theory, functional connectivity network was estimated from a set of comparison ROIs (7 nodes from each hemisphere) related to visual, auditory, motor, and language processing that were hypothesized to be unrelated to susceptibility to anxiety and depression. Similar procedures were utilized to obtain ROI coordinates: specific terms were used as keywords in NeuroSynth (i.e., "audio", "fusiform", "language", "sensor", "supplementary motor area", "visual"); corresponding voxel coordinates were then extracted and then utilized to create an 8mm-diameter ROI sphere using fslmaths (see Supplemental Table 3-3 for MNI coordinates of ROIs in comparison network). These ROIs were then registered to subject-specific anatomical images and time-series data were extracted for S-GIMME processing. S-GIMME arrived at a 2-subgroup solution, but there were no statistically significant differences in anxiety or depression between the two subgroups in the comparison network adjusting for initial symptoms (anxiety: β=.026, p=.706; depression: β=.053, p=.490). Furthermore, no significant subgroup-adversity interaction was found in relation to anxiety (β=.054, p=.630) or depression (β=.148, p=.188) during the pandemic. Results from comparison network analyses are reported in Supplemental Table 3-4.

3.6.6 Measures for anxiety and depressive symptoms

Anxiety at wave 1 and wave 2 was measured using the 38-item Screen for Anxiety Related Disorders (Birmaher et al., 1997) (Cronbach's α = .92 at wave 1; Cronbach's α = .95 at wave 2). Anxiety at wave 3 was measured using the 21-item Beck Anxiety Inventory (Beck et al., 1988) (Cronbach's α = .95). Depression at wave 1 and wave 2 was measured using the Mood and Feelings Questionnaire (Angold et al., 1995) (34 items at wave 1, 30 items at wave 2)

(Cronbach's α = .91 at wave 1; Cronbach's α = .96 at wave 2). Depression at wave 3 was measured using the 20-item Beck Depression Inventory (Beck et al., 1996) (Cronbach's α = .91).

3.6.7 Covariates

Sex was parent-report at child aged 1 (0 = female, 1 = male). Pubertal development was measured at wave 1 by youth report on the Pubertal Development Scale (Petersen et al., 1988) that measured changes in child height, body hair, skin, facial hair and voice (males only), breast development and menarche (females only). Responses were coded on 4-point scale: 1 = no development to 4 = completed development; and score was a sum of all items endorsed. Ethnoracial identity was self-identified by youth at age 15 (wave 1): Black, non-Hispanic; white, non-Hispanic; Hispanic or LatinX; and Other. In cases where youth did not identify race/ethnicity (N = 8), parent report of race/ethnicity was utilized. Three dummy-coded variables were created to represent ethnoracial identity with Black as the reference variable. Annual household income was reported by primary caregiver at wave 1. If caregiver did not report annual household income, income was determined by other caregiver's report who are cohabitating with child. In the case that neither caregiver reported income, annual income was imputed by regression-based imputation. Framewise displacement was computed in FSL as a measure of in-scanner motion by averaging differences in rotation and translation parameter (Power et al., 2012). Early adverse experiences (i.e., violence exposure, social deprivation) were included as covariates to account for early childhood experiences that may relate to neurobiological development as found by previous investigation using this sample (Goetschius, Hein, McLanahan, et al., 2020; Goetschius, Hein, Mitchell, et al., 2020; Hein et al., 2020; Peckins et al., 2020). Both violence exposure and social deprivation were measured using

composite scores of exposure at ages 3, 5, and 9. Violence exposure was based on: (1) parent responses on child physical and emotional abuse questions in the Parent-Child Conflict Tactics Scale (Straus et al., 1998); (2) child exposure to neighborhood violence; (3) maternal report of intimate partner violence. Social deprivation was based on: (1) parent report on physical and emotional neglect on the Parent-Child Conflict Tactics Scale (Straus et al., 1998); (2) neighborhood cohesion. For both measures, scores were first standardized and z-scores across each dimension of early adversity (violence exposure; social deprivation) across each timepoint were summed. Cognitive abilities (i.e., reading comprehension, mathematical abilities) were measured at age 9 using the Passage Comprehension and Applied Problems subtests taken from then Woodcock Johnson test (Woodcock et al., 2001). Passage Comprehension involves matching symbolic pictures to word representation as well as reading a passage and identifying missing words in the passage. The items progressively become more difficult by increasing passage length and complexity of vocabulary, syntactic, and semantic cues. Applied Problems subtest involves solving math problems, which increases in difficulty with item level. Child's percentile rank was used for both subtests. Cohabitation status was self-reported at wave 3 (during the pandemic). Participants reported whether they are living with spouse, partner, or girlfriend/boyfriend during the pandemic (1 = yes, 0 = no). Similarly, parental status was self-reported at wave 3. Participants reported whether they are living with biological, step, adopted or foster children during the pandemic (1 = yes, 0 = no). All continuous variables were mean centered for further statistical analyses.

3.6.8 S-GIMME

S-GIMME begins with a null model. First, group-level connections are added for everyone if they significantly improve model fit for at least 75% of the sample as assessed by the Lagrange Multiplier tests (Gates et al., 2010). Individuals are then classified into subgroups using a Walktrap community detection algorithm (Gates et al., 2017), allowing for an unsupervised model search that reflects personalized network without averaging across individuals. Subgroup-level connections are then added for everyone in a given subgroup if they significantly improve models for at least 51% of individuals within each subgroup. Lastly, individual-level connections (i.e., connections unique for each person) are added until individual model well-fit the observed data. After person-specific networks were generated, contemporaneous edges were extracted for subsequent analyses, consistent with previous investigations (Goetschius, Hein, McLanahan, et al., 2020) as lagged connections are amenable to hemodynamic temporal dependencies (Gates et al., 2010; Smith, 2012). See Supplemental Figure 3-3 for an illustration of S-GIMME process.

3.6.9 Robustness checks for functional connectivity estimation

To establish reliability in the functional data, split-half reliability test was performed by applying S-GIMME separately to odd and even volumes of the data (Elliott et al., 2021; Pronk et al., 2022). Results show good correspondence between the resulting subgroups. Two subgroups emerged from analyses of both datasets with high correspondence in subgroup membership and connectivity (subgroups did not differ across runs: $\chi^2(1)= 0.299$, $p=.585$; $r=.83$, $p<.001$ for subgroup A path count; $r=.82$, $p<.001$ for subgroup B path count) (Supplemental Table 3-10). Anxiety and depressive symptoms for each subgroup did not differ between the datasets (Subgroup A anxiety: $t(90)=.360$, $p=.720$; depression: $t(92)=-.034$, $p=.973$; Subgroup B anxiety: $t(144)=-.331$, $p=.741$; depression: $t(142)=-.047$, $p=.963$). Furthermore, to establish robustness in

functional connectivity estimation for the sample, S-GIMME was applied to five randomly drawn subsamples (80%, sampled with replacement; *N*=139). Consistent with original results, two subgroups were derived with good correspondence in subgroup membership and connectivity between all five subsamples and the full sample (Supplemental Table 3-11; Supplemental Figure 3-5).

3.6.10 Robustness checks in predictive models

Several robustness checks were performed to all models. First, models were re-examined without inclusion of subjects that had standardized network model psi values of above 1 (*N*=18 for subgroup A; *N*=20 for subgroup B), which would reflect greater than 100% unexplained variation for an ROI in the model – an impossible value that could reflect model overfitting (Lütkepohl, 2005). Next, model residuals were examined, and any influential outliers identified using Cook's distance were excluded in subsequent models for sensitivity checks. Finally, sensitivity analyses were performed to account for covariates that may explain variance in the outcome (i.e., age, sex, pubertal development, ethnoracial identity, annual household income, days since study commenced) and additional covariates (i.e., scanner framewise displacement, violence exposure, social deprivation, reading comprehension, mathematical abilities, residential status with partner during pandemic, residential status with child during pandemic).

Supplemental Table 3-1. Full and included sample comparisons

	Full sample (*N*=237)	**Wave 1 (baseline) sample (*N*=174)**
Age (years)	*M* = 15.87 | *SD* = 0.54	*M* = 15.86 | *SD* = 0.53
Sex	F = 124 (52.3%) | M = 113 (47.7%)	F = 94 (54.0%) | M = 80 (46.0%)
Ethnoracial identity	Black = 181 (76.4%)	Black = 133 (76.4%)
	White = 32 (13.5%)	White = 21 (12.1%)
	Hispanic/LatinX = 13 (5.5%)	Hispanic/LatinX = 12 (6.9%)
	Other/Multiracial = 11 (4.6%)	Other/Multiracial = 8 (4.6%)
Annual Income	<$15,000 = 57 (24.1%)	<$15,000 = 41 (23.6%)
	$15,000-39,999 = 70 (29.5%)	$15,000-39,999 = 49 (28.2%)
	$40,000-69,999 = 58 (24.5%)	$40,000-69,999 = 40 (23.0%)
	>$70,000 = 51 (21.5%)	>$70,000 = 43 (24.7%)
	Missing/Not reported = 1 (0.4%)	Missing/Not reported = 1 (0.6%)

	Wave 2 sample (*N*=128)	**Wave 3 (COVID-19) (*N*=119)**
Age (years)	*M* = 15.85 | *SD* = 0.54	*M* = 15.87 | *SD* = 0.54
Sex	F = 77 (60.2%) | M = 51 (39.8%)	F = 74 (62.2%) | M = 45 (37.8%)
Ethnoracial identity	Black = 92 (71.9%)	Black = 83 (69.7%)
	White = 18 (14.1%)	White = 19 (16.0%)
	Hispanic/LatinX = 11 (8.6%)	Hispanic/LatinX = 10 (8.4%)
	Other/Multiracial = 7 (5.5%)	Other/Multiracial = 7 (5.9%)
Annual Income	<$15,000 = 25 (19.5%)	<$15,000 = 27 (22.7%)
	$15,000-39,999 = 31 (24.2%)	$15,000-39,999 = 28 (23.5%)
	$40,000-69,999 = 34 (26.6%)	$40,000-69,999 = 26 (21.8%)
	>$70,000 = 38 (29.7%)	>$70,000 = 37 (31.1%)
	Missing/Not reported = 0 (0%)	Missing/Not reported = 1 (0.8%)

[a] Samples did not differ in age: $F(3,654)=.038$, $p=.99$; sex: $\chi^2(3)=4.323$, $p=.229$; race: $\chi^2(9)=3.419$, $p=.943$; annual income: $F(3,651)=1.194$, $p=.311$.

Supplemental Table 3-2. MNI coordinates of individual Regions of Interest (ROI)

Hemisphere	***Regions of Interest (ROI)***	***MNI coordinates***
Left	Amygdala	-18, -6, -20
	Dorsal anterior cingulate cortex	-10, 26, 26
	Dorsomedial prefrontal cortex	-16, 46, 36
	Insula	-34, 22, 0
	Orbitofrontal prefrontal cortex	-10, 38, -18
	Subgenual cingulate cortex	-10, 22, -16
	Ventral striatum	-10, 10, -6
Right	Amygdala	18, -6, -20
	Dorsal anterior cingulate cortex	10, 26, 26
	Dorsomedial prefrontal cortex	16, 46, 36
	Insula	34, 22, 0
	Orbitofrontal prefrontal cortex	10, 38, -18

	Subgenual cingulate cortex	10, 22, -16
	Ventral striatum	10, 10, -6

Supplemental Table 3-3. MNI coordinates of ROIs in comparison network

Hemisphere	***NeuroSynth key terms***	***MNI coordinates***
Left	Audio	-50, -18, 6
	Fusiform	-42, -50, -20
	Language	-56, -42, 4
	Language	-46, 16, 22
	Sensorimotor	-36, -20, 54
	Supplementary motor area	-5, -6, 60
	Visual	-46, 70, 2
Right	Audio	50, -18, 6
	Fusiform	42, -50, -20
	Language	56, -42, 4
	Language	46, 16, 22
	Sensorimotor	36, -20, 54
	Supplementary motor area	5, -6, 60
	Visual	46, 70, 2

Supplemental Table 3-4. Results from predictive models using comparison network

	Change in anxiety		Change in depression	
	β	*p*	*β*	*p*
Subgroup	0.026	0.706	0.053	0.490
Initial symptoms	-0.451	<.001	-0.091	0.236
	$F(2,170)=22.02$, $p<.001$		$F(2,170)=1.01$, $p=.366$	

	Anxiety at wave 3		Depression at wave 3	
	β	*p*	*β*	*p*
Subgroup	-0.102	0.243	-0.101	0.246
COVID-19 adversity	0.339	0.003	0.268	0.018
Subgroup x COVID-19 adversity	0.054	0.630	0.148	0.188
	$F(3,114)=6.52$, $p<.001$		$F(3,114)=6.66$, $p<.001$	

Supplemental Table 3-5. Node centrality for each subgroup

Hemisphere	***Node***	***Subgroup A***		***Subgroup B***		***t-test results[1]***
		Mean	*SD*	*Mean*	*SD*	
Left	**Amygdala**	**.123**	**.033**	**.101**	**.042**	$t(170.72)= 3.93$, $p_{adjust}=.002$
	Dorsal anterior cingulate cortex	**.131**	**.043**	**.159**	**.047**	$t(171.32)= -4.09$, $p_{adjust}<.001$

	Dorsomedial prefrontal cortex	.152	.043	.172	.051	$t(172)= -2.75$, $p_{\text{-adjust}}= .092$
	Insula	**.141**	**.044**	**.164**	**.048**	**$t(171.14)= -3.28$, $p_{\text{-adjust}}= .017$**
	Orbitofrontal prefrontal cortex	.147	.041	.161	.038	$t(163.08)= -2.33$, $p_{\text{-adjust}}= .298$
	Subgenual cingulate cortex	.153	.040	.144	.042	$t(170)= 1.43$, $p_{\text{-adjust}}= 1.00$
	Ventral striatum	**.162**	**.043**	**.108**	**.043**	**$t(167.23)= 8.17$, $p_{\text{-adjust}}<.001$**
Right	Amygdala	.102	.044	.107	.048	$t(171.16)= -.80$, $p_{\text{-adjust}}= 1.00$
	Dorsal anterior cingulate cortex	.158	.040	.154	.045	$t(171.89)= .74$, $p_{\text{-adjust}}= 1.00$
	Dorsomedial prefrontal cortex	.117	.047	.130	.053	$t(171.5)= -1.66$, $p_{\text{-adjust}}= 1.00$
	Insula	**.156**	**.037**	**.184**	**.051**	**$t(167.95)= -4.28$, $p_{\text{-adjust}}<.001$**
	Orbitofrontal prefrontal cortex	.138	.035	.147	.047	$t(168.57)= -1.46$, $p_{\text{-adjust}}= 1.00$
	Subgenual cingulate cortex	**.195**	**.043**	**.134**	**.047**	**$t(171.19)= 8.92$, $p_{\text{-adjust}}<.001$**
	Ventral striatum	.124	.040	.135	.037	$t(163.33)= -1.80$, $p_{\text{-adjust}}= 1.00$

[1] p-values were Bonferroni-corrected ($p_{\text{-adjust}}$) for multiple 14 model comparisons

Supplemental Table 3-6. Models predicting anxiety and depressive symptoms, adjusted for covariates

Model: Change in symptoms (slope) ~ subgroup + initial symptoms (intercept) + all covariates

	Change in anxiety		Change in depression	
	β	p	β	p
Subgroup (A)	**0.257**	**0.011**	0.145	0.182
Initial symptoms	-0.315	0.002	0.119	0.246
Male	0.099	0.427	0.248	0.067
Puberty	0.076	0.525	0.024	0.853
Age	0.127	0.172	0.010	0.919
White	0.211	0.037	-0.019	0.860
Hispanic	0.081	0.391	0.151	0.142
Other	-0.114	0.211	-0.102	0.305
Baseline income	0.012	0.902	0.109	0.318
Pandemic duration	0.012	0.899	-0.077	0.461
Motion	-0.082	0.394	0.002	0.987
Violence exposure	0.004	0.968	0.032	0.784
Social deprivation	0.057	0.598	-0.068	0.563
Reading comprehension	0.171	0.146	0.158	0.218

Math abilities	-0.045	0.707	0.074	0.574
Living w/ partner	0.142	0.124	0.131	0.198
Living w/ child	0.194	0.040	0.139	0.179
	$F(17,92)=2.68$, $p=.001$		$F(17,92)=1.35$, $p=.178$	

Model: Symptoms during pandemic ~ subgroup * COVID-19 economic adversity + initial level of symptom + all covariates

	Anxiety at wave 3		Depression at wave 3	
	β	p	β	p
Subgroup (A)	0.238	0.007	0.037	0.624
COVID-19 adversity	0.133	0.263	0.030	0.771
Subgroup x COVID-19 adversity	**0.259**	**0.031**	0.145	0.160
Initial symptoms	0.406	0.000	0.735	0.000
Male	0.024	0.827	0.084	0.362
Puberty	0.039	0.705	-0.051	0.569
Age	0.109	0.184	-0.030	0.674
White	0.247	0.005	0.007	0.921
Hispanic	0.096	0.241	0.139	0.052
Other	-0.041	0.604	-0.003	0.966
Baseline income	0.021	0.816	0.041	0.602
Pandemic duration	0.030	0.726	-0.011	0.881
Motion	-0.146	0.094	-0.036	0.628
Violence exposure	-0.087	0.374	-0.025	0.763
Social deprivation	0.093	0.324	-0.036	0.660
Reading comprehension	0.147	0.157	0.098	0.280
Math abilities	-0.075	0.480	0.028	0.762
Living w/ partner	0.113	0.164	0.058	0.407
Living w/ child	0.105	0.228	0.052	0.486
	$F(19,89)=4.90$, $p<.001$		$F(19,88)=8.20$, $p<.001$	

Supplemental Table 3-7. Models with individual node centrality predicting change in symptoms, adjusting for initial levels

Models / Predictor (tested in separate models)	Change in anxiety		Change in depression	
	β	$p_{\text{-adjust}}$	β	$p_{\text{-adjust}}$
L. Amygdala	.042	1.00	.042	1.00
R. Amygdala	-.049	1.00	-.188	.183
L. Dorsal anterior cingulate	.058	1.00	.043	1.00
R. Dorsal anterior cingulate	-.030	1.00	.022	1.00
L. Dorsomedial prefrontal	.059	1.00	.084	1.00
R. Dorsomedial prefrontal	-.018	1.00	.072	1.00
L. Insula	-.022	1.00	.047	1.00
R. Insula	-.106	1.00	-.205	.096
L. Orbitofrontal	-.018	1.00	.105	1.00
R. Orbitofrontal	-.016	1.00	.004	1.00

L. Subgenual cingulate	-.055	1.00	-.151	.666
R. Subgenual cingulate	.160	.263	.124	1.00
L. Ventral striatum	.085	1.00	.026	1.00
R. Ventral striatum	-.164	.221	-.063	1.00

Supplemental Table 3-8. Average path estimates for group- and subgroup-level connections

Path type	***Connection*[1]**	***N***	***Mean***	***SD***	***Max***	***Min***
Group	L. Amyg – R. Amyg	174	.412	.204	1.01	-.297
	L. dACC – R. dACC	174	.446	.267	1.03	-.604
	R. dmPFC – L. dmPFC	174	.414	.252	1.07	-.238
	R. Ins – L. Ins	174	.414	.245	.852	-.438
	L. Ins – L. dACC	174	.215	.213	.993	-.393
	R. OFC – R. sgACC	174	.394	.244	1.19	-1.03
	L. sgACC – L. OFC	174	.365	.257	1.36	-.546
	L. sgACC – R. VS	174	.253	.212	.897	-.557
	R. VS – L. VS	174	.478	.197	.891	-.376
Subgroup (A)	L. dmPFC – L. dACC	80	.223	.288	1.26	-.276
	R. OFC – L. OFC	80	.196	.317	.673	-1.16
	R. sgACC – L. Amyg	80	.103	.210	.531	-.494
	R. sgACC – L. sgACC	80	.355	.305	1.06	-.649
	R. sgACC – L.VS	80	.222	.201	.712	-.394
	L. VS – R. Ins	80	.182	.223	.747	-.313
Subgroup (B)	L. dmPFC – R. Ins	94	-.151	.199	.464	-.732
	R. Ins – R. dACC	94	.180	.186	.536	-.306
	L. OFC – R. OFC	94	.367	.200	.857	-.044

[1] L. and R. indicate left/right hemisphere; Amyg = amygdala; dACC = dorsal anterior cingulate; dmPFC = dorsomedial prefrontal; Ins = insula; OFC = orbitofrontal; sgACC = subgenual cingulate; VS = ventral striatum

Supplemental Table 3-9. Comparison between extracted data using 4mm-radii and 6.5mm-radii node spheres

Region	***Mean* (*SD*) (8mm-diameter)**	***Mean* (*SD*) (6.5mm-radii)**	***t*-test results**
Left Amygdala	6785.061 (781.231)	6749.546 (704.276)	$t(346)=.445$, $p=.657$
Right Amygdala	7294.925 (885.737)	7205.825 (783.190)	$t(346)=.995$, $p=.320$

Supplemental Table 3-10. Split-half reliability test results

GIMME subgroups	**Count (%)**	**Path (non-lagged) count *M* (*SD*)**
Subgroup A	Odd = 73 (41.95%) Even = 67 (38.51%)	Odd = 29.00 (5.68) Even = 24.75 (6.44)
Subgroup B	Odd = 101 (58.05%) Even = 107 (61.49%)	Odd = 28.70 (3.82) Even = 24.56 (4.40)

	Subgroup A	Subgroup B
Odd	73	101
Even	67	107

$\chi^2(1)= 0.299$, $p = .585$

Supplemental Table 3-11. Results from 80% randomly drawn subsample test

Sample	**Subgroup membership [1] Count (%)**	**Path (non-lagged) [1] *M* (*SD*)**	**Anxiety comparison with full sample**
Full sample (*N*=174)	A = 80 (45.98%) B = 94 (54.02%)	A = 32.4 (4.69) B = 27.0 (3.62)	N/A
Subsample 1 (*N* =139)	A = 60 (43.17%) B = 79 (56.83%)	A = 32.0 (4.95) B = 27.4 (3.75)	*t*(89)=-.400, *p*=.690 *t*(119)=.090, *p*=.929
Subsample 2 (*N* =139)	A = 69 (49.64%) B = 70 (50.36%)	A = 33.3 (4.57) B = 26.9 (3.64)	*t*(98)=-.027, *p*=.979 *t*(110)=.004, *p*=.997
Subsample 3 (*N* =139)	A = 76 (54.68%) B = 63 (45.32%)	A = 32.8 (5.06) B = 27.1 (3.51)	*t*(102)=-.367, *p*=.714 *t*(110)=.213, *p*=.832
Subsample 4 (*N* =139)	A = 55 (39.57%) B = 84 (60.43%)	A = 35.5 (4.50) B = 26.8 (3.39)	*t*(88)=.181, *p*=.857 *t*(121)=.551, *p*=.583
Subsample 5 (*N* =139)	A = 65 (46.76%) B = 74 (53.24%)	A = 34.0 (4.40) B = 27.1 (3.58)	*t*(95)=.146, *p*=.884 *t*(117)=.046, *p*=.963

Chi-square test results comparing subgroup membership of original sample and subsamples

	Subgroup A	Subgroup B
Subgroup membership in original sample	62	77
Subgroup membership in Subsample 1	60	79

$\chi^2(1)= .015$, $p = .904$

Subgroup membership in original sample	69	70
Subgroup membership in Subsample 2	69	70

$\chi^2(1)= 1$, $p = 1$

Subgroup membership in original sample	67	72
Subgroup membership in Subsample 3	76	63

$\chi^2(1)= .922$, $p = .337$

Subgroup membership in original sample	63	76
Subgroup membership in Subsample 4	55	84

$\chi^2(1)= .722$, $p = .396$

Subgroup membership in original sample	65	74
Subgroup membership in Subsample 5	65	74

$\chi^2(1)= 1$, $p = 1$

Supplemental Figure 3-1. Exclusionary criteria for neuroimaging data

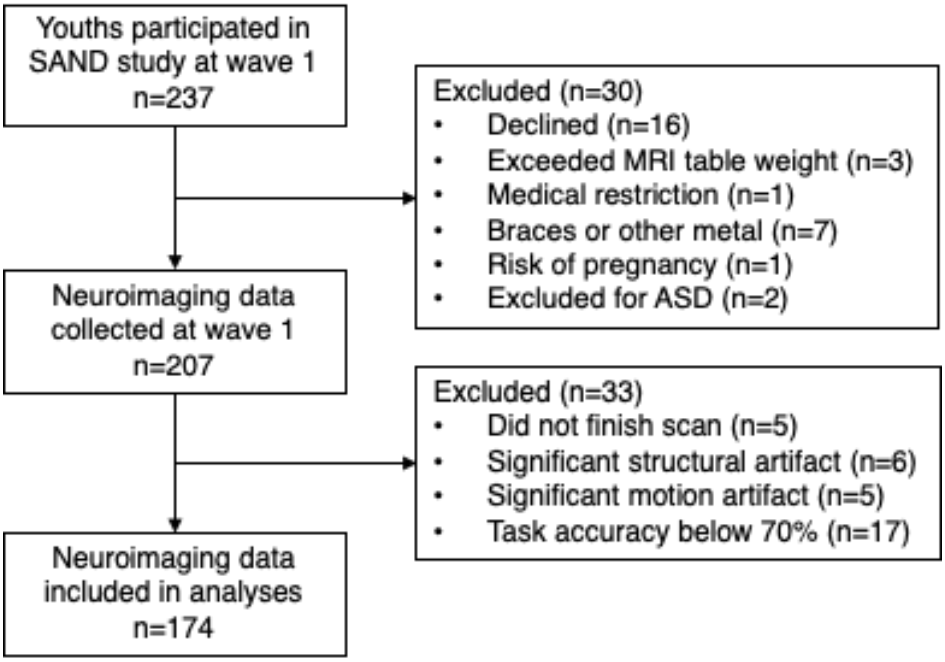

Supplemental Figure 3-2. fMRI task paradigm

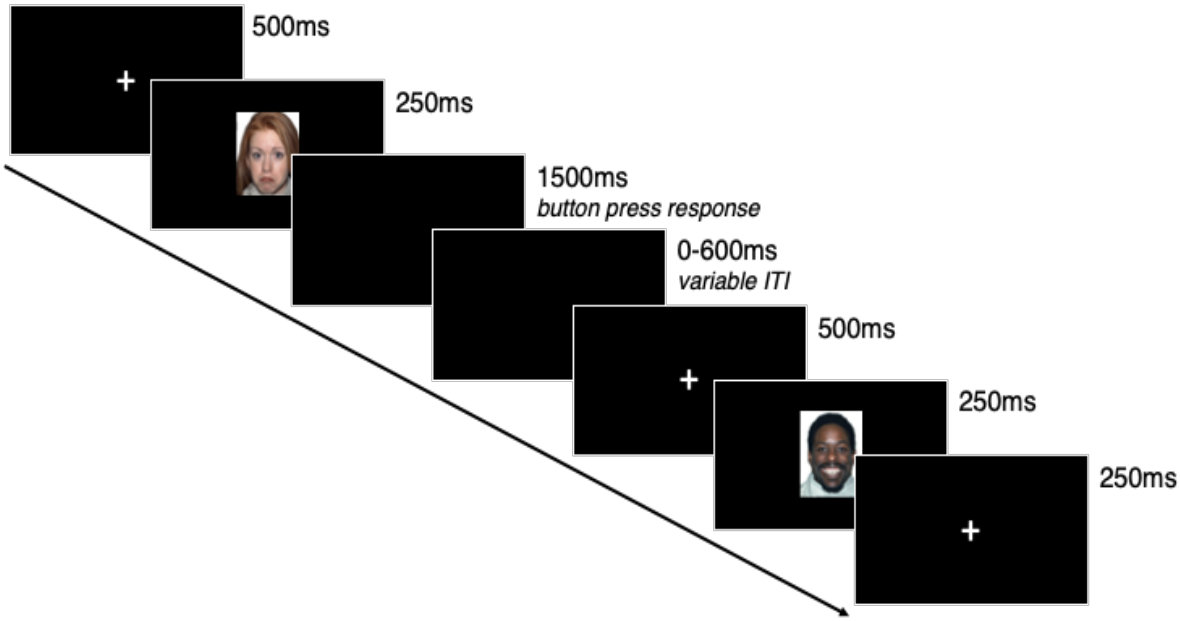

Supplemental Figure 3-3. S-GIMME flowchart

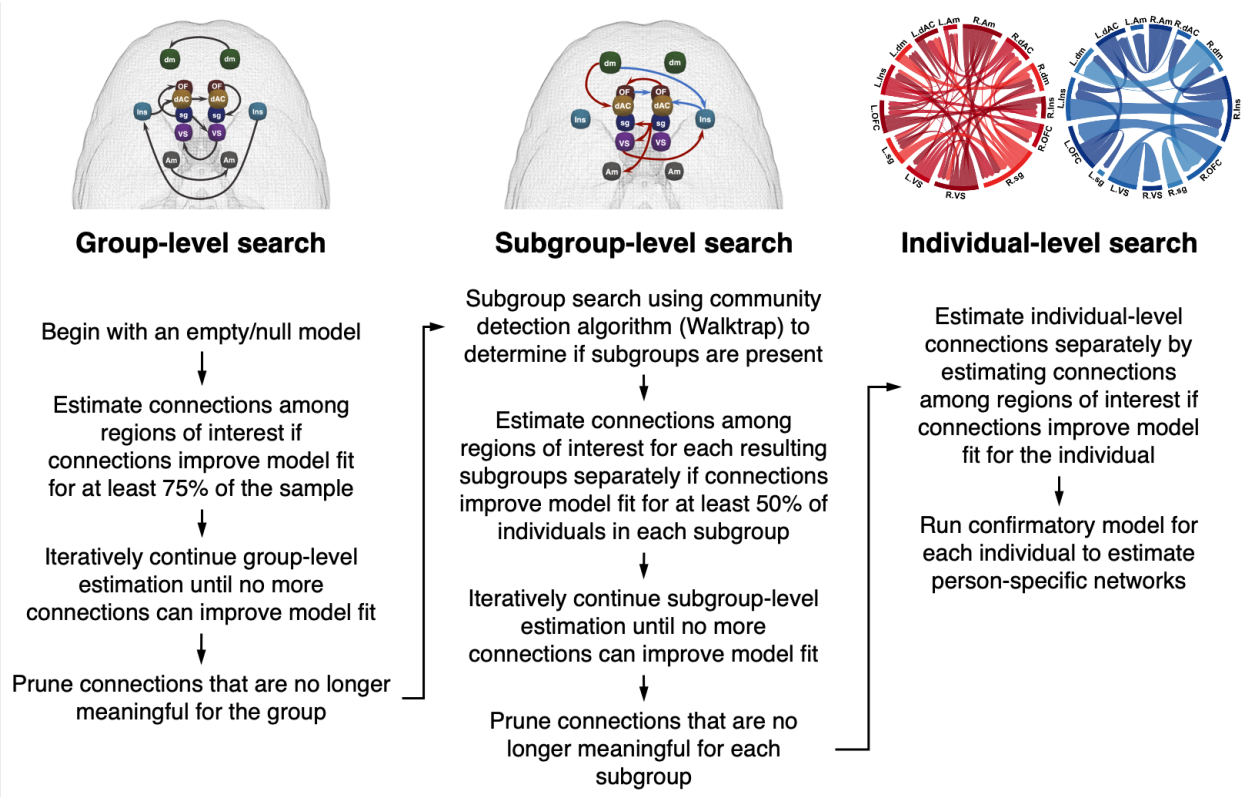

Supplemental Figure 3-4. GIMME results based on 5 randomly drawn 80% subsamples

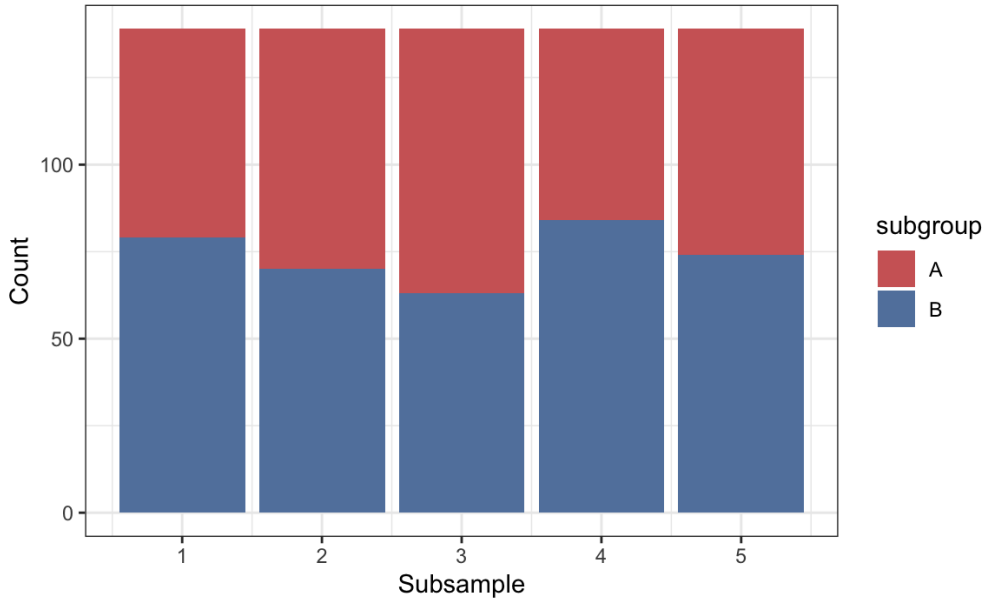

Supplemental Figure 3-5. Anxiety and depression for each subgroup, stratified by sex

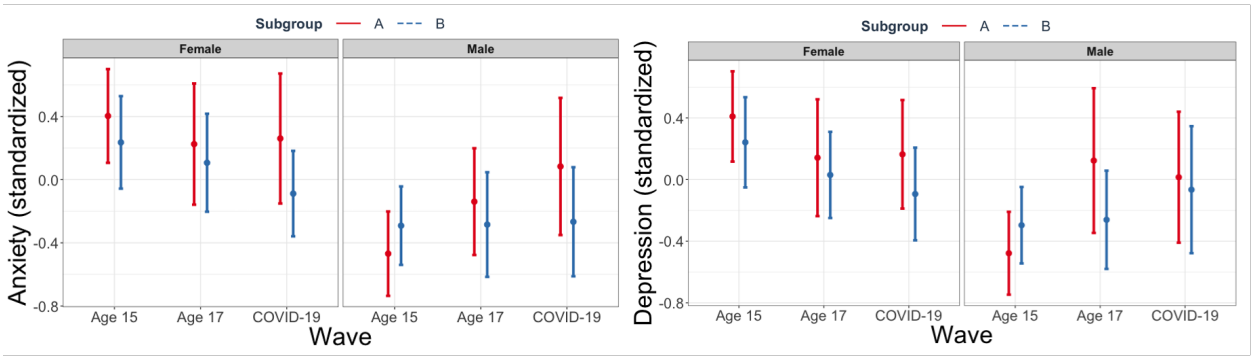

Anxiety and depression for each subgroup stratified by sex. Sex differences in both anxiety and depression were most pronounced at adolescence (age 15) where females were reporting greater symptoms, especially those with denser network profiles. Observed sex differences were markedly diminished during COVID-19 for both subgroups. Both males and females with Subgroup A denser network profiles (in red) showed greater anxiety symptoms during COVID-19 compared to Subgroup B (in blue). Each point represents mean value, and the bars indicate standard errors.

Chapter 4

Latent Profiles of Childhood Adversity Identify Distinct Patterns of Mental Health Outcomes and Emotion-Related Neural Network Connectivity in Adolescence

4.1 Introduction

Adverse childhood experiences are prevalent risk factors for health across the lifespan and are associated with nearly 30% of all psychiatric disorders (Green et al., 2010; Hughes et al., 2017; McLaughlin et al., 2012). Childhood adversity have been linked with differences in brain function during emotion processing in human and animal research (Anda et al., 2006; Gee, 2021; Goetschius, Hein, McLanahan, et al., 2020; Hardi, Goetschius, McLoyd, et al., 2023; Hosseini-Kamkar et al., 2023; McLaughlin et al., 2019), thus providing insight into how adversity could disrupt critical domains of development that contribute to psychopathology later in life.

Adverse experiences, ranging from maltreatment and family violence to household instability and community violence, often co-occur and interact (Dong et al., 2004; Felitti et al., 1998; Finkelhor et al., 2015; Hughes et al., 2017; McLaughlin et al., 2012). Nevertheless, exposure to one adversity does not necessarily indicate the presence of another; variations in additional adverse experiences exist within groups exposed to specific adversity (Dong et al., 2004; Hughes et al., 2017), underscoring the broad heterogeneity of adverse environments. However, most studies examining neural correlates of adversity focused on singular exposures or the cumulative indices of multiple adversities. While the additive effect of multiple adversities on mental health is widely recognized (Felitti et al., 1998; Hughes et al., 2017; Rutter et al., 1978), cumulative approaches assume that each adverse experience operates in a similar manner

and holds equal importance for each individual (Bergman & Magnusson, 1997; Briggs et al., 2021; Lacey & Minnis, 2020; Laursen & Hoff, 2006). These limitations undercut the identification of precise adversity-linked neural correlates that can improve interventions.

Thus, more work is needed to parse heterogeneity within individuals' multifaceted adverse environments. To improve precision in clinical interventions, a growing body of work has sought to identify latent subpopulations that share similar characteristics (Feczko et al., 2019; Mori et al., 2020; Sterba & Bauer, 2010). While these person-oriented approaches have largely been applied to classify subgroups of individuals with complex health outcomes (Beijers et al., 2019; Hack et al., 2023; Karalunas & Nigg, 2020; Mattoni et al., 2021; Xiao et al., 2024), they have not focused on explaining variations in adolescent mental health and brain function simultaneously, specifically in population-based samples with rich contextual information about adverse experiences across multiple developmental years. Additionally, person-centered clustering methods, which identify data-driven hidden classes or subtypes of individuals, can be combined with person-specific network neuroscience methods that allow for estimation of neural patterns across the group, subgroups, and individual-levels (Gates & Molenaar, 2012; Henry et al., 2019). Thus, increasing the ability to reveal commonalities and differences within the population and capturing more granularity in modeling individual processes.

Work in clinical neuroscience postulates that disrupted communication within brain networks such as the default mode network (DMN) (Raichle, 2015), salience network (SN) (Seeley, 2019), and fronto-parietal network (FPN) (Zanto & Gazzaley, 2013) underlies vulnerabilities to psychiatric disorders (Menon, 2011). Adversities such as threat, neglect, and unpredictability have been found to be differentially associated with these neural networks during rest (Chahal et al., 2022; Goetschius, Hein, McLanahan, et al., 2020); however, the extent

to which they differ among distinct broad-based adverse environments during active emotion processing is unknown. Neuroimaging data collected during behavioral tasks may characterize neural patterns that are more representative of processes implicated in psychopathology, thus can improve the prediction of clinical traits (Finn, 2021; Ooi et al., 2022).

This study aimed to characterize heterogeneity in mental health and network function during emotion processing among subgroups of youth with different profiles of multi-domain childhood adversity. We used longitudinal data from a population-based birth-cohort sample that includes a substantial proportion of marginalized individuals who are at a greater risk for adversity (Sacks & Murphey, 2018) and are underrepresented in biomedical research (Falk et al., 2013). Individuals were first clustered based on reported adversity across multiple contexts experienced during childhood (0-9 years) and the resulting adversity profiles were then examined to predict mental health in adolescence (age 15). This clustering method was then combined with person-specific connectivity approach to allow for estimation of profile-specific emotion-linked network patterns in a neuroimaging subsample. We hypothesize that this data-driven approach would identify distinct patterns of mental health and functional network connectivity in youth based on their exposures to adverse childhood experiences across multiple contexts.

4.2 Methods

4.2.1 Setting and Participants

Participants were from the Future Families and Child Wellbeing study, a birth cohort population-based sample of children born in large U.S. cities (population over 200,000) between 1998 and 2000, with oversampling (3:1) of non-marital births (Reichman et al., 2001). Data collected at ages 1, 3, 5, 9, and 15, capturing information about the child environment from birth

to age 9, from 4210 individuals were included in the present study (Supplemental Table 4-1). Participants who did not reside with the mother at least half of the time at any point (*n*=290) and those with adversity data at fewer than two timepoints were excluded from analyses (*n*=398). There were no differences between the samples (Supplemental Table 4-1). When the children were 15, a cohort of families participated in the Study of Adolescent Neural Development at the University of Michigan, Ann Arbor, where neuroimaging data were collected. After exclusions for ineligibility for scanning and quality control (*n*=63), neuroimaging data from 167 individuals were included in the present study (Supplemental Table 4-2; Supplemental Figure 4-1).

4.2.2 Childhood adversity measures

Ten indicators measured in the first 9 years of child life were selected to represent adverse experiences within and outside of the home that could contribute to youth mental health problems: childhood maltreatment (emotional abuse, physical abuse, neglect; measured by Parent-Child Conflict Tactics Scale) (Straus et al., 1998), intimate partner violence (measured by relationship quality questionnaire) (Hunt et al., 2017), maternal depression (measured by Composite International Diagnostic Interview – Short Form) (Kessler et al., 1998), parental stress (measured by Parent Stress Inventory) (Abidin et al., 2006), residential moves (measured by frequency of moves between waves) (Hardi, Goetschius, Tillem, et al., 2023), and neighborhood-level factors such as neighborhood violence (measured by neighborhood violence questions) (Zhang & Anderson, 2010) and lack of protective influences (community cohesion measured by Social Cohesion and Trust Scale (Sampson, 1997; Sampson et al., 1997); and social control measured by Informal Social Control Scale) (Sampson, 1997; Sampson et al., 1997) (more information in the Appendix 4.5.1).

4.2.3 Functional Magnetic Resonance Imaging (fMRI) data

Neuroimaging data were acquired using a 3T GE Discovery MR750 scanner with an 8-channel head coil. Two types of fMRI data were collected: while participants completed an in-scanner emotion task (task-based data) in which they were asked to identify the gender of the actor who was displaying affective facial expressions (fear, happy, sad, neutral, angry) (Supplemental Figure 4-2); and while participants were passively looking at a fixation cross (resting-state data) (Appendix 4.5.5). Consistent with a previous investigation (Hardi, Goetschius, McLoyd, et al., 2023), task-based functional data were extracted across the entire task (including all emotion conditions and cross-hair presentations) and standard fMRI preprocessing pipeline (Beltz et al., 2019) were applied using FSL v6.0 (Appendix 4.5.6). Preprocessed time-series data were extracted from 9 bilateral regions of interest (ROIs) representing the DMN, SN, and FPN. Coordinates for each node were established using NeuroSynth (Goetschius, Hein, McLanahan, et al., 2020; Hardi, Goetschius, McLoyd, et al., 2023; Yarkoni et al., 2011) (Supplemental Table 4-3).

4.2.4 Youth mental health outcomes

Internalizing and externalizing problems were measured using separate second-order multi-informant latent factors (Appendix 4.5.2). Confirmatory factor analyses were conducted on both parent- and youth-reported measures collected at age 15. The internalizing symptoms factor was comprised of three scales: parent-reported internalizing scale of the Child Behavioral Checklist (CBCL) 6-18 (Achenbach, 2001); youth-reported items from the Brief Symptom Inventory 18 (Derogatis & Kathryn, 2000); and youth-reported items from the Center for Epidemiologic Studies Depression Scale (Radloff, 1977) (Supplemental Figure 4-3). The

externalizing behaviors factor comprised of three scales: parent-report externalizing scale of the CBCL (Achenbach, 2001); youth-reported items from the Delinquency scale adopted from the National Longitudinal Study of Adolescent Health (Harris, 2013); and youth-reported substance use (Supplemental Figure 4-4).

4.2.5 Statistical Analysis

4.2.5.1 Latent Profile Analysis (LPA)

LPA was used to identify latent profiles of childhood adversity and was modeled using Mplus v8.8 (Muthén & Muthén, 2017) on the full sample (*n*=4,210). LPA is a data-driven latent variable modeling approach which identifies unobserved subpopulations (i.e., clusters of individuals) using a set of selected indicators (e.g., multiple types of childhood adversity). In this study, latent profiles were identified using within-person mean exposure to each adversity across childhood (age 0-9). Multiple model parameters (AIC, BIC, ABIC, LMR) and classification characteristics (Entropy, average posterior probabilities) were then compared to determine the most parsimonious best-fitting model (Berlin et al., 2014; Faubert, 2020; Nylund et al., 2007; Sinha et al., 2021; Vermunt & Magidson, 2002) (Appendix 4.5.4). Missing data were addressed using maximum likelihood estimation with robust standard errors.

4.2.5.2 Estimation of profile-specific functional network connectivity

In the neuroimaging subsample (*n*=167), person-specific functional network connectivity was estimated for each latent profile using Confirmatory Subgrouping Group Iterative Multiple Model Estimation (GIMME) in R v4.2.1 (Team, 2013). GIMME iteratively estimates

connections among preselected ROIs using a unified structural equation model framework that includes estimation of group-level (present for at least 75% of all individuals), subgroup-level (present for at least 50% of individuals in each latent profile subgroup), and individual-level (present for each individual) connections group (Gates & Molenaar, 2012; Henry et al., 2019) (Appendix 4.5.6.2).

Two types of connectivity metrics were computed using the resulting network maps: overall network density (i.e., network connectivity across all three networks) and network density specific to each network (i.e., DMN density, SN density, FPN density). Network density was represented as a proportion of corresponding connections (e.g., number of connections involving all DMN ROIs) from the overall network connections. Procedures were first applied to task-based neuroimaging data. Then, to determine that resulting functional connectivity networks were unique to emotion-related processes, GIMME analyses were repeated using resting-state functional neuroimaging data and compared to the task-based results (Appendix 4.5.7).

4.2.6 Analyses examining symptom and functional network differences among profiles

A one-way analysis of variance was used to test differences among adversity profiles in both internalizing/externalizing symptoms and connectivity metrics (overall, DMN, SN, FPN density). Pairwise comparisons were conducted with adjustment for multiple comparisons using the Tukey-Kramer test. Several robustness checks were then conducted. Sensitivity analyses with covariates were conducted to adjust models for important sociodemographic differences (see Appendix 4.5.3). Further, to account for sex as a biological variable, statistical analyses were repeated separately for males and females (Appendix 4.5.8).

4.3 Results

4.3.1 Adversity latent profiles

Zero-order correlations between adversity measures are in Supplemental Table 4-4 (associations ranged from r=.05 to .64*)*. A four-class model was the final selected model (Appendix 4.5.4; profile-specific sociodemographic characteristics are in Table 4-1). Individuals in the first profile (n=1,230; 29.2%) scored the lowest in all adversity indicators (Figure 4-1). Individuals in the second (n=1,973; 46.9%) and third profiles (n=550; 13.1%) had similarly moderate levels of adversity, except that maternal depression was distinctly elevated in profile 3 (Supplemental Table 4-10). Individuals in profiles 2 and 3 did not differ in levels of physical abuse, neglect, intimate partner violence, lack of neighborhood cohesion, and neighborhood violence (Supplemental Table 4-12). Differences between other indicators (i.e., emotional abuse, parental stress, residential move, lack of social control) were statistically significant, but small in magnitude compared to a relatively large elevation in maternal depression in profile 3. Lastly, relative to all other profiles, individuals in profile 4 (n=457; 10.9%) scored the highest in all adversity indicators, except for maternal depression. To reflect these patterns, in subsequent sections, profile 1 was referred as “Low-adversity”, profile 2 “Medium-adversity”, profile 3 “Maternal Depression” (MD), and profile 4 “High-adversity”.

4.3.2 Profile comparison in youth internalizing and externalizing symptoms

Adolescent internalizing and externalizing scores were the lowest in the Low-adversity profile followed by Medium, MD, and High-adversity profiles (Figure 4-2) (Internalizing: $F(3,3333)=37.84$, $p<.001$; Externalizing: $F(3,3332)=60.04$, $p<.001$). Adolescent internalizing

symptoms did not differ between the MD and High-adversity profiles (mean difference 0.11, p=.177) (Supplemental Table 4-13), despite MD and Medium-adversity profiles sharing the most similarities in adversity levels. Mean differences in externalizing symptoms differ among all profiles (all adjusted-ps<.05) (Supplemental Table 4-13). These findings remained after adjusting for sociodemographic covariates (Supplemental Table 4-14). Exploratory analysis found that the non-significant difference between MD and High-adversity profiles was particularly important for females (Supplemental Table 4-18).

4.3.3 Profile-specific subgroup comparison in functional network connectivity

Confirmatory Subgrouping GIMME generated person-specific models with excellent fit (average indices: root mean square error of approximation = .057, standard root mean residual = .047, non-normed fit index = .922, confirmatory fit index = .951). Group-level connections pertaining to individuals across all profiles were detected within the DMN, SN, and FPN (Supplemental Figure 4-6). Subgroup-level and individual-level connections that are specific to each profile were also identified across all three networks, with more person-specific connections present for the High-adversity profile (Figure 4-3). There were also profile differences in both the overall density across the entire network as well as specific network densities. Overall network density differed among profiles (F(3,163)=10.65, p<.001) (Figure 4-3). Relative to the High-adversity profile, other adversity profiles showed decreased density in the overall network (Supplemental Table 4-15). There were also differences in specific network features and specific pairwise differences among adversity profiles (Figure 4-4). First, for the DMN, MD and High-adversity profiles showed higher density relative to the other profiles (F(3,163)=11.14, p<.001; Supplemental Table 4-15). The High-adversity profile also showed

lower SN density compared to Low-adversity ($F(3,163)=3.16$, $p=.026$; Supplemental Table 4-15), and the highest FPN density compared to other profiles ($F(3,163)=18.96$, $p<.001$; Supplemental Table 4-15). These profile differences remained when the models were adjusted for sociodemographic covariates (Supplemental Table 4-16). Moreover, these network connectivity profile differences were observed using task-based functional networks, but not resting-state networks, providing evidence of the specificity of effects to emotion processes (Supplemental Table 4-17; Supplemental Figure 4-7).

4.4 Discussion

This study investigated the relationships between person-centered childhood adversity profiles and youth behavior and emotion-related brain function within a population-based birth cohort, characterized by a substantial representation of marginalized individuals and those facing substantial adversity. Four person-centered, latent, multi-domain childhood adversity profiles were identified: Low, Medium, Maternal Depression (MD), and High. Whereas individuals in the Medium and MD profiles shared similar levels of exposure to adversity, the MD profile exhibited elevated internalizing symptoms similar to the High-adversity profile. Individuals in the MD and High-adversity profiles displayed the highest DMN density compared to those in the other two profiles. Additionally, those in the High-adversity profile exhibited attenuated SN density relative to the Low-adversity profile and the highest FPN density relative to those in all other profiles. These network patterns were observed during an emotion task, but not at rest.

The differences in symptomatic presentation among adversity profiles highlight the significant impact of clustered multi-domain childhood adversity on adolescent mental health. Consistent with evidence indicating that the accumulation of exposures to various risk factors

could result in adverse health outcomes (Evans et al., 2013), the present study found that high exposure to adversity across multiple domains was associated with the highest mental health symptoms. Notably, a profile emerged with moderate levels of adversity exposure and a high level of maternal depression (the MD profile) that most closely resembling levels of adversity of the Medium-adversity profile across multiple adversities. Despite those similarities, youth with the MD profile showed mental health outcomes akin to those who were exposed to high levels of adversity across all domains (the High-adversity profile), especially for internalizing symptoms. This suggests that exposure to maternal depression may exert a particularly influential role in shaping youth mental health.

The intergenerational transmission of depression from mothers to children is widely recognized to involve both genetic and environmental mechanisms (Goodman et al., 2011; Goodman & Gotlib, 1999; Monk et al., 2008). Infants born to mothers with depression are at heightened risk of increased stress sensitivity and negative caregiving behaviors (Goodman et al., 2011). In the present study, youth with high maternal depression in childhood had elevated levels of internalizing problems, consistent with studies indicating strong links between maternal depression and child psychopathology. Moreover, these patterns were particularly important for females relative to males, consistent with previous work showing sex differences in stress-linked anxiety and depression (Goodman et al., 2011; Hankin et al., 2007).

There were also profile-specific differences in brain function that underlie youth mental health differences. Youth with the MD profile exhibited distinct patterns closely resembling those of the High-adversity profile, specifically in the DMN. Notably, these findings emerged for functional connectivity during emotion task but not at rest, suggesting that these network patterns were specific to affective conditions. Given that the DMN is typically deactivated during tasks

(Raichle et al., 2001), these findings suggest a more pronounced neural disengagement to emotional cues in youth who had relatively high exposure to maternal depression and those who were exposed to many forms of adversity. Moreover, youth with the High-adversity profile also showed network differences across the SN and FPN networks compared to youth in other profiles. Whereas weak SN engagement has been attributed to disruptions in brain network communications (Menon, 2011; Uddin, 2015), increased connectivity within the control regions within the FPN could be indicative of a compensatory mechanism that is reflected in increased regulatory processes (Bertocci et al., 2023; Etkin et al., 2009). Thus, the present study suggests that multi-domain exposures to adverse childhood experiences can potentially underlie these aberrant network communications within key emotion regulatory regions.

4.4.1 Limitations

First, there could be other adverse experiences that were not measured or collected in the sample. Nonetheless, the present investigation used information from broad-based measures of adversity across development and multiple levels of risk factors, which have likely captured most of the variance in the child's adverse experiences. Second, although youth psychopathology was represented by multi-informant measures, many of the childhood adversity measures were parent-reported. Thus, further research is needed to include data from other informants (e.g., teachers) that could provide important information about children's early environment. Third, as this is not a genetically-informed study, we are not able to disentangle genetic versus environmental influences, particularly among the links with maternal depression and child psychopathology outcomes. Fourth, the neuroimaging sample examined here is modestly sized, which precluded the examination of brain-behavior associations; thus, more research is needed to

reproduce these results in larger neuroimaging samples. Fifth, GIMME requires *a priori* specification of ROI and networks, thus these findings need to be examined across large-scale networks across the entire brain. Finally, there are limitations inherent in the latent profile approach. First, LPA is unable to capture developmentally specific variations in adverse experiences. Thus, although the present results represent adversities across the first 9 years of age, they could not address differences in the effects of adversity experienced at specific developmental periods. Moreover, while LPA well describes specific samples, the extent to which these profiles generalize to other samples need to be tested in subsequent studies; though notably, the latent profiles identified in present investigation were modeled in a large representative sample, which serves to improve generalizability to the population.

4.4.2 Conclusion

In this 15-year longitudinal study of a population-based birth cohort sample with a large proportion of individuals facing adversity, four latent profiles of childhood adversity with distinct patterns of adolescent mental health and emotion-related brain function were identified. Adolescents who were exposed to high maternal depression and multi-domain risks in childhood were at the highest risk for psychopathology and had differential patterns across brain networks implicated in emotion processing relative to those with low- and medium-adversity risks. This study is the first to combine subtyping with individualized network estimation methods to parse heterogeneity both within childhood adverse environment and subsequent brain networks in a longitudinal population-based sample. This study demonstrates the benefit of individual-oriented approaches to increase precision of neural mechanisms linked to adverse childhood experiences.

Table 4-1. Sociodemographic descriptive of each adversity latent profile (*N*=4,210)

	Low-adversity (*n*=1,230)	**Medium-adversity (*n*=1,973)**	**Maternal Depression (*n*=550)**	**High-adversity (*n*=457)**	**Statistical test**
Ethnoracial identity, No. (%)					
Black (non-Hispanic)	308 (25)	791 (40)	221 (40)	165 (36)	$\chi(12) = 185.9$, $p < .001$
White (non-Hispanic)	252 (20)	185 (9)	92 (17)	22 (5)	
Hispanic	213 (17)	383 (19)	67 (12)	96 (21)	
Other/multi	68 (6)	105 (5)	27 (5)	36 (8)	
Unknown	389 (32)	509 (26)	143 (26)	138 (30)	
Sex at birth, No. (%)					
Female	581 (47)	948 (48)	254 (46)	216 (47)	$\chi(3) = 0.665$, $p = .881$
Male	649 (53)	1025 (52)	296 (54)	241 (53)	
Parental marital status, No. (%)					
Married	468 (38)	404 (20)	116 (21)	80 (18)	$\chi(3) = 149.64$, $p < .001$
Unmarried	762 (62)	1569 (80)	434 (79)	377 (82)	
Poverty ratio	3.25 (3.09)	1.98 (2.08)	2.01 (2.13)	1.52 (1.69)	$F(3,4206) = 95.31$, $p < .001$

Figure 4-1. Childhood adversity latent profiles

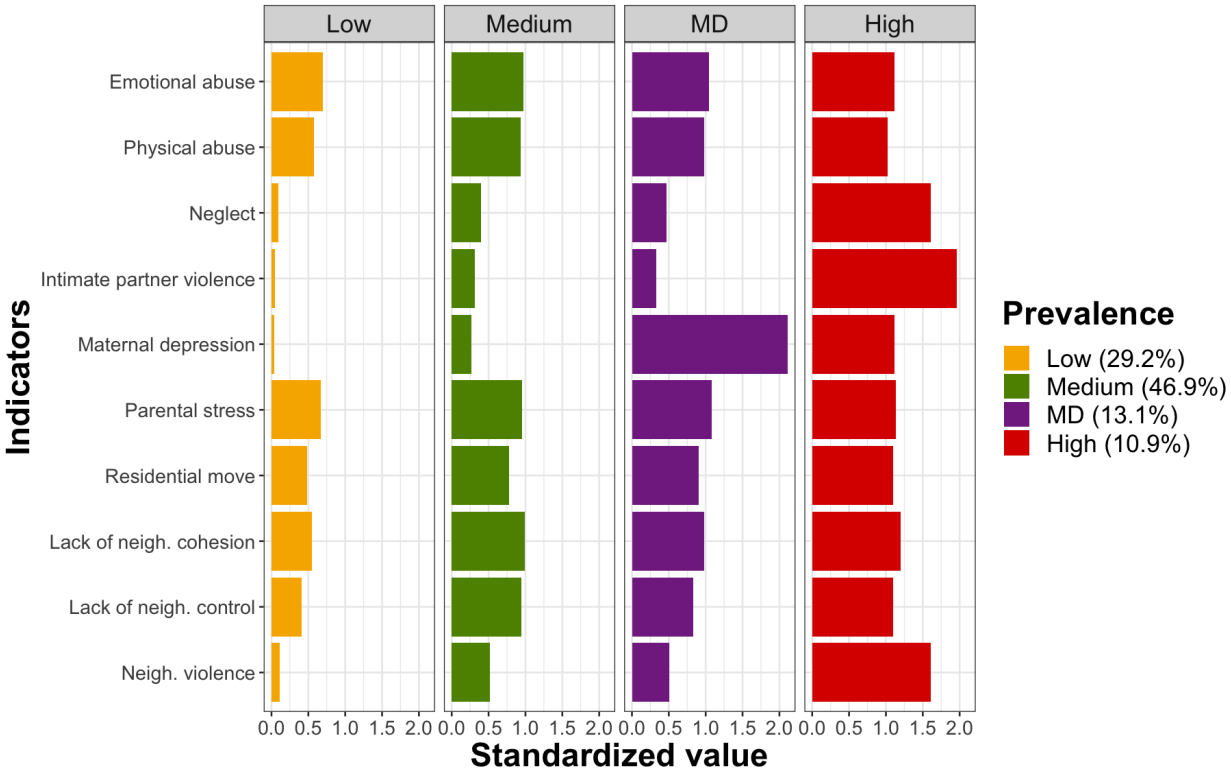

Standardized values of each adversity indicator in the four-class model of childhood adversity profiles. Of *N*=4,210 individuals in the included sample, *N*=1,230 (29.2%; in yellow) experienced the lowest rate of adversity; *N*=1,973 (46.9%; in green) were exposed to medium-level adversity risk; and *N*=457 (10.9%; in red) experienced the highest level of risk across the ten adversity types. *N*=550 (13.1%; in purple) individuals had similar levels of exposures with the medium-risk profile (green), but with markedly elevated levels of maternal depression (MD) compared to all other profiles.

Figure 4-2. Internalizing and externalizing symptoms among adversity profiles

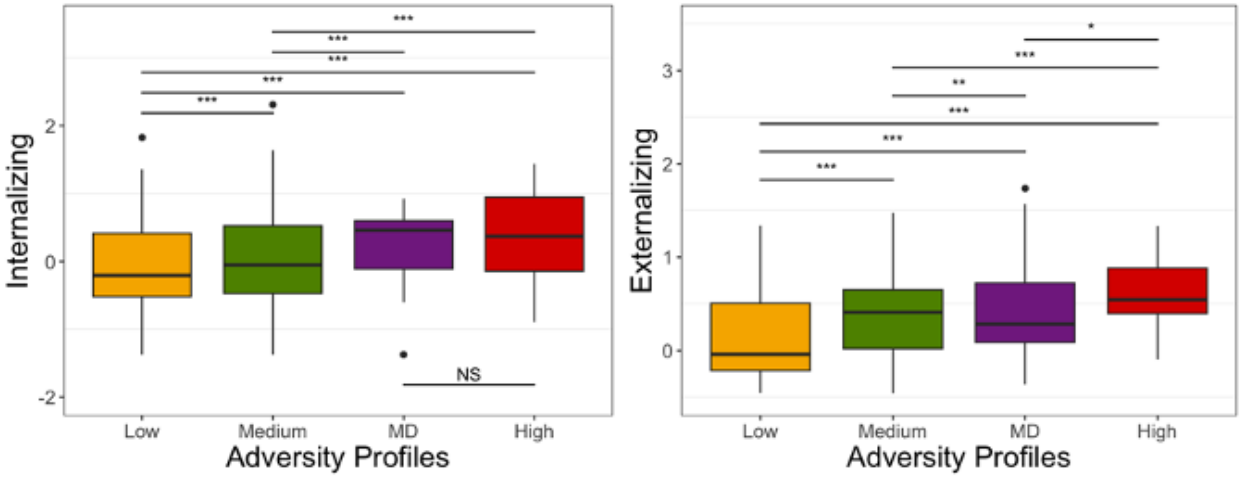

Boxplots comparing levels of internalizing and externalizing symptoms. The MD and High-adversity profiles do not differ for internalizing symptoms, but differ among all profiles for externalizing symptoms. *** $p_{adj} < .001$; ** $p_{adj} < .01$; * $p_{adj} < .05$; NS $p_{adj} > .05$

Figure 4-3. Network connectivity properties of adversity profiles

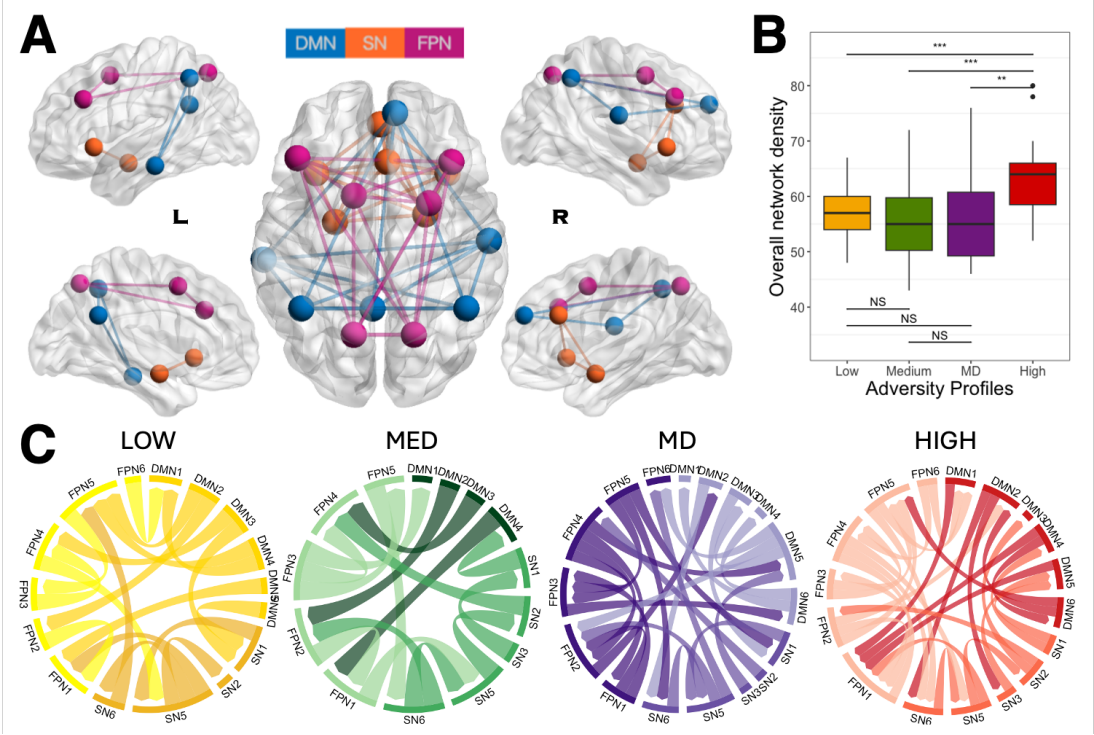

A: Regions of interest and large-scale network connectivity. The Default Mode Network (DMN; blue) included the bilateral inferior parietal lobule, posterior cingulate cortex, and medial temporal gyrus. The Salience Network (SN; orange) included the bilateral insula, amygdala, and dorsal anterior cingulate cortex. The Fronto Parietal Network (FPN; pink) included the bilateral dorsolateral prefrontal cortex, anterior inferior parietal lobule, and posterior parietal cortex.

B: Boxplots comparing the overall network density of individual connectivity maps across adversity profiles. Individuals with the high-adversity profile (red) have the highest overall network density compared to individuals with the low- (yellow), medium-adversity (green), and maternal depression (purple) profiles. *** $p_{adj} < .001$; ** $p_{adj} < .01$; NS $p_{adj} > .05$

C: Subgroup-specific connectivity maps of each adversity profile. Subgroup-specific connections were the highest for individuals with the maternal depression (MD; purple) and high-adversity (red) profiles.

Figure 4-4. Comparison of functional connectivity within subnetworks among adversity profiles

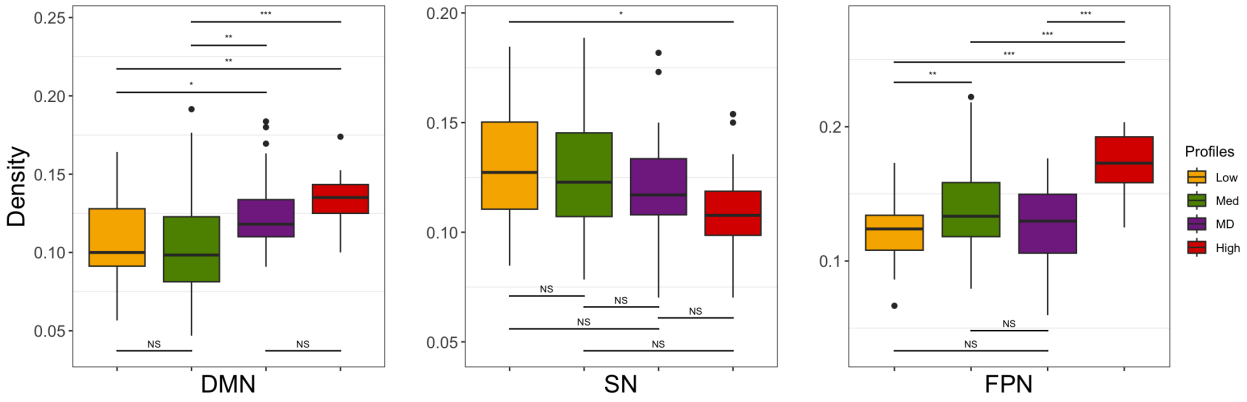

Boxplots showing differences in subnetwork-specific connections across adversity profiles. From left to right: Individuals in the maternal depression (MD) and high-adversity profiles showed the highest density of DMN compared to low- and medium-risk adversity profiles; The high-adversity profile showed the lowest SN density compared to low-adversity profile; The high-adversity profile showed the highest FPN density compared to the all other groups.

*** $p_{adj} < .001$; ** $p_{adj} < .01$; * $p_{adj} < .05$; NS $p_{adj} > .05$

4.5 Appendix

4.5.1 Childhood adversity measures

Ten variables were examined as indicators of childhood adversity spanning across four waves (ages 1, 3, 5, and 9) capturing information about the child environment from birth to age 9. Use of these variables was justified in past publications (Goetschius, Hein, McLanahan, et al., 2020; Goetschius, Hein, Mitchell, et al., 2020; Hardi, Goetschius, Tillem, et al., 2023; Hein et al., 2020; Peckins et al., 2020) as available constructs representing salient childhood adversities in this sample. These variables provide information on child maltreatment (physical abuse, emotional abuse, and neglect), intimate partner violence (IPV), maternal depression, parental stress, residential moves, and neighborhood adversities (lack of cohesion, lack of social control, neighborhood violence), each types of adversities with large literatures connecting them to negative outcomes, particularly internalizing and externalizing psychopathology.

Childhood maltreatment data were collected at child ages 3, 5, and 9. Each maltreatment type (physical abuse, emotional abuse, and neglect) was measured by separate subscales in the Parent-Child Conflict Tactics Scale (Straus et al., 1998). Emotional abuse was parent-reported using the 5-item psychological aggression subscale capturing past year frequency that primary caregiver reported to have engaged in behaviors such as “shouted, yelled, or screamed at” or “swore or cursed at” child (0 = did not happen, 1 = has happened one or more times) (Straus et al., 1998). Physical abuse was parent-reported using the 5-item physical assault subscale capturing past year frequency that primary caregiver reported to have engaged in behaviors such as “spanked [child] on the bottom with their bare hand” or “hit [child] on the bottom with something like a belt, hairbrush, a stick or some other hard object.” (0 = did not happen, 1 = has

happened one or more times) (Straus et al., 1998). Neglect was parent-reported using the 5-item neglect subscale capturing past year frequency that primary caregiver reported to have engaged in behaviors such as "had to leave their child home alone, even when they thought some adult should be with him/her" or "was not able to make sure their child got to a doctor or hospital when he/she needed it." (0 = did not happen, 1 = has happened one or more times) (Straus et al., 1998). Average scores for each subscale across all waves were computed to represent the extent of childhood physical abuse, emotional abuse, and neglect.

Intimate partner violence (IPV) data were collected at child ages 1, 3, 5, and 9 using parent-reported 6-item questions on physical, emotional, or sexual intimate partner violence such as "how often does father slap or kick you?" or "how often does father try to isolate you from friends/family?" (0 = never, 1 = sometimes, 3 = often) perpetrated by the child's father or parent's romantic partner. These items were selected based on a previous study on adverse childhood experiences in this sample (Hunt et al., 2017). In cases where mother was no longer in a relationship with the child's biological father during data collection wave, mother reported information about her current partner. An average score across all waves were computed to represent IPV.

Maternal depression was measured using self-reported data on the Composite International Diagnostic Interview – Short Form (CIDI-SF) (Kessler et al., 1998) across child age 1, 3, 5, 9. The CIDI-SF, consistent with the Diagnostic and Statistical Manual of Mental Disorders – Fourth Edition (Bell, 1994), included questions on mother's feelings of depressed mood or anhedonia (loss in pleasure or interest in activities that they usually found enjoyable) in the past year that lasted two weeks or more (1 = yes, 0 = no). If so, they were asked more detailed questions about losing interest, tiredness, changes in weight, sleep, concentration,

worthlessness, and any suicidal ideation. Diagnostic criteria were met if mother endorsed depressed mood or anhedonia lasting at least half of the day nearly every day and two or more additional symptoms. Average scores across all waves were computed to represent maternal depression across childhood.

Parental stress was measured at child ages 1, 3, 5, and 9 using 4-item parent-reported questionnaire adapted from the Child Development Supplement of the Panel of Study of Income Dynamics (Hofferth et al., 1997) such as "I often feel tired, worn out, or exhausted from raising a family" and "I feel trapped by my responsibilities as a parent." (0 = strongly disagree, 1 = somewhat disagree, 2 = somewhat agree, 3 = strongly agree). Several items for this scale were taken from the Parent Stress Inventory (Abidin et al., 2006), which measures stress triggered by changes in employment, income or other factors. An average score across all waves was computed to represent parental stress.

Frequency of residential moves or household instability was parent-reported at child ages 1, 3, 5, and 9 to capture changes occurring in between waves (i.e., between ages 0-1, 1-3, 3-5, and 5-9). At each wave, mothers or primary caregivers provided answers on whether the family has moved since the prior wave, and if yes, how many times. Average scores across all waves were computed to represent residential moves across childhood.

Three neighborhood factors (lack of community cohesion, lack of social control, neighborhood violence) were reported at child ages 3, 5, and 9. Lack of neighborhood cohesion was measured using parent-reported reverse-coded 4-item questions taken from the Social Cohesion and Trust Scale (Sampson, 1997; Sampson et al., 1997) such as "people around here are willing to help their neighbors" and "this is a close-knit neighborhood" (0 = strongly agree, 1 = agree, 2 = disagree, 3 = strongly disagree). Lack of neighborhood social control was measured

using reverse-coded 5-item questions taken from the Informal Social Control Scale (Sampson, 1997; Sampson et al., 1997) such as "how likely neighbors intervene if children skipping school and hanging on street?" and "how likely neighbors intervene if fight broke out in front of the house?" (0 = very likely, 1 = somewhat, 2 = not very unlikely, 3 = very unlikely). Neighborhood violence was measured using 3 parent-reported items such as "in the past year, how often did you see person get hit, slapped, punched?" and "in the past year, how often did you see person attacked with weapon?" (0 = never, 1 = once, 2 = 2-3 times, 3 = 4-10 times, 4 = more than 10 times) based on prior investigations (Zhang & Anderson, 2010). Average scores across all waves for each construct were computed to represent lack of community cohesion, lack of social control, and neighborhood violence during childhood.

4.5.2 Youth internalizing and externalizing symptoms

Internalizing symptoms were measured as a multi-informant latent factor comprised of all available FFCWS measures of internalizing symptoms at age 15: parent-reported internalizing scale (i.e., anxious/depressed and withdrawn items) from the Child Behavioral Checklist 6-18 (CBCL) (Achenbach, 2001); youth-reported items from the Brief Symptom Inventory 18 (BSI-18) (Derogatis & Kathryn, 2000); and youth-reported items from the Center for Epidemiologic Studies Depression Scale (CES-D) (Radloff, 1977). The CBCL is comprised of 8 questions (6 anxious/depressed items and 2 withdrawn items) (0 = not true, 1 = sometimes true, 2 = often true), and higher scores indicate greater youth internalizing symptoms. The BSI-18 contains 6 questions from the anxiety subscale (0 = strongly disagree, 1 = somewhat disagree, 2 = somewhat agree, 3 = strongly agree), and higher scores indicate greater anxiety symptoms. The CES-D contains 4 questions (0 = strongly disagree, 1 = somewhat disagree, 2 = somewhat agree,

3 = strongly agree), and higher scores indicate greater youth depressive symptoms. Confirmatory factor analysis was conducted using MPlus v8.8 (Muthén & Muthén, 2017) with WLSMV estimator to account for categorical variables. Each question was loaded onto three latent factors reflecting the measures (CBCL, BSI-18, CES-D), which were then loaded onto a higher-order latent factor of overall internalizing symptoms. Model fit indices indicate adequate model fit (CFI = .931, TLI = .921, RMSEA = .065, SRMR = .075) (Hu & Bentler, 1999) (Supplemental Figure 4-3). Internalizing factor scores were extracted as individual scores for further analysis.

Externalizing behaviors were measured as a multi-informant latent factor comprised of all available FFCWS measures of externalizing behavior at age 15: parent-reported externalizing scale (i.e., aggressive and rule-breaking items) from the Child Behavioral Checklist 6-18 (CBCL) (Achenbach, 2001); youth-reported items from the Delinquency scale adopted from the National Longitudinal Study of Adolescent Health (Add Health) (Harris, 2013); and youth-reported substance use. The parent-reported CBCL items comprise of 19 questions (10 aggressive behavior items and 9 rule-breaking behavior items) (0 = not true, 1 = sometimes true, 2 = often true), and higher scores indicate greater youth externalizing symptoms. Youth-reported delinquency was measured by 13 questions (0 = never, 1 = sometimes, 2 = often), and higher scores indicate greater youth delinquent behavior. Substance use was measured using 5 binary questions (0 = no, 1 = yes) capturing alcohol use (more than 2 drinks without parents), tobacco, and other substances (marijuana, illicit drugs or nonmedical use of prescription drugs). Confirmatory factor analysis was conducted using Mplus v8.8 (Muthén & Muthén, 2017) with WLSMV estimator to account for categorical variables. Each question was loaded onto three latent factors reflecting the measures (CBCL, Delinquency, Substance), which were then loaded onto a higher-order latent factor of overall externalizing behavior. Model fit indices indicate

excellent model fit (CFI = .955, TLI = .952, RMSEA = .031, SRMR = .092) (Hu & Bentler, 1999) (Supplemental Figure 4-4). Externalizing factor scores were then extracted as individual participant scores for further analysis.

4.5.3 Sociodemographic covariates

The following covariates were included in sensitivity analyses: ethnoracial identity, parental marital status, household income. Two additional covariates were included in the neuroimaging subsample analysis: age of youth during the neuroimaging scan and in-scanner motion. Ethnoracial identity was included to account for unequal exposures to experiences of race-related adversity such as discrimination and structural racism, and was youth-reported at age 15 (Black/African American, non-Hispanic; white, non-Hispanic; Hispanic/Latino, all races; multi-racial, non-Hispanic; other, non-Hispanic). As the group with the highest prevalence in the sample, the Black group was used as the reference group in statistical models. Parental marital status was included to account for FFCWS sampling strategy (Reichman et al., 2001), and was parent-reported when each child was age 1 (0 = Unmarried, 1 = Married). Household income was included to account for differences in family socioeconomic resources, and was measured by poverty ratio (ratio of total household income to the official poverty thresholds designated by the U.S. census bureau), which was parent-reported at age 1 (higher poverty ratio indicated higher socioeconomic status). Youth age was included to account for differences in stages of normative brain development and was computed using youth-reported date of birth at age 15. In-scanner motion was measured using the framewise displacement metric computed in FSL by averaging differences in rotation and translation parameters (Power et al., 2012), and was included to ensure that results were robust after adjustment for motion differences. Analysis of covariance

(ANCOVA) models were first tested to examine differences in network connectivity metrics among profiles, accounting for all covariates. Pairwise multiple comparisons were then conducted with adjustment for multiple comparisons using the Tukey-Kramer test.

4.5.4 Procedures and robustness checks for LPA

Latent profile analysis was conducted using Mplus v8.8 (Muthén & Muthén, 2017). Latent class models were estimated by adding classes in consecutive order; starting with a two-class model, classes were added iteratively until the final model was identified. In all models, proportional covariance structure was used to assist in convergence for complex models (Liu & Rubin, 1998). Here, covariance in a class was freely estimated and used as a referent, resulting in equal correlation matrices without constrained homogeneity of covariance structures across classes (Barnard et al., 2000; Liu & Rubin, 1998; McNeish et al., 2022; Proust-Lima et al., 2017). Classes were initially fitted using 500 random starts with 20 iterations, and then repeated with 1000 and, subsequently, 2000 starting values to ensure that results reflect a global maximum (Nylund et al., 2008).

Multiple model fit indices and classification characteristics (log-likelihood (LL), Akaike Information Criteria (AIC), Bayesian Information Criteria (BIC), adjusted BIC (ABIC), Lo-Mendell-Rubin Adjusted Likelihood Ratio test (LMR), Entropy, average latent class posterior probabilities, class sizes) were used to determine model selection (Faubert, 2020; Nylund et al., 2008; Sinha et al., 2021). LL represents the goodness-of-fit of the model, with higher values indicating a better fit. AIC (Akaike, 1987), BIC (Schwarz, 1978), and ABIC (Sclove, 1987) are statistical information criteria, with lower values indicating a better model fit. LMR (Lo et al., 2001) is a test comparing the specified model *k* with *k*-1 class (model with one less class), and

assesses if there are statistically meaningful improvements in model fit with the addition of one class. Classifications diagnostics were also examined for class selection (Masyn, 2013). Entropy is a measure of class separation and assesses the classification accuracy (Celeux & Soromenho, 1996), where high values (1.0 being the maximum, .80 to be acceptable) (Celeux & Soromenho, 1996) indicate high separation among classes. The average posterior probabilities represent the certainty of latent profile assignment, whereby high classification quality is achieved when the diagonal values are high (as close to the maximum value of 1.0) and off-diagonal values are low (as close to the minimum value of 0) (Muthén & Muthén, 2000). Finally, class sizes were examined to ensure that no classes have fewer than 50 individuals or 5% of the sample, which are prone to model misspecifications (Faubert, 2020; Nylund et al., 2008).

Loglikelihood was replicated for all fitted classes across different starting values in exception for the 6-class model. Multiple model fit indices improved with greater number of classes (i.e., increases in LL and decreases in AIC, BIC, and ABIC values with more fitted classes) until the 6-class model, for which poorer model fit and classification were examined across multiple parameters (Supplemental Table 4-5), suggesting that a 6-class model may be too high in complexity for the present data. Thus, no additional models beyond the 6-class model were estimated. The model fit and classification indices were then compared among the remaining estimated classes for final model selection.

Results demonstrate a 4-class model to be the best-fitting solution with the greatest parsimony. Specifically, the 4-class model showed improvements across all model fit indices (highest LL and lowest AIC, BIC, and ABIC values) compared to the 2- and 3-class models, and the highest classification accuracy (highest Entropy and average posterior probabilities) among all other class models (Supplemental Table 4-5). In the four-class model, average posterior

probabilities ranged from .874 to .919 (Supplemental Table 4-6), with approximately 11.8% of the sample with values below .70. These statistics indicate greater classification quality of the 4-class model compared to the 3-class and the 5-class models (Supplemental Table 4-7), for which several diagonal class posterior probabilities fall below the optimal range of .80 to .90 (Faubert, 2020; Muthén & Muthén, 2000), and contained a greater proportion of individuals with low posterior probability of below .70 (Nagin, 2009) (3-class: 12.9%; 5-class: 19.8%).

To determine the internal consistency and robustness of the selected final model, LPA with a fitted 4-class model was repeated for a total of 20 supplementary analyses leaving out one site (i.e., sample city) (Reichman et al., 2001) at a time. The consistency of model fit parameters and prevalence of resulting class memberships were then examined across these analyses. Results demonstrated convergence across these separate supplementary analyses, which reflect highly similar model fit and class memberships to the full sample (Supplemental Table 4-8), demonstrating internal consistency of the selected latent profile 4-class model. Resulting profile membership of the 4-class model was extracted for additional analysis.

4.5.5 Neuroimaging data acquisition and preprocessing

MRI data were acquired using a 3T GEDiscovery MR750 scanner with an 8-channel head coil. Head padding and instructions limited movement. T1-weighted gradient echo images were first captured (TR=12ms, TE=5ms, TI=500ms, flip angle=15°, FOV=26cm, slice thickness=1.44mm, 256x192 matrix, 110 slices). fMRI T2*-weighted blood oxygenation level dependent (BOLD) images were then captured using reverse spiral sequence (Glover & Law, 2001) of 40 contiguous axial 3mm slices (TR = 2000ms, TE = 30ms, flip angle = 90°, FOV = 22cm, voxel size = 3.44mm x 3.44mm x 3mm, ascending acquisition, parallel to AC-PC line).

Task-based functional neuroimaging (fMRI) data were collected using an event-related emotion (faces) task (see Supplemental Figure 4-2 for visual representation of task paradigm design). Participants were shown a series of emotional faces (Tottenham et al., 2009) and indicated if they were viewing a female or male face. Gender (female, male), race (European American, African American), and emotion (fearful, happy, sad, neutral, angry) of the actor were counterbalanced and randomly presented across 100 trials. Each trial consisted of a fixation cross (500ms) followed by 250ms of an emotional face, then 1500ms of blank screen during which participants are expected to respond using a button press. Functional data from each participant across all trials of the emotion task (without any contrasting across emotion conditions) were extracted for subsequent processing. Resting-state neuroimaging data were collected while participants were awake and passively viewing a fixation cross.

Identical preprocessing steps were applied to both task-fMRI and resting-state fMRI data. Anatomical images were first skull-stripped (f=.25) using Brain Extraction Tool (BET) in FSL version 6.0 (Jenkinson et al., 2012) and segmented into gray matter, white matter, and cerebrospinal fluid using FSL FAST. After large temporal spikes in the k-space functional data (>2 *SD*) were removed, field maps were corrected and functional images were reconstructed using MATLAB. Noise from cardiac and respiratory motion were removed using RETROICOR and slice-timing correction using SPM8 (Wellcome Department of Cognitive Neurology, London, UK; http://www.fil.ion.ucl.ac.uk). Moreover, the first ten volumes of functional data were removed to ensure the stability of signal intensity. Following these steps, the functional data were further preprocessed using FSL fMRI Expert Analysis Tool (FEAT). Functional images were skull-stripped and spatially smoothed using FSL FMRIB's Automated Segmentation Tool (Woolrich et al., 2001), and registered to subject-specific previously skull-

stripped and segmented anatomical images. Motion correction was performed using MCFLIRT and spatial smoothing using a Gaussian kernel of FWHM 6.0mm was applied. Grand-mean intensity of the entire 4D dataset was normalized by a single multiplicative factor and FSL motion outliers were ran to extract framewise displacement motion parameters.(Power et al., 2012) ICA-AROMA was used to remove motion-related artifacts in the data, nuisance signal derived from white matter and cerebrospinal fluid were regressed out, and data with signal below 0.01Hz were then high-pass filtered. These preprocessing steps were applied using detailed scripts (Beltz et al., 2019) similar to prior work (Goetschius, Hein, McLanahan, et al., 2020; Hardi, Goetschius, McLoyd, et al., 2023).

4.5.6 Functional connectivity across neural networks estimation

4.5.6.1 ROI selection and data extraction

The present investigation focused on eighteen bilateral regions that represent the tripartite network (Menon, 2011): Default Mode Network (DMN), Salience Network (SN), Frontoparietal Network (FPN) (Supplemental Table 4-3). The DMN extends across the lateral parietal, posterior cingulate, and medial temporal cortices (Raichle, 2015). It is often linked to introspective self-referential mental processes, and is conventionally believed to deactivate during task engagement (Raichle et al., 2001). The SN includes the anterior insula, cingulate cortex, and amygdala, and plays a central role in detecting important environmental cues (Seeley, 2019) and facilitating bottom-up signals to other networks (Menon, 2011). The FPN, which encompasses the inferior lobule, dorsolateral prefrontal, and posterior parietal cortices, is implicated in cognitive control and goal-directed processes (Zanto & Gazzaley, 2013).

Consistent with our previous investigations (Goetschius, Hein, McLanahan, et al., 2020; Hardi, Goetschius, McLoyd, et al., 2023), ROI coordinates were extracted from NeuroSynth (Yarkoni et al., 2011), a meta-analytic tool that combines results from published neuroimaging articles using an automated parser. Specific ROI names (i.e., "Default Mode", "Salience", "Frontoparietal") were used as keywords to search for peak activity on the NeuroSynth website and corresponding association maps were then downloaded. Voxel coordinates from downloaded images were subsequently extracted using FSL and then utilized to create an ROI 6.5mm-diameter sphere using *fslmaths* (Goetschius, Hein, McLanahan, et al., 2020). The ROIs for DMN and SN in this study were consistent with a previous investigation (Goetschius, Hein, McLanahan, et al., 2020), and three additional nodes were selected to represent the FPN.

4.5.6.2 Confirmatory Subgrouping Group Iterated Multiple Model Estimation (GIMME)

Confirmatory Subgrouping GIMME (Henry et al., 2019) is an extension of GIMME (Gates & Molenaar, 2012), a functional connectivity analysis method that iteratively fits unified structural equation models to arrive at person-specific networks that contain group-, subgroup-, and individual-level connections. GIMME estimates both directed contemporaneous (occurring at the same time or functional volume) and lagged (occurring at a different time or functional volume) connections among *a priori* regions of interests (ROIs). GIMME has been validated in multiple largescale simulations, outperformed 38 other commonly-used approaches in estimation connectivity maps among neural nodes (Gates & Molenaar, 2012), and has been discussed in over 400 scientific articles (Beltz & Gates, 2017; Gates & Molenaar, 2012). GIMME begins search for group model with autoregressive paths freed for estimation. GIMME first estimates connections among preselected brain ROIs that pertain to at least 75% of the entire sample if the

connections significantly improve individual model fit (as assessed by Lagrange Multiplier tests) (Gates et al., 2010). In the Confirmatory Subgrouping extension (Henry et al., 2019), subgroup-specific connections are then estimated for individuals in each prespecified subgroup if the connections significantly improve model fit for at least 51% of individuals within each subgroup. Finally, individual-level connections that are specific to each person in the sample are estimated until the connectivity model fits the observed data for each individual well, according to traditional model fit indices. Contemporaneous connections estimated using GIMME were then extracted for subsequent analyses, consistent with previous investigations (Goetschius, Hein, McLanahan, et al., 2020; Hardi, Goetschius, McLoyd, et al., 2023).

4.5.7 Analyses comparing functional connectivity networks during emotion task vs non-task

There were differential patterns of resting-state network connectivity among adversity profiles compared to task-based network connectivity (Supplemental Table 4-17). Repeated measures ANOVAs were conducted with Greenhouse–Geisser correction to examine the differences between scan type (task vs. rest) in predicting network density (DMN, SN, FPN). Results demonstrated that task-based network connectivity significantly differed from network connectivity during the resting-state (Supplemental Table 4-17). Results from repeated-measure ANOVA comparing task-based from resting-state network connectivity found differences between scan type and by profiles (Supplemental Table 4-17). In particular, there were significant differences between scan type within person for overall network density ($F(1,150)=0.78$, ges=.092, $p<.001$) and SN density ($F(1,150)=9.71$, ges=.026, $p=.001$). Moreover, there were significant scan type by profiles differences. Specifically, there were differences between task-based and resting-state data network connectivity in the DMN for low

and medium-adversity profiles ($F(3,150)=7.52$, ges=0.63, $p<.001$); SN for maternal depression and high-adversity profiles ($F(3,150)=5.22$, ges=0.42, $p=.001$); and FPN for low-adversity and high-adversity profiles ($F(3,150)=16.56$, ges=.133, $p<.001$) (Supplemental Table 4-17).

4.5.8 Exploratory analysis examining differences among adversity profiles, stratified by sex

In exploratory analyses, sex was accounted for as a biological variable by separately examining the mean differences in mental health outcomes and metrics of functional connectivity networks among adversity profiles for males and females. Sex was mother-reported at child birth (baseline wave) as "Male" or "Female". For youth internalizing and externalizing outcomes, similar patterns to the analysis with the entire sample were observed. Youth internalizing and externalizing outcomes increased from Low-adversity to Medium-adversity, MD, High-adversity profiles. For females, internalizing and externalizing symptoms do not differ between the MD and High-adversity profiles; whereas for males, internalizing and externalizing symptoms do not differ between the Medium-adversity and the MD profiles (Supplemental Figure 4-8; Supplemental Table 4-18). There were no notable sex differences between males and females groups in stratified analyses examining mean difference in brain network metrics (Supplemental Table 4-19).

Supplemental Table 4-1. Statistical comparison between the full FFCWS and included samples

	FFCWS sample (n = 4,898)	**Included sample (n = 4,210)**	**Test**
Ethno-racial identity *No.* (%)	Black non-Hispanic = 1,601 (33%) White non-Hispanic = 590 (12%) Hispanic = 813 (17%) Other/multi = 261 (5%) Unknown = 1,633 (33%)	Black non-Hispanic = 1,485 (35%) White non-Hispanic = 551 (13%) Hispanic = 759 (18%) Other/multi = 236 (6%) Unknown = 1,179 (28%)	$\chi(3) = 0.109$, $p = .991$
Child sex *No.* (%)	Female = 2,568 (52%) Male = 2,329 (48%) Unknown = 1 (0.02%)	Female = 1,999 (48%) Male = 2,211 (53%)	$\chi(1) = .003$, $p = .958$
Parental marital status *No.* (%)	Married = 1,187 (24%) Unmarried = 3,710 (76%) Unknown = 1 (0.02%)	Married = 1,068 (25%) Unmarried = 3,142 (75%)	$\chi(1) = 1.488$, p=.222
Poverty ratio *M* (*SD*)	2.22 (2.41)	2.30 (2.47)	t(8838.4) = -1.589, p=.112
Child birth city *No.* (%)	Oakland, CA = 330 (7%) Austin, TX = 326 (7%) Baltimore, MD = 338 (9%) Detroit, MI = 327 (7%) Newark, NJ = 342 (7%) Philadelphia, PA = 337 (7%) Richmond, VA = 327 (7%) Corpus Christi, TX = 331 (7%) Indianapolis, IN = 325 (7%) Milwaukee, WI = 348 (7%) New York, NY = 384 (8%) San Jose, CA = 326 (7%) Boston, MA = 99 (2%) Nashville, TN = 102 (2 %) Chicago, IL = 155 (3%) Jacksonville, FL = 100 (2%) Toledo, OH = 101 (2%) San Antonio, TX = 100 (2%) Pittsburgh, PA = 100 (2%) Norfolk, VA = 99 (2%) Unknown = 1 (0.02%)	Oakland, CA = 281 (7%) Austin, TX = 282 (7%) Baltimore, MD = 294 (7%) Detroit, MI = 283 (7%) Newark, NJ = 274 (7%) Philadelphia, PA = 300 (7%) Richmond, VA = 267 (6%) Corpus Christi, TX = 296 (7%) Indianapolis, IN = 286 (7%) Milwaukee, WI = 312 (7%) New York, NY = 312 (7%) San Jose, CA = 270 (6%) Boston, MA = 90 (2%) Nashville, TN = 86 (2%) Chicago, IL = 136 (3%) Jacksonville, FL = 88 (2%) Toledo, OH = 89 (2%) San Antonio, TX = 88 (2%) Pittsburgh, PA = 91 (2%) Norfolk, VA = 85 (2%)	$\chi(19) = 3.187$, $p = 1.00$

Note. Unknown group was omitted in chi-square estimation; Poverty ratio represents a ratio of total household income to the official poverty threshold and higher values represent higher socioeconomic status, and was measured at baseline (child birth).

Supplemental Table 4-2. Descriptives and statistical comparison between included and neuroimaging samples

	Included FFCWS sample (*n* = 4,210)	**Neuroimaging subsample (*n* = 167)**	**Comparison**
Ethno-racial identity *No.* (%)	Black non-Hispanic = 1,485 (35%) White non-Hispanic = 551 (13%) Hispanic = 759 (18%) Other/multi = 236 (6%) Unknown = 1,179 (28%)	Black non-Hispanic = 128 (77 %) White non-Hispanic = 20 (12%) Hispanic = 11 (7%) Other/multi = 8 (5%)	$\chi(3) = 51.66$, $p < .001$
Child sex *No.* (%)	Male = 2,211 (53%) Female = 1,999 (48%)	Male = 76 (46%) Female = 91 (55%)	$\chi(1) = 2.89$, $p = .09$
Parental marital status *No.* (%)	Married = 1,068 (25%) Unmarried = 3,142 (75%)	Married = 37 (22%) Unmarried = 130 (78%)	$\chi(1) = 0.72$, $p = .40$
Poverty ratio *M* (*SD*)	2.30 (2.47)	2.11 (2.31)	$t(181.31) = 1.07$, $p = .28$
Child birth city *No.* (%)	Oakland, CA = 281 (7%) Austin, TX = 282 (7%) Baltimore, MD = 294 (7%) Detroit, MI = 283 (7%) Newark, NJ = 274 (7%) Philadelphia, PA = 300 (7%) Richmond, VA = 267 (6%) Corpus Christi, TX = 296 (7%) Indianapolis, IN = 286 (7%) Milwaukee, WI = 312 (7%) New York, NY = 312 (7%) San Jose, CA = 270 (6%) Boston, MA = 90 (2%) Nashville, TN = 86 (2%) Chicago, IL = 136 (3%) Jacksonville, FL = 88 (2%) Toledo, OH = 89 (2%) San Antonio, TX = 88 (2%) Pittsburgh, PA = 91 (2%) Norfolk, VA = 85 (2%)	Baltimore = 1 (0.6%) Detroit = 113 (68%) Indianapolis = 2 (1%) Chicago = 24 (14%) Toledo = 26 (16%) Pittsburgh = 1 (0.6%)	$\chi(5) = 193.52$, $p < .001$

Note. Unknown group was omitted in chi-square estimation; Poverty ratio represents a ratio of total household income to the official poverty threshold and higher values represent higher socioeconomic status, and was measured at baseline (child birth); Only the six birth cities in the neuroimaging subsample were included in chi-square estimation.

Supplemental Table 4-3. MNI coordinates of neural Regions of Interest (ROIs)

Default Mode Network (DMN)		
DMN_1	R. Inferior Parietal Lobule	46 -52 48
DMN_2	L. Inferior Parietal Lobule	-42 -52 48
DMN_3	R. Posterior Cingulate Cortex	8 -52 28
DMN_4	L. Posterior Cingulate Cortex	-4 -52 28
DMN_5	R. Medial Temporal Gyrus	58 -16 20
DMN_6	L. Medial Temporal Gyrus	-62 -26 -18
Salience Network (SN)		
SN_1	R. Insula	36 20 -4
SN_2	L. Insula	-34 20 -4
SN_3	R. Amygdala	24 -2 -16
SN_4	L. Amygdala	-24 -6 -16
SN_5	R. Dorsal Anterior Cingulate Cortex	4 26 28
SN_6	L. Dorsal Anterior Cingulate Cortex	0 46 6
Fronto Parietal Network (FPN)		
FPN_1	R. Dorsolateral Prefrontal Cortex	38 26 34
FPN_2	L. Dorsolateral Prefrontal Cortex	-44 28 32
FPN_3	R. Anterior Inferior Parietal Lobule	26 4 50
FPN_4	L. Anterior Inferior Parietal Lobule	-14 8 50
FPN_5	R. Posterior Parietal Cortex	18 -66 50
FPN_6	L. Posterior Parietal Cortex	-14 -66 52

Supplemental Table 4-4. Zero-order correlations of adversity variables

Variables (avg. 0-9yo)	**1**	**2**	**3**	**4**	**5**	**6**	**7**	**8**	**9**
1. Physical abuse									
2. Emotional abuse	.64**								
3. Neglect	.27**	.22**							
5. Maternal depression	.22**	.13**	.19**						
4. Intimate partner violence	.10**	.05*	.14**	.19**					
6. Parental stress	.23**	.18**	.24**	.26**	.15**				
7. Residential moves	.14**	.12**	.09**	.20**	.06**	.08**			
8. Lack of community cohesion	.22**	.16**	.14**	.19**	.14**	.19**	.14**		
9. Lack of community control	.09**	.09**	.12**	.09**	.13**	.14**	.11**	.56**	
10. Neighborhood violence	.18**	.14**	.13**	.15**	.07**	.13**	.08**	.31**	.15**

*Note. * indicates p < .05. ** indicates p < .01.*

Supplemental Table 4-5. Model fit indices between latent profile classes

Model	Log-likelihood (LL) (df)	% reduction in LL	AIC	BIC	ABIC	Entropy
2-class	-45462.39 (32)	NA	90988.77	91191.82	91090.14	0.78
3-class	-44309.84 (44)	2.54***	88707.68	88986.87	88847.06	0.76
4-class	-43538.83 (56)	1.74***	87189.66	87544.99	87367.05	0.82
5-class	-43033.89 (68)	1.16***	86203.79	86635.26	86419.19	0.79
6-class	-48469.01 (80)	-12.63	97098.02	97605.64	97351.43	0.78

*Note. ***p<.001 in likelihood ratio test. AIC indicates Akaike Information Criteria. BIC indicates Bayesian Information Criteria. ABIC indicates adjusted BIC.*

Supplemental Table 4-6. Average posterior probabilities of assigned profile membership (4-class model)

Class membership	Probability of being assigned to latent profile				Descriptive	
	Class 1	Class 2	Class 3	Class 4	Range	% <.70
1	**.87**	*.13*	*.00*	*.00*	.43 – 1.00	4 %
2	*.06*	**.91**	*.01*	*.02*	.50 – 1.00	5 %
3	*.00*	*.02*	**.92**	*.06*	.42 – 1.00	1 %
4	*.00*	*.05*	*.03*	**.92**	.47 – 1.00	1 %

Note. High classification quality is determined by high diagonal average posterior probabilities values (as close to 1; in bold) and low off-diagonal values (as close to 0; in italics) (Muthén & Muthén, 2000)*. Range indicates the range of posterior probabilities within the specific class. % <.70 indicates the sample proportion with posterior probability of less than .70 with the specific class membership.*

Supplemental Table 4-7. Average posterior probabilities of the 3-class and 5-class models

Class membership	**Probability of latent profile assignment**			**Descriptive**	
	Class 1	Class 2	Class 3	Range	% <.70
1	**.87**	*.13*	*.00*	.43 – 1.00	5 %
2	*.06*	**.90**	*.05*	.46 – 1.00	6 %
3	*.00*	*.09*	**.91**	.50 – 1.00	2 %

Class membership	**Probability of latent profile assignment**					**Descriptive**	
	Class 1	Class 2	Class 3	Class 4	Class 5	Range	% < .70
1	**.82**	*.12*	*.06*	*.00*	*.00*	.35 – 1.00	5 %
2	*.10*	**.77**	*.13*	*.00*	*.00*	.36 – 1.00	8 %
3	*.02*	*.05*	**.89**	*.01*	*.02*	.33 – 1.00	5 %
4	*.00*	*.00*	*.03*	**.93**	*.05*	.48 – 1.00	1 %
5	*.00*	*.00*	*.05*	*.04*	**.92**	.49 – 1.00	0.9 %

Note. High classification quality is determined by high diagonal average posterior probabilities values (as close to 1; in bold) and low off-diagonal values (as close to 0; in italics) (Muthén & Muthén, 2000)*. Range indicates the range of posterior probabilities within the specific class. % <.70 indicates the sample proportion with posterior probability of less than .70 with the specific class membership.*

Supplemental Table 4-8. Supplementary latent profile analyses (4-class model) leaving one site out

	N	AIC	BIC	ABIC	Entropy	Low-adversity *No.* (%)	Medium-adversity *No.* (%)	Maternal Depression *No.* (%)	High-adversity *No.* (%)
All sites	4210	87189.66	87544.99	87367.05	0.82	1230 (29%)	1230 (47%)	550 (13%)	457 (11%)
Site 1 out	3929	81222.94	81574.40	81396.46	0.82	1204 (31%)	1204 (46%)	507 (13%)	401 (10%)
Site 2 out	3928	81504.20	81855.65	81677.71	0.82	1182 (30%)	1182 (46%)	505 (13%)	423 (11%)
Site 3 out	3916	80857.59	81208.87	81030.93	0.82	1167 (30%)	1167 (46%)	522 (13%)	424 (11%)
Site 4 out	3927	80808.92	81160.36	80982.42	0.82	1180 (30%)	1180 (46%)	504 (13%)	430 (11%)
Site 5 out	3936	81203.29	81554.85	81376.91	0.82	1167 (30%)	1167 (46%)	513 (13%)	438 (11%)
Site 6 out	3910	80574.01	80925.20	80747.26	0.82	1160 (30%)	1160 (47%)	495 (13%)	427 (11%)
Site 7 out	3943	81422.73	81774.40	81596.45	0.82	1147 (29%)	1147 (47%)	512 (13%)	422 (11%)
Site 8 out	3914	81318.65	81669.90	81491.96	0.82	1115 (28%)	1115 (47%)	517 (13%)	429 (11%)
Site 9 out	3924	81173.05	81524.44	81346.50	0.82	1169 (30%)	1169 (47%)	517 (13%)	407 (10%)
Site 10 out	3898	80571.40	80922.42	80744.47	0.82	1145 (29%)	1145 (47%)	500 (13%)	415 (11%)
Site 11 out	3898	81485.90	81836.92	81658.97	0.82	1092 (28%)	1092 (47%)	520 (13%)	443 (11%)
Site 12 out	3940	81872.98	82224.60	82046.66	0.82	1179 (30%)	1179 (46%)	531 (13%)	414 (11%)
Site 13 out	4120	85330.99	85685.11	85507.17	0.82	1197 (29%)	1197 (47%)	537 (13%)	443 (11%)
Site 14 out	4124	85470.72	85824.90	85646.96	0.82	1198 (29%)	1198 (47%)	524 (13%)	460 (11%)
Site 15 out	4074	84521.67	84875.16	84697.22	0.82	1199 (29%)	1199 (46%)	542 (13%)	443 (11%)
Site 16 out	4122	85385.23	85739.38	85561.44	0.82	1204 (29%)	1204 (47%)	539 (13%)	442 (11%)
Site 17 out	4121	85481.38	85835.52	85657.57	0.82	1214 (29%)	1214 (47%)	537 (13%)	450 (11%)
Site 18 out	4122	85403.94	85758.09	85580.15	0.82	1150 (28%)	1150 (48%)	528 (13%)	467 (11%)
Site 19 out	4119	85515.74	85869.84	85691.90	0.82	1191 (29%)	1191 (47%)	534 (13%)	456 (11%)
Site 20 out	4125	85416.84	85771.03	85593.08	0.82	1206 (29%)	1206 (47%)	534 (13%)	454 (11%)

Note. AIC indicates Akaike Information Criteria. BIC indicates Bayesian Information Criteria. ABIC indicates adjusted BIC. A list of each site is available on Supplemental Table 4-1 and Supplemental Table 4-2.

Supplemental Table 4-9. Descriptives of each adversity latent profile in the neuroimaging subsample (*N*=167)

	Low-adversity (*n*=38)	**Medium-adversity (*n*=83)**	**Maternal Depression (*n*=22)**	**High-adversity (*n*=24)**	**Statistical test**
Ethnoracial identity, No. (%)					
Black (non-Hispanic)	24 (63.2)	66 (79.5)	18 (81.8)	20 (83.3)	$\chi(3) = 5.17$, $p = .16$
White (non-Hispanic)	8 (21.1)	8 (9.6)	3 (13.6)	1 (4.2)	
Hispanic	3 (7.9)	8 (9.6)	0 (0)	0 (0)	
Other/multi	3 (7.9)	1 (1.2)	1 (4.6)	3 (12.5)	
Sex at birth, No. (%)					
Female	26 (68.4)	43 (51.8)	9 (40.9)	13 (54.2)	$\chi(3) = 4.85$, $p = .18$
Male	12 (31.6)	40 (48.2)	13 (59.1)	11 (45.8)	
Parental marital status, No. (%)					
Married	13 (34.2)	16 (19.3)	6 (27.3)	2 (8.3)	$\chi(3) = 6.59$, $p = .09$
Unmarried	25 (65.8)	67 (80.7)	16 (72.7)	22 (91.7)	
Poverty ratio *M* (*SD*)	3.33 (3.19)	1.93 (2.03)	1.84 (1.69)	1.04 (1.07)	$F(3,163) = 5.97$, $p < .001$

Note. Chi-square test for ethnoracial identity was conducted using two groups (Black vs non).

Supplemental Table 4-10. Mean and standard deviation of adversity for each profile (N=4210)

Indicators	**Low-adversity *M (SD)***	**Medium-adversity *M (SD)***	**Maternal depression *M (SD)***	**High-adversity *M (SD)***	***F* value**
Emotional abuse	0.69 (0.29)	0.97 (0.37)	1.04 (0.34)	1.11 (0.43)	169.2***
Physical abuse	0.58 (0.38)	0.94 (0.51)	0.98 (0.49)	1.02 (0.58)	124.4***
Neglect	0.09 (0.27)	0.39 (0.41)	0.47 (0.69)	0.58 (1.74)	313***
Maternal depression	0.04 (0.16)	0.27 (0.38)	2.11 (0.59)	1.12 (1.03)	2675***
Intimate partner violence	0.05 (0.16)	0.31 (0.51)	0.33 (0.51)	1.96 (1.83)	666.9***
Parental stress	0.67 (0.30)	0.95 (0.42)	1.08 (0.40)	1.13 (0.48)	242.1***
Residential moves	0.48 (0.40)	0.78 (0.62)	0.91 (0.71)	1.09 (1.05)	127***
Lack of social cohesion	0.55 (0.30)	0.99 (0.41)	0.98 (0.43)	1.20 (0.50)	347.4***
Lack of social control	0.41 (0.34)	0.95 (0.59)	0.83 (0.57)	1.09 (0.73)	236.6***

Neighborhood violence	0.11 (0.23)	0.52 (0.65)	0.51 (0.62)	1.60 (1.57)	341.9***

*Note. Mean and standard deviation above are based on standardized values. ***p < .001.*

Supplemental Table 4-11. Mean and standard deviation of adversity in the neuroimaging subsample (N=167)

Indicators	**Low-adversity** ***M (SD)***	**Medium-adversity** ***M (SD)***	**Maternal depression** ***M (SD)***	**High-adversity** ***M (SD)***	***F* value**
Emotional abuse	0.67 (0.20)	0.93 (0.34)	1.06 (0.29)	1.22 (0.35)	15.6***
Physical abuse	0.60 (0.29)	0.92 (0.43)	0.99 (0.38)	1.17 (0.42)	10.1***
Neglect	0.02 (0.11)	0.26 (0.44)	0.5 (0.55)	1.73 (1.71)	27.55***
Maternal depression	0.02 (0.11)	0.28 (0.37)	1.85 (0.55)	1.40 (0.9)	104***
Intimate partner violence	0.07 (0.22)	0.34 (0.60)	0.55 (0.76)	1.46 (1.62)	13.69***
Parental stress	0.68 (0.28)	0.87 (0.41)	1.04 (0.40)	1.27 (0.35)	13.39***
Residential moves	0.42 (0.36)	0.72 (0.56)	0.89 (0.67)	1.25 (0.97)	9.59***
Lack of social cohesion	0.58 (0.32)	0.95 (0.37)	0.91 (0.36)	1.29 (0.41)	18.21***
Lack of social control	0.40 (0.32)	0.82 (0.57)	0.85 (0.49)	1.29 (0.77)	11.98***
Neighborhood violence	0.14 (0.22)	0.62 (0.62)	0.40 (0.54)	1.70 (0.996)	30.4***

*Note. Mean and standard deviation above are based on standardized values. ***p < .001.*

Supplemental Table 4-12. Pairwise test comparing adversity levels among latent profiles

	Pairwise contrast	**Mean difference**	**95% CI Lower bound**	**95% CI Upper bound**	p_{adjust}
Emotional abuse	Med – Low	0.278	0.238	0.318	<.001
	MD – Low	0.348	0.293	0.403	<.001
	High – Low	0.419	0.360	0.479	<.001
	MD – Med	0.070	0.020	0.120	.002
	High – Med	0.141	0.086	0.197	<.001
	High – MD	0.072	0.004	0.139	.031
Physical abuse	Med – Low	0.359	0.305	0.413	<.001
	MD – Low	0.398	0.323	0.473	<.001
	High – Low	0.444	0.363	0.526	<.001
	MD – Med	0.039	-0.030	0.108	.469
	High – Med	0.085	0.009	0.161	.020
	High – MD	0.046	-0.046	0.138	.566
Neglect	Med – Low	0.300	0.213	0.387	<.001
	MD – Low	0.380	0.260	0.500	<.001

	High – Low	1.52	1.391	1.650	<.001
	MD – Med	0.080	-0.030	0.189	.245
	High – Med	1.220	1.100	1.340	<.001
	High – MD	1.141	0.995	1.287	<.001
Maternal depression	Med – Low	0.235	0.189	0.282	<.001
	MD – Low	2.077	2.011	2.142	<.001
	High – Low	1.082	1.012	1.152	<.001
	MD – Med	1.841	1.780	1.903	<.001
	High – Med	0.847	0.781	0.913	<.001
	High – MD	-0.995	-1.075	-0.914	<.001
Intimate partner violence	Med – Low	0.266	0.192	0.340	<.001
	MD – Low	0.283	0.174	0.392	<.001
	High – Low	1.909	1.797	2.022	<.001
	MD – Med	0.017	-0.086	0.120	.974
	High – Med	1.645	1.537	1.751	<.001
	High – MD	1.626	1.493	1.760	<.001
Parental stress	Med – Low	0.284	0.247	0.321	<.001
	MD – Low	0.408	0.356	0.460	<.001
	High – Low	0.462	0.407	0.518	<.001
	MD – Med	0.124	0.076	0.173	<.001
	High – Med	0.178	0.126	0.231	<.001
	High – MD	0.054	-0.010	0.118	.136
Residential moves	Med – Low	0.295	0.235	0.355	<.001
	MD – Low	0.425	0.341	0.510	<.001
	High – Low	0.612	0.522	0.703	<.001
	MD – Med	0.131	0.051	0.210	<.001
	High – Med	0.317	0.232	0.403	<.001
	High – MD	0.187	0.082	0.291	<.001
Lack of social cohesion	Med – Low	0.442	0.400	0.483	<.001
	MD – Low	0.425	0.367	0.483	<.001
	High – Low	0.647	0.584	0.710	<.001
	MD – Med	-0.017	-0.037	0.071	.852
	High – Med	0.205	0.146	0.264	<.001
	High – MD	0.222	0.150	0.294	<.001
Lack of social control	Med – Low	0.538	0.481	0.595	<.001
	MD – Low	0.420	0.339	0.500	<.001
	High – Low	0.687	0.600	0.773	<.001
	MD – Med	-0.119	-0.193	-0.044	<.001
	High – Med	0.148	0.067	0.230	<.001
	High – MD	0.267	0.168	0.366	<.001
Neighborhood violence	Med – Low	0.408	0.328	0.489	<.001
	MD – Low	0.397	0.285	0.508	<.001
	High – Low	1.490	1.370	1.610	<.001
	MD – Med	-0.011	-0.091	0.114	.992
	High – Med	1.093	0.971	1.193	<.001
	High – MD	1.082	0.958	1.229	<.001

Supplemental Table 4-13. Comparison of youth internalizing and externalizing among adversity profiles

Internalizing				
		95% confidence interval		
Contrast	**Mean Difference**	**Lower bound**	**Upper bound**	**Adjusted *p***
Med – Low	0.188	0.104	0.272	<.001
MD – Low	0.348	0.231	0.466	<.001
High – Low	0.462	0.336	0.589	<.001
Med – MD	-0.160	-0.269	-0.051	.001
High – Med	0.274	0.155	0.393	<.001
High – MD	0.114	-0.030	0.259	.177

Externalizing				
		95% confidence interval		
Contrast	**Mean Difference**	**Lower bound**	**Upper bound**	**Adjusted *p***
Med – Low	0.247	0.175	0.319	<.001
MD – Low	0.370	0.269	0.471	<.001
High – Low	0.496	0.387	0.605	<.001
Med – MD	-0.123	-0.217	-0.029	.004
High – Med	0.249	0.147	0.351	<.001
High – MD	0.126	0.002	0.250	.046

Supplemental Table 4-14. Comparison of youth internalizing and externalizing among adversity profiles, adjusting for covariates

Internalizing					
	df	**Sum Sq**	**Mean Sq**	***F* value**	***p* value**
Adversity profiles	3	64.6	21.520	33.857	<.001
White non-Hispanic	1	4.3	4.273	6.722	.010
Hispanic	1	7.4	7.422	11.677	<.001
Other/multi	1	3.0	3.000	4.719	.030
Parental marital status	1	4.8	4.783	7.525	.006
Poverty ratio	1	0.5	0.538	0.846	.358
Residuals	3022	1920.8	0.636		

Pairwise test				
		95% confidence interval		
Contrast	**Mean Difference**	**Lower bound**	**Upper bound**	**Adjusted *p***
Med – Low	0.196	0.107	0.285	<.001
MD – Low	0.351	0.227	0.474	<.001
High – Low	0.462	0.327	0.597	<.001

Med – MD	-0.155	-0.270	-0.040	.003
High – Med	0.266	0.140	0.393	<.001
High – MD	0.112	-0.042	0.265	.241

Externalizing					
	df	**Sum Sq**	**Mean Sq**	***F* value**	***p* value**
Adversity profiles	3	75.3	25.114	55.884	<.001
White non-Hispanic	1	1.4	1.366	3.040	.081
Hispanic	1	2.6	2.612	5.812	.016
Other/multi	1	0.9	0.855	1.903	.168
Parental marital status	1	22.4	22.387	49.816	<.001
Poverty ratio	1	10.8	10.773	23.972	<.001
Residuals	3021	1357.6	0.449		

Pairwise test		**95% confidence interval**		
Contrast	**Mean Difference**	**Lower bound**	**Upper bound**	**Adjusted *p***
Med – Low	0.251	0.176	0.326	<.001
MD – Low	0.365	0.261	0.469	<.001
High – Low	0.498	0.385	0.612	<.001
Med – MD	-0.114	-0.211	-0.017	.013
High – Med	0.247	0.141	0.354	<.001
High – MD	0.133	0.005	0.262	.039

Supplemental Table 4-15. Comparison of functional connectivity density among adversity profiles

Overall Network Density		**95% confidence interval**		
Contrast	**Mean Difference**	**Lower bound**	**Upper bound**	**Adjusted *p***
Med – Low	-2.373	-5.608	0.863	.231
MD – Low	-1.450	-5.875	2.975	.830
High – Low	5.868	1.562	10.175	.003
Med – MD	-0.923	-4.884	3.038	.930
High – Med	8.241	4.413	12.069	<.001
High – MD	7.318	2.443	12.194	<.001

DMN Density		
	95% confidence interval	

Contrast	Mean Difference	95% confidence interval		Adjusted *p*
		Lower bound	Upper bound	
Med – Low	-0.005	-0.019	0.008	.724
MD – Low	0.019	0.0002	0.037	.046
High – Low	0.026	0.007	0.044	.002
Med – MD	-0.024	-0.041	-0.008	.001
High – Med	0.031	0.015	0.047	<.001
High – MD	0.007	-0.014	0.027	.834

SN Density				
Contrast	Mean Difference	95% confidence interval		Adjusted *p*
		Lower bound	Upper bound	
Med – Low	-0.005	-0.018	0.007	.672
MD – Low	-0.010	-0.027	0.008	.496
High – Low	-0.020	-0.037	-0.003	.017
Med – MD	0.004	-0.012	0.020	.906
High – Med	-0.014	-0.030	0.001	.075
High – MD	-0.010	-0.030	0.009	.527

FPN Density				
Contrast	Mean Difference	95% confidence interval		Adjusted *p*
		Lower bound	Upper bound	
Med – Low	0.016	0.002	0.030	.015
MD – Low	0.005	-0.014	0.024	.903
High – Low	0.052	0.033	0.070	<.001
Med – MD	0.011	-0.006	0.028	.326
High – Med	0.036	0.019	0.052	<.001
High – MD	0.047	0.026	0.068	<.001

Supplemental Table 4-16. Comparison of functional connectivity density among profiles, adjusting for covariates

Overall Network Density					
	df	**Sum Sq**	**Mean Sq**	***F* value**	***p* value**
Adversity profiles	3	1294	431.2	12.637	<.001
White non-Hispanic	1	45	45.3	1.328	.251
Hispanic	1	64	64.2	1.882	.172
Other/multi	1	0	0.1	0.002	.964
Parental marital status	1	87	86.9	2.545	.113

Poverty ratio	1	135	144.9	4.245	.041
Age during neuroimaging scan	1	4	4.2	0.124	.725
Framewise displacement	1	932	931.7	27.303	<.001
Residuals	156	5323	34.1		

Pairwise test		95% confidence interval		
Contrast	**Mean Difference**	**Lower bound**	**Upper bound**	**Adjusted *p***
Med – Low	-2.373	-5.344	0.599	.166
MD – Low	-1.450	-5.514	2.614	.791
High – Low	5.868	1.913	9.824	.001
Med – MD	-0.923	-4.560	2.715	.912
High – Med	8.241	4.725	11.757	<.001
High – MD	7.318	2.841	11.796	<.001

DMN Density					
	df	**Sum Sq**	**Mean Sq**	**F value**	***p* value**
Adversity profiles	3	0.024	0.008	11.178	<.001
White non-Hispanic	1	0.004	0.004	5.993	.016
Hispanic	1	0.000	0.000	0.027	.870
Other/multi	1	0.000	0.000	0.263	.609
Parental marital status	1	0.000	0.000	0.238	.627
Poverty ratio	1	0.000	0.000	0.095	.759
Age during neuroimaging scan	1	0.000	0.001	0.964	.328
Framewise displacement	1	0.000	0.000	0.001	.970
Residuals	156	0.112	0.001		

Pairwise test		95% confidence interval		
Contrast	**Mean Difference**	**Lower bound**	**Upper bound**	**Adjusted *p***
Med – Low	-0.005	0.019	0.008	.723
MD – Low	0.019	0.0002	0.037	.046
High – Low	0.026	0.007	0.044	.002
Med – MD	-0.024	-0.041	-0.008	.001
High – Med	0.031	0.015	0.047	<.001
High – MD	0.006	-0.014	0.027	.833

SN Density					
	df	**Sum Sq**	**Mean Sq**	**F value**	***p* value**
Adversity profiles	3	0.006	0.002	3.241	.024

White non-Hispanic	1	0.000	0.000	0.159	.691
Hispanic	1	0.002	0.002	3.702	.056
Other/multi	1	0.001	0.001	1.218	.271
Parental marital status	1	0.001	0.001	1.92	.168
Poverty ratio	1	0.002	0.002	3.288	.072
Age during neuroimaging scan	1	0.000	0.000	0.11	.740
Framewise displacement	1	0.001	0.001	0.868	.353
Residuals	156	0.098	0.001		

Pairwise test		95% confidence interval		
Contrast	**Mean Difference**	**Lower bound**	**Upper bound**	**Adjusted *p***
Med – Low	-0.005	-0.018	0.007	.683
MD – Low	-0.010	-0.027	0.008	.485
High – Low	-0.020	-0.037	-0.003	.015
Med – MD	0.004	-0.012	0.020	.902
High – Med	-0.014	-0.029	0.001	.070
High – MD	-0.010	-0.029	0.009	.516

FPN Density					
	df	**Sum Sq**	**Mean Sq**	**F value**	***p* value**
Adversity profiles	3	0.043	0.014	18.897	<.001
White non-Hispanic	1	0.000	0.000	0.311	.578
Hispanic	1	0.002	0.002	3.246	.073
Other/multi	1	0.000	0.000	0.076	.782
Parental marital status	1	0.000	0.000	0.251	.617
Poverty ratio	1	0.000	0.000	0.053	.817
Age during neuroimaging scan	1	0.000	0.000	0.373	.542
Framewise displacement	1	0.002	0.002	2.124	.147
Residuals	156	0.119	0.001		

Pairwise test		95% confidence interval		
Contrast	**Mean Difference**	**Lower bound**	**Upper bound**	**Adjusted *p***
Med – Low	0.016	0.002	0.030	.016
MD – Low	0.005	-0.014	0.024	.903
High – Low	0.052	0.033	0.070	<.001
Med – MD	0.011	-0.006	0.028	.327
High – Med	0.036	0.019	0.052	<.001
High – MD	0.047	0.026	0.068	<.001

Supplemental Table 4-17. Comparison of network connectivity metrics estimated using neuroimaging data during emotional faces task vs resting state data

Overall density	**df**	**SSn**	**SSd**	***F***	**ges**	***p* value**
Between groups	3, 150	2138.24	7609.44	14.05	.136	<.001
Within (scan type)	1, 150	1372.49	6001.06	34.31	.092	<.001
Between:Within	3, 150	93.50	6001.06	0.78	.007	.507

DMN density						
	df	**SSn**	**SSd**	***F***	**ges**	***p* value**
Between groups	3, 150	0.01	0.12	5.81	.061	<.001
Within (scan type)	1, 150	0.00	0.09	0.03	<.001	.857
Between:Within	3, 150	0.01	0.09	7.52	.063	<.001
Task – Rest pairwise test						
Profile	**Estimate**	***SE***	**df**	***t***	**Adjusted *p***	
Low-adversity	0.014	0.006	150	2.329	.021	
Medium-adversity	-0.014	0.004	150	-3.568	.001	
Maternal Depression	0.014	0.008	150	1.891	.061	
High-adversity	-0.012	0.007	150	-1.614	.109	

SN density	**df**	**SSn**	**SSd**	**F**	**ges**	***p* value**
Between groups	3, 150	0.01	0.12	3.71	.041	.013
Within (scan type)	1, 150	0.01	0.09	9.71	.026	.002
Between:Within	3, 150	0.01	0.09	5.22	.042	.002
Task – Rest pairwise test						
Profile	**Estimate**	***SE***	**df**	***t***	**Adjusted *p***	
Low-adversity	0.008	0.006	150	1.364	.175	
Medium-adversity	-0.005	0.004	150	-1.184	.238	
Maternal Depression	-0.027	0.007	150	-3.696	<.001	
High-adversity	-0.015	0.007	150	-2.068	.040	

FPN density	**df**	**SSn**	**SSd**	**F**	**ges**	***p* value**
Between groups	3, 150	0.03	0.11	11.47	.109	<.001
Within (scan type)	1, 150	0.00	0.10	0.26	<.001	.613
Between:Within	3, 150	0.03	0.10	16.56	.133	<.001
Task – Rest pairwise test						
Profile	**Estimate**	***SE***	**df**	***t***	**Adjusted *p***	
Low-adversity	-0.034	0.006	150	-5.469	<.001	
Medium-adversity	0.006	0.004	150	1.447	.150	
Maternal Depression	0.003	0.008	150	0.378	.706	
High-adversity	0.032	0.008	150	4.194	<.001	

Supplemental Table 4-18. Exploratory analysis comparing youth internalizing and externalizing among adversity profiles, stratified by sex

Internalizing (Females)					
	df	**Sum Sq**	**Mean Sq**	**F value**	***p* value**
Adversity profiles	3	31.200	10.393	15.190	<.001
Residuals	1589	1087.200	0.684		

Pairwise test		**95% confidence interval**		
Contrast	**Mean Difference**	**Lower bound**	**Upper bound**	**Adjusted *p***
Med – Low	0.183	0.058	0.309	.001
MD – Low	0.385	0.206	0.565	<.001
High – Low	0.402	0.206	0.597	<.001
Med – MD	-0.202	-0.370	-0.034	.011
High – Med	0.218	0.034	0.403	.013
High – MD	0.016	-0.208	0.241	.998

Internalizing (Males)					
	df	**Sum Sq**	**Mean Sq**	**F value**	***p* value**
Adversity profiles	3	43.200	14.400	25.700	<.001
Residuals	1740	975.000	0.560		

Pairwise test		**95% confidence interval**		
Contrast	**Mean Difference**	**Lower bound**	**Upper bound**	**Adjusted *p***
Med – Low	0.195	0.084	0.306	<.001
MD – Low	0.326	0.174	0.479	<.001
High – Low	0.524	0.360	0.687	<.001
Med – MD	-0.131	-0.272	0.010	.080
High – Med	0.329	0.176	0.482	<.001
High – MD	0.198	0.012	0.383	.032

Externalizing (Females)					
	df	**Sum Sq**	**Mean Sq**	**F value**	***p* value**
Adversity profiles	3	43.400	14.461	34.630	<.001
Residuals	1589	663.500	0.418		

Pairwise test		**95% confidence interval**		
Contrast	**Mean Difference**	**Lower bound**	**Upper bound**	**Adjusted *p***
Med – Low	0.277	0.179	0.375	<.001
MD – Low	0.468	0.328	0.608	<.001

High – Low	0.427	0.274	0.579	<.001
Med – MD	-0.191	-0.322	-0.060	.001
High – Med	0.149	0.005	0.293	.038
High – MD	-0.042	-0.217	0.134	.929

Externalizing (Males)					
	df	**Sum Sq**	**Mean Sq**	**F value**	***p* value**
Adversity profiles	3	43.100	14.350	29.350	<.001
Residuals	1739	850.100	0.489		
Pairwise test		**95% confidence interval**			
Contrast	**Mean Difference**	**Lower bound**	**Upper bound**	**Adjusted *p***	
Med – Low	0.216	0.112	0.319	<.001	
MD – Low	0.276	0.133	0.418	<.001	
High – Low	0.540	0.387	0.693	<.001	
Med – MD	-0.060	-0.192	0.072	.645	
High – Med	0.324	0.181	0.467	<.001	
High – MD	0.264	0.091	0.438	.001	

Supplemental Table 4-19. Exploratory analysis comparing functional connectivity density among adversity profiles, stratified by sex

Overall Network Density (Females)					
	df	**Sum Sq**	**Mean Sq**	**F value**	***p* value**
Adversity profiles	3	465.600	155.200	5.465	.002
Residuals	87	2470.900	28.400		
Pairwise test		**95% confidence interval**			
Contrast	**Mean Difference**	**Lower bound**	**Upper bound**	**Adjusted *p***	
Med – Low	-2.261	-5.729	1.207	.326	
MD – Low	-2.863	-8.262	2.536	.509	
High – Low	4.154	-0.588	8.896	.107	
Med – MD	0.602	-4.515	5.719	.990	
High – Med	6.415	1.997	10.833	.001	
High – MD	7.017	0.964	13.070	.016	

Overall Network Density (Males)					
	df	**Sum Sq**	**Mean Sq**	**F value**	***p* value**
Adversity profiles	3	928.000	309.250	5.526	.002

Residuals	72	4029.000	55.960		

Pairwise test		95% confidence interval		
Contrast	**Mean Difference**	**Lower bound**	**Upper bound**	**Adjusted *p***
Med – Low	-2.300	-8.776	4.176	.787
MD – Low	-0.212	-8.088	7.664	1.000
High – Low	8.068	-0.144	16.281	.056
Med – MD	-2.088	-8.370	4.193	.818
High – Med	10.368	3.670	17.066	.001
High – MD	8.280	0.220	16.340	.042

DMN Density (Females)					
	df	**Sum Sq**	**Mean Sq**	**F value**	***p* value**
Adversity profiles	3	0.014	0.005	5.770	.001
Residuals	87	0.071	0.001		

Pairwise test		95% confidence interval		
Contrast	**Mean Difference**	**Lower bound**	**Upper bound**	**Adjusted *p***
Med – Low	-0.009	-0.028	0.009	.572
MD – Low	0.015	-0.014	0.044	.517
High – Low	0.026	0.000	0.051	.048
Med – MD	-0.024	-0.052	0.003	.100
High – Med	0.035	0.011	0.058	.001
High – MD	0.010	-0.022	0.043	.837

DMN Density (Males)					
	df	**Sum Sq**	**Mean Sq**	**F value**	***p* value**
Adversity profiles	3	0.010	0.003	5.548	.002
Residuals	72	0.045	0.001		

Pairwise test		95% confidence interval		
Contrast	**Mean Difference**	**Lower bound**	**Upper bound**	**Adjusted *p***
Med – Low	0.000	-0.021	0.022	1.000
MD – Low	0.024	-0.002	0.050	.087
High – Low	0.027	0.000	0.055	.054
Med – MD	-0.024	-0.045	-0.003	.022
High – Med	0.027	0.004	0.049	.013
High – MD	0.003	-0.024	0.030	.989

SN Density (Females)					
	df	**Sum Sq**	**Mean Sq**	**F value**	***p* value**
Adversity profiles	3	0.004	0.001	1.692	.175
Residuals	87	0.070	0.001		

SN Density (Males)					
	df	**Sum Sq**	**Mean Sq**	**F value**	***p* value**
Adversity profiles	3	0.002	0.001	1.358	.263
Residuals	72	0.035	0.000		

FPN Density (Females)					
	df	**Sum Sq**	**Mean Sq**	**F value**	***p* value**
Adversity profiles	3	0.030	0.010	12.800	<.001
Residuals	87	0.067	0.001		

Pairwise test		**95% confidence interval**		
Contrast	**Mean Difference**	**Lower bound**	**Upper bound**	**Adjusted *p***
Med – Low	0.016	-0.002	0.034	.110
MD – Low	0.002	-0.026	0.030	.998
High – Low	0.056	0.032	0.081	<.001
Med – MD	0.014	-0.013	0.040	.528
High – Med	0.041	0.018	0.064	<.001
High – MD	0.054	0.023	0.086	<.001

FPN Density (Males)					
	df	**Sum Sq**	**Mean Sq**	**F value**	***p* value**
Adversity profiles	3	0.014	0.005	6.090	.001
Residuals	72	0.056	0.001		

Pairwise test		**95% confidence interval**		
Contrast	**Mean Difference**	**Lower bound**	**Upper bound**	**Adjusted *p***
Med – Low	0.016	-0.008	0.041	.284
MD – Low	0.007	-0.023	0.036	.933
High – Low	0.046	0.016	0.077	.001
Med – MD	0.010	-0.014	0.033	.688
High – Med	0.030	0.005	0.055	.013
High – MD	0.040	0.009	0.070	.005

Supplemental Figure 4-1. Exclusionary criteria for the neuroimaging subsample

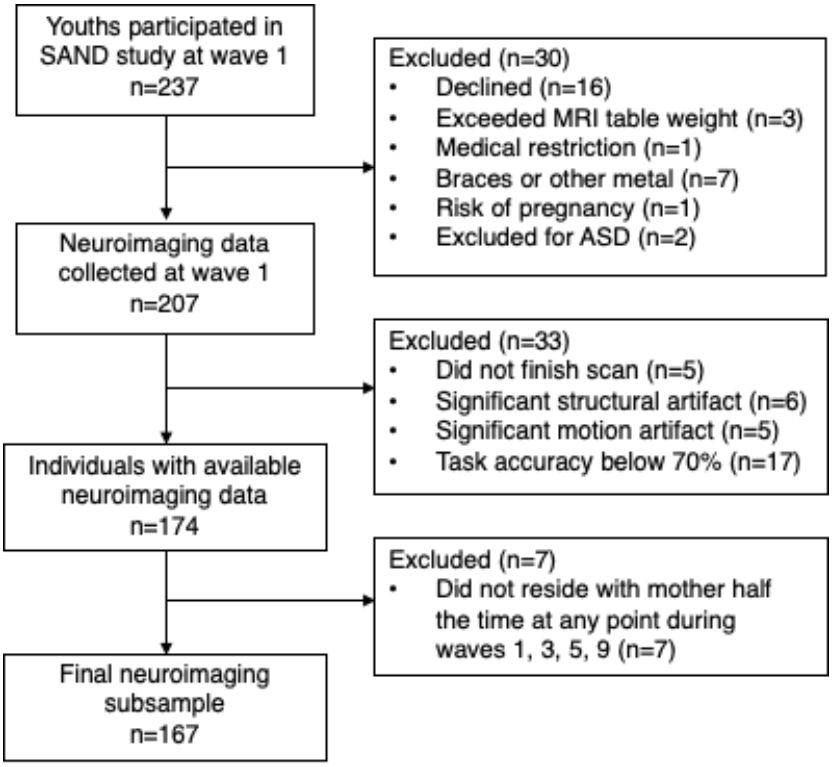

Supplemental Figure 4-2. fMRI task paradigm

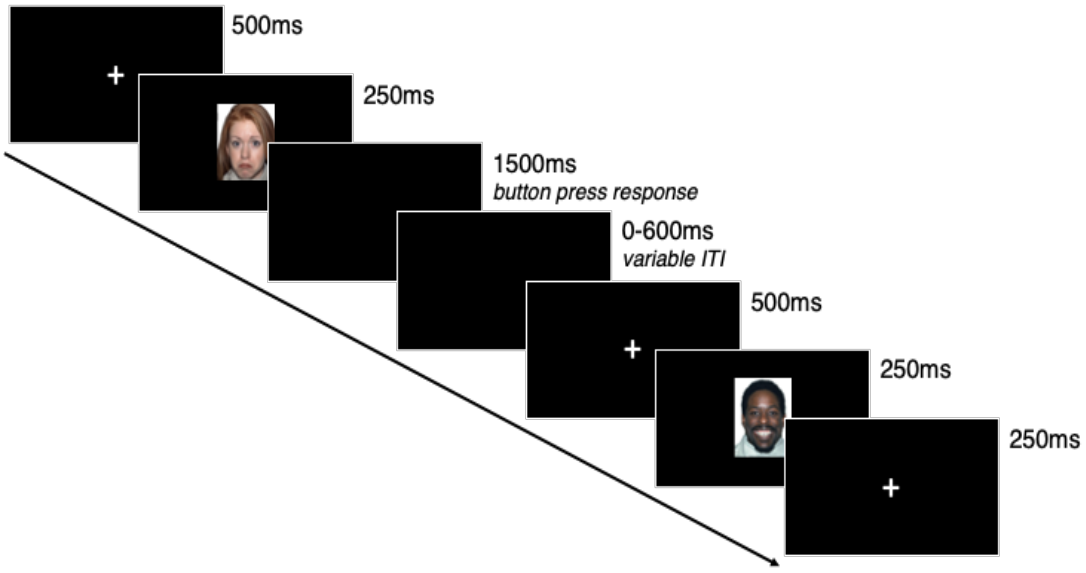

Note. Figure was previously reported in;(Hardi, Goetschius, McLoyd, et al., 2023)
ms denotes milliseconds. ITI denotes Inter Trial Interval.

Supplemental Figure 4-3. Internalizing latent factor structure and loadings

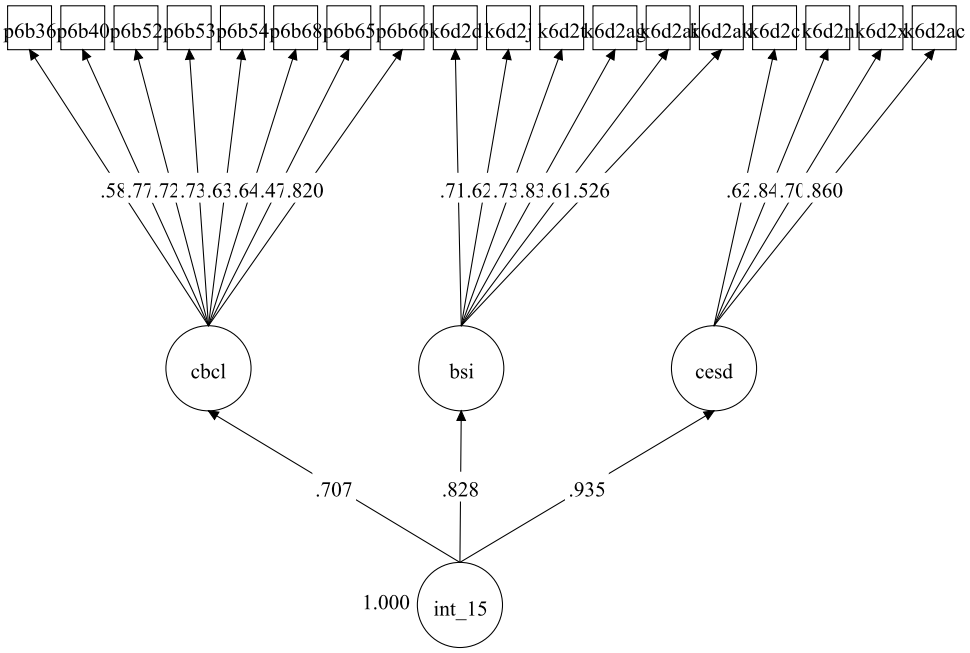

Note. CBCL indicates the Child Behavioral Checklist. BSI indicates the Brief Symptom Inventory 18. CES-D indicates the Center for Epidemiologic Studies Depression Scale. Model fit indices indicate adequate model fit (CFI = .931, TLI = .921, RMSEA = .065, SRMR = .075).

Supplemental Figure 4-4. Externalizing latent factor structure and loadings

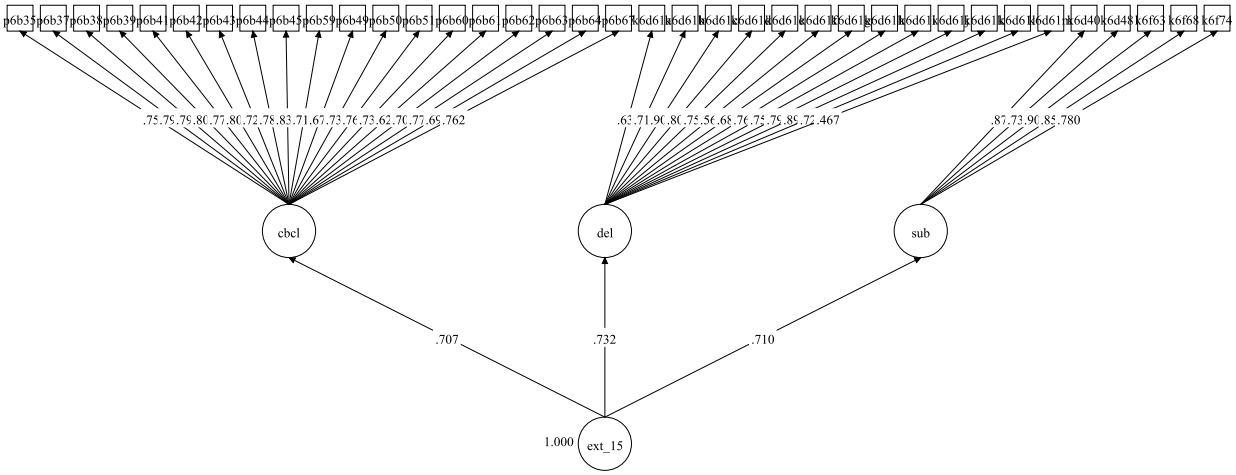

Note. CBCL indicates the Child Behavioral Checklist. DEL indicates the Delinquency scale adopted from the National Longitudinal Study of Adolescent Health (Add Health). SUB indicates youth-reported substance use. Model fit indices indicate excellent model fit (CFI = .955, TLI = .952, RMSEA = .031, SRMR = .092).

Supplemental Figure 4-5. Prevalence of adversity indicators for the 4-class model within the neuroimaging subsample (N=167)

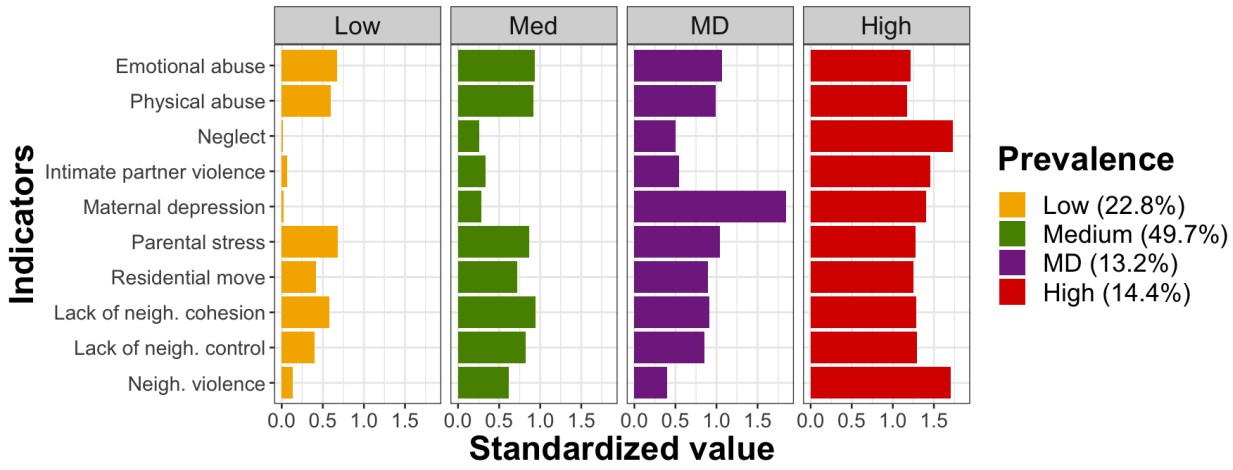

Note. MD denotes Maternal Depression profile

Supplemental Figure 4-6. Confirmatory Subgrouping Group Iterative Multiple Model Estimation network plots for each adversity profile

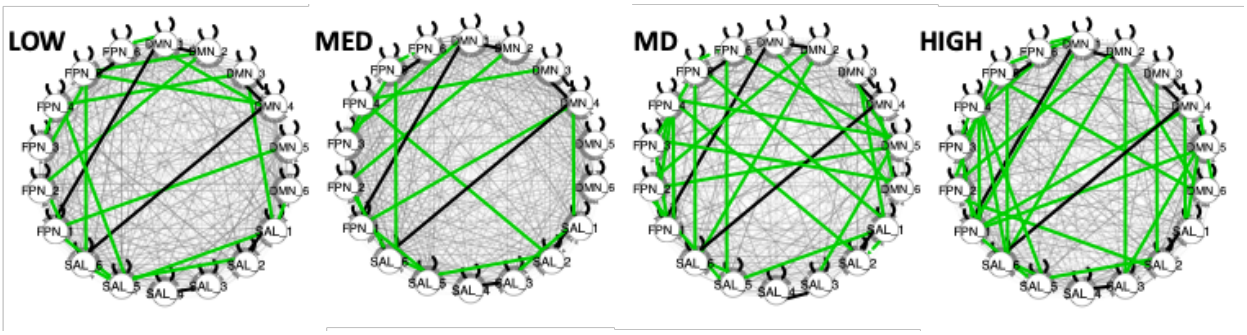

Note. Group-level connections (present for at least 75% of all individuals in the sample) are shown in black. Subgroup-level connections (present for at least 50% of individuals in each latent profile subgroup) are shown in green. Individual-level connections (present for each person) are shown in grey. Specific labels for the ROI represented by individual nodes (e.g., DMN_1) can be found on Supplementary Table 4-3 .

Supplemental Figure 4-7. Boxplot showing network density estimated using resting-state functional neuroimaging data

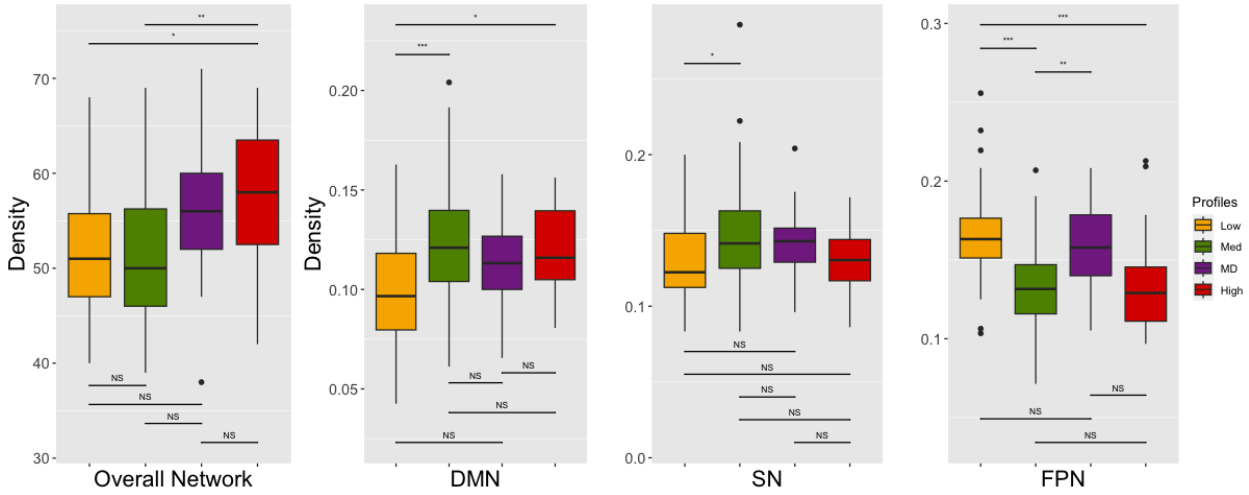

Note. *** $p_{adj} < .001$; ** $p_{adj} < .01$; * $p_{adj} < .05$; NS $p_{adj} > .05$

Supplemental Figure 4-8. Youth mental health, stratified by sex

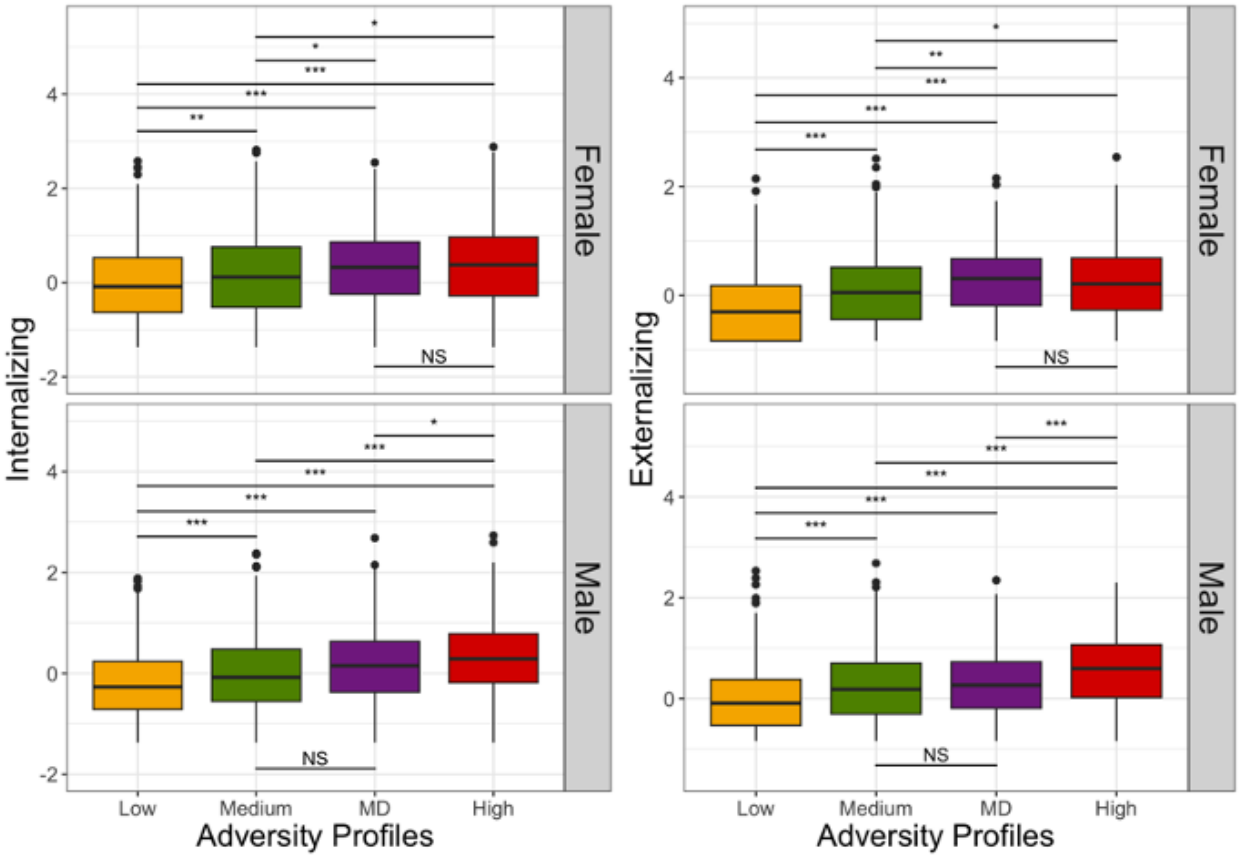

Note. *** $p_{adj} < .001$; ** $p_{adj} < .01$; * $p_{adj} < .05$; NS $p_{adj} > .05$

Chapter 5
General Discussion

Adverse and stressful experiences are significant contributors for the emergence of psychopathology across development. Existing research has focused on the neural mechanisms underlying adversity to establish how these experiences could differentially influence mental health. Despite progress, existing mechanistic processes have not adequately explained the broad heterogeneity in outcomes, nor have they predicted who may be at the greatest risk. This hinders our ability to identify precise targets for prevention and intervention. This dissertation aims to address these limitations by examining the neural mechanisms of adversity and psychopathology within a longitudinal, population-based birth cohort sample.

5.1 Summary

5.1.1 Chapter 2

The study described in Chapter 2 examines differential neural mechanisms underlying the effects of adversity on mental health. The study employed a longitudinal design over 21 years to demonstrate the long-term neural and behavioral consequences of childhood adversity. Findings revealed that increased household instability was associated with more efficient structural networks, and that adolescent structural brain networks indirectly explained the impact of early childhood household instability on depressive symptoms in young adulthood. These findings suggest a neural adaptation to an unpredictable environment, aligned with faster life history

strategies, with a potentially developmental cost later in life. Moreover, these associations remained evident after accounting for other types of adverse experiences, such as harsh parenting, neglect, economic deprivation, and various sociodemographic covariates, indicating that structural network development could represent a specific neural mechanism that explains the influence of environmental unpredictability on mental health.

5.1.2 Chapter 3

The study described in Chapter 3 utilized person-specific, data-driven functional connectivity subgroups to predict future mental health outcomes and susceptibility to stress. In this study, youth were initially clustered based on their network maps across key emotion-linked regions. The resulting subgroup memberships were then used to predict patterns of anxiety and depression across adolescence and young adulthood, and were examined in association with financial adversity during a highly stressful period (the COVID-19 pandemic). Results revealed two subgroups: one more heterogeneous, characterized by greater variation in individual-specific networks and higher network density, especially in regions such as the amygdala, subgenual anterior cingulate, and striatum; and one more homogeneous, characterized by lower network density and greater involvement of the insula and dorsal anterior cingulate cortex. Compared to the homogeneous subgroup, the heterogeneous subgroup experienced escalating trajectories of anxiety symptoms from ages 15 to 21 and exhibited greater anxiety symptoms in response to economic adversity during the pandemic. These findings collectively suggest the potential neural signatures of susceptibility and resilience to stress related to anxiety, established using a data-driven personalized network approach in connectivity mapping and clustering.

5.1.3 Chapter 4

The study described in Chapter 4 addressed heterogeneity in childhood adverse experiences by identifying data-driven, person-centered adversity profiles based on experiences across multiple contexts. Subsequent mental health outcomes and functional brain networks associated with these profiles were then examined. Findings identified four latent, multi-domain childhood adversity profiles: Low-adversity, Medium-adversity, High-adversity, and one profile with markedly high exposure to maternal depression (MD profile). Despite the similarities in levels of childhood adversity between individuals in the Medium-adversity and MD profiles, youth in the MD profile had characteristics of mental health and brain function more closely resembling to those in the High-adversity profile. Notably, internalizing and externalizing symptoms were the highest among youths in the MD and High-adversity profiles, particularly for internalizing symptoms. The MD and high-adversity profiles also exhibited increased default mode network (DMN) density during an emotion task. Furthermore, the High-adversity profile showed attenuated salience network density compared to the Low-adversity profile and the highest frontoparietal network density relative to all other profiles. These findings suggest that interventions targeting multiple risk factors and placing additional focus on maternal mental health could yield the most substantial benefits for youth well-being.

5.2 Integrative Themes

The work discussed here supports several notable themes that will inform future research. First, more consideration for the individual operationalization of adversity is needed in the literature. The findings from all three chapters demonstrate that adverse experiences do not affect individuals uniformly; neural mechanisms may be specific to the types of adversity and to the

individuals. The findings from Chapter 2 indicate specific neural mechanisms related to instability that were not apparent for other types of adversity. The findings Chapter 3 show that stress susceptibility and anxiety may be specific to certain brain regions or to particular groups of individuals. Chapter 4 illustrates how individual-focused characterizations of adversity reveal differences in youth mental health outcomes and brain function. Collectively, these studies highlight the differential neural mechanisms that may underlie specific experiences.

Second, all three chapters of this dissertation demonstrate that novel methodological approaches can enhance precision in understanding the neural mechanisms of adversity. In Chapter 2, the combination of cutting-edge tractography and graph analytic approaches allowed for the individualized estimation of structural brain networks' topological organization. In Chapter 3, the application of a person-specific network mapping approach and a data-driven community detection method enabled the identification of groups of individuals who were more or less susceptible to adversity. Chapter 4 employed a person-centered method that clustered individuals into childhood adversity profiles, coupled with a data-driven connectivity estimation method, facilitating the identification of distinct connectivity patterns specific to each adversity profile. Collectively, these approaches introduce novel multivariate methods that extend beyond conventional techniques, advancing the research on environmental influences on development.

Finally, the work featured in this dissertation underscores the lifelong consequences of childhood adversity on brain and mental health in a population-based sample. All three studies utilized longitudinal designs spanning multiple developmental stages—childhood, adolescence, and young adulthood—in a birth cohort sample that includes a high representation of minority and low-income families. This work builds upon the growing appreciation of representative sampling in neuroimaging research, especially when studying experiences of adversity that

disproportionately impact marginalized identities in the US, contributing to vast health inequalities. Thus, this dissertation contributes valuable insights that will inform future research focused on improving population health across the lifespan.

5.3 Future Directions

This dissertation demonstrates the critical importance of adverse experiences in shaping both brain and socioemotional development, while also highlighting several future directions.

5.3.1 Refining neurobiological mechanisms of adversity

The evidence presented in this dissertation suggest that more research is needed to parse the significant heterogeneity in early experiences, specifically to identify precise mechanisms underlying the effects of stress on development. In particular, as demonstrated in the first and third study of this dissertation, specific types of adverse experiences (e.g., instability, maternal depression) could have differential neural pathways that underlie individual outcomes in mental health. Building upon these findings, more research is needed to establish greater specificity in current mechanistic models of adversity.

Parallel to initiatives such as the Research Domain Criteria (RDoC) (Cuthbert, 2014) or Hierarchical Taxonomy of Psychopathology (HITOP) (Kotov et al., 2017), which aim to refine psychiatric nosology across heterogeneous symptomatic presentations of mental disorders, similar principles could be applied to discern specific neurobiological mechanisms underlying various domains of early experience. In addition to further research to establish neural correlates associated with the three identified dimensions of adversity—threat, deprivation, and

unpredictability—identifying other elements of adversity that cut across multiple types of events could enhance the precision of the resulting neural markers (Cohodes et al., 2021; Gee, 2021). Cohodes and colleagues (2021) have recently proposed additional dimensions such as controllability, an element thus far absent in current dimensional models. Another element previously unconsidered is the processes underlying the harmful effects of racism. Despite growing evidence of the consequences of racial trauma on mental health (Bernard et al., 2021) and neural effects of racial disparities (Harnett, 2020), current models of adversity do not yet account for processes specific to these experiences. In particular, the experience of identity threat due to discrimination constitutes a chronic risk to psychological safety (Wanless, 2016) and may be differentially internalized than threats in other contexts.

These research directions could be enhanced by greater integration of cross-species translational work, which can provide foundational bases for understanding these mechanistic processes. Crucially, refining the basic elements of adverse experiences could facilitate efforts to align work based on animal models with human findings. One direction that warrants further exploration is how children's perception of adverse events can drive neural variations in the effects of adversity (Smith & Pollak, 2021). To this end, integrating well-established cognitive science principles could illuminate specific systems involved in event perception and memory (Norman & Rumelhart, 1970), as well as how their underlying neural processes may differ during stress (Schwabe et al., 2022). As suggested this dissertation, this may require expanding the focus of investigation beyond key neural regions that have informed existing theoretical models. For instance, future research can further explore how the crosstalk between critical brain regions involved in basic cognitive and emotion processes might lead to variations in how individuals process and experience adversity across different contexts and development stages.

5.3.2 Distinguishing universality and individuality

Human development is defined by processes that are ubiquitous, as well as attributes that are unique to each individual. As discussed earlier in this dissertation, most neuroimaging studies have focused on characterizing group-based neural patterns to maximize statistical power and signal-to-noise ratio (Dubois & Adolphs, 2016), despite the acknowledged importance of individual differences. On the other extreme, examining individual-level patterns carry concerns about the generalizability of resulting neural markers for population-level prediction. This dissertation work has demonstrated how person-oriented methods can be leveraged to achieve a balance between capturing population-level inferences and individual-level patterns (e.g., by combining person-centered and person-specific approaches that can simultaneously parse population heterogeneity and heterogeneous brain network connectivity). While this approach can increase the precision of the identified neural correlates of adversity, additional studies using other samples are needed to formally distinguish neural pathways and processes that are universal and those that are specific to certain individuals.

A major constraint in studying neural development in individuals is the limited availability of neuroimaging data that provide representative information about the population. These efforts are becoming more feasible with the increasing availability of longitudinal datasets accessible to the scientific community (Monk & Hardi, 2023). The utility of these datasets is enhanced by large-scale sampling and increased computational resources (Fair et al., 2021), enabling the implementation of more sophisticated neural models. However, to understand universal processes versus individual-specific ones, population-level findings using big data need to be complemented by insights from developmental psychology that focus on rich individual-level processes in smaller samples (Gratton et al., 2022; McLaughlin, 2014). Moreover,

increasing the frequency of neuroimaging data collection, as in the case of dense sampling (Poldrack, 2017), could also enhance our understanding of individual differences.

An increasing focus on sampling also highlights the importance of examining characteristics of individuals who deviate from common patterns. For instance, Greene and colleagues (2022) investigated model failures in brain-behavior predictive models and examined characteristics of individuals for whom these models poorly represent. They found that model misclassifications were associated with a host of sociodemographic and behavioral indices, including age, race, education, and cognitive ability. Misclassifications occurred in individuals who defied expected patterns across these indices (e.g., in individuals with high education but low cognitive scores, or vice versa) (Greene et al., 2022). These findings suggest that universal models may not apply uniformly to all individuals, and there is a need to establish which processes could apply to whom. These inferences can also be complemented with other resources that are becoming more publicly available. For instance, recent progress in large-scale data sharing has yielded human brain charts that aggregate structural neuroimaging data from more than 100,000 individuals ranging from birth to 100 years of age (Bethlehem et al., 2022). Such a resource can help quantify individual deviations from normative developmental trajectories, similar to how pediatric growth charts are used to track children's physical growth (Rutherford et al., 2022). Applying these cutting-edge approaches will forge a new frontier in distinguishing universal developmental processes from those specific to individuals.

5.3.3 Modeling adaptation to adversity as a dynamic process across the life course

Human development is understood to be a complex and dynamic process, as discussed earlier in this dissertation. However, despite the understanding that these dynamic interactions

result in a probabilistic course of development (Gottlieb, 2007), research on adversity has heavily relied on examining exposures-outcomes processes with deterministic approaches. As demonstrated by study three, person-oriented approaches that capture the interaction of multiple intersecting factors within person can better account for this dynamic patterns of human development. When applied to scientific questions pertaining to the influence of adversity on mental health, it can lead to greater specificity in the neural regions implicated in this association, and revealed experiences that are particularly important for individuals in the sample. This work can inform future research to begin integrating person-oriented approaches in capturing the complexity of rich environmental contexts as large-scale longitudinal data become more readily available. Moreover, the application of computational approaches to modeling developmental change could also provide novel insights. For instance, generative network models have been proposed as a framework to model dynamic systems (Astle et al., 2023) and could be employed to provide empirical evidence of the link between random neural variation and early life stress (Carozza et al., 2023).

A potential extension of this work is the integration of a life course approach to model stress exposure. In addition to accounting for the complexities of developmental processes, considering fluctuations that occur throughout the life course is also necessary to characterize neural adaptation to adversity. For instance, although much research has focused on the developmental timing of early adversity (Gard et al., 2021; Gee, 2021; Hardi et al., 2022; Tottenham & Sheridan, 2010), with specific emphasis on the critical importance of early experiences as potential sensitive periods (Hensch & Bilimoria, 2012; Knudsen, 2004; Luby et al., 2020), less work has addressed environmental variability across the lifetime. Moreover, a mismatch between early and adult environments could increase risks for disease, as neural

mechanisms resulting from adaptation to adverse environments may not be optimized to other contexts (Nederhof & Schmidt, 2012). More research is needed to test this hypothesis, especially to determine which neural properties could be least accommodating to changing contexts and which may be malleable regardless of the environment. Neural flexibility, in this regard, may reflect a resilience factor against the harmful effects of adversity, thus providing a tangible mechanistic target for intervention. Moreover, certain adversity may exert greater influence at specific developmental stages, as experience-expectant processes differ across development.

5.4 Conclusion

Research on the neural embedding of adversity has burgeoned in the past decade, attracting scientists and scholars from incredibly diverse disciplines. This interdisciplinary research continues to forge new directions and exciting work on this topic. However, it is imperative not to lose sight of the ultimate goal: to improve individual well-being by centering this work on the individuals it serves. Despite decades of research, adverse childhood experiences remain one of the leading causes of mental disorders (Centers for Disease Control and Prevention, 2021), imposing an annual economic cost of $14.1 trillion nationally, $88,000 for each affected adult, and $2.4 million over their lifetime (Peterson et al., 2023). Moreover, childhood adversity is disproportionately experienced by children in marginalized communities (Slopen et al., 2016), further contributing to health disparities in the US. Thus, research focused on understanding how children learn and develop in stressful environments should continue to prioritize how findings could be leveraged to improve policies that protect children from adverse events and interventions that can reverse the harmful effects of adversity.

Bibliography

Abidin, R., Flens, J. R., & Austin, W. G. (2006). *The parenting stress index.* Lawrence Erlbaum Associates Publishers.

Achenbach, T. M. (2001). Manual for ASEBA school-age forms & profiles. *University of Vermont, Research Center for Children, Youth & Families*.

Adriene M. Beltz, Hailey L. Dotterer, & Leigh G. Goetschius. (2019). *GIMME Preprocessing: Initial Release* [Computer software]. Zenodo. https://doi.org/10.5281/zenodo.2692522

Akaike, H. (1987). Factor analysis and AIC. *Psychometrika*, *52*, 317–332.

Anda, R. F., Felitti, V. J., Bremner, J. D., Walker, J. D., Whitfield, C., Perry, B. D., Dube, S. R., & Giles, W. H. (2006). The enduring effects of abuse and related adverse experiences in childhood. *European Archives of Psychiatry and Clinical Neuroscience*, *256*(3), 174–186. https://doi.org/10.1007/s00406-005-0624-4

Andersson, J. L. R., Graham, M. S., Zsoldos, E., & Sotiropoulos, S. N. (2016). Incorporating outlier detection and replacement into a non-parametric framework for movement and distortion correction of diffusion MR images. *NeuroImage*, *141*, 556–572. https://doi.org/10.1016/j.neuroimage.2016.06.058

Angold, A., Costello, E. J., Messer, S. C., & Pickles, A. (1995). Development of a short questionnaire for use in epidemiological studies of depression in children and adolescents. *International Journal of Methods in Psychiatric Research*, *5*(4), 237–249.

Appleyard, K., Egeland, B., van Dulmen, M. H. M., & Alan Sroufe, L. (2005). When more is not better: The role of cumulative risk in child behavior outcomes. *Journal of Child Psychology and Psychiatry*, *46*(3), 235–245. https://doi.org/10.1111/j.1469-7610.2004.00351.x

Astle, D. E., Johnson, M. H., & Akarca, D. (2023). Toward computational neuroconstructivism: A framework for developmental systems neuroscience. *Trends in Cognitive Sciences*, *27*(8), 726–744. https://doi.org/10.1016/j.tics.2023.04.009

Atkinson, L., Beitchman, J., Gonzalez, A., Young, A., Wilson, B., Escobar, M., Chisholm, V., Brownlie, E., Khoury, J. E., Ludmer, J., & Villani, V. (2015). Cumulative Risk, Cumulative Outcome: A 20-Year Longitudinal Study. *PLOS ONE*, *10*(6), e0127650. https://doi.org/10.1371/journal.pone.0127650

Barnard, J., McCulloch, R., & Meng, X.-L. (2000). Modeling covariance matrices in terms of standard deviations and correlations, with application to shrinkage. *Statistica Sinica*, 1281–1311.

Bassett, D. S., & Bullmore, E. T. (2017). Small-World Brain Networks Revisited. *The Neuroscientist*, *23*(5), 499–516. https://doi.org/10.1177/1073858416667720

Bath, K. G., Manzano-Nieves, G., & Goodwill, H. (2016). Early life stress accelerates behavioral and neural maturation of the hippocampus in male mice. *Hormones and Behavior*, *82*, 64–71. https://doi.org/10.1016/j.yhbeh.2016.04.010

Bauman, K. J. (1999). Shifting family definitions: The effect of cohabitation and other nonfamily household relationships on measures of poverty. *Demography*, *36*(3), 315–325. https://doi.org/10.2307/2648055

Beck, A. T., & Clark, D. A. (1988). Anxiety and depression: An information processing perspective. *Anxiety Research*, *1*(1), 23–36. https://doi.org/10.1080/10615808808248218

Beck, A. T., Epstein, N., Brown, G., & Steer, R. A. (1988). An inventory for measuring clinical anxiety: Psychometric properties. *Journal of Consulting and Clinical Psychology*, 893–897.

Beck, A. T., Steer, R. A., & Brown, G. (1996). *Beck Depression Inventory–II* (Vol. 10). Pearson.

Beijers, L., Wardenaar, K. J., van Loo, H. M., & Schoevers, R. A. (2019). Data-driven biological subtypes of depression: Systematic review of biological approaches to depression subtyping. *Molecular Psychiatry*, *24*(6), Article 6. https://doi.org/10.1038/s41380-019-0385-5

Bell, C. C. (1994). DSM-IV: diagnostic and statistical manual of mental disorders. *Jama*, *272*(10), 828–829.

Belsky, J., Bakermans-Kranenburg, M. J., & van IJzendoorn, M. H. (2007). For Better and For Worse: Differential Susceptibility to Environmental Influences. *Current Directions in Psychological Science*, *16*(6), 300–304. https://doi.org/10.1111/j.1467-8721.2007.00525.x

Belsky, J., & Pluess, M. (2009). Beyond diathesis stress: Differential susceptibility to environmental influences. *Psychological Bulletin*, *135*, 885–908. https://doi.org/10.1037/a0017376

Belsky, J., Schlomer, G., & Ellis, B. (2011). Beyond Cumulative Risk: Distinguishing Harshness and Unpredictability as Determinants of Parenting and Early Life History Strategy. *Developmental Psychology*, *48*, 662–673. https://doi.org/10.1037/a0024454

Beltz, A., Dotterer, H., & Goetschius, L. (2019). *GIMME preprocessing: Initial release (version v1. 0). Zenodo*.

Beltz, A. M., & Gates, K. M. (2017). Network Mapping with GIMME. *Multivariate Behavioral Research*, *52*(6), 789–804. https://doi.org/10.1080/00273171.2017.1373014

Benjamini, Y., & Hochberg, Y. (1995). Controlling the False Discovery Rate: A Practical and Powerful Approach to Multiple Testing. *Journal of the Royal Statistical Society. Series B (Methodological)*, *57*(1), 289–300. JSTOR.

Berens, A. E., Jensen, S. K. G., & Nelson, C. A. (2017). Biological embedding of childhood adversity: From physiological mechanisms to clinical implications. *BMC Medicine*, *15*(1), 135. https://doi.org/10.1186/s12916-017-0895-4

Bergman, L. R., & Magnusson, D. (1997). A person-oriented approach in research on developmental psychopathology. *Development and Psychopathology*, *9*(2), 291–319. https://doi.org/10.1017/S095457949700206X

Berlin, K. S., Williams, N. A., & Parra, G. R. (2014). An introduction to latent variable mixture modeling (part 1): Overview and cross-sectional latent class and latent profile analyses. *Journal of Pediatric Psychology*, *39*(2), 174–187.

Bernard, D. L., Calhoun, C. D., Banks, D. E., Halliday, C. A., Hughes-Halbert, C., & Danielson, C. K. (2021). Making the "C-ACE" for a Culturally-Informed Adverse Childhood Experiences Framework to Understand the Pervasive Mental Health Impact of Racism on Black Youth. *Journal of Child & Adolescent Trauma*, *14*(2), 233–247. https://doi.org/10.1007/s40653-020-00319-9

Bertocci, M. A., Afriyie-Agyemang, Y., Rozovsky, R., Iyengar, S., Stiffler, R., Aslam, H. A., Bebko, G., & Phillips, M. L. (2023). Altered patterns of central executive, default mode

and salience network activity and connectivity are associated with current and future depression risk in two independent young adult samples. *Molecular Psychiatry*, *28*(3), 1046–1056. https://doi.org/10.1038/s41380-022-01899-8

Bethlehem, R. a. I., Seidlitz, J., White, S. R., Vogel, J. W., Anderson, K. M., Adamson, C., Adler, S., Alexopoulos, G. S., Anagnostou, E., Areces-Gonzalez, A., Astle, D. E., Auyeung, B., Ayub, M., Bae, J., Ball, G., Baron-Cohen, S., Beare, R., Bedford, S. A., Benegal, V., … Alexander-Bloch, A. F. (2022). Brain charts for the human lifespan. *Nature*, *604*(7906), Article 7906. https://doi.org/10.1038/s41586-022-04554-y

Bickel, G., Nord, M., Price, C., Hamilton, W., & Cook, J. (2000). *Guide to measuring household food security*.

Birmaher, B., Khetarpal, S., Brent, D., Cully, M., Balach, L., Kaufman, J., & Neer, S. M. (1997). The Screen for Child Anxiety Related Emotional Disorders (SCARED): Scale construction and psychometric characteristics. *Journal of the American Academy of Child and Adolescent Psychiatry*, *36*(4), 545–553. https://doi.org/10.1097/00004583-199704000-00018

Boyce, W. T., & Ellis, B. J. (2005). Biological sensitivity to context: I. An evolutionary–developmental theory of the origins and functions of stress reactivity. *Development and Psychopathology*, *17*(2), 271–301. https://doi.org/10.1017/s0954579405050145

Briggs, E. C., Amaya-Jackson, L., Putnam, K. T., & Putnam, F. W. (2021). All adverse childhood experiences are not equal: The contribution of synergy to adverse childhood experience scores. *American Psychologist*, *76*(2), 243–252. https://doi.org/10.1037/amp0000768

Bronfenbrenner, U., & Ceci, S. J. (1995). Nature-nuture reconceptualized in developmental perspective: A bioecological model. *Psychological Review*, *101*(4), 568. https://doi.org/10.1037/0033-295X.101.4.568

Bronfenbrenner, U., & Morris, P. A. (2007). The bioecological model of human development. *Handbook of Child Psychology*, *1*.

Brooks-Gunn, J., & Duncan, G. J. (1997). The effects of poverty on children. *The Future of Children*, *7*(2), 55–71.

Brown, J. D., & McGill, K. L. (1989). The cost of good fortune: When positive life events produce negative health consequences. *Journal of Personality and Social Psychology*, *57*(6), 1103–1110. https://doi.org/10.1037/0022-3514.57.6.1103

Buehler, C., & Gerard, J. M. (2013). Cumulative Family Risk Predicts Increases in Adjustment Difficulties across Early Adolescence. *Journal of Youth and Adolescence*, *42*(6), 905–920. https://doi.org/10.1007/s10964-012-9806-3

Bullmore, E., & Sporns, O. (2012). The economy of brain network organization. *Nature Reviews Neuroscience*, *13*(5), Article 5. https://doi.org/10.1038/nrn3214

Bullmore, E. T., & Sporns, O. (2009). Complex brain networks: Graph theoretical analysis of structural and functional systems. *Nature Reviews Neuroscience*, *10*(3), 186–198. https://doi.org/10.1038/nrn2575

Calabrese, J. R., Goetschius, L. G., Murray, L., Kaplan, M. R., Lopez-Duran, N., Mitchell, C., Hyde, L. W., & Monk, C. S. (2022). Mapping frontostriatal white matter tracts and their association with reward-related ventral striatum activation in adolescence. *Brain Research*, *1780*, 147803. https://doi.org/10.1016/j.brainres.2022.147803

Callaghan, B. L., & Tottenham, N. (2016). The Stress Acceleration Hypothesis: Effects of early-life adversity on emotion circuits and behavior. *Current Opinion in Behavioral Sciences*, *7*, 76–81. https://doi.org/10.1016/j.cobeha.2015.11.018

Careau, V., Bininda-Emonds, O. R. P., Thomas, D. W., Réale, D., & Humphries, M. M. (2009). Exploration Strategies Map along Fast-Slow Metabolic and Life-History Continua in Muroid Rodents. *Functional Ecology*, *23*(1), 150–156.

Carozza, S., Akarca, D., & Astle, D. (2023). *The adaptive stochasticity hypothesis: Modelling equifinality, multifinality and adaptation to adversity* (p. 2023.05.02.539045). bioRxiv. https://doi.org/10.1101/2023.05.02.539045

Cattell, R. B. (1952). The three basic factor-analytic research designs—Their interrelations and derivatives. *Psychological Bulletin*, *49*(5), 499–520. https://doi.org/10.1037/h0054245

Celeux, G., & Soromenho, G. (1996). An entropy criterion for assessing the number of clusters in a mixture model. *Journal of Classification*, *13*(2), 195–212. https://doi.org/10.1007/BF01246098

Centers for Disease Control and Prevention. (2021). Adverse childhood experiences prevention strategy. *Atlanta, GA: National Center for Injury Prevention and Control, Centers for Disease Control and Prevention*.

Chahal, R., Miller, J. G., Yuan, J. P., Buthmann, J. L., & Gotlib, I. H. (2022). An exploration of dimensions of early adversity and the development of functional brain network connectivity during adolescence: Implications for trajectories of internalizing symptoms. *Development and Psychopathology*, *34*(2), 557–571. https://doi.org/10.1017/S0954579421001814

Champagne, F. A., Francis, D. D., Mar, A., & Meaney, M. J. (2003). Variations in maternal care in the rat as a mediating influence for the effects of environment on development. *Physiology & Behavior*, *79*(3), 359–371. https://doi.org/10.1016/S0031-9384(03)00149-5

Chang, L., Schwartz, D., Dodge, K. A., & McBride-Chang, C. (2003). Harsh Parenting in Relation to Child Emotion Regulation and Aggression. *Journal of Family Psychology*, *17*(4), 598–606. https://doi.org/10.1037/0893-3200.17.4.598

Chapman, D. P., Whitfield, C. L., Felitti, V. J., Dube, S. R., Edwards, V. J., & Anda, R. F. (2004). Adverse childhood experiences and the risk of depressive disorders in adulthood. *Journal of Affective Disorders*, *82*(2), 217–225. https://doi.org/10.1016/j.jad.2003.12.013

Chen, Z., Liu, M., Gross, D., & Beaulieu, C. (2013). Graph theoretical analysis of developmental patterns of the white matter network. *Frontiers in Human Neuroscience*, *7*. https://www.frontiersin.org/articles/10.3389/fnhum.2013.00716

Chetty, R., Hendren, N., & Katz, L. F. (2016). The Effects of Exposure to Better Neighborhoods on Children: New Evidence from the Moving to Opportunity Experiment. *American Economic Review*, *106*(4), 855–902. https://doi.org/10.1257/aer.20150572

Cicchetti, D., & Lynch, M. (1993). Toward an Ecological/Transactional Model of Community Violence and Child Maltreatment: Consequences for Children's Development. *Psychiatry*, *56*(1), 96–118. https://doi.org/10.1080/00332747.1993.11024624

Cicchetti, D., & Rogosch, F. A. (1996). Equifinality and multifinality in developmental psychopathology. *Development and Psychopathology*, *8*(4), 597–600. https://doi.org/10.1017/s0954579400007318

Civier, O., Smith, R. E., Yeh, C.-H., Connelly, A., & Calamante, F. (2019). Is removal of weak connections necessary for graph-theoretical analysis of dense weighted structural

connectomes from diffusion MRI? *NeuroImage*, *194*, 68–81. https://doi.org/10.1016/j.neuroimage.2019.02.039

Cohodes, E. M., Kitt, E. R., Baskin-Sommers, A., & Gee, D. G. (2021). Influences of early-life stress on frontolimbic circuitry: Harnessing a dimensional approach to elucidate the effects of heterogeneity in stress exposure. *Developmental Psychobiology*, *63*(2), 153–172.

Coplan, J. D., Andrews, M. W., Rosenblum, L. A., Owens, M. J., Friedman, S., Gorman, J. M., & Nemeroff, C. B. (1996). Persistent elevations of cerebrospinal fluid concentrations of corticotropin-releasing factor in adult nonhuman primates exposed to early-life stressors: Implications for the pathophysiology of mood and anxiety disorders. *Proceedings of the National Academy of Sciences*, *93*(4), 1619–1623. https://doi.org/10.1073/pnas.93.4.1619

Coplan, J. D., Smith, E. L. P., Altemus, M., Scharf, B. A., Owens, M. J., Nemeroff, C. B., Gorman, J. M., & Rosenblum, L. A. (2001). Variable foraging demand rearing: Sustained elevations in cisternal cerebrospinal fluid corticotropin-releasing factor concentrations in adult primates. *Biological Psychiatry*, *50*(3), 200–204. https://doi.org/10.1016/S0006-3223(01)01175-1

Curran, P. J., & Bauer, D. J. (2011). The Disaggregation of Within-Person and Between-Person Effects in Longitudinal Models of Change. *Annual Review of Psychology*, *62*(1), 583–619. https://doi.org/10.1146/annurev.psych.093008.100356

Cuthbert, B. N. (2014). The RDoC framework: Facilitating transition from ICD/DSM to dimensional approaches that integrate neuroscience and psychopathology. *World Psychiatry*, *13*(1), 28–35. https://doi.org/10.1002/wps.20087

Dallman, M. F., Akana, S. F., Strack, A. M., Scribner, K. S., Pecoraro, N., La Fleur, S. E., Houshyar, H., & Gomez, F. (2004). Chronic Stress-Induced Effects of Corticosterone on Brain: Direct and Indirect. *Annals of the New York Academy of Sciences*, *1018*(1), 141–150. https://doi.org/10.1196/annals.1296.017

Dantzer, B., Newman, A. E. M., Boonstra, R., Palme, R., Boutin, S., Humphries, M. M., & McAdam, A. G. (2013). Density Triggers Maternal Hormones That Increase Adaptive Offspring Growth in a Wild Mammal. *Science*, *340*(6137), 1215–1217. https://doi.org/10.1126/science.1235765

Davidson, R. J. (2002). Anxiety and affective style: Role of prefrontal cortex and amygdala. *Biological Psychiatry*, *51*(1), 68–80. https://doi.org/10.1016/S0006-3223(01)01328-2

Davis, E. P., Stout, S. A., Molet, J., Vegetabile, B., Glynn, L. M., Sandman, C. A., Heins, K., Stern, H., & Baram, T. Z. (2017). Exposure to unpredictable maternal sensory signals influences cognitive development across species. *Proceedings of the National Academy of Sciences*, *114*(39), 10390–10395. https://doi.org/10.1073/pnas.1703444114

Davis, M. (1992). The role of the amygdala in fear and anxiety. *Annual Review of Neuroscience*, *15*(1), 353–375.

Derogatis, L. R., & Kathryn, L. (2000). The SCL-90-R and Brief Symptom Inventory (BSI) in primary care. In *Handbook of psychological assessment in primary care settings* (pp. 310–347). Routledge.

Dong, M., Anda, R. F., Felitti, V. J., Dube, S. R., Williamson, D. F., Thompson, T. J., Loo, C. M., & Giles, W. H. (2004). The interrelatedness of multiple forms of childhood abuse, neglect, and household dysfunction. *Child Abuse & Neglect*, *28*(7), 771–784. https://doi.org/10.1016/j.chiabu.2004.01.008

Doom, J. R., Vanzomeren-Dohm, A. A., & Simpson, J. A. (2016). Early unpredictability predicts increased adolescent externalizing behaviors and substance use: A life history perspective. *Development and Psychopathology*, *28*(4 Pt 2), 1505–1516. https://doi.org/10.1017/S0954579415001169

Drevets, W. C. (2007). Orbitofrontal Cortex Function and Structure in Depression. *Annals of the New York Academy of Sciences*, *1121*(1), 499–527. https://doi.org/10.1196/annals.1401.029

Drevets, W. C., Savitz, J., & Trimble, M. (2008). The Subgenual Anterior Cingulate Cortex in Mood Disorders. *CNS Spectrums*, *13*(8), 663–681.

Dubois, J., & Adolphs, R. (2016). Building a Science of Individual Differences from fMRI. *Trends in Cognitive Sciences*, *20*(6), 425–443. https://doi.org/10.1016/j.tics.2016.03.014

Eickhoff, S. B., Laird, A. R., Fox, P. T., Bzdok, D., & Hensel, L. (2016). Functional Segregation of the Human Dorsomedial Prefrontal Cortex. *Cerebral Cortex*, *26*(1), 304–321. https://doi.org/10.1093/cercor/bhu250

Elliott, M. L., Knodt, A. R., & Hariri, A. R. (2021). Striving toward translation: Strategies for reliable fMRI measurement. *Trends in Cognitive Sciences*, *25*(9), 776–787. https://doi.org/10.1016/j.tics.2021.05.008

Elliott, M. L., Knodt, A. R., Ireland, D., Morris, M. L., Poulton, R., Ramrakha, S., Sison, M. L., Moffitt, T. E., Caspi, A., & Hariri, A. R. (2020). What Is the Test-Retest Reliability of Common Task-Functional MRI Measures? New Empirical Evidence and a Meta-Analysis. *Psychological Science*, *31*(7), 792–806. https://doi.org/10.1177/0956797620916786

Ellis, B. J., Sheridan, M. A., Jay Belsky, & Katie A McLaughlin. (2022). Why and how does early adversity influence development? Toward an integrated model of dimensions of environmental experience. *Development and Psychopathology*, 1–25. https://doi.org/10.1017/s0954579421001838

Etkin, A., Prater, K. E., Schatzberg, A. F., Menon, V., & Greicius, M. D. (2009). Disrupted Amygdalar Subregion Functional Connectivity and Evidence of a Compensatory Network in Generalized Anxiety Disorder. *Archives of General Psychiatry*, *66*(12), 1361–1372. https://doi.org/10.1001/archgenpsychiatry.2009.104

Etkin, A., & Wager, T. D. (2007). Functional Neuroimaging of Anxiety: A Meta-Analysis of Emotional Processing in PTSD, Social Anxiety Disorder, and Specific Phobia. *American Journal of Psychiatry*, *164*(10), 1476–1488. https://doi.org/10.1176/appi.ajp.2007.07030504

Evans, G. W., Li, D., & Whipple, S. S. (2013). Cumulative risk and child development. *Psychological Bulletin*, *139*, 1342–1396. https://doi.org/10.1037/a0031808

Fair, D. A., Bathula, D., Nikolas, M. A., & Nigg, J. T. (2012). Distinct neuropsychological subgroups in typically developing youth inform heterogeneity in children with ADHD. *Proceedings of the National Academy of Sciences*, *109*(17), 6769–6774. https://doi.org/10.1073/pnas.1115365109

Fair, D. A., Dosenbach, N. U. F., Moore, A. H., Satterthwaite, T. D., & Milham, M. P. (2021). Developmental Cognitive Neuroscience in the Era of Networks and Big Data: Strengths, Weaknesses, Opportunities, and Threats. *Annual Review of Developmental Psychology*, *3*(1), 249–275. https://doi.org/10.1146/annurev-devpsych-121318-085124

Falk, E. B., Hyde, L. W., Mitchell, C., Faul, J. D., Gonzalez, R., Heitzeg, M. M., Keating, D. P., Langa, K. M., Martz, M. E., Maslowsky, J., Morrison, F. J., Noll, D. C., Patrick, M. E., Pfeffer, F. T., Reuter-Lorenz, P. A., Thomason, M. E., Davis-Kean, P. E., Monk, C. S., & Schulenberg, J. E. (2013). What is a representative brain? Neuroscience meets population science. *Proceedings of the National Academy of Sciences of the United States of America*, *110*(44), 17615–17622. https://doi.org/10.1073/pnas.1310134110

Farquharson, S., Tournier, J.-D., Calamante, F., Fabinyi, G., Schneider-Kolsky, M., Jackson, G. D., & Connelly, A. (2013). White matter fiber tractography: Why we need to move beyond DTI: Clinical article. *Journal of Neurosurgery*, *118*(6), 1367–1377. https://doi.org/10.3171/2013.2.JNS121294

Faubert, B. E. W., Natasha K. Bowen, Sarah J. (2020). Latent Class Analysis: A Guide to Best Practice - Bridget E. Weller, Natasha K. Bowen, Sarah J. Faubert, 2020. *Journal of Black Psychology*. https://journals.sagepub.com/doi/full/10.1177/0095798420930932

Feczko, E., Miranda-Dominguez, O., Marr, M., Graham, A. M., Nigg, J. T., & Fair, D. A. (2019). The Heterogeneity Problem: Approaches to Identify Psychiatric Subtypes. *Trends in Cognitive Sciences*, *23*(7), 584–601. https://doi.org/10.1016/j.tics.2019.03.009

Felitti, V. J., Anda, R. F., Nordenberg, D., Williamson, D. F., Spitz, A. M., Edwards, V., & Marks, J. S. (1998). Relationship of childhood abuse and household dysfunction to many of the leading causes of death in adults: The Adverse Childhood Experiences (ACE) Study. *American Journal of Preventive Medicine*, *14*(4), 245–258.

Finkelhor, D. (1995). The victimization of children: A developmental perspective. *American Journal of Orthopsychiatry*, *65*(2), 177–193.

Finkelhor, D., Turner, H. A., Shattuck, A., & Hamby, S. L. (2015). Prevalence of Childhood Exposure to Violence, Crime, and Abuse: Results From the National Survey of Children's Exposure to Violence. *JAMA Pediatrics*, *169*(8), 746–754. https://doi.org/10.1001/jamapediatrics.2015.0676

Finn, E. S. (2021). Is it time to put rest to rest? *Trends in Cognitive Sciences*, *25*(12), 1021–1032. https://doi.org/10.1016/j.tics.2021.09.005

Finn, E. S., Glerean, E., Khojandi, A. Y., Nielson, D., Molfese, P. J., Handwerker, D. A., & Bandettini, P. A. (2020). Idiosynchrony: From shared responses to individual differences during naturalistic neuroimaging. *NeuroImage*, *215*, 116828. https://doi.org/10.1016/j.neuroimage.2020.116828

Finn, E. S., Scheinost, D., Finn, D. M., Shen, X., Papademetris, X., & Constable, R. T. (2017). Can brain state be manipulated to emphasize individual differences in functional connectivity? *NeuroImage*, *160*, 140–151. https://doi.org/10.1016/j.neuroimage.2017.03.064

Finn, E. S., Shen, X., Scheinost, D., Rosenberg, M. D., Huang, J., Chun, M. M., Papademetris, X., & Constable, R. T. (2015). Functional connectome fingerprinting: Identifying individuals using patterns of brain connectivity. *Nature Neuroscience*, *18*(11), Article 11. https://doi.org/10.1038/nn.4135

Fisher, A. J., Medaglia, J. D., & Jeronimus, B. F. (2018). Lack of group-to-individual generalizability is a threat to human subjects research. *Proceedings of the National Academy of Sciences*, *115*(27), E6106–E6115. https://doi.org/10.1073/pnas.1711978115

Fomby, P., & Osborne, C. (2017). Family Instability, Multipartner Fertility, and Behavior in Middle Childhood. *Journal of Marriage and Family*, *79*(1), 75–93. https://doi.org/10.1111/jomf.12349

Foulkes, L., & Blakemore, S.-J. (2018). Studying individual differences in human adolescent brain development. *Nature Neuroscience*, *21*(3), Article 3. https://doi.org/10.1038/s41593-018-0078-4

Garcini, L. M., Arredondo, M. M., Berry, O., Church, J. A., Fryberg, S., Thomason, M. E., & McLaughlin, K. A. (2022). Increasing diversity in developmental cognitive neuroscience: A roadmap for increasing representation in pediatric neuroimaging research. *Developmental Cognitive Neuroscience*, *58*, 101167. https://doi.org/10.1016/j.dcn.2022.101167

Gard, A. M., Maxwell, A. M., Shaw, D. S., Mitchell, C., Brooks-Gunn, J., McLanahan, S. S., Forbes, E. E., Monk, C. S., & Hyde, L. W. (2021). Beyond family-level adversities: Exploring the developmental timing of neighborhood disadvantage effects on the brain. *Developmental Science*, *24*(1), e12985. https://doi.org/10.1111/desc.12985

Gard, A. M., Waller, R., Shaw, D. S., Forbes, E. E., Hariri, A. R., & Hyde, L. W. (2017). The Long Reach of Early Adversity: Parenting, Stress, and Neural Pathways to Antisocial Behavior in Adulthood. *Biological Psychiatry: Cognitive Neuroscience and Neuroimaging*, *2*(7), 582–590. https://doi.org/10.1016/j.bpsc.2017.06.005

Gates, K. M., Lane, S. T., Varangis, E., Giovanello, K., & Guiskewicz, K. (2017). Unsupervised Classification During Time-Series Model Building. *Multivariate Behavioral Research*, *52*(2), 129–148. https://doi.org/10.1080/00273171.2016.1256187

Gates, K. M., & Molenaar, P. C. M. (2012). Group search algorithm recovers effective connectivity maps for individuals in homogeneous and heterogeneous samples. *NeuroImage*, *63*(1), 310–319. https://doi.org/10.1016/j.neuroimage.2012.06.026

Gates, K. M., Molenaar, P. C. M., Hillary, F. G., Ram, N., & Rovine, M. J. (2010). Automatic search for fMRI connectivity mapping: An alternative to Granger causality testing using formal equivalences among SEM path modeling, VAR, and unified SEM. *NeuroImage*, *50*(3), 1118–1125. https://doi.org/10.1016/j.neuroimage.2009.12.117

Gee, D. G. (2021). Early Adversity and Development: Parsing Heterogeneity and Identifying Pathways of Risk and Resilience. *American Journal of Psychiatry*, *178*(11), 998–1013. https://doi.org/10.1176/appi.ajp.2021.21090944

Gee, D. G., Gabard-Durnam, L. J., Flannery, J., Goff, B., Humphreys, K. L., Telzer, E. H., Hare, T. A., Bookheimer, S. Y., & Tottenham, N. (2013). Early developmental emergence of human amygdala–prefrontal connectivity after maternal deprivation. *Proceedings of the National Academy of Sciences*, *110*(39), 15638–15643. https://doi.org/10.1073/pnas.1307893110

Geronimus, A. T. (1992). The Weathering Hypothesis and the Health of African-American Women and Infants: Evidence and Speculations. *Ethnicity & Disease*, *2*(3), 207–221.

Giano, Z., Wheeler, D. L., & Hubach, R. D. (2020). The frequencies and disparities of adverse childhood experiences in the U.S. *BMC Public Health*, *20*(1), 1327. https://doi.org/10.1186/s12889-020-09411-z

Glover, G. H., & Law, C. S. (2001). Spiral-in/out BOLD fMRI for increased SNR and reduced susceptibility artifacts. *Magnetic Resonance in Medicine*, *46*(3), 515–522. Scopus. https://doi.org/10.1002/mrm.1222

Glynn, L. M., & Baram, T. Z. (2019). The Influence of Unpredictable, Fragmented Parental Signals on the Developing Brain. *Frontiers in Neuroendocrinology*, *53*, 100736. https://doi.org/10.1016/j.yfrne.2019.01.002

Goetschius, L. G., Hein, T. C., Mattson, W. I., Lopez-Duran, N., Dotterer, H. L., Welsh, R. C., Mitchell, C., Hyde, L. W., & Monk, C. S. (2019). Amygdala-prefrontal cortex white matter tracts are widespread, variable and implicated in amygdala modulation in adolescents. *NeuroImage*, *191*, 278–291. https://doi.org/10.1016/j.neuroimage.2019.02.009

Goetschius, L. G., Hein, T. C., McLanahan, S. S., Brooks-Gunn, J., McLoyd, V. C., Dotterer, H. L., Lopez-Duran, N., Mitchell, C., Hyde, L. W., Monk, C. S., & Beltz, A. M. (2020). Association of Childhood Violence Exposure With Adolescent Neural Network Density. *JAMA Network Open*, *3*(9). https://doi.org/10.1001/jamanetworkopen.2020.17850

Goetschius, L. G., Hein, T. C., Mitchell, C., Lopez-Duran, N. L., McLoyd, V. C., Brooks-Gunn, J., McLanahan, S. S., Hyde, L. W., & Monk, C. S. (2020). Childhood violence exposure and social deprivation predict adolescent amygdala-orbitofrontal cortex white matter connectivity. *Developmental Cognitive Neuroscience*, *45*, 100849. https://doi.org/10.1016/j.dcn.2020.100849

Goldfarb, W. (1945). Effects of psychological deprivation in infancy and subsequent stimulation. *American Journal of Psychiatry*, *102*(1), 18–33. https://doi.org/10.1176/ajp.102.1.18

Goodman, S. H., & Gotlib, I. H. (1999). Risk for psychopathology in the children of depressed mothers: A developmental model for understanding mechanisms of transmission. *Psychological Review*, *106*, 458–490. https://doi.org/10.1037/0033-295X.106.3.458

Goodman, S. H., Rouse, M. H., Connell, A. M., Broth, M. R., Hall, C. M., & Heyward, D. (2011). Maternal Depression and Child Psychopathology: A Meta-Analytic Review. *Clinical Child and Family Psychology Review*, *14*(1), 1–27. https://doi.org/10.1007/s10567-010-0080-1

Gordon, E. M., Laumann, T. O., Gilmore, A. W., Newbold, D. J., Greene, D. J., Berg, J. J., Ortega, M., Hoyt-Drazen, C., Gratton, C., Sun, H., Hampton, J. M., Coalson, R. S., Nguyen, A. L., McDermott, K. B., Shimony, J. S., Snyder, A. Z., Schlaggar, B. L., Petersen, S. E., Nelson, S. M., & Dosenbach, N. U. F. (2017). Precision Functional Mapping of Individual Human Brains. *Neuron*, *95*(4), 791-807.e7. https://doi.org/10.1016/j.neuron.2017.07.011

Gottlieb, G. (2007). Probabilistic epigenesis. *Developmental Science*, *10*(1), 1–11. https://doi.org/10.1111/j.1467-7687.2007.00556.x

Granger, S. J., Glynn, L. M., Sandman, C. A., Small, S. L., Obenaus, A., Keator, D. B., Baram, T. Z., Stern, H., Yassa, M. A., & Davis, E. P. (2021). Aberrant Maturation of the Uncinate Fasciculus Follows Exposure to Unpredictable Patterns of Maternal Signals. *The Journal of Neuroscience*, *41*(6), 1242–1250. https://doi.org/10.1523/JNEUROSCI.0374-20.2020

Gratton, C., Laumann, T. O., Nielsen, A. N., Greene, D. J., Gordon, E. M., Gilmore, A. W., Nelson, S. M., Coalson, R. S., Snyder, A. Z., Schlaggar, B. L., Dosenbach, N. U. F., & Petersen, S. E. (2018). Functional Brain Networks Are Dominated by Stable Group and Individual Factors, Not Cognitive or Daily Variation. *Neuron*, *98*(2), 439-452.e5. https://doi.org/10.1016/j.neuron.2018.03.035

Gratton, C., Nelson, S. M., & Gordon, E. M. (2022). Brain-behavior correlations: Two paths toward reliability. *Neuron*, *110*(9), 1446–1449. https://doi.org/10.1016/j.neuron.2022.04.018

Green, J. G., McLaughlin, K. A., Berglund, P. A., Gruber, M. J., Sampson, N. A., Zaslavsky, A. M., & Kessler, R. C. (2010). Childhood Adversities and Adult Psychiatric Disorders in the National Comorbidity Survey Replication I: Associations With First Onset of DSM-IV Disorders. *Archives of General Psychiatry*, *67*(2), 113–123. https://doi.org/10.1001/archgenpsychiatry.2009.186

Greene, A. S., Gao, S., Scheinost, D., & Constable, R. T. (2018). Task-induced brain state manipulation improves prediction of individual traits. *Nature Communications*, *9*(1), Article 1. https://doi.org/10.1038/s41467-018-04920-3

Greene, A. S., Shen, X., Noble, S., Horien, C., Hahn, C. A., Arora, J., Tokoglu, F., Spann, M. N., Carrión, C. I., Barron, D. S., Sanacora, G., Srihari, V. H., Woods, S. W., Scheinost, D., & Constable, R. T. (2022). Brain–phenotype models fail for individuals who defy sample stereotypes. *Nature*, *609*(7925), Article 7925. https://doi.org/10.1038/s41586-022-05118-w

Greenough, W. T., Volkmar, F. R., & Juraska, J. M. (1973). Effects of rearing complexity on dendritic branching in frontolateral and temporal cortex of the rat. *Experimental Neurology*, *41*(2), 371–378. https://doi.org/10.1016/0014-4886(73)90278-1

Greicius, M. D., Flores, B. H., Menon, V., Glover, G. H., Solvason, H. B., Kenna, H., Reiss, A. L., & Schatzberg, A. F. (2007). Resting-State Functional Connectivity in Major Depression: Abnormally Increased Contributions from Subgenual Cingulate Cortex and

Thalamus. *Biological Psychiatry*, *62*(5), 429–437. https://doi.org/10.1016/j.biopsych.2006.09.020

Gu, Z., Gu, L., Eils, R., Schlesner, M., & Brors, B. (2014). Circlize implements and enhances circular visualization in R. *Bioinformatics*, *30*(19), 2811–2812. https://doi.org/10.1093/bioinformatics/btu393

Guadagno, A., Verlezza, S., Long, H., Wong, T. P., & Walker, C.-D. (2020). It Is All in the Right Amygdala: Increased Synaptic Plasticity and Perineuronal Nets in Male, But Not Female, Juvenile Rat Pups after Exposure to Early-Life Stress. *Journal of Neuroscience*, *40*(43), 8276–8291. https://doi.org/10.1523/JNEUROSCI.1029-20.2020

Guassi Moreira, J. F., McLaughlin, K. A., & Silvers, J. A. (2021). Characterizing the Network Architecture of Emotion Regulation Neurodevelopment. *Cerebral Cortex*, *31*(9), 4140–4150. https://doi.org/10.1093/cercor/bhab074

Gunnar, M. R., Van Dulmen, M. H. M., & The International Adoption Team. (2007). Behavior problems in postinstitutionalized internationally adopted children. *Development and Psychopathology*, *19*(01). https://doi.org/10.1017/S0954579407070071

Gur, R. E., Moore, T. M., Rosen, A. F. G., Barzilay, R., Roalf, D. R., Calkins, M. E., Ruparel, K., Scott, J. C., Almasy, L., Satterthwaite, T. D., Shinohara, R. T., & Gur, R. C. (2019). Burden of Environmental Adversity Associated With Psychopathology, Maturation, and Brain Behavior Parameters in Youths. *JAMA Psychiatry*, *76*(9), 966–975. https://doi.org/10.1001/jamapsychiatry.2019.0943

Hack, L. M., Tozzi, L., Zenteno, S., Olmsted, A. M., Hilton, R., Jubeir, J., Korgaonkar, M. S., Schatzberg, A. F., Yesavage, J. A., O'Hara, R., & Williams, L. M. (2023). A Cognitive Biotype of Depression Linking Symptoms, Behavior Measures, Neural Circuits, and

Differential Treatment Outcomes: A Prespecified Secondary Analysis of a Randomized Clinical Trial. *JAMA Network Open*, *6*(6), e2318411. https://doi.org/10.1001/jamanetworkopen.2023.18411

Hagmann, P., Sporns, O., Madan, N., Cammoun, L., Pienaar, R., Wedeen, V. J., Meuli, R., Thiran, J.-P., & Grant, P. E. (2010). White matter maturation reshapes structural connectivity in the late developing human brain. *Proceedings of the National Academy of Sciences*, *107*(44), 19067–19072. https://doi.org/10.1073/pnas.1009073107

Hankin, B. L., Mermelstein, R., & Roesch, L. (2007). Sex Differences in Adolescent Depression: Stress Exposure and Reactivity Models. *Child Development*, *78*(1), 279–295. https://doi.org/10.1111/j.1467-8624.2007.00997.x

Hanson, J. L., Adluru, N., Chung, M. K., Alexander, A. L., Davidson, R. J., & Pollak, S. D. (2013). Early Neglect Is Associated With Alterations in White Matter Integrity and Cognitive Functioning. *Child Development*, *84*(5), 1566–1578. https://doi.org/10.1111/cdev.12069

Hanson, J. L., Knodt, A. R., Brigidi, B. D., & Hariri, A. R. (2015). Lower structural integrity of the uncinate fasciculus is associated with a history of child maltreatment and future psychological vulnerability to stress. *Development and Psychopathology*, *27*(4pt2), 1611–1619. https://doi.org/10.1017/S0954579415000978

Hardi, F. A., Goetschius, L. G., McLoyd, V., Lopez-Duran, N. L., Mitchell, C., Hyde, L. W., Beltz, A. M., & Monk, C. S. (2023). Adolescent functional network connectivity prospectively predicts adult anxiety symptoms related to perceived COVID-19 economic adversity. *Journal of Child Psychology and Psychiatry*, *64*(6), 918–929. https://doi.org/10.1111/jcpp.13749

Hardi, F. A., Goetschius, L. G., Peckins, M. K., Brooks-Gunn, J., McLanahan, S. S., McLoyd, V., Lopez-Duran, N. L., Mitchell, C., Hyde, L. W., & Monk, C. S. (2022). Differential Developmental Associations of Material Hardship Exposure and Adolescent Amygdala–Prefrontal Cortex White Matter Connectivity. *Journal of Cognitive Neuroscience*, *34*(10), 1866–1891. https://doi.org/10.1162/jocn_a_01801

Hardi, F. A., Goetschius, L. G., Tillem, S., McLoyd, V., Brooks-Gunn, J., Boone, M., Lopez-Duran, N., Mitchell, C., Hyde, L. W., & Monk, C. S. (2023). Early childhood household instability, adolescent structural neural network architecture, and young adulthood depression: A 21-year longitudinal study. *Developmental Cognitive Neuroscience*, *61*, 101253. https://doi.org/10.1016/j.dcn.2023.101253

Harnett, N. G. (2020). Neurobiological consequences of racial disparities and environmental risks: A critical gap in understanding psychiatric disorders. *Neuropsychopharmacology*, *45*(8), Article 8. https://doi.org/10.1038/s41386-020-0681-4

Harris, K. M. (2013). The add health study: Design and accomplishments. *Chapel Hill: Carolina Population Center, University of North Carolina at Chapel Hill*, *1*, 1–22.

He, L., Wei, D., Yang, F., Zhang, J., Cheng, W., Feng, J., Yang, W., Zhuang, K., Chen, Q., Ren, Z., Li, Y., Wang, X., Mao, Y., Chen, Z., Liao, M., Cui, H., Li, C., He, Q., Lei, X., … Qiu, J. (2021). Functional Connectome Prediction of Anxiety Related to the COVID-19 Pandemic. *American Journal of Psychiatry*, appi.ajp.2020.20070979. https://doi.org/10.1176/appi.ajp.2020.20070979

Hein, T. C., Goetschius, L. G., McLoyd, V. C., Brooks-Gunn, J., McLanahan, S. S., Mitchell, C., Lopez-Duran, N. L., Hyde, L. W., & Monk, C. S. (2020). Childhood violence exposure and social deprivation are linked to adolescent threat and reward neural function. *Social*

Cognitive and Affective Neuroscience, *15*(11), 1252–1259. https://doi.org/10.1093/scan/nsaa144

Hein, T. C., Mattson, W. I., Dotterer, H. L., Mitchell, C., Lopez-Duran, N., Thomason, M. E., Peltier, S. J., Welsh, R. C., Hyde, L. W., & Monk, C. S. (2018). Amygdala habituation and uncinate fasciculus connectivity in adolescence: A multi-modal approach. *NeuroImage*, *183*, 617–626. https://doi.org/10.1016/j.neuroimage.2018.08.058

Hein, T. C., & Monk, C. S. (2017). Research Review: Neural response to threat in children, adolescents, and adults after child maltreatment – a quantitative meta-analysis. *Journal of Child Psychology and Psychiatry*, *58*(3), 222–230. https://doi.org/10.1111/jcpp.12651

Henry, T. R., Feczko, E., Cordova, M., Earl, E., Williams, S., Nigg, J. T., Fair, D. A., & Gates, K. M. (2019). Comparing directed functional connectivity between groups with confirmatory subgrouping GIMME. *NeuroImage*, *188*, 642–653. https://doi.org/10.1016/j.neuroimage.2018.12.040

Hensch, T. K., & Bilimoria, P. M. (2012). Re-opening Windows: Manipulating Critical Periods for Brain Development. *Cerebrum: The Dana Forum on Brain Science*, *2012*. https://www.ncbi.nlm.nih.gov/pmc/articles/PMC3574806/

Hertzman, C. (2012). Putting the concept of biological embedding in historical perspective. *Proceedings of the National Academy of Sciences of the United States of America*, *109*(Suppl 2), 17160–17167. https://doi.org/10.1073/pnas.1202203109

Hofferth, S., Davis-Kean, P. E., Davis, J., & Finkelstein, J. (1997). The child development supplement to the Panel Study of Income Dynamics: 1997 user guide. *Ann Arbor: Survey Research Center, Institute for Social Research, University of Michigan*.

Holz, N. E., Berhe, O., Sacu, S., Schwarz, E., Tesarz, J., Heim, C. M., & Tost, H. (2023). Early Social Adversity, Altered Brain Functional Connectivity, and Mental Health. *Biological Psychiatry*, *93*(5), 430–441. https://doi.org/10.1016/j.biopsych.2022.10.019

Hosseini-Kamkar, N., Varvani Farahani, M., Nikolic, M., Stewart, K., Goldsmith, S., Soltaninejad, M., Rajabli, R., Lowe, C., Nicholson, A. A., Morton, J. B., & Leyton, M. (2023). Adverse Life Experiences and Brain Function: A Meta-Analysis of Functional Magnetic Resonance Imaging Findings. *JAMA Network Open*, *6*(11), e2340018. https://doi.org/10.1001/jamanetworkopen.2023.40018

Howard, M. C., & Hoffman, M. E. (2018). Variable-Centered, Person-Centered, and Person-Specific Approaches: Where Theory Meets the Method. *Organizational Research Methods*, *21*(4), 846–876. https://doi.org/10.1177/1094428117744021

Hu, L., & Bentler, P. M. (1999). Cutoff criteria for fit indexes in covariance structure analysis: Conventional criteria versus new alternatives. *Structural Equation Modeling*, *6*(1), 1–55. https://doi.org/10.1080/10705519909540118

Hughes, K., Bellis, M. A., Hardcastle, K. A., Sethi, D., Butchart, A., Mikton, C., Jones, L., & Dunne, M. P. (2017). The effect of multiple adverse childhood experiences on health: A systematic review and meta-analysis. *The Lancet Public Health*, *2*(8), e356–e366. https://doi.org/10.1016/S2468-2667(17)30118-4

Hunt, T. K. A., Berger, L. M., & Slack, K. S. (2017). Adverse Childhood Experiences and Behavioral Problems in Middle Childhood. *Child Abuse & Neglect*, *67*, 391–402. https://doi.org/10.1016/j.chiabu.2016.11.005

Janak, P. H., & Tye, K. M. (2015). From circuits to behaviour in the amygdala. *Nature*, *517*(7534), Article 7534. https://doi.org/10.1038/nature14188

Janiri, D., Moser, D. A., Doucet, G. E., Luber, M. J., Rasgon, A., Lee, W. H., Murrough, J. W., Sani, G., Eickhoff, S. B., & Frangou, S. (2020). Shared Neural Phenotypes for Mood and Anxiety Disorders: A Meta-analysis of 226 Task-Related Functional Imaging Studies. *JAMA Psychiatry*, *77*(2), 172–179. https://doi.org/10.1001/jamapsychiatry.2019.3351

Jenkinson, M., Beckmann, C. F., Behrens, T. E. J., Woolrich, M. W., & Smith, S. M. (2012). FSL. *NeuroImage*, *62*(2), 782–790. https://doi.org/10.1016/j.neuroimage.2011.09.015

Karalunas, S. L., & Nigg, J. T. (2020). Heterogeneity and Subtyping in Attention-Deficit/Hyperactivity Disorder—Considerations for Emerging Research Using Person-Centered Computational Approaches. *Biological Psychiatry*, *88*(1), 103–110. https://doi.org/10.1016/j.biopsych.2019.11.002

Kessler, R. C., Andrews, G., Mroczek, D., Ustun, B., & Wittchen, H. (1998). The World Health Organization composite international diagnostic interview short-form (CIDI-SF). *International Journal of Methods in Psychiatric Research*, *7*(4), 171–185.

Kessler, R. C., Berglund, P., Demler, O., Jin, R., Merikangas, K. R., & Walters, E. E. (2005). Lifetime Prevalence and Age-of-Onset Distributions of DSM-IV Disorders in the National Comorbidity Survey Replication. *Archives of General Psychiatry*, *62*(6), 593. https://doi.org/10.1001/archpsyc.62.6.593

Kessler, R. C., Davis, C. G., & Kendler, K. S. (1997). Childhood adversity and adult psychiatric disorder in the US National Comorbidity Survey. *Psychological Medicine*, *27*(5), 1101–1119. https://doi.org/10.1017/S0033291797005588

Kessler, R. C., McGonagle, K. A., Zhao, S., Nelson, C. B., Hughes, M., Eshleman, S., Wittchen, H.-U., & Kendler, K. S. (1994). Lifetime and 12-Month Prevalence of DSM-III-R Psychiatric Disorders in the United States: Results From the National Comorbidity

Survey. *Archives of General Psychiatry*, *51*(1), 8–19. https://doi.org/10.1001/archpsyc.1994.03950010008002

Kessler, R. C., McLaughlin, K. A., Green, J. G., Gruber, M. J., Sampson, N. A., Zaslavsky, A. M., Aguilar-Gaxiola, S., Alhamzawi, A. O., Alonso, J., Angermeyer, M., Benjet, C., Bromet, E., Chatterji, S., de Girolamo, G., Demyttenaere, K., Fayyad, J., Florescu, S., Gal, G., Gureje, O., … Williams, D. R. (2010). Childhood adversities and adult psychopathology in the WHO World Mental Health Surveys. *The British Journal of Psychiatry: The Journal of Mental Science*, *197*(5), 378–385. https://doi.org/10.1192/bjp.bp.110.080499

Klumpp, H., Angstadt, M., & Phan, K. L. (2012). Insula reactivity and connectivity to anterior cingulate cortex when processing threat in generalized social anxiety disorder. *Biological Psychology*, *89*(1), 273–276. https://doi.org/10.1016/j.biopsycho.2011.10.010

Klumpp, H., Post, D., Angstadt, M., Fitzgerald, D. A., & Phan, K. L. (2013). Anterior cingulate cortex and insula response during indirect and direct processing of emotional faces in generalized social anxiety disorder. *Biology of Mood & Anxiety Disorders*, *3*(1), Article 1. https://doi.org/10.1186/2045-5380-3-7

Knudsen, E. I. (2004). Sensitive Periods in the Development of the Brain and Behavior. *Journal of Cognitive Neuroscience*, *16*(8), 1412–1425. https://doi.org/10.1162/0898929042304796

Koenis, M. M. G., Brouwer, R. M., Swagerman, S. C., van Soelen, I. L. C., Boomsma, D. I., & Hulshoff Pol, H. E. (2018). Association between structural brain network efficiency and intelligence increases during adolescence. *Human Brain Mapping*, *39*(2), 822–836. https://doi.org/10.1002/hbm.23885

Koenis, M. M. G., Brouwer, R. M., van den Heuvel, M. P., Mandl, R. C. W., van Soelen, I. L. C., Kahn, R. S., Boomsma, D. I., & Hulshoff Pol, H. E. (2015). Development of the brain's structural network efficiency in early adolescence: A longitudinal DTI twin study. *Human Brain Mapping*, *36*(12), 4938–4953. https://doi.org/10.1002/hbm.22988

Kotov, R., Krueger, R. F., Watson, D., Achenbach, T. M., Althoff, R. R., Bagby, R. M., Brown, T. A., Carpenter, W. T., Caspi, A., Clark, L. A., Eaton, N. R., Forbes, M. K., Forbush, K. T., Goldberg, D., Hasin, D., Hyman, S. E., Ivanova, M. Y., Lynam, D. R., Markon, K., … Zimmerman, M. (2017). The Hierarchical Taxonomy of Psychopathology (HiTOP): A dimensional alternative to traditional nosologies. *Journal of Abnormal Psychology*, *126*(4), 454–477. https://doi.org/10.1037/abn0000258

Kragel, P. A., Han, X., Kraynak, T. E., Gianaros, P. J., & Wager, T. D. (2021). Functional MRI Can Be Highly Reliable, but It Depends on What You Measure: A Commentary on Elliott et al. (2020). *Psychological Science*, *32*(4), 622–626. https://doi.org/10.1177/0956797621989730

Lacey, R. E., & Minnis, H. (2020). Practitioner Review: Twenty years of research with adverse childhood experience scores – Advantages, disadvantages and applications to practice. *Journal of Child Psychology and Psychiatry*, *61*(2), 116–130. https://doi.org/10.1111/jcpp.13135

Lane, S. T., Gates, K. M., Pike, H. K., Beltz, A. M., & Wright, A. G. C. (2019). Uncovering general, shared, and unique temporal patterns in ambulatory assessment data. *Psychological Methods*, *24*(1), 54–69. https://doi.org/10.1037/met0000192

Lanza, S. T., & Cooper, B. R. (2016). Latent Class Analysis for Developmental Research. *Child Development Perspectives*, *10*(1), 59–64. https://doi.org/10.1111/cdep.12163

Latora, V., & Marchiori, M. (2001). Efficient Behavior of Small-World Networks. *Physical Review Letters*, *87*(19), 198701. https://doi.org/10.1103/PhysRevLett.87.198701

Latora, V., & Marchiori, M. (2003). Economic small-world behavior in weighted networks. *The European Physical Journal B - Condensed Matter and Complex Systems*, *32*(2), 249–263. https://doi.org/10.1140/epjb/e2003-00095-5

Laursen, B., & Hoff, E. (2006). Person-Centered and Variable-Centered Approaches to Longitudinal Data. *Merrill-Palmer Quarterly*, *52*(3), 377–389.

Lee, C. M., Cadigan, J. M., & Rhew, I. C. (2020). Increases in Loneliness Among Young Adults During the COVID-19 Pandemic and Association With Increases in Mental Health Problems. *Journal of Adolescent Health*, *67*(5), 714–717. https://doi.org/10.1016/j.jadohealth.2020.08.009

Levine, S. (2005). Developmental determinants of sensitivity and resistance to stress. *Psychoneuroendocrinology*, *30*(10), 939–946. https://doi.org/10.1016/j.psyneuen.2005.03.013

Liu, C., & Rubin, Donald. B. (1998). Ellipsoidally symmetric extensions of the general location model for mixed categorical and continuous data. *Biometrika*, *85*(3), 673–688. https://doi.org/10.1093/biomet/85.3.673

Lo, Y., Mendell, N. R., & Rubin, D. B. (2001). Testing the number of components in a normal mixture. *Biometrika*, *88*(3), 767–778. https://doi.org/10.1093/biomet/88.3.767

Loman, M. M., & Gunnar, M. R. (2010). Early experience and the development of stress reactivity and regulation in children. *Neuroscience & Biobehavioral Reviews*, *34*(6), 867–876.

Luby, J. L., Baram, T. Z., Rogers, C. E., & Barch, D. M. (2020). Neurodevelopmental Optimization after Early-Life Adversity: Cross-Species Studies to Elucidate Sensitive Periods and Brain Mechanisms to Inform Early Intervention. *Trends in Neurosciences*. https://doi.org/10.1016/j.tins.2020.08.001

Lütkepohl, H. (2005). *New Introduction to Multiple Time Series Analysis*. Springer Science & Business Media.

Machlin, L., Miller, A. B., Snyder, J., McLaughlin, K. A., & Sheridan, M. A. (2019). Differential Associations of Deprivation and Threat With Cognitive Control and Fear Conditioning in Early Childhood. *Frontiers in Behavioral Neuroscience*, *13*. https://www.frontiersin.org/articles/10.3389/fnbeh.2019.00080

Magnusson, D. (2001). The holistic-interactionistic paradigm: Some directions for empirical developmental research. *European Psychologist*, *6*(3), 153–162. https://doi.org/10.1027/1016-9040.6.3.153

Magnusson, D., & Stattin, H. (2007). The Person in Context: A Holistic-Interactionistic Approach. In *Handbook of Child Psychology*. John Wiley & Sons, Ltd. https://doi.org/10.1002/9780470147658.chpsy0108

Manuck, S. B., & McCaffery, J. M. (2014). Gene-environment interaction. *Annual Review of Psychology*, *65*, 41–70. https://doi.org/10.1146/annurev-psych-010213-115100

Margulies, D. S., Kelly, A. M. C., Uddin, L. Q., Biswal, B. B., Castellanos, F. X., & Milham, M. P. (2007). Mapping the functional connectivity of anterior cingulate cortex. *NeuroImage*, *37*(2), 579–588. https://doi.org/10.1016/j.neuroimage.2007.05.019

Martf, O., & Armario, A. (1997). Influence of Regularity of Exposure to Chronic Stress on the Pattern of Habituation of Pituitary-Adrenal Hormones, Prolactin and Glucose. *Stress*, *1*(3), 179–189. https://doi.org/10.3109/10253899709001107

Martin, T. E. (1995). Avian Life History Evolution in Relation to Nest Sites, Nest Predation, and Food. *Ecological Monographs*, *65*(1), 101–127. https://doi.org/10.2307/2937160

Masten, A. S. (2001). Ordinary magic: Resilience processes in development. *American Psychologist*, *56*(3), 227.

Masyn, K. E. (2013). Latent Class Analysis and Finite Mixture Modeling. In T. D. Little (Ed.), *The Oxford Handbook of Quantitative Methods in Psychology: Vol. 2: Statistical Analysis* (p. 0). Oxford University Press. https://doi.org/10.1093/oxfordhb/9780199934898.013.0025

Mattoni, M., Wilson, S., & Olino, T. M. (2021). Identifying profiles of brain structure and associations with current and future psychopathology in youth. *Developmental Cognitive Neuroscience*, *51*, 101013. https://doi.org/10.1016/j.dcn.2021.101013

Mattson, W. I., Hyde, L. W., Shaw, D. S., Forbes, E. E., & Monk, C. S. (2016). Clinical neuroprediction: Amygdala reactivity predicts depressive symptoms 2 years later. *Social Cognitive and Affective Neuroscience*, *11*(6), 892–898. https://doi.org/10.1093/scan/nsw018

Mayberg, H. S., Lozano, A. M., Voon, V., McNeely, H. E., Seminowicz, D., Hamani, C., Schwalb, J. M., & Kennedy, S. H. (2005). Deep Brain Stimulation for Treatment-Resistant Depression. *Neuron*, *45*(5), 651–660. https://doi.org/10.1016/j.neuron.2005.02.014

Mayer, S. E., & Jencks, C. (1989). Poverty and the Distribution of Material Hardship. *The Journal of Human Resources*, *24*(1), 88–114. JSTOR. https://doi.org/10.2307/145934

McEwen, B. S. (1998). Stress, adaptation, and disease. Allostasis and allostatic load. *Annals of the New York Academy of Sciences*, *840*(1), 33–44. https://doi.org/10.1111/j.1749-6632.1998.tb09546.x

McEwen, B. S. (2007). Physiology and Neurobiology of Stress and Adaptation: Central Role of the Brain. *Physiological Reviews*, *87*(3), 873–904. https://doi.org/10.1152/physrev.00041.2006

McEwen, B. S. (2008). Central effects of stress hormones in health and disease: Understanding the protective and damaging effects of stress and stress mediators. *European Journal of Pharmacology*, *583*(2), 174–185. https://doi.org/10.1016/j.ejphar.2007.11.071

McLaughlin, K. A. (2014). Developmental epidemiology. In *Handbook of developmental psychopathology* (pp. 87–107). Springer.

McLaughlin, K. A., Greif Green, J., Gruber, M. J., Sampson, N. A., Zaslavsky, A. M., & Kessler, R. C. (2012). Childhood adversities and first onset of psychiatric disorders in a national sample of US adolescents. *Archives of General Psychiatry*, *69*(11), 1151–1160. https://doi.org/10.1001/archgenpsychiatry.2011.2277

McLaughlin, K. A., & Nolen-Hoeksema, S. (2012). Interpersonal Stress Generation as a Mechanism Linking Rumination to Internalizing Symptoms in Early Adolescents. *Journal of Clinical Child & Adolescent Psychology*, *41*(5), 584–597. https://doi.org/10.1080/15374416.2012.704840

McLaughlin, K. A., Sheridan, M. A., Humphreys, K. L., Belsky, J., & Ellis, B. J. (2021). The Value of Dimensional Models of Early Experience: Thinking Clearly About Concepts

and Categories. *Perspectives on Psychological Science*, *16*(6), 1463–1472. https://doi.org/10.1177/1745691621992346

McLaughlin, K. A., Weissman, D., & Bitrán, D. (2019). Childhood Adversity and Neural Development: A Systematic Review. *Annual Review of Developmental Psychology*, *1*(1), 277–312. https://doi.org/10.1146/annurev-devpsych-121318-084950

McLoyd, V. C. (1998). Socioeconomic Disadvantage and Child Development. *American Psychologist*, 20.

McNeish, D., Harring, J. R., & Bauer, D. J. (2022). Nonconvergence, covariance constraints, and class enumeration in growth mixture models. *Psychological Methods*.

Meaney, M. J. (2001). Maternal Care, Gene Expression, and the Transmission of Individual Differences in Stress Reactivity Across Generations. *Annual Review of Neuroscience*, *24*(1), 1161–1192. https://doi.org/10.1146/annurev.neuro.24.1.1161

Menon, V. (2011). Large-scale brain networks and psychopathology: A unifying triple network model. *Trends in Cognitive Sciences*, *15*(10), 483–506. https://doi.org/10.1016/j.tics.2011.08.003

Menon, V., & Uddin, L. Q. (2010). Saliency, switching, attention and control: A network model of insula function. *Brain Structure and Function*, *214*(5–6), 655–667. https://doi.org/10.1007/s00429-010-0262-0

Miller, A. B., Machlin, L., McLaughlin, K. A., & Sheridan, M. A. (n.d.). Deprivation and psychopathology in the Fragile Families Study: A 15-year longitudinal investigation. *Journal of Child Psychology and Psychiatry*, *n/a*(n/a). https://doi.org/10.1111/jcpp.13260

Miller, A. B., Sheridan, M. A., Hanson, J. L., McLaughlin, K. A., Bates, J. E., Lansford, J. E., Pettit, G. S., & Dodge, K. A. (2018). Dimensions of deprivation and threat,

psychopathology, and potential mediators: A multi-year longitudinal analysis. *Journal of Abnormal Psychology*, *127*(2), 160–170. https://doi.org/10.1037/abn0000331

Mitchell, C., McLanahan, S., Hobcraft, J., Brooks-Gunn, J., Garfinkel, I., & Notterman, D. (2015). Family Structure Instability, Genetic Sensitivity, and Child Well-Being. *American Journal of Sociology*, *120*(4), 1195–1225. https://doi.org/10.1086/680681

Molenaar, P. C. M. (2004). A Manifesto on Psychology as Idiographic Science: Bringing the Person Back Into Scientific Psychology, This Time Forever. *Measurement: Interdisciplinary Research and Perspectives*, *2*(4), 201–218. https://doi.org/10.1207/s15366359mea0204_1

Molenaar, P. C. M. (2015). On the relation between person-oriented and subject-specific approaches. *Journal for Person-Oriented Research*, *1*(1–2), 34–41. https://doi.org/10.17505/jpor.2015.04

Molenaar, P. C. M., & Campbell, C. G. (2009). The New Person-Specific Paradigm in Psychology. *Current Directions in Psychological Science*, *18*(2), 112–117. https://doi.org/10.1111/j.1467-8721.2009.01619.x

Monk, C. S., & Hardi, F. A. (2023). Poverty, Brain Development, and Mental Health: Progress, Challenges, and Paths Forward. *Annual Review of Developmental Psychology*, *5*(1). https://doi.org/10.1146/annurev-devpsych-011922-012402

Monk, C. S., Klein, R. G., Telzer, E. H., Schroth, E. A., Mannuzza, S., Moulton, J. L., Guardino, M., Masten, C. L., McClure-Tone, E. B., Fromm, S., Blair, R. J., Pine, D. S., & Ernst, M. (2008). Amygdala and Nucleus Accumbens Activation to Emotional Facial Expressions in Children and Adolescents at Risk for Major Depression. *American Journal of Psychiatry*, *165*(1), 90–98. https://doi.org/10.1176/appi.ajp.2007.06111917

Mori, M., Krumholz, H. M., & Allore, H. G. (2020). Using Latent Class Analysis to Identify Hidden Clinical Phenotypes. *JAMA*, *324*(7), 700–701. https://doi.org/10.1001/jama.2020.2278

Morin, A. J. S., Gagne, M., & Bujacz, A. (2016). *Feature topic: Person-centered methodologies in the organizational sciences*. https://doi.org/10.1177/1094428115617592

Moses-Kolko, E. L., Perlman, S. B., Wisner, K. L., James, J., Saul, A. T., & Phillips, M. L. (2010). Abnormally Reduced Dorsomedial Prefrontal Cortical Activity and Effective Connectivity With Amygdala in Response to Negative Emotional Faces in Postpartum Depression. *American Journal of Psychiatry*, *167*(11), 1373–1380. https://doi.org/10.1176/appi.ajp.2010.09081235

Muir, J. L., & Pfister, H. P. (1986). Corticosterone and prolactin responses to predictable and unpredictable novelty stress in rats. *Physiology & Behavior*, *37*(2), 285–288. https://doi.org/10.1016/0031-9384(86)90234-9

Muthén, B., & Muthén, L. (2017). Mplus. In *Handbook of item response theory* (pp. 507–518). Chapman and Hall/CRC.

Muthén, B., & Muthén, L. K. (2000). Integrating Person-Centered and Variable-Centered Analyses: Growth Mixture Modeling With Latent Trajectory Classes. *Alcohol: Clinical and Experimental Research*, *24*(6), 882–891. https://doi.org/10.1111/j.1530-0277.2000.tb02070.x

Nagin, D. S. (2009). Group-Based Modeling of Development. In *Group-Based Modeling of Development*. Harvard University Press. https://doi.org/10.4159/9780674041318

Nederhof, E., & Schmidt, M. V. (2012). Mismatch or cumulative stress: Toward an integrated hypothesis of programming effects. *Physiology & Behavior*, *106*(5), 691–700. https://doi.org/10.1016/j.physbeh.2011.12.008

Nelson, C. A., & Gabard-Durnam, L. J. (2020). Early Adversity and Critical Periods: Neurodevelopmental Consequences of Violating the Expectable Environment. *Trends in Neurosciences*, *43*(3), 133–143. https://doi.org/10.1016/j.tins.2020.01.002

Newman, M. E. J. (2003). The Structure and Function of Complex Networks. *SIAM Review*, *45*(2), 167–256. https://doi.org/10.1137/S003614450342480

Newman, M. E. J. (2004). Fast algorithm for detecting community structure in networks. *Physical Review E*, *69*(6), 066133. https://doi.org/10.1103/PhysRevE.69.066133

Newman, M. E. J. (2006). Finding community structure in networks using the eigenvectors of matrices. *Physical Review E*, *74*(3), 036104. https://doi.org/10.1103/PhysRevE.74.036104

Noble, S., Scheinost, D., & Constable, R. T. (2019). A decade of test-retest reliability of functional connectivity: A systematic review and meta-analysis. *NeuroImage*, *203*, 116157. https://doi.org/10.1016/j.neuroimage.2019.116157

Noble, S., Scheinost, D., & Constable, R. T. (2021). A guide to the measurement and interpretation of fMRI test-retest reliability. *Current Opinion in Behavioral Sciences*, *40*, 27–32. https://doi.org/10.1016/j.cobeha.2020.12.012

Norman, D. A., & Rumelhart, D. E. (1970). A system for perception and memory. In *Models of human memory* (pp. 19–64). Academic Press New York.

Nucifora, P. G. P., Verma, R., Lee, S.-K., & Melhem, E. R. (2007). Diffusion-Tensor MR Imaging and Tractography: Exploring Brain Microstructure and Connectivity. *Radiology*, *245*(2), 367–384. https://doi.org/10.1148/radiol.2452060445

Nylund, K. L., Asparouhov, T., & Muthén, B. O. (2007). Deciding on the number of classes in latent class analysis and growth mixture modeling: A Monte Carlo simulation study. *Structural Equation Modeling: A Multidisciplinary Journal*, *14*(4), 535–569.

Nylund, K. L., Asparouhov, T., & Muthén, B. O. (2008). Deciding on the number of classes in latent class analysis and growth mixture modeling: A Monte Carlo simulation study. *Structural Equation Modeling*, *15*(1), 182–182. https://doi.org/10.1080/10705510701793320

Onnela, J.-P., Saramäki, J., Kertész, J., & Kaski, K. (2005). Intensity and coherence of motifs in weighted complex networks. *Physical Review E*, *71*(6), 065103. https://doi.org/10.1103/PhysRevE.71.065103

Ono, M., Kikusui, T., Sasaki, N., Ichikawa, M., Mori, Y., & Murakami-Murofushi, K. (2008). Early weaning induces anxiety and precocious myelination in the anterior part of the basolateral amygdala of male Balb/c mice. *Neuroscience*, *156*(4), 1103–1110. https://doi.org/10.1016/j.neuroscience.2008.07.078

Ooi, L. Q. R., Chen, J., Shaoshi, Z., Kong, R., Tam, A., Li, J., Dhamala, E., Zhou, J. H., Holmes, A. J., & Yeo, B. T. T. (2022). Comparison of individualized behavioral predictions across anatomical, diffusion and functional connectivity MRI. *NeuroImage*, 119636. https://doi.org/10.1016/j.neuroimage.2022.119636

Opsahl, T., & Panzarasa, P. (2009). Clustering in weighted networks. *Social Networks*, *31*(2), 155–163. https://doi.org/10.1016/j.socnet.2009.02.002

Pagnoni, G., Zink, C. F., Montague, P. R., & Berns, G. S. (2002). Activity in human ventral striatum locked to errors of reward prediction. *Nature Neuroscience*, *5*(2), Article 2. https://doi.org/10.1038/nn802

Pechtel, P., & Pizzagalli, D. A. (2011). Effects of early life stress on cognitive and affective function: An integrated review of human literature. *Psychopharmacology*, *214*(1), 55–70. https://doi.org/10.1007/s00213-010-2009-2

Peckins, M. K., Roberts, A. G., Hein, T. C., Hyde, L. W., Mitchell, C., Brooks-Gunn, J., McLanahan, S. S., Monk, C. S., & Lopez-Duran, N. L. (2020). Violence exposure and social deprivation is associated with cortisol reactivity in urban adolescents. *Psychoneuroendocrinology*, *111*, 104426. https://doi.org/10.1016/j.psyneuen.2019.104426

Pereira, M. E., & Fairbanks, L. A. (2002). *Juvenile Primates: Life History, Development and Behavior, with a New Foreword*. University of Chicago Press.

Pessoa, L. (2017). A Network Model of the Emotional Brain. *Trends in Cognitive Sciences*, *21*(5), 357–371. https://doi.org/10.1016/j.tics.2017.03.002

Petersen, A. C., Crockett, L., Richards, M., & Boxer, A. (1988). A self-report measure of pubertal status: Reliability, validity, and initial norms. *Journal of Youth and Adolescence*, *17*(2), 117–133. https://doi.org/10.1007/BF01537962

Peterson, C., Aslam, M. V., Niolon, P. H., Bacon, S., Bellis, M. A., Mercy, J. A., & Florence, C. (2023). Economic Burden of Health Conditions Associated With Adverse Childhood Experiences Among US Adults. *JAMA Network Open*, *6*(12), e2346323. https://doi.org/10.1001/jamanetworkopen.2023.46323

Poldrack, R. A. (2017). Precision Neuroscience: Dense Sampling of Individual Brains. *Neuron*, *95*(4), 727–729. https://doi.org/10.1016/j.neuron.2017.08.002

Pollak, S. D., Cicchetti, D., Hornung, K., & Reed, A. (2000). Recognizing emotion in faces: Developmental effects of child abuse and neglect. *Developmental Psychology*, *36*(5), 679.

Power, J. D., Barnes, K. A., Snyder, A. Z., Schlaggar, B. L., & Petersen, S. E. (2012). Spurious but systematic correlations in functional connectivity MRI networks arise from subject motion. *Neuroimage*, *59*(3), 2142–2154. https://doi.org/10.1016/j.neuroimage.2011.10.018

Price, J. L., & Drevets, W. C. (2010). Neurocircuitry of mood disorders. *Neuropsychopharmacology: Official Publication of the American College of Neuropsychopharmacology*, *35*(1), 192–216. https://doi.org/10.1038/npp.2009.104

Promislow, D. E. L., & Harvey, P. H. (1990). Living fast and dying young: A comparative analysis of life-history variation among mammals. *Journal of Zoology*, *220*(3), 417–437. https://doi.org/10.1111/j.1469-7998.1990.tb04316.x

Pronk, T., Molenaar, D., Wiers, R. W., & Murre, J. (2022). Methods to split cognitive task data for estimating split-half reliability: A comprehensive review and systematic assessment. *Psychonomic Bulletin & Review*, *29*(1), 44–54. https://doi.org/10.3758/s13423-021-01948-3

Proust-Lima, C., Philipps, V., & Liquet, B. (2017). Estimation of Extended Mixed Models Using Latent Classes and Latent Processes: The R Package lcmm. *Journal of Statistical Software*, *78*, 1–56. https://doi.org/10.18637/jss.v078.i02

Radloff, L. S. (1977). The CES-D scale: A self-report depression scale for research in the general population. *Applied Psychological Measurement*, *1*(3), 385–401.

Raichle, M. E. (2015). The Brain's Default Mode Network. *Annual Review of Neuroscience*, *38*(1), 433–447. https://doi.org/10.1146/annurev-neuro-071013-014030

Raichle, M. E., MacLeod, A. M., Snyder, A. Z., Powers, W. J., Gusnard, D. A., & Shulman, G. L. (2001). A default mode of brain function. *Proceedings of the National Academy of Sciences*, *98*(2), 676–682. https://doi.org/10.1073/pnas.98.2.676

Rauch, S. L., Shin, L. M., & Wright, C. I. (2003). Neuroimaging Studies of Amygdala Function in Anxiety Disorders. *Annals of the New York Academy of Sciences*, *985*(1), 389–410. https://doi.org/10.1111/j.1749-6632.2003.tb07096.x

Reichardt, J., & Bornholdt, S. (2006). Statistical mechanics of community detection. *Physical Review E*, *74*(1), 016110. https://doi.org/10.1103/PhysRevE.74.016110

Reichman, N. E., Teitler, J. O., Garfinkel, I., & McLanahan, S. (2001). Fragile Families: Sample and Design. *Children and Youth Services Review*, *23*. https://doi.org/10.1016/s0190-7409(01)00141-4

Ricard, J. A., Parker, T. C., Dhamala, E., Kwasa, J., Allsop, A., & Holmes, A. J. (2022). Confronting racially exclusionary practices in the acquisition and analyses of neuroimaging data. *Nature Neuroscience*, 1–8. https://doi.org/10.1038/s41593-022-01218-y

Richmond, S., Johnson, K. A., Seal, M. L., Allen, N. B., & Whittle, S. (2016). Development of brain networks and relevance of environmental and genetic factors: A systematic review. *Neuroscience & Biobehavioral Reviews*, *71*, 215–239. https://doi.org/10.1016/j.neubiorev.2016.08.024

Robinson, O. J., Cools, R., Carlisi, C. O., Sahakian, B. J., & Drevets, W. C. (2012). Ventral Striatum Response During Reward and Punishment Reversal Learning in Unmedicated Major Depressive Disorder. *American Journal of Psychiatry*, *169*(2), 152–159. https://doi.org/10.1176/appi.ajp.2011.11010137

Rolls, E. T., Joliot, M., & Tzourio-Mazoyer, N. (2015). Implementation of a new parcellation of the orbitofrontal cortex in the automated anatomical labeling atlas. *NeuroImage*, *122*, 1–5. https://doi.org/10.1016/j.neuroimage.2015.07.075

Rosenblum, L. A., & Paully, G. S. (1984). The Effects of Varying Environmental Demands on Maternal and Infant Behavior. *Child Development*, *55*(1), 305–314. https://doi.org/10.2307/1129854

Rubinov, M., & Sporns, O. (2010). Complex network measures of brain connectivity: Uses and interpretations. *NeuroImage*, *52*(3), 1059–1069. https://doi.org/10.1016/j.neuroimage.2009.10.003

Rudolph, K. D., Lansford, J. E., & Rodkin, P. C. (2016). Interpersonal Theories of Developmental Psychopathology. In *Developmental Psychopathology* (pp. 1–69). John Wiley & Sons, Ltd. https://doi.org/10.1002/9781119125556.devpsy307

Rutherford, S., Kia, S. M., Wolfers, T., Fraza, C., Zabihi, M., Dinga, R., Berthet, P., Worker, A., Verdi, S., Ruhe, H. G., Beckmann, C. F., & Marquand, A. F. (2022). The normative modeling framework for computational psychiatry. *Nature Protocols*, *17*(7), Article 7. https://doi.org/10.1038/s41596-022-00696-5

Rutter, M. (1998). Developmental catch-up, and deficit, following adoption after severe global early privation. *The Journal of Child Psychology and Psychiatry and Allied Disciplines*, *39*(4), 465–476.

Rutter, M., Hersov, L., & Shaffer, D. (1978). Aggression and anti-social behavior in childhood and adolescence. *Family, Area, and School Influences in the Genesis of Conduct Disorder*, 95–113.

Rutter, M., Kent, M. W., & Rolf, J. (1979). Primary prevention of psychopathology, vol. 3: Social competence in children. *Psychiatric Services*, *31*(4), 279–280.

Rutter, M., & Silberg, J. (2002). Gene-environment interplay in relation to emotional and behavioral disturbance. *Annual Review of Psychology*, *53*(1), 463–490.

Sacks, V., & Murphey, D. (2018). The prevalence of adverse childhood experiences, nationally, by state, and by race or ethnicity. *Child Trends*, *20*, 2018.

Sameroff, A. (1975). Transactional models in early social relations. *Human Development*, *18*(1–2), 65–79.

Sameroff, A. (2010). A unified theory of development: A dialectic integration of nature and nurture. *Child Development*, *81*(1), 6–22. https://doi.org/10.1111/j.1467-8624.2009.01378.x

Sameroff, A., Seifer, R., Zax, M., & Barocas, R. (1987). Early indicators of developmental risk: Rochester Longitudinal Study. *Schizophrenia Bulletin*, *13*(3), 383–394.

Sampson, R. J. (1997). Collective regulation of adolescent misbehavior: Validation results from eighty Chicago neighborhoods. *Journal of Adolescent Research*, *12*(2), 227–244.

Sampson, R. J., Raudenbush, S. W., & Earls, F. (1997). Neighborhoods and Violent Crime: A Multilevel Study of Collective Efficacy. *Science*, *277*(5328), 918–924. https://doi.org/10.1126/science.277.5328.918

Sánchez, M. M., Ladd, C. O., & Plotsky, P. M. (2001). Early adverse experience as a developmental risk factor for later psychopathology: Evidence from rodent and primate

models. *Development and Psychopathology*, *13*(3), 419–449. https://doi.org/10.1017/S0954579401003029

Sapolsky, R. M. (1992). *Stress, the aging brain, and the mechanisms of neuron death.* the MIT Press.

Schultz, W., Apicella, P., Scarnati, E., & Ljungberg, T. (1992). Neuronal activity in monkey ventral striatum related to the expectation of reward. *Journal of Neuroscience*, *12*(12), 4595–4610. https://doi.org/10.1523/JNEUROSCI.12-12-04595.1992

Schumacker, R., Robinson, C., & Schumacker, R. E. (2009). *Interacting effects: Centering, variance inflation factor and interpretation issues. Multiple Linear Regression Viewpoints*.

Schwabe, L., Hermans, E. J., Joëls, M., & Roozendaal, B. (2022). Mechanisms of memory under stress. *Neuron*, *110*(9), 1450–1467. https://doi.org/10.1016/j.neuron.2022.02.020

Schwartz, C. E., Wright, C. I., Shin, L. M., Kagan, J., & Rauch, S. L. (2003). Inhibited and Uninhibited Infants "Grown Up": Adult Amygdalar Response to Novelty. *Science*, *300*(5627), 1952–1953. https://doi.org/10.1126/science.1083703

Schwarz, G. (1978). Estimating the dimension of a model. *The Annals of Statistics*, 461–464.

Sclove, S. L. (1987). Application of model-selection criteria to some problems in multivariate analysis. *Psychometrika*, *52*, 333–343.

Scotto Rosato, N., & Baer, J. C. (2012). Latent Class Analysis: A Method for Capturing Heterogeneity. *Social Work Research*, *36*(1), 61–69. https://doi.org/10.1093/swr/svs006

Seeley, W. W. (2019). The Salience Network: A Neural System for Perceiving and Responding to Homeostatic Demands. *Journal of Neuroscience*, *39*(50), 9878–9882. https://doi.org/10.1523/JNEUROSCI.1138-17.2019

Sheridan, M. A., Fox, N. A., Zeanah, C. H., McLaughlin, K. A., & Nelson, C. A. (2012). Variation in neural development as a result of exposure to institutionalization early in childhood. *Proceedings of the National Academy of Sciences*, *109*(32), 12927–12932. https://doi.org/10.1073/pnas.1200041109

Sheridan, M. A., & McLaughlin, K. A. (2014). Dimensions of early experience and neural development: Deprivation and threat. *Trends in Cognitive Sciences*, *18*(11), 580–585. https://doi.org/10.1016/j.tics.2014.09.001

Sinha, P., Calfee, C. S., & Delucchi, K. L. (2021). Practitioner's Guide to Latent Class Analysis: Methodological Considerations and Common Pitfalls. *Critical Care Medicine*, *49*(1), e63. https://doi.org/10.1097/CCM.0000000000004710

Slopen, N., Shonkoff, J. P., Albert, M. A., Yoshikawa, H., Jacobs, A., Stoltz, R., & Williams, D. R. (2016). Racial Disparities in Child Adversity in the U.S.: Interactions With Family Immigration History and Income. *American Journal of Preventive Medicine*, *50*(1), 47–56. https://doi.org/10.1016/j.amepre.2015.06.013

Smith, K. E., & Pollak, S. D. (2021). Rethinking Concepts and Categories for Understanding the Neurodevelopmental Effects of Childhood Adversity. *Perspectives on Psychological Science*, *16*(1), 67–93. https://doi.org/10.1177/1745691620920725

Smith, R. E., Tournier, J.-D., Calamante, F., & Connelly, A. (2012). Anatomically-constrained tractography: Improved diffusion MRI streamlines tractography through effective use of anatomical information. *NeuroImage*, *62*(3), 1924–1938. https://doi.org/10.1016/j.neuroimage.2012.06.005

Smith, S. M. (2012). The future of FMRI connectivity. *NeuroImage*, *62*(2), 1257–1266. https://doi.org/10.1016/j.neuroimage.2012.01.022

Spisak, T., Bingel, U., & Wager, T. D. (2023). Multivariate BWAS can be replicable with moderate sample sizes. *Nature*, *615*(7951), Article 7951. https://doi.org/10.1038/s41586-023-05745-x

Sporns, O. (2002). Network analysis, complexity, and brain function. *Complexity*, *8*(1), 56–60. https://doi.org/10.1002/cplx.10047

Sporns, O., Tononi, G., & Kötter, R. (2005). The Human Connectome: A Structural Description of the Human Brain. *PLOS Computational Biology*, *1*(4), e42. https://doi.org/10.1371/journal.pcbi.0010042

Stein, M. B., Simmons, A. N., Feinstein, J. S., & Paulus, M. P. (2007). Increased Amygdala and Insula Activation During Emotion Processing in Anxiety-Prone Subjects. *American Journal of Psychiatry*, *164*(2), 318–327. https://doi.org/10.1176/ajp.2007.164.2.318

Sterba, S. K., & Bauer, D. J. (2010). Matching method with theory in person-oriented developmental psychopathology research. *Development and Psychopathology*, *22*(2), 239–254. https://doi.org/10.1017/S0954579410000015

Stevens, F. L., Hurley, R. A., Taber, K. H., Hurley, R. A., Hayman, L. A., & Taber, K. H. (2011). Anterior Cingulate Cortex: Unique Role in Cognition and Emotion. *The Journal of Neuropsychiatry and Clinical Neurosciences*, *23*(2), 121–125. https://doi.org/10.1176/jnp.23.2.jnp121

Straus, M. A., Hamby, S. L., Finkelhor, D., Moore, D. W., & Runyan, D. (1998). Identification of Child Maltreatment With the Parent-Child Conflict Tactics Scales: Development and Psychometric Data for a National Sample of American Parents. *Child Abuse & Neglect*, *22*(4), 249–270. https://doi.org/10.1016/S0145-2134(97)00174-9

Strzelewicz, A. R., Ordoñes Sanchez, E., Rondón-Ortiz, A. N., Raneri, A., Famularo, S. T., Bangasser, D. A., & Kentner, A. C. (2019). Access to a high resource environment protects against accelerated maturation following early life stress: A translational animal model of high, medium and low security settings. *Hormones and Behavior*, *111*, 46–59. https://doi.org/10.1016/j.yhbeh.2019.01.003

Swartz, J. R., Knodt, A. R., Radtke, S. R., & Hariri, A. R. (2015). A Neural Biomarker of Psychological Vulnerability to Future Life Stress. *Neuron*, *85*(3), 505–511. https://doi.org/10.1016/j.neuron.2014.12.055

Swedo, E. A. (2023). Prevalence of Adverse Childhood Experiences Among US Adults—Behavioral Risk Factor Surveillance System, 2011–2020. *MMWR. Morbidity and Mortality Weekly Report*, *72*.

Tahedl, M. (2018). BATMAN: Basic and Advanced Tractography with MRtrix for All Neurophiles. *OSF Home, Doi*, *10*.

Tai, D. B. G., Shah, A., Doubeni, C. A., Sia, I. G., & Wieland, M. L. (2021). The Disproportionate Impact of COVID-19 on Racial and Ethnic Minorities in the United States. *Clinical Infectious Diseases*, *72*(4), 703–706. https://doi.org/10.1093/cid/ciaa815

Taxali, A., Angstadt, M., Rutherford, S., & Sripada, C. (2021). Boost in Test–Retest Reliability in Resting State fMRI with Predictive Modeling. *Cerebral Cortex*, *bhaa390*. https://doi.org/10.1093/cercor/bhaa390

Team, R. C. (2013). R: A language and environment for statistical computing. R Foundation for Statistical Computing, Vienna, Austria. *Http://Www. R-Project. Org/*.

Teicher, M. H., Samson, J. A., Anderson, C. M., & Ohashi, K. (2016). The effects of childhood maltreatment on brain structure, function and connectivity. *Nature Reviews Neuroscience*, *17*(10), 652–666. https://doi.org/10.1038/nrn.2016.111

Thelen, E., & Smith, L. B. (1994). *A dynamic systems approach to the development of cognition and action*. MIT press.

Thomas, K. M., Drevets, W. C., Dahl, R. E., Ryan, N. D., Birmaher, B., Eccard, C. H., Axelson, D., Whalen, P. J., & Casey, B. J. (2001). Amygdala Response to Fearful Faces in Anxious and Depressed Children. *Archives of General Psychiatry*, *58*(11), 1057–1063. https://doi.org/10.1001/archpsyc.58.11.1057

Tottenham, N. (2020). Early Adversity and the Neotenous Human Brain. *Biological Psychiatry*, *87*(4), 350–358. https://doi.org/10.1016/j.biopsych.2019.06.018

Tottenham, N., Hare, T. A., Quinn, B. T., McCarry, T. W., Nurse, M., Gilhooly, T., Millner, A., Galvan, A., Davidson, M. C., Eigsti, I.-M., Thomas, K. M., Freed, P. J., Booma, E. S., Gunnar, M. R., Altemus, M., Aronson, J., & Casey, B. j. (2010). Prolonged institutional rearing is associated with atypically large amygdala volume and difficulties in emotion regulation. *Developmental Science*, *13*(1), 46–61. https://doi.org/10.1111/j.1467-7687.2009.00852.x

Tottenham, N., & Sheridan, M. A. (2010). A review of adversity, the amygdala and the hippocampus: A consideration of developmental timing. *Frontiers in Human Neuroscience*, *3*. https://doi.org/10.3389/neuro.09.068.2009

Tottenham, N., Tanaka, J. W., Leon, A. C., McCarry, T., Nurse, M., Hare, T. A., Marcus, D. J., Westerlund, A., Casey, B. J., & Nelson, C. (2009). The NimStim set of facial

expressions: Judgments from untrained research participants. *Psychiatry Research*, *168*(3), 242–249. https://doi.org/10.1016/j.psychres.2008.05.006

Tournier, J.-D., Calamante, F., & Connelly, A. (2007). Robust determination of the fibre orientation distribution in diffusion MRI: Non-negativity constrained super-resolved spherical deconvolution. *NeuroImage*, *35*(4), 1459–1472. https://doi.org/10.1016/j.neuroimage.2007.02.016

Tournier, J.-D., Calamante, F., & Connelly, A. (2012). MRtrix: Diffusion tractography in crossing fiber regions. *International Journal of Imaging Systems and Technology*, *22*(1), 53–66. https://doi.org/10.1002/ima.22005

Tournier, J.-D., Calamante, F., Gadian, D. G., & Connelly, A. (2004). Direct estimation of the fiber orientation density function from diffusion-weighted MRI data using spherical deconvolution. *NeuroImage*, *23*(3), 1176–1185. https://doi.org/10.1016/j.neuroimage.2004.07.037

Trentacosta, C. J., Hyde, L. W., Shaw, D. S., Dishion, T. J., Gardner, F., & Wilson, M. (2008). The relations among cumulative risk, parenting, and behavior problems during early childhood. *Journal of Child Psychology and Psychiatry*, *49*(11), 1211–1219. https://doi.org/10.1111/j.1469-7610.2008.01941.x

Uddin, L. Q. (2015). Salience processing and insular cortical function and dysfunction. *Nature Reviews Neuroscience*, *16*(1), Article 1. https://doi.org/10.1038/nrn3857

Vannucci, A., Fields, A., Hansen, E., Katz, A., Kerwin, J., Tachida, A., Martin, N., & Tottenham, N. (2023). Interpersonal early adversity demonstrates dissimilarity from early socioeconomic disadvantage in the course of human brain development: A meta-analysis.

Neuroscience & Biobehavioral Reviews, *150*, 105210. https://doi.org/10.1016/j.neubiorev.2023.105210

Vermunt, J. K., & Magidson, J. (2002). Latent class cluster analysis. *Applied Latent Class Analysis*, *11*(89–106), 60.

Vértes, P. E., & Bullmore, E. T. (2015). Annual Research Review: Growth connectomics – the organization and reorganization of brain networks during normal and abnormal development. *Journal of Child Psychology and Psychiatry*, *56*(3), 299–320. https://doi.org/10.1111/jcpp.12365

Walker, C.-D., Bath, K. G., Joels, M., Korosi, A., Larauche, M., Lucassen, P. J., Morris, M. J., Raineki, C., Roth, T. L., Sullivan, R. M., Taché, Y., & Baram, T. Z. (2017a). Chronic early life stress induced by limited bedding and nesting (LBN) material in rodents: Critical considerations of methodology, outcomes and translational potential. *Stress (Amsterdam, Netherlands)*, *20*(5), 421–448. https://doi.org/10.1080/10253890.2017.1343296

Walker, C.-D., Bath, K. G., Joels, M., Korosi, A., Larauche, M., Lucassen, P. J., Morris, M. J., Raineki, C., Roth, T. L., Sullivan, R. M., Taché, Y., & Baram, T. Z. (2017b). Chronic early life stress induced by limited bedding and nesting (LBN) material in rodents: Critical considerations of methodology, outcomes and translational potential. *Stress*, *20*(5), 421–448. https://doi.org/10.1080/10253890.2017.1343296

Wang, Y., Ghumare, E., Vandenberghe, R., & Dupont, P. (2017). Comparison of Different Generalizations of Clustering Coefficient and Local Efficiency for Weighted Undirected Graphs. *Neural Computation*, *29*(2), 313–331. https://doi.org/10.1162/NECO_a_00914

Wang, Y.-P., & Gorenstein, C. (2013). Psychometric properties of the Beck Depression Inventory-II: A comprehensive review. *Revista Brasileira de Psiquiatria (Sao Paulo, Brazil*, *35*(4), 416–431. https://doi.org/10.1590/1516-4446-2012-1048

Wang, Z., Goerlich, K. S., Ai, H., Aleman, A., Luo, Y., & Xu, P. (2021). Connectome-Based Predictive Modeling of Individual Anxiety. *Cerebral Cortex*, *31*(6), 3006–3020. https://doi.org/10.1093/cercor/bhaa407

Wanless, S. B. (2016). The Role of Psychological Safety in Human Development. *Research in Human Development*, *13*(1), 6–14. https://doi.org/10.1080/15427609.2016.1141283

Warmingham, J. M., Handley, E. D., Rogosch, F. A., Manly, J. T., & Cicchetti, D. (2019). Identifying maltreatment subgroups with patterns of maltreatment subtype and chronicity: A latent class analysis approach. *Child Abuse & Neglect*, *87*, 28–39. https://doi.org/10.1016/j.chiabu.2018.08.013

Whalen, P. J., Shin, L. M., Somerville, L. H., McLean, A. A., & Kim, H. (2002). Functional neuroimaging studies of the amygdala in depression. *Seminars in Clinical Neuropsychiatry*, *7*(4), 234–242. https://doi.org/10.1053/scnp.2002.35219

Wiggins, J. L., Mitchell, C., Hyde, L. W., & Monk, C. S. (2015). Identifying early pathways of risk and resilience: The codevelopment of internalizing and externalizing symptoms and the role of harsh parenting. *Development and Psychopathology*, *27*(4pt1), 1295–1312. https://doi.org/10.1017/S0954579414001412

Woodcock, R. W., McGrew, K. S., & Mather, N. (2001). *Woodcock-Johnson III tests of achievement*.

Woolrich, M. W., Ripley, B. D., Brady, M., & Smith, S. M. (2001). Temporal autocorrelation in univariate linear modeling of FMRI data. *NeuroImage*, *14*(6), 1370–1386. https://doi.org/10.1006/nimg.2001.0931

Xia, M., Wang, J., & He, Y. (2013). BrainNet Viewer: A Network Visualization Tool for Human Brain Connectomics. *PLOS ONE*, *8*(7), e68910. https://doi.org/10.1371/journal.pone.0068910

Xiao, Y., Bi, K., Yip, P. S.-F., Cerel, J., Brown, T. T., Peng, Y., Pathak, J., & Mann, J. J. (2024). Decoding Suicide Decedent Profiles and Signs of Suicidal Intent Using Latent Class Analysis. *JAMA Psychiatry*. https://doi.org/10.1001/jamapsychiatry.2024.0171

Xiong, J., Lipsitz, O., Nasri, F., Lui, L. M. W., Gill, H., Phan, L., Chen-Li, D., Iacobucci, M., Ho, R., Majeed, A., & McIntyre, R. S. (2020). Impact of COVID-19 pandemic on mental health in the general population: A systematic review. *Journal of Affective Disorders*, *277*. https://doi.org/10.1016/j.jad.2020.08.001

Yarkoni, T., Poldrack, R. A., Nichols, T. E., Van Essen, D. C., & Wager, T. D. (2011). Large-scale automated synthesis of human functional neuroimaging data. *Nature Methods*, *8*(8), 665–670. https://doi.org/10.1038/nmeth.1635

Zanto, T. P., & Gazzaley, A. (2013). Fronto-parietal network: Flexible hub of cognitive control. *Trends in Cognitive Sciences*, *17*(12), 602–603. https://doi.org/10.1016/j.tics.2013.10.001

Zeanah, C., Nelson, C., Fox, N., Smyke, A., Marshall, P., Parker, S., & Koga, S. (2003). Designing research to study the effects of institutionalization on brain and behavioral development: The Bucharest Early Intervention Project. *Development and Psychopathology*, *15*, 885–907. https://doi.org/10.1017/S0954579403000452

Zeytinoglu, S., Morales, S., Lorenzo, N. E., Chronis-Tuscano, A., Degnan, K. A., Almas, A. N., Henderson, H., Pine, D. S., & Fox, N. A. (2021). A Developmental Pathway From Early Behavioral Inhibition to Young Adults' Anxiety During the COVID-19 Pandemic. *Journal of the American Academy of Child & Adolescent Psychiatry*, S0890856721000733. https://doi.org/10.1016/j.jaac.2021.01.021

Zhang, S., & Anderson, S. G. (2010). Low-income single mothers' community violence exposure and aggressive parenting practices. *Children and Youth Services Review*, *32*(6), 889–895.

Ziol-Guest, K. M., & McKenna, C. C. (2014). Early Childhood Housing Instability and School Readiness. *Child Development*, *85*(1). https://doi.org/10.1111/cdev.12105